SMALL SIGNAL STABILITY ENHANCEMENT USING POWER SYSTEM STABILIZER

Ph.D. THESIS

by

DHANESH KUMAR SAMBARIYA

DEPARTMENT OF ELECTRICAL ENGINEERING
INDIAN INSTITUTE OF TECHNOLOGY ROORKEE
ROORKEE – 247 667 (INDIA)
MARCH, 2015

SMALL SIGNAL STABILITY ENHANCEMENT USING POWER SYSTEM STABILIZER

A THESIS

Submitted in partial fulfilment of the requirements for the award of the degree of

DOCTOR OF PHILOSOPHY
in
ELECTRICAL ENGINEERING

by

DHANESH KUMAR SAMBARIYA

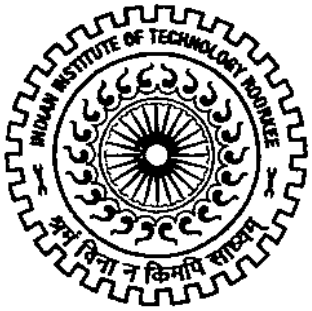

DEPARTMENT OF ELECTRICAL ENGINEERING
INDIAN INSTITUTE OF TECHNOLOGY ROORKEE
ROORKEE – 247 667 (INDIA)
MARCH, 2015

INDIAN INSTITUTE OF TECHNOLOGY ROORKEE
ROORKEE

CANDIDATE'S DECLARATION

I hereby certify that the work which is being presented in this thesis entitled **"SMALL SIGNAL STABILITY ENHANCEMENT USING POWER SYSTEM STABILIZER"** in partial fulfilment of the requirements for the award of *the Degree of Doctor of Philosophy* and submitted in the Department of Electrical Engineering of the Indian Institute of Technology Roorkee, Roorkee is an authentic record of my own work carried out during a period from July, 2011 to March, 2015 under the supervision of Dr. Rajendra Prasad, Professor, Department of Electrical Engineering, Indian Institute of Technology Roorkee, Roorkee.

The matter presented in this thesis has not been submitted by me for the award of any other degree of this or any other Institution.

Signature of Candidate

This is to certify that the above statement made by the candidate is correct to the best of my knowledge.

Signature of Supervisor (s)

The Ph.D. Viva-Voce Examination of ***Mr. Dhanesh Kumar Sambariya***, Research Scholar, has been held on August 17, 2015.

Chairman, SRC **Signature of External Examiner**

This is to certify that the student has made all the corrections in the thesis.

Signature of Supervisor (s) **Head of the Department**

Dated: August 17, 2015

ABSTRACT

Modern power systems are large, complex and multi-component dynamic systems being prone to fluctuating characteristics with varying generation schedules and loads. These power systems suffer with small signal oscillations (SSOs) on occurrence of fault on system network and sudden changes in load changes of low magnitude and in the frequency range of 0.2 – 3.0 Hz. The power transfer capability of the system is restricted over the weak transmission lines because of the persistent oscillations.

In late 1950s, the generators were equipped with high gain and fast acting automatic voltage regulators (AVRs) to improve the system voltage profile. The application of AVRs has invited the problem of small signal oscillations in the power system. The power system stabilizer (PSS) was added to AVR for modulate the excitation of the generator by improving electrical damping torque component in phase with rotor speed deviation, which in turn reduces the SSOs in the power system. The uniformly adopted type of PSS is known as conventional PSS (CPSS), which consists of the lead-lag type components. The CPSS suffers from some limitations as (a) these are designed off-line, therefore, requires re-tuning during commissioning, (b) these are tuned for one operating condition, therefore, may not perform properly for varying operating conditions and (c) because of changing conditions and configuration throughout the power system, they require retuning for good performance, regularly. The power system and control researchers have presented significant efforts to the design of CPSS after the pioneering contribution made by deMello and Concordia in 1969 [1]. The designs of PSS were followed by using modern control theory like adaptive control, optimal control and eigenvalue (pole) assignment. It is reported that the selection of PSS and design methodology is a complex iterative method around an operating point resulting to unsatisfactory operation. Lyapunov based adaptive control and self-tuning are effective methods but requires knowledge of power system dynamics.

Artificial intelligence (AI) based tuning and learning processes such as fuzzy logic, adaptive fuzzy, neuro-fuzzy, artificial neural networks (ANNs) and type-2 fuzzy have been used to design effective PSS. In case of ANN, the gradient algorithm is being used to learn its parameters; either input/output parameters or online data at different operating points of a power system network. Another technological development was based on optimization methods to design PSS. The classical optimization methods were unable to converge for non-linear and non-differential engineering problems. Some of the optimization methods such as the genetic algorithm (GA), particle swarm optimization (PSO), simulated annealing (SA), and differential evolution (DE) algorithm, have been applied to large and complex power systems.

It is worth mentioning that the designed PSS by every method (forth-coming) has been applied to three well known test power system models, such as single-machine infinite-bus (SMIB) power system, two-area four-machine ten-bus power system and New England ten-machine thirty nine-bus power system. In this thesis, Bat algorithm is used to tune the gain, pole - zero parameters of CPSS and tested with all three power system models. The designed BA-CPSS for SMIB system is compared to performance with that of CPSSs designed with different methods in [2-11]. The performance comparison of BA-CPSS over a wide range of operating conditions along with fault condition is compared with each above CPSSs. The performance comparing parameters such as integral of square of error (ISE) and integral of time weighted squares of error (ITSE) performance indices are initially introduced in [12]. In 1999 [12], Prof. Malik has used these indices to differentiate, two superimposed responses by two different PSSs. Therefore, the performance comparison is carried out using integral of time weighted absolute error (ITAE), integral of absolute error (IAE) and ISE as performance indices of speed response and found better as compared to others. The superiority of BA-CPSS is also validated for 231 plant conditions by plot of eigenvalue on s-plane and found to be within the D-shape sector which is the requirement of guaranteeing stability.

In case of four-machine ten-bus power system, BA-CPSSs are compared with the controllers designed by different methods in [11, 13-19]. Again the better value of performance indices (ITAE, IAE and ISE) of speed response with proposed BA-CPSS as compared to others is able to prove its effectiveness over the others.

The application of the bat algorithm to tune CPSS is also extended to New England 39-bus power system and performance are compared to that of with CPSSs reported in [11, 19-26].

The application of the bat algorithm is also applied to tune a proportional-integral-derivative based PSS and compared to PID-PSSs reported in [27-33] for SMIB power system. The application is extended to four-machine system and compared to Iterative Linear Matrix Inequality [34]. The bat algorithm based PID is also designed for New England ten-machine power system and compared with CPSSs reported in [11, 24, 35].

In continuation, the small signal stability is analyzed through the application of a fuzzy logic controller. The distinct fuzzy rule bases proposed by different researchers are arranged in groups with similar entries and numbered from 1 to 21 as reported in [12, 36-71]. Total 21 different fuzzy rule matrices (FRMs) have been detected and applied to SMIB system with a nominal operating condition for small signal stability analysis. It is worth mentioning that some of the rule bases have appeared with similar performances. Therefore, these 21 rule bases are re-arranged in categories with similar performances and resulting to 6 categories in the number. Based on superior performance, category-6 rule bases show the unstable results and category-1

[36-45, 52-54, 61] shows the best performance. As a core work, a new rule table is designed, and the performance is compared to rule base in category-1 [36-45, 52-54, 61] and category-2 [12, 49, 50, 55-59] with SMIB, four-machine and New England power system test systems and found superior in performance.

The fuzzy logic controller lacks the mathematical reasoning, and the performance is reviewed by transient response of the closed-loop system. A small-signal model of the fuzzy logic power system stabilizer (FPSS) is derived to optimize the scaling factors using Harmony Search Algorithm (HSA) and Bat algorithm (BA). The derived such a small signal model of FPSS is proven to be a Proportional Derivative controller. Since the input of a fuzzy PSS can be error and derivative of error, therefore, changes in speed and acceleration are applied to input of FPSS. The parameters of the PD controller are considered as the normalized factors of the FPSS and are tuned using HSA and BA. The optimized PD controller is placed just before the FPSS and results to optimize the scaling factors of the FPSS. Such optimized FPSS using harmony search (HS-FPSS) and bat algorithm (BA-FPSS) is connected to SMIB, four-machine and ten-machine power system and the performance are compared to FPSS as in [72, 73]. Superior performance of BA-FPSS is validated for the wide range of operating conditions along with fault application.

Another way of optimization of scaling factors is introduced by El-Hawary, 1998 as a book chapter in [74]. The main aspect to this approach is to apply a change in speed and change in power as input to FPSS and correction voltage at output. The scaling factors for input as well as output signals are optimized by Zonkoly in 2009 using particle swarm optimization [65]. The same approach is applied to three power system models using harmony search and bat algorithm and performance is compared to PSO-FPSS [65] and FPSS [72, 73] for SMIB system and FPSS [40, 41] for multimachine system. In both approaches, BA-FPSS proves to be the best performer as compared to its counter parts.

The next generation of type-1 fuzzy sets is the interval type-2 fuzzy sets (IT2-FS) were again introduced by Zadeh in 1975. The stronger part of an interval type-2 fuzzy set is to model imprecision and uncertainty in a better way. These IT2-FS were developed by Mendel, who characterized IT2-FS as the footprint of uncertainty (FOU). In most of the cases, IT2 FS performance is better than its type-1 counterpart. Therefore, the evaluation and performance analysis of an interval type-2 fuzzy logic controller (IT2 FLC) as a power system stabilizer (PSS) is carried out. The single machine infinite bus (SMIB) system is considered for evaluation and implementation of IT2 FLC as PSS. The input signals to the controller are considered as speed deviation and acceleration. The evaluation of the controller is considered with 20 separate types of membership functions (MFs) and treated as IT2 FPSS on SMIB system to evaluate the performance of each. The performance of these MFs is evaluated graphically as well as in terms of

ISE, IAE and ITAE as the performance index. The better suitable MF as FPSS is decided out of considered 20 MFs. The selected MF based IT2 FPSS is tested for small signal performance analysis of an SMIB system with wide operating conditions of a power system and extended to the four-machine system and ten-machine power systems. The thesis work may be a good source of different type of PSSs with application of new techniques in the field of small signal stability enhancement.

ACKNOWLEDGEMENT

I take this opportunity to express my deepest sense of gratitude to my research supervisor Dr. Rajendra Prasad, Professor in the Department of Electrical Engineering, Indian Institute of Technology Roorkee for his substantive guidance and moral support. It has my proud privilege to work with Dr. Prasad, a luminary in the field of control system engineering. His support, proficient, advice and continuous encouragement, were the constant source of inspiration for the completion of this research work. I sincerely appreciate his pronounced individualities, humanistic and warm personal approach, which has given me strength to carry out this research work on steady and smooth course. *I* humbly acknowledge a lifetime's gratitude to him.

I keep a deep sense of gratitude to the Head, Department of Electrical Engineering, Prof. S. P. Srivastava, Indian Institute of Technology Roorkee, for providing excellent work environment and computing facilities in the department for the research work. The cooperation and encouragement from former Head of Department of Electrical Engineering, Prof. Promod Agrawal is also gratefully acknowledged. I express my sincere appreciation to Prof. B. Das as SRC, Chairman, Dr. Y. V. Hote as SRC, Member (Internal Expert) and Prof. S. P. Yadav as SRC, Member (External Expert). I am thankful to Prof. G. N. Pillai (Chairman, Doctoral Research Committee, Department of Electrical Engineering) for his invaluable support and encouragement.

I would like to place my heartfelt thanks to my research colleagues, who helped me in every respect, during my stay at Roorkee. I am highly grateful to Dr. Rajeev Gupta, Director, UCE, RTU, Kota and Prof. in the Department of EIC, UCE, RTU, Kota for his technical help in the modeling of test systems and preparation of Simulink model in MATLAB Software. Special thanks to Mr. Sajan, research scholar, IIT Roorkee for helping in the design of multi-objective function and to solve software compatibility issues. I am thankful to Dr. D. K. Palwalia, who helped me by detecting notable issues during thesis writing. I am grateful to University College of Engineering, Rajasthan Technical University, Kota for sponsoring me under Quality Improvement Programme. I also thank my colleagues for sharing the responsibility at the parent Institute during my stay at Roorkee.

This research work was carried under Quality Improvement Programme (QIP) of Govt. of India. I acknowledge my gratitude to the coordinator, Quality Improvement Programme (QIP) centre, Indian Institute of Technology Roorkee, for her kind co-operation.

Special, sincere heartfelt gratitude to my father Shri Bahori Lal, whose sincere prayers, best wishes and support have been a constant source of assurance and strength to me, during the entire period of this work. Thanks to my relatives and friends, who have contributed directly and

indirectly to the completion of this research work. I am especially thankful to my wife Preeti, for her unfailing support and patience during the many months, weekends and nights; I worked for this thesis. I am also thankful to my daughter Shuhangi, who was always a source of inspiration and motivation.

(Dhanesh Kumar Sambariya)

CONTENTS

LIST OF FIGURES

LIST OF TABLES

LIST OF SYMBOLS

Symbol	Description
t	Time
T	Transpone operator
Δ	Perturbing operator
ρ	Derivative operator ($\partial/\partial t$)
x	State vectors
y	Output vectors
X_l	Transmission line reactance
X	Total reactance
ω_0	Rated angular speed in radians per second
V_0, I_0	Pre-fault voltage and current signals
E'_{qi}	Transient EMF in quadrature axis of i^{th} machine in per unit
E'_{di}	Direct axis based transient EMF of i^{th} machine in per unit
E_{fdi}	Excitation field voltage of i^{th} machine in per unit
P_{ei}	Electrical power of i^{th} machine in per unit
P_{mi}	Mechanical power of i^{th} machine in per unit
V_{ti}	Terminal voltage of i^{th} machine in per unit
V_{refi}	Reference voltage at terminal of i^{th} machine in per unit
I_{qi}	Current in quadrature axis of i^{th} machine in per unit
I_{di}	Current in direct axis of i^{th} machine in per unit
K_{Di}	Damping constant of i^{th} machine in per unit
H_i	Inertia coefficient representation of i^{th} machine in seconds
T'_{d0}	Direct open circuit time constant representation in seconds
X'_{di}	Transient reactance in direct axis of i^{th} machine in per unit
X_{di}	Reactance in direct axis of i^{th} machine in per unit
K_{Ai}	Gain of voltage regulator of i^{th} machine in per unit
T_{Ai}	Time constant representation of AVR of i^{th} machine in seconds

G_{ij}	Element of conductance matrix in per unit
B_{ij}	Element representation of susceptance matrix in per unit
V_{ref}	Reference voltage
A	State matrix of the system
B	Control input matrix
C	Output matrix
δ_i	Rotor Angle of the i^{th} machine
ω_i	Rotor Speed of the i^{th} machine
M_i	Machine inertia coefficient of the i^{th} machine
ω_0	Synchronous speed of the machine
T_{mi}	Mechanical Torque of the i^{th} machine
K_{Ai}	Automatic voltage regulator gain of the i^{th} machine
T_{Ai}	Automatic voltage regulator time constant of the i^{th} machine
U_i	PSS output signal of the i^{th} machine
$K_{1ij} - K_{6ij}$	Heffron-Phillip Constants
T_m	Mechanical torque
T_e	Tectrical torque
T_s	Synchronizing torque
$K_s,\ K_D$	Syncheronizing and Damping torque coefficients, respectively
$E_0\angle 0^0$	Infinite bus representation in SMIB system
$E\angle\delta$	Generator EMF behind transient reactance in SMIB system

Objective function

λ_i	ith electromechanical mode eigenvalue ($\lambda_i = \sigma_i \pm j\omega_i$)
σ_i	Real part of ith electromechanical mode eigenvalue
ω_i	Imaginary part of ith electromechanical mode eigenvalue
ξ_i	Damping ratio corresponding to ith electromechanical mode eigenvalue
σ_0	Critical value of real part of eigenvalue selected for D-shape sector
ξ_0	Critical value of damping ratio D-shape sector

Harmony search algorithm

x_i	ith design variable
X_i	Set of possible range of values for each design variable ($x_i^L \le x_i \le x_i^U$)
x_i^L	Lower limit of ith design variable
x_i^U	Upper limit of ith design variable
N	*C*ount of design variable
x'_i	New Harmony vector of ith design variable
dw	*D*istance band-width
$b(i)$	Step size for ith design variable

Bat algorithm

A	Loudness of sound
r	Pulse rate
$f_{\min}$	Minimum frequency
$f_{\max}$	Maximum frequency
ε	Elite percentage
N	Number of maximum iterations

Interval type-2 FS

$\tilde{A}$	Type-2 fuzzy set
$\mu(x)$	Membership grade of type-1 fuzzy membership function (FMF)
$\mu_{\tilde{A}}(x,u)$	Membership grade of type-2 FMF, with $x \in X$ and $u \in J_X \subseteq [0,1]$
$x \in X$	Universe of discourse
[0,1]	Membership Grade
x'	Verticle Slice
$\tilde{A}_e^j$	jth type-2 embedded fuzzy set of $\tilde{A}$
$\overline{\mu}_{\tilde{A}}(x)$	Upper bound of Membership Function (UMF)
$\underline{\mu}_{\tilde{A}}(x)$	Lower bound of Membership Function (LMF)
FOU	Footprint of Uncertainty

LIST OF ACRONYMS

Acronym	Description
PSS	Power system stabilizer
CPSS	Conventional power system stabilizer
FLC	Fuzzy logic controller
FRM	Fuzzy rule matrix
FPSS	Fuzzy logic power system stabilizer
IT2 FPSS	Interval type-2 fuzzy power system stabilizer
SMIB	Single-machine infinite-bus power
SISO	Single-input single-output
MIMO	Multi-input multi-output
AVR	Automatic voltage regulator
LHS	Left hand side
RHS	Right hand side
ITAE	Integral of time weighted absolute error
IAE	Integral absolute error
ISE	Integral of squared error
NVAR	Number of Variables
HMS	Harmony memory size
HMCR	Harmony consideration rate
PARmin	Minimum pitch adjusting rate
PARmax	Maximum pitch adjusting rate
bwmin	Minumum bandwidth
bwmax	Maxiumum bandwidth
PVB	Range of variables
EPS	Electrical power system
SSO	Small signal oscillation
LFO	Low frequency oscillation
BA	Bat algorithm
HSA	Harmony search algorithm
EMO	Electromechanical mode of oscillation
TAFMTB	Two-area four-machine ten-bus
NETMTB	New England ten-machine thirty nine-bus
PI	Performance index

Chapter 1

INTRODUCTION

Electrical power systems (EPSs) are large, interconnected and complex; it generally consists of generating units; transmission lines and load centres; are prone to disturbances of temporary or permanent in nature; and may result to develop small signal oscillations (SSOs). These SSOs are low in magnitude and frequency within the range of 0.2 - 3.0 Hz. Most of SSOs may be damped out but some of them may persist for a while, grow gradually and result to system separation. During late 1950s and early 1960s, most of the generating units in EPS were equipped with high gain, fast and continuously acting automatic voltage regulator (AVR). Voltage and reactive power are being regulated by controlling the excitation current using AVRs. The output of the excitation is controlled by sensing and comparing generator terminal voltage to a reference voltage. A loss of synchronism may be avoided using high gain fast acting AVRs. However, the AVRs introduces negative damping torque to hinder the damping of the power system [75]. However, the EPS is dynamically complicated, which often confront with the changes of operating conditions and disturbances. Therefore, usage of fast acting, high-gain AVRs in modern EPS invites the problem of SSOs. To mitigate the problem of SSOs; a supplementary control action has been employed to an excitation system to add damping torque in phase with rotor speed and is termed as a power system stabilizer (PSS). The art and science of applying PSS have been developed over the past fifty to fifty-five years since the first widespread application to the Western systems of the United States [76-78].

The CPSS design methodology based on eigenvalue analysis reported to use two basic tuning methods such as root locus and phase compensation [76]. The widely accepted phase compensation tuning technique provides phase compensation to provide damping torque. This is the straight-forward, easily understandable and being implemented in the field. It requires the determination of some parameters of each machine in EPS. These are wash-out circuit time constant, DC gain and the time constants of the phase compensator circuit. Much on the sequential and simultaneous approaches to tune these parameters has been reported in literature [79].

Root locus involves shifting of eigenvalue related to the power system modes of oscillation by adjusting stabilizer pole and zero locations in s-plane [76-78]. It gives additional insight to the performance by considering the closed-loop characteristic of the system, contrary to deal with open loop nature in the phase compensation technique, but involve complications in this field. The performance of these controllers is degraded with variations in operating conditions within the

power system. The eigenvalue assignment is too involved in complicated multimachine power systems and may not provide satisfactory performance [20].

An EPS with varying operating condition's results to face uncertainties; therefore, an effective PSS design is always the requirement of the system. The available methodologies for PSSs design for considering these uncertainties are adaptive and robust control. In adaptive control, the parameters of the EPS are determined on-line to design PSS. It involves intensive care to persistent excitation conditions and satisfactory performance during learning phase [80]. However, it is considered during the design of PSS using different adaptive techniques [81-84] and works with enhanced performance. In real large and complex EPS, whose parameters are time varying, an on-line controller for adaptive techniques in which the parameters have to be estimated, may not be easy or may be erroneous, and may result with degraded performance. In real EPS, not all of the states are available for measurement, thus the applicability of these PSS is limited. Robust techniques such as H_∞ [85, 86] and μ-synthesis [87] have been used for PSS design. In H_∞ control the uncertainties in the considered system are extracted and modelled in terms of bounds in frequency response. Such H_∞ controller guarantees the robust stability in a closed-loop system. The extraction of uncertainties in EPS is not easy and sometimes very hard and time consuming in large-scale power systems. It involves an iterative and sophisticated process to design PSS. The problem associated with pole-zero cancellations and choice of weighting functions used for the design of PSS; limits the power engineers to adopt it. It results with very high-order controllers, which may not be feasible to implement [88]. H_∞ involves frequency domain; therefore, it does not provide control action in transient behaviour. On the other hand, the variable structure control is designed to drive the system to a sliding surface on which the error decays to zero [89]. Perfect performance is achieved even if parameter uncertainties are presented. However, such performance is obtained at the cost of high control activities (chattering). Despite the use of boundary layer to reduce the chattering phenomenon, the design of the switching signal remains unresolved. An approximation of the sliding gain by an adaptive fuzzy system to eliminate the chattering phenomenon without requiring any particular knowledge about the upper bounds of both approximation errors and external disturbances have been suggested in literature. However, the global stability of the closed-loop system in these approaches is guaranteed only for a good approximation level or for a particular choice of the initial values of the adjustable parameters [90].

The PSS design using above techniques needs to have state-space or transfer function model of the EPS, but for large and complex systems, linearized model is very hard to obtain, it leads to invention/adoption of optimization techniques. Gradient based procedure for optimization of CPSS parameters for a wide range of operating conditions had been reported in [91]. It requires

computations of sensitivity factors and eigenvectors at each iteration and resulting rise to heavy computational burden and slow convergence. The search processed likely to be trapped in local minima, and the solution obtained may not be optimal. As the optimization problem with the PSS design reported to be multimodal, i.e. with more than one local optimum. Therefore, local optimization techniques, are unsuitable for PSS design problem [92].

To mitigate above limitations in PSS design, a remarkable attempt to use intelligent optimization techniques is reported in literature [25]. The tuning of PSS parameters can be broadly classified as sequential and simultaneous tuning. In sequential tuning, optimal set of PSS parameters under different operating conditions (OCs) is achieved by repeated tuning and testing of PSS with different OCs of EPS [93, 94]. Design of PSS parameters using the simultaneous tuning process, could be carried out by formulating as a very large-scale nonlinear and non-differentiable optimization problem. It is very difficult to solve such problems using classical differentiable optimization techniques. The sequential design of PSSs is avoided in [2, 95-99] where various methods for simultaneous tuning of PSSs in multimachine power systems are proposed. These techniques are iterative and require heavy computation burden due to system reduction procedure and time-consuming computer codes. To mitigate the above mentioned problems, many random search algorithms have been reported in literature. Recently, intelligent optimization based CPSS design is adopted by many researchers. These are as Tabu search algorithm [2], real coded genetic algorithm (RCGA) [3], genetic algorithm [4], LMI approach [5], particle swarm optimization (PSO) [6], and breeder genetic algorithm (BGA) [7] where in a single-stage lead type PSS is considered. Similarly, the CPSS parameters of double-stage are designed using genetic algorithm (GA) [8], bacteria foraging algorithm (BFA) [8], simulated annealing (SA) [9], robust simulated annealing (RSA) [9], differential evolution (DE) [10] and strength pareto evolutionary algorithms (SPEA) [11]. In these methods, the power system model is considered as single-machine connected to the infinite-bus (SMIB) power system. The use of an optimization algorithm in literature such as particle swarm optimization (PSO) [13], small-population-based particle swarm optimization (SPPSO) [13], bacterial foraging algorithm [13], genetic algorithm (GA) [14, 24], PSO with passive congregation (PSOPC) [14], modified PSO (MPSO) [15], combinatorial discrete and continuous action reinforcement learning automata (CDCARLA) [16], modified artificial immune network (MAINet) [17], multiobjective immune algorithm (MOIA) [17], bacterial foraging optimization algorithm (BFOA) [18], adaptive mutation breeder genetic algorithm (ABGA) [19], strength-pareto evolutionary algorithm (SPEA) [11], differential evolution (DE) [23], fuzzy gravitational search algorithm (FGSA) [26], cultural algorithm (CA) [25], have gained acceptance in CPSS design for multimachine power system because of effectiveness and ability to investigate near-global optimal results for the problem

space. It has been established that the GA is satisfactory in finding the optimal set of solutions, but it often yields revisiting the same sub-optimal set of solutions. It needs a long-run time may be up to several hours depending on the size of the system under investigation. However, these may trap to local minima, slow convergence and hard to optimize problems with epistatic objective function. Fortunately, Yang [100], reported a promising bat algorithm (BA) under the category of meta-heuristic algorithms. It is a search algorithm and based on the echolocation behaviour of Microbats. It has been reported based on benchmark problem studies that the BA is superior to GA and PSO for solving unconstraint optimization problems [100] because these methods fail to solve the multimodal optimization problems. The initialization step in GA and PSO is crucial and affects the final dynamic response of the controlled system. The BA utilizes (i) frequency-tuning technique to enhance the spectrum of the solutions to the population (ii) the automatic zooming for balancing exploitation and exploration during the search process by mimicking the changes of loudness and pulse emission rates of bats when searching for prey. It proves to be very efficient with a typical quick start.

Recently, an artificial intelligence based techniques such as neural networks and fuzzy logic control have been reported in literature [46, 60, 101-108]. Unlike the most conventional methods, an explicit mathematical model of the system dynamics is not required to design a controller using neural networks and/ or fuzzy logic systems. Artificial neural network (ANN) has gained popularity in the design of PSS because of its extremely fast processing facility and to cope with nonlinear mapping from input to output space. The application of neural networks to the PSS design includes online tuning of conventional PSS parameters, the implementation of inverse mode control, direct control, and indirect adaptive control [109-111]. Performance reported by ANN based PSS is to stabilize power systems is satisfactory over the wider spectrum of operating conditions, but it suffers with long training time, selection of layers and the selection of the number of neurons in a layer.

Fuzzy logic controllers (FLCs) have attracted considerable attention because of the variety of the advantages they offer over the conventional computational systems [103, 104]. The FLCs have a number of advantages in comparison with global nonlinear models, such as neural networks. The structure of FLCs is reported as understandable and sometimes interpretable. Knowledge of power engineers could be integrated with the model, including statistical objects and empirical knowledge [90, 112]. These These are model-free controllers having rapidity and robustness as their most profound and interesting properties in comparison to the other classical schemes [113]. These have been successfully applied to the control of non-linear dynamical systems [36, 43] especially in the field of adaptive control by making use of on-line training. The flexibility and subjectivity of knowledge representation are a distinct feature of fuzzy logic, which

allows the technique to be a notable candidate for PSS design, as reported in [106]. An FLC designed with appropriate membership functions works like a PD or PID controller with variable gains. The equivalence between the scaling factor of a fuzzy controller and linear PID controller coefficients is examined in [114]. FLCs are reported to provide superior performance in terms of nonlinear control because of the variable gains [114]. In the design of fuzzy logic based PSS (FPSS), it is necessary to define membership functions for all of the input and output variables of the controller. Moreover, a rule table should be selected to relate the input and output variables to each other. The control rule table and membership functions are chosen by the time consuming trial and error procedure. To overcome this drawback, some researchers have designed the FPSS with the aid of searching algorithms such as genetic algorithms, particle swarm optimisation, bacteria foraging optimisation, the chaotic optimisation algorithms and so forth [65, 113, 115-123]. However, optimum tuning of FPSS parameters using heuristic optimization techniques is further required for better performance under a wide range of OCs. The generation of membership functions, selection of scaling factors, selection of input signals, fuzzification and defuzzification methods and "if – then" based rule generation have been done either by trial-and-error, iteratively or by human experts. Therefore, it becomes the time-consuming and laborious task to design FPSS[124].

Zadeh in 1975 [125] have generalized the concept of ordinary fuzzy systems as reported [126], and termed as Type-2 (T2) fuzzy systems to handle uncertainties involved in type-1 fuzzy logic systems. Mendel et al. [127, 128], extend this concept and explore many aspects of type-2 fuzzy sets and systems. The reported four possible sources of uncertainty present in type-1 fuzzy logic systems are (1) the antecedents and consequents of rules can be uncertain because linguistic terms mean different things to different people, (2) consequents may have a set of values associated with them, especially when knowledge is extracted from a group of experts, who do not agree at all, (3) measurements that activate a type -1 fuzzy logic system may be noisy and, therefore, uncertain and (4) the data that are used to tune the parameters of a type -1 fuzzy logic system may also be noisy. Recent research reported the limitations of traditional type-1 fuzzy logic theory in treating large uncertainty factors due to unexpected severe faults on the power system [129]. Application of type-2 fuzzy logic in various fields shows compensation to the limitations with type-1 fuzzy logic [128, 130, 131]. Castillo et al. have proposed GA and PSO optimized type-2 fuzzy logic controllers and demonstrated better performance as compared to type-1 controllers [132-135].Type-2 fuzzy logic is computationally intensive because its inference and type reduction are very intensive. Type-2 fuzzy set can be converted to interval type-2 by considering secondary memberships equal to zero or one [136]. Because of such a better performance and applicability, interval type-2 fuzzy logic may be considered for PSS design.

In this chapter, a review on heuristic optimization and artificial intelligent control techniques has been considered for design of optimal PSS as reported in literature and included in section 1.1. A brief review on modern heuristic optimization techniques has been discussed in section 1.2. These are harmony search algorithm and bat algorithm would be used in design of PSS parameters in this thesis. Section 1.3, elaborates the different objective functions used by different researchers in literature. The detail on performance indices to compare the system responses has been included in section 1.4. The section 1.5 includes the detail on objectives considered in this thesis. Mathematical modelling of single-machine connected to an infinite bus is given in section 1.6. The Heffron-Phillip constants are mathematically derived in section 1.7. The state space representation of the SMIB power system is incorporated in section 1.8 and extended to multimachine power system in section 1.9. The outline of the thesis is included in section 1.10 and followed by the conclusion in section 1.11.

1.1. Literature Review on PSS Design Techniques

Over the last five decades, a large number of research papers have appeared over the area of the power system stabilizer (PSS). Research has been directed towards obtaining such a PSS that can provide an optimal performance for a wide range of machine and system parameters. In the design of PSS, several techniques have been investigated and introduced time to time, but every method has its limitation. Various control strategies and optimization techniques have found their applications in this area as also various degrees of system modelling have been attempted. It is difficult to bring out a detailed discussion of the historical development of PSS and its applications; therefore, a modest attempt has been made in this section to discuss the most significant works in the area of the thesis.

1.1.1. Heuristic optimization techniques

Abido and Abdel-Magid, 1999 [2] have proposed the design of excitation system and static phase shifter (SPS) for small signal stability enhancement. An eigenvalue-based objective function to maximize the damping ratio has been considered to formulate the design problem of excitation with lead-lag type PSS and SPS controllers using tabu search (TS) algorithm. It has been presented that although excitation control enhances the power system stability; the SPS controller provides enhanced voltage profile for the SMIB power system.

The application of TS in multimachine scenario has been examined by Abido and Abdel-Magid, 2002 [20]. The problem of optimization of CPSS parameters for three-machine nine-bus and New England power system was formulated with shifting of eigenvalue to the left of s-plane.

The performance evaluation of designed PSSs had been considered under different disturbances and loading conditions. The effectiveness had been validated to damp out the inter area and intra area modes using nonlinear simulations and eigenvalue analysis.

Simulated annealing (SA) have been well explored by Abido in 1999 [137] for tuning of parameters of CPSS connected to the SMIB power system. The problem of optimization has been considered as maximization of damping ratio to determine optimal setting of stabilizer parameters. The performance is evaluated by applying a 6-cycle three-phase fault at the infinite bus. The first swing in the torque angle and the terminal voltage has been greatly improved.

In [138], the SA had been considered to determine optimal setting of CPSS parameters in a three-machine and New England power system. The problem of optimization has been considered simultaneous shifting of electromechanical modes (EMOs) in the left of s-plane. The application of SA in optimization has greatly reduced the computation burden without an initial guess of the solutions.

Abido, 2000 [139] have applied SA to search optimal setting of CPSS and TCSC based stabilizer parameters using a pole-placement objective function to shift dominant EMOs to the left of s-plane. The effectiveness and robustness of the stabilizers have been evaluated for efficient damping using eigenvalue and nonlinear simulations under different disturbances and parameter variations.

Abido and Abdel-Magid, 2002 [13] have presented the PSSs design for New England 39-bus power system using evolutionary programming (EP) optimization technique. The problem of parameter setting has been formulated with an objective function such as to shift the eigenvalue associated with the electromechanical modes to be left of s-plane. The performance of the proposed PSSs under different disturbances, loading conditions, and system configurations have been investigated in terms of eigenvalue analysis and the nonlinear simulation results and concluded to as outperforming to the performance with CPSS[140].

Abdel-Magid et al., 1997 [141] have proposed a genetic algorithm (GA) based simultaneous tuning of stabilizers for a wide range of operating conditions with a single-machine system. The effectiveness was validated using eigenvalue analysis and simultaneous plotting on the s-plane. The approach of simultaneous stabilization of PSSs using GA was extended to multimachine systems in [142]. The GA based problem formulation with ISE, and ITAE based objective function for optimal setting of PSS parameters has been proposed in [143].

Abido and Abdel-Magid, 1998 [4] have proposed a genetic algorithm (GA) based optimized CPSS using a simple objective function that reflects small steady-state errors and overshoots and termed as integral of square of time weighted error. The performance of optimized

PSS has found to be outperforming as compared with conventional PSS on a single-machine infinite-bus power system under different loading conditions.

The application of GA to optimal selection of CPSS parameters in ten-machine scenario was proposed by Abdel-Magid and Abido, 2003 [24]. The problem of optimization is formulated with three different objective functions as minimization of damping factor, maximization of damping ratio and the combination of these two with a prespecified region in s-plane. The stabilizer parameters have been selected by simultaneously shifting of lightly damped EMOs to a defined zone in s-plane. The system performance with these (three optimal sets of CPSS parameters) stabilizers have been compared. The performance with stabilizers tuned with the combination of two; it reported to be outperforming to its counterparts.

Eslami et al., 2013 [144] have employed Genetic algorithm (GA) optimization method for optimal design of the power system stabilizer (PSS). The problem of optimization is formulated as multiobjective as to increase damping factor, damping ratio and the sum of both to tune CPSS parameters for two-area four-machine power system. The eigenvalue analysis and non-linear simulation results are presented and compared to show the effectiveness to enhance power system stability.

Phiri and Folly, 2008 [145] have proposed a relatively new variant of GA based on survival of the fittest; termed as breeder genetic algorithm (BGA), in this field. They reported that the performance with BGA-PSS is better than that of the GA-PSS and CPSS based on simulation results with an SMIB power system. BGA was again explored for optimal setting of CPSS parameters in [7]. Sheetekela et al. 2010 [7] have formulated the problem of optimization PSS parameters using BGA under maximization of minimum damping ratio as an objective function. Again, the performance reported as best in comparison to GA-CPSS and CPSS on an SMIB power system. It had been reported to be the optimum performer as compared to population-based incremental learning (PBIL) algorithms based CPSS in [146, 147].

Mary-Linda and Kesavan-Nair, 2013 [19] have proposed BGA with Adaptive Mutation (ABGA) to tune the parameters of CPSS. The problem of optimization has been formulated as shifting of EMOSs as maximization of minimum damping ratio for three power systems viz. 3-machine 9-bus, two-area four-machine and New England power system. The ABGA based CPSSs have been reported as the better performer as compared to GA based CPSSs in all three power systems.

Abido and Abdel-Magid, 2004 [3] have proposed excitation and FACTS based PSS for stability enhancement. The PSS parameters have been optimized using real coded genetic algorithm (RCGA) with increasing the damping factor as an objective function. The proposed stabilizers have been applied to a weakly connected power system with different loading

conditions. The eigenvalue analysis and nonlinear simulation results have reported the effectiveness and robustness of the proposed stabilizers to enhance the system stability.

Duman and Öztürk, 2010 [30] have considered RCGA to tune parameters of PID based PSS on SMIB power system. They have used integral absolute error (IAE) and integral squared error (ISE) performance indices as an objective function. They reported better performance with ISE based RCGA-PID as compared to IAE based RCGA-PID and CPSS based on simulation results over a wide range of operating conditions within the power system.

The application of RCGA in the design of optimal setting of PSS parameters was reported in [148]. Falehi, 2013 has considered RCGA and particle swarm optimization (PSO) as optimization tools for determining optimal settings of PSS in single-machine and multimachine scenario under ITAE as an objective function. The simulation results have been reported to be same with RCGA and PSO based PSS.

Abido, 2001[22, 149] have introduced the application of particle swarm optimization (PSO) in optimal setting of PSS parameters. The problem of optimization of PSS parameters in multimachine scenario has been carried out with two eigenvalue-based objective functions for enhancing damping to the system. The performance with PSO-PSS has been examined over three-machine and ten-machine power systems. The performance with PSO-PSS, based on simulation results and eigenvalue analysis, reported to be better as compared to GA-PSS and gradient based CPSS.

Soliman et al., 2008 [6] have used PSO for optimal design of CPSS parameters of an SMIB power system under different loading conditions. The concept or objective function is based on minimization of maximum overshoot of the speed response to alleviate generator shaft fatigue.

Das et al., 2008 [13] have introduced small population- based particle swarm optimization (SPPSO) and bacterial foraging algorithm (BFA) to tune the PSS parameters. Both algorithms are used with time domain based objective function in tuning process. The effectiveness of the two algorithms is evaluated and compared for damping the system oscillations during small and large disturbances, and their robustness is illustrated using the transient energy analysis on two area power system. In addition, the computational complexities of the two algorithms have also been presented. The SPPSO with the regeneration concept reported to have faster convergence with fewer numbers of fitness evaluations and algebraic operations. BFA, owing to its unique processes, can find good optimal solutions. The SPPSO, however, have been found to be superior to the BFA and PSO in terms of computational complexity. Simulation results with SPPSO-PSS have been reported as compared against the performance that of with CPSS, PSO-PSS and BFA-PSS.

El-Zonkoly et al., 2009 [65] have proposed the design of PSS using PSO. They have considered CPSS and fuzzy logic based PSS (FPSS) for improving stability of SMIB and two-area four-machine power system. The problem of optimization has been formulated with an eigenvalue based objective function to maximize the damping ratio for tuning CPSS parameters and scale factors of FPSS. It has been reported by simulation results that PSO-FPSS works better as compared to PSO-CPSS for a wide range of operating conditions and system configurations.

Shayeghi et al., 2010 [150] have extended the application of PSO for coordinated design of PSS, and thyristor controlled series capacitor TCSC parameters. The problem has been formulated as optimization using a time domain-based objective function (as ITAE) to determine optimal settings of PSS and TCSC controllers. The effectiveness of the proposed controllers has been validated using simulation results on a four-machine power system.

Eslami et al., 2010 [14] have introduced the application of PSO with passive congregation (PSOPC) to tune the PSS parameters. The combination of maximization of the damping ratio and damping factor as a multiobjective objective function is considered for optimization. The performance of the proposed PSOPC is compared to the SPSO and GA in terms of parameter accuracy and computational time. The PSOPC has been reported, much better optimization technique, in terms of accuracy and convergence, as compared to PSO and GA. Furthermore, nonlinear simulation and eigenvalue analysis results have confirmed the efficiency of the proposed technique.

Eslami et al., 2012 [15] have proposed a modified particle swarm optimization (MPSO) which integrates the PSOPC and the chaotic sequence to tune the parameters of PSS and number of PSS placement in a two-area four-machine power system. The tuning and placement of PSS over a wide range of system configurations have been formulated as a multi-objective function as to maximize the damping ratio and damping factor and the optimal number of PSS. The performance from the system with MPSO has been compared that of with CPSS, GA-PSS, PSO-PSS and PSOPC-PSS through eigenvalue analysis and nonlinear time-domain simulation. It resulted as the best performer as compared to its counter controllers.

The application of PSO with linear matrix inequality (LMI) has been to design PSS for single-machine power system in [151]. Soliman and Mahmoud, 2013, have reported the robustness of PSO-LMI based PSS, against uncertainties wherein power systems operations are changing continuously due to load changes.

G. Kasilingam, 2014 [31] have proposed design of PID type PSS for SMIB power system using PSO. The problem of optimization is formulated by considering time domain based objective function. Such designed PID type PSS performance is examined on the system and compared to conventional tuning method called as Ziegler-Nichols and another tuned PID type

PSS by the trial-and-error method. The superiority is proved by nonlinear simulations over the wide range of the power system as compared with the others designed PID type PSSs.

Kiani et al., 2013 [18] have investigated the Bacterial Foraging Optimization algorithm (BFOA) to design the parameters of the PSS in the two-area four-machine power system. The performance of proposed PSS is compared to the genetic algorithm tuned PSS and found better in damping the inter-area oscillations.

Abd-Elazim and Ali, 2013 [8] have explored Becterial Foreaging optimization algorithm (BFOA) to search optimal controller parameters by minimizing the time-domain objective function as ITAE. The problem of optimization for optimal settings of controllers has been carried out with SMIB and 3-machine 9-bus power system. The performance of systems with BFOA-CPSS has been compared to that of with GA-CPSS, CPSS and without PSS. The performance with BFOA-CPSS has reported to be enhanced as compared to others.

Hameed and Palani, 2013 [28] have proposed a bacterial foraging algorithm (BFA) to tune the PID-PSS for SMIB power system. The performance from a system with BFO-PID-PSS has compared to GA-PID-PSS and CPSS using eigenvalue analysis and nonlinear simulation over a wide range of operating conditions. The performance with BFO-PID-PSS has been reported to be better as compared to others.

Abdul-Ghaffar et al., 2013 [29] have made modification to BFA using benefits of PSO and such hybrid Particle Swarm-Bacteria Foraging Optimization (PSO-BFA) has used to design PID type PSS parameters for SMIB power system to improve damping. The performance of such a designed PID type PSS (PSO-BFA-PID-PSS) has examined and compared the response without PSS and with BFA tuned PID type PSS to establish its effectiveness through simulation study.

Ali and Mehdi, 2013 [152] have designed CPSS parameters using the gravitational search algorithm (GSA) for SMIB power system. The optimization problem has been formulated as the eigenvalue based multi-objective function to improve damping factor and damping ratio and the sum of these two. The performance of the GSA-CPSS has examined over a wide range of operating conditions.

Abido, 2010 [23] have proposed Differential Evolution (DE) technique to search for optimal settings of PSS parameters in New England power system environment. The performance of the proposed DE based PSS (DEPSS) under different disturbances, loading conditions, and system configurations is investigated and examined for different multimachine power systems. The eigenvalue analysis and the nonlinear simulation results show the robustness and the effectiveness of the DEPSSs to damp out the local as well as the inter-area modes of oscillations and work effectively over a wide range of loading conditions. The performance is compared to performance without PSS, with PSO-PSSs [22] and with GA-PSSs[142].

Mulumba and Folly, 2011 [153] have considered DE and BGA as optimization techniques for the optimal setting of CPSSs in a four-machine system. Based on simulation results, they have reported better performance with DE-CPSS as compared to BGA-CPSS.

Tripathi and Panda, 2011 [10] have explored the application of Differential Evolution (DE) as an optimization algorithm to tune the PSS parameters with time domain based fitness function as in [8]. The enhanced performance with DE-CPSS has been validated by simultaion study of an SMIB power system over a wide range of operating and system conditions and compared without controller and with CPSS.

Yassami et al., 2010 [11] have presented the application of Strength Pareto approach in tuning parameters of CPSS. They have presented multi-objective optimization by considering maximization of the damping factor and the damping ratio of power system modes as two different objective functions for designing the PSS parameters. The proposed approach is implemented and examined in the system comprising an SMIB, four-machine and ten-machine power system. The performance with SPEA-CPSS has reported to be better as compared against the performance with GA-CPSS.

Shayeghi and Ghasemi, 2014 [154] have proposed the Parallel Vector Evaluated Improved Honey Bee Mating Optimization (VEIHBMO) as a novel multi objective technique to obtain a set of optimal PSSs parameters for four-machine and 16-machine five-area power system under different loading conditions. The objectives considered throughout this paper are the time domain based integral square time of square error (ISTSE), and eigenvalue based comprising the damping factor. The effectiveness of the proposed method is demonstrated through the time multiplied absolute value of the error (ITAE), eigenvalue and figure of demerit (FD) analysis performance indices. The performance of the VEIHBMO based CPSS with different objective functions is compared with the BFA based CPSS [13] and CPSS; It resulted in superior performance.

Kashki et al., 2010 [16] have introtuced a novel Combinatorial Discrete and Continuous Action Reinforcement Learning Automata (CDCARLA) based approach for optimal design PSS parameters for two-area four-machine power system. The proposed CDCARLA based design approach reported to a combined procedure into two optimization stages in discrete and continuous spaces for fast convergence and high optimization efficiency. The performance of such a designed PSSs has been evaluated under different power system disturbances and compared with other stabilizers reported throughout the literature, including the multi-band PSSs for a two-area four-machine power system. The effectiveness and robustness of the proposed CDCARLA-PSS in damping local and inter-area oscillation modes and confirmed its better performance in comparison with CPSSs.

Khaleghi et al., 2011 [17] have presented two approaches for multiobjective simultaneous coordinated tuning of damping controllers, a modified artificial immune network (MAINet) algorithm and a multiobjective immune algorithm (MOIA). The weighted-sum approach in the MAINet and the Pareto-optimization approach have been used in the MOIA. The performance of such a designed MAINet and MOIA based PSS has been compared by simulation study with a two-area four-machine power system and reported to be more effective with MOIA as compared to MAINet.

Khodabakhshian and Hemmati, 2013 [25] have employed cultural algorithms (CAs) to tune the PSS parameters for New England power system. The effective and robustness of the performance with CA-CPSSs have reported through nonlinear simulation results as compared with a GA based PSSs.

Linda and Nair, 2012 [35] have proposed a multi-objective design of CPSS for the New England Power System using Ant Colony Optimization (ACO). The outcomes of the proposed ACOPSS are compared with the Conventional PSS, Genetic Local Search-based PSS, Chaotic Optimization-based PSS and PSO-CPSS. From the simulation results it can be inferred that the ACOPSS reduces the settling time, and maximum overshoot more than the other techniques.

Ghasemi, Shayeghi and Alkhatib, 2013 [26] have proposed a novel Fuzzy Gravitational Search Algorithm (FGSA) for optimal design of multimachine power system stabilizers (PSSs). They have formulated as an optimization problem within the time-domain based objective function over a wide range of operating conditions and solved by the proposed FGSA technique. The performance of FGSA-PSS design has been carried out with a 3-machine 9-bus system and a 10-machine 39-bus power system. The effectiveness and robustness of proposed method have been demonstrated using many performance indices. They established the effectiveness of the performance with FGSA-PSSs over SPEA-PSSs and CPSSs via nonlinear simulations.

Hameed and Palani, 2014 [27] have proposed Harmony search algorithm (HSA) to tune proportional integral derivative type PSS (PID-PSS) parameters. The performance of such HSA tuned PID-PSS is comapared with CPSS, and GA based PID-PSS and reported with better performance in nonlinear simulation results on an SMIB power system.

Theja et al., 2013 [32] have proposed the design of PID type PSS for SMIB power system using the Ant Bee Colony (ABC) optimization algorithm. The ABC algorithm is used to tune the PID type PSS and CPSS parameters and performance is compared. The superior performance of PID type, ABC tuned PSS is compared with the ABC tuned CPSS and found better in terms of settling time of the speed response.

Karthikeyan and Lakshmi, 2012 [33] have proposed biogeographical based optimization algorithm to tune the PID based PSS parameters for SMIB power system. The problem of

optimzation has been formulated as a sum of ISE and ITAE error reduction of speed error. They tuned the CPSS parameters, and PID based PSS using the BBO. The performance with BBO-PID-PSS has been reported to be better as compared that of with BBO-CPSS and CPSS through nonlinear simulations over the wide range of operating conditions of the power system.

1.1.2. Artificial intelligent techniques

Artificial Intelligence (AI) techniques have been emerged as very effective and powerful tools in the field of designing PSS. It could be more effective when properly joined together with conventional mathematical approaches [155-157]. The AI techniques have been classified as Fuzzy logic, Artificial Neural Network (ANN), hybrid artificial intelligent techniques and expert system. Several designed PSSs have been reported in literature using these AI techniques. The serious attempt is made to present a comprehensive analysis of fuzzy logic control for designing PSS, which has been proposed by researchers recently.

1.1.2.1. Artificial neural network

ANN is a mathematical or computational model which mimics the biological neural networks. It consists numerous nodes (neurons) which are connected to form one or multiple layers in the network. The connections between neurons are weights that needed to be trained. Connections from one layer back to a previous layer, and connections between neurons in the same layer are called feedback connections. The Neural Networks (NNs) have been classified as (i) feed forwarded network, it does have any loop, therefore, the information moves through layers to the forward direction and (ii) a recurrent NN is a network that has more than one cycle.

ANN has been reported with two distinct properties such as (i) fast processing capability, and (ii) realization of nonlinear mapping from input to output space. The application of NN to PSS design includes online tuning of conventional PSS parameters, direct and indirect-adaptive control and inverse mode control [109, 110]. Nearest to this work was the design of an indirect-adaptive neural network based PSS by Liu and his co-workers in [158] and by Shamsollahi and Malik in [159]. In [159, 160], the authors mitigated the effect of the trapped delay lines in the controller structure by incorporating a neuro-identifier to identify the plant in real-time and a neuro-controller to damp the power system oscillations. The layered and multi-layer feed-forward NN as in [161] and [101, 102] respectively have been reported in literature. Yilmaz et al. [162] have proposed back propagation NN to seek for strong correlation between the state variables. In addition, while one radial basis function (RBF) network has been used in PSS design in [163-165]; two recurrent ones were employed in [163].

1.1.2.2. Fuzzy logic systems

The fuzzy logic concept was introduced by Zadeh in 1965. The concept was derived from fuzzy set theory. It allows an infinite number of membership functions, and the degree of membership function is represented by a number between 0 and 1.

The conventional controllers are designed to a linearized model of a power system around an operating point. The control laws are derived the linearized system and accordingly the controller is designed. Fuzzy logic controller (FLC) is nonlinear in nature and does not need a mathematical model of the system. It is immune to parameter variation of the controlled system. Human experience and expertise can be used in the design of the fuzzy controller.

The main component of FLC is its rule-base. The control action is defined by the rules in rule-base and is written in natural language. In FLC, the crisp signal value is converted to fuzzy sets using fuzzyfication process with appropriate membership function. The knowledge-base consists of membership function and necessary rules, which in turn are used to derive the control laws. The inference engine processes the proper control action based on the rules designed by engineers. The results of an inference process depend on the method such as the max-minimum, etc. The last stage of FLC is called defuzzyfication, where in the fuzzy value is converted to crisp value based on a defuzzification method and commonly used method is 'centroid'.

El-Sherbiny et al. [164] have reported design of a controller based on the state feedback control systems. The control signal to excitation consists a fuzzy controller and a conventional PI controller output signal. The efficacy of the fuzzy controller is tested for both heavy and light load conditions as compared to conventional PSS. The further extension to study is presented in [165]. It presents two linear PSSs design based on the frequency-domain method to accommodate above conditions. The single stabilizing signal is developed by fuzzy reasoning in such a way that the signal matches the operating condition optimally.

Hossein-Zadeh and Kalam [166] reported an indirect adaptive fuzzy PSS based on fuzzy basis function. The power system was represented by two unknown nonlinear differential equations with some known linguistic information. Two fuzzy logic systems developed, and the respective controllers have been designed with adaptive law using Lyapunov's synthesis method.

Elshafei et al. [167] have presented a fuzzy PSS with adaptively tuning of fuzzy rule base online. Rule base is updated using variable structure adaptive algorithm with predefined control objectives. It significantly reduces the size of rule base and improves performance as compared to non-adaptive FPSS. The online adaptive tuning based FPSS is considered for SMIB and multimachine power system.

Mitra et al. [168] reported an FPSS with new input signals as deviation in active power and change in speed. It reported better performance as compared to CPSS and FPSS with speed

deviation and acceleration as input signals. It reported reduced cost and scanning time during the approach because the same signal can be fed to each of the FPSSs. A new global tuning technique based on minimization of a multiextremal black-box function over a multidimensional hyperinterval for multi-machine power system in order to damp the power system oscillations [54]. It is based on an iterative adaptive efficient partition algorithm and found the optimal global solution faster than a genetic algorithm (GA).

Soliman et al. [169] have reported a model-based FPSS that guarantees stability and performance of the system. It presented a linear matrix inequalities (LMI) design of a model-based fuzzy static output-feedback PSS. It guarantees pole-clustering in an acceptable region to cover the wide range of operating conditions of the power system. The capability to damp inter-area oscillations is tested on the two-area four-machine ten-bus power system.

In [54], the problem of global tuning of FPSSs in the four-machine ten-bus power system has been considered. The problem has been formulated as a global minimization of a multiextremal black-box function over a multidimensional hyper interval. On each evaluation, the objective function is connected to a sophisticated simulation which in turn results to a high computational burden. In iterative adaptive efficient partition algorithm (EPA) as reported technique, the search hyper interval is partitioned into smaller ones, and the objective function is evaluated only at two vertices corresponding to the main diagonal of the generated hyper intervals, thus avoiding unnecessary cumbersome simulations. The performance of the system with proposed tuned FPSS (TFPSS) is compared to the base FPSS (BFPSS), and the CPSS considered in [170]. The ISE performance of the system response has been calculated with TFPSS, BFPSS and CPSS and reported as 179, 191 and 213, respectively.

In [41], a topology of rule reduction of a symmetrical rule base is proposed. The IAE performance index of the response on SMIB system was reported to be with FPSS and with simplified FPSS in the range of 1.18 - 1.59 for a wide range of operating conditions.

In [40], a self-tuned fuzzy logic power system stabilizer (STFPSS) is designed, where in the self-tuning technique consists of the simple fuzzy logic controller (FPSS) and a fuzzy tuner (FT). The fuzzy tuner is used to non-linearly modify the on-line the sensitivity of the simple fuzzy logic controller to its input variable, which indirectly changes the relative sensitivity of areas of associated input membership functions. The performance of the STFPSS is compared to that of with FPSS and CPSS. The performance in terms of IAE with STFPSS, FPSS and CPSS has been reported in the range of 8.48 - 48.56, 8.66 - 50.79 and 9.28 - 54.88 for a wide range of SMIB operating conditions and system configuration.

In [171], a robust adaptive fuzzy controller as a power system stabilizer (RFPSS) has been proposed for four-machine system and used to damp inter-area modes of oscillation following

disturbances in power systems. It has been proved to be a better performer as compared to the IEEE multi-band power system stabilizer (MB-PSS). The performance index as ISE has been reported with both controllers. The value of ISE with RFPSS is addressed as 10-20% of the value as that of with IEEE MB-PSS. However, the range of ISE with RFPSS is ranging in 100s to 1000s, which is a very higher value and needs to be analyzed for improved.

In [172], indirect adaptive fuzzy sliding mode PSS (AFSMPSS) for four-machine system is presented. The performance of the system equipped with AFSMPSS is compared that of with FPSS, AFPSS and CPSS[173]. The ITAE type performance index of the system response when equipped with AFSMPSS, AFPSS, FPSS and CPSS are reported as 0.38032, 0.5524, 0.82547 and 0.93253, respectively under 3-phase fault condition.

In [174], an indirect adaptive fuzzy based power system stabilizer (AFPSS) has been designed to damp inter-area modes of oscillation following disturbances in four-machine power systems. The performance of AFPSS is compared to the IEEE standard multi-band power system stabilizer (MB-PSS) and to be better in performance at different operating points of the power system. The performance index (ISE) of the speed response of generators equipped with proposed AFPSS and that of with MB-PSS have been reported in the range of 22-790 and 100-2460, respectively.

In [113], bacterial foraging optimization (BFO) and genetic algorithm (GA) are utilized to tune the parameters of both single input and dual-input power system stabilizers (PSSs). The performance with BFO as compared to that of with either genetic algorithm is reported to be more effective than the others in finding the optimal transient performance of a PSS equipped on SMIB system. The parameters of CPSS and the three dual-input PSSs (PSS2B, PSS3B, and PSS4B) [175] have been optimally tuned and revealed that the transient performance with dual-input PSS is better than single-input PSS. The PSS3B offers superior performance among dual-input PSSs under subject. The off-nominal operating conditions based on-line has been determined using Takagi Sugeno fuzzy logic (SFL). The BFO based PSSs outperforms GA and the minimum value of damping ratio with CPSS, PSS2B, PSS3B and PSS4B have been reported as 0.38, 0.49, 0.72 and 0.37, respectively with system configuration. In [119], chaotic ant swarm optimization (CASO) is utilized to tune the parameters of both single input and dual-input power system stabilizers (PSSs) as in [113]. This algorithm explores the chaotic and self-organization behaviour of ants in the foraging process. A novel concept, like craziness, is introduced in the CASO to achieve improved performance of the algorithm. The performance with CASO as compared to that of with genetic algorithm is reported to be more effective than the others in finding the optimal transient performance of a PSS equipped on SMIB system. The performance of these PSS tuned with CASO and GA is comparCASO,n terms of damping ratio. CASO based PSSs outperforms

GA and the minimum value of damping ratio with CPSS, PSS2B, PSS3B and PSS4B have been reported as 0.41, 0.69, 0.79 and 0.72, respectively. It could be easy to reveal that the CASO based performance is better as compared to BFO and GA. It has been reported that the use of MB three-stage CPSSs, increases the size of a system in online tuning process, which results to increase in computational burden and complexity to a system.

1.2. Modern Heuristic Optimization Techniques

1.2.1. Harmony search algorithm

This algorithm is an evolutionary meta-heuristic which is inspired by a natural phenomenon. It is inspired by the method used by musicians to improvise new optimal harmonies. In this algorithm, an analogy in between optimization and improvisation has been designed such that to mimic the process used by musicians to get the note that results to a finest pleasing harmony, whenever, musicians are synchronized with other musicians [176, 177]. Each row of HM, consists of N decision variables and the fitness score w ($[x^1, x^2 \ldots w]$). The HM is initialized with HMS randomly generated solution vectors [178, 179].

Step 1: Initialization Process: Let in an optimization problem, the objective function is represented by Minimization of $F(x)$ which is subjected to $x_i \in X_i$, $i=1, 2, 3 \ldots N$. Where, x is the set of design variables (x_i), ($x_i^L \le x_i \le x_i^U$), and N is the count of design variables.

1. Define the variable limits as lower (x_i^L) and upper (x_i^U) or $x_i^L \le x_i \le x_i^U$.
2. Deciding the value of harmony memory size (HMS), from the range $10 \le \text{HMS} \le 100$.
3. Decide value of HMCR (harmony memory consideration rate) within the range $0.0 \le \text{HMCR} \le 1.0$.

$$x_1^{'} \leftarrow \begin{cases} x_i^{'} \quad l\{x_i^1, x_i^2, \cdots, x_i^{HMS} \ with\ probability\ HMCR \\ x_i^{'} \in X_i \quad with\ probability\ (1-HMCR) \end{cases} \tag{1.1}$$

4. Decide the value of PAR (pitch adjustment rate) from the range $0.0 \le PAR \le 1.0$

$$x_j^i = x_j^L + rand(0,1)(x_j^U - x_j^L) \tag{1.2}$$

$$x'_i \leftarrow \begin{cases} yes \quad with\ probability\ PAR \\ no \quad with\ probability\ (1-PAR) \end{cases} \tag{1.3}$$

5. Compute the step size (b_i) as $b(i) = (x_i^U - x_i^L)/N$

6. Specify the maximum limit of iteration number.

Step 2: HM Initiation: The HM matrix as in Eqn. (1.4)[180] is filled with randomly generated possible solution vectors for HMS and is sorted by the values of the objective function f(x).

$$HM = \begin{bmatrix} x_1^1 & x_2^1 & \cdots & x_{N-1}^1 & x_N^1 \\ x_1^2 & x_2^2 & \cdots & x_{N-1}^2 & x_N^2 \\ \vdots & \vdots & \vdots & \vdots & \vdots \\ x_1^{HMS-1} & x_2^{HMS-1} & \cdots & x_{N-1}^{HMS-1} & x_N^{HMS-1} \\ x_1^{HMS} & x_2^{HMS} & \cdots & x_{N-1}^{HMS} & x_N^{HMS} \end{bmatrix} \Rightarrow \begin{bmatrix} f(x^1) \\ f(x^2) \\ \vdots \\ f(x^{HMS-1}) \\ f(x^{HMS}) \end{bmatrix} \quad (1.4)$$

Step 3: Improvisation Process: A New Harmony vector $x' = (x_x', x_2', \cdots, x_n')$ is generated based on three criteria: random selection, memory consideration, and pitch adjustment.

Random Selection: To decide the value of x'_1 for the New Harmony $x' = (x'_1, x'_2, ..., x'_n)$, the HS algorithm randomly selects a value from range with a probability of "*1 - HMCR*".

Memory Consideration: To decide the value of x'_1, the HS algorithm randomly selects a value x_1^j from the HM with a probability of "*HMCR*", where *j = 1, 2,…, HMS*. It can be represented as in Eqn. (1.4).

Pitch Adjustment: Each element of the New HM vector $x' = (x'_1, x'_2, ..., x'_n)$ is subjected to determine whether it should be pitch-adjusted or not. The selected x'_i is further adjusted by adding an amount to the value with a probability of PAR. The PAR parameter is called the probability of pitch adjustment and is represented by Eqn. (1.3).

The *'no'* with probability *'1 - PAR'* represents that the probability of not adding any amount. On the other hand, if the pitch adjustment decision for x'_i is yes, then x'_i is replaced by $x'_i \leftarrow x'_i \pm bw$; where, *bw* is distance bandwidth in case a continuous variable. The pitch adjustment is performed on every variable of the New HM vector.

Step 4: Updating the HM: Let the HM vector is $x' = (x_x', x_2', \cdots, x_n')$, which is resolved by minimization of objective function is better than the worst harmony present in the HM. Therefore, the New Harmony is inserted into the HM, while, the worst harmony is removed from the HM.

Step 5: Checking the stopping criterion: If the maximum count of improvisations is reached and the stopping criterion as maximum number of iterations is satisfied, then the process of computation is terminated. Otherwise, go to steps 3 and 4 to repeat the process. The HS algorithm is shown in the Figure 1.1 and the Pseudo code is written in the Table 1.1.

Table 1.1: Pseudo code representation for Harmony search algorithm

Minimize F(x), xi∈Xi, i=1,2, ...,N % N=20, Range according to section 1.2.1 in vector form
Initialize HS Parameters as HMS = 60; HMCR =0.9; PAR∈[0.4 0.9]; BW∈[0.0001 0.99], and Max. Iteration =200.
PVB (Parameter range)=[Ki, T1i;...;Ki, T1i]=20×2: % the solution vector is improved by PAR and HMCR parameters
for *(i, j)*
HM =randval(PVB∈HMS,NVAR), % HM filled with solution vectors as in Eqn. 1.4 and sorting by using F(x) // i=1,2,...,HMS and j=1,2,...,NVAR
end *for*
begin
while *(t < tmax) % tmax is the maximum number of iterations*
Improvise a new HM using probability of Memory consideration [HMCR×(1-PAR)], pitch adjustment [HMCR×PAR] and randomization [1-HMCR] as in Eqn. 1.1 and pitch adjusting is carried out using Eqn. 1.3-1.4.
for *(j=0:k)*
if *(r_1<HMCR), then*
$x_j^{new} = x_j^a$ *% a∈(1,2,...,HMS)*
if *(r2<PAR), then*
$$x_j^{new} = x_j^{new} \pm r_3 \times BW \quad \% \quad r_1, r_2, r_3 \in [0,1]$$
end *if*
else
$$x_j^{new} = Para_j^{new} + r \times (Para_j^{\max} - para_j^{\min})$$
end *if*
end *for*
for worst harmony vector (existing) being worse than new harmony vector in HM in terms of OF value as $F(X^{new})<F(X^{worst})$, update HM by new harmony vector and exclude worst harmony vector again sort HM by OF value.
Fhs(t,:)=fmin; save Fhs.mat % store fmin (minimum fitness function value) for each iteration.
Phs(t,:)=best; save Phs.mat % store best (optimized parameters) for each iteration and record cor comparision pupose.
t=t+1; % update i.e. advance the iteration count by 1
end *while*
show last iteration based fmin (minimum function value) and best (optimized parameter value

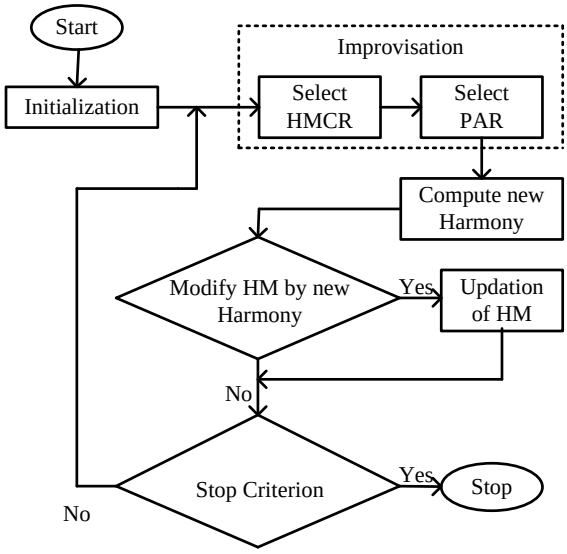

Figure 1.1: Flow chart representation of harmony search algorithm

1.2.2. Bat algorithm

As the bat algorithm is based on the echolocation behaviour of Micro bats [100]. In echolocation, each pulse generated by a micro bat may last only for 8 to 10 milliseconds with a frequency ranging 25 kHz to 150 kHz, which corresponds to the wavelengths of two mm to 14 mm. In BA, the echolocation characteristics of Micro bats can be idealized with the following assumptions.

1. It is assumed that the bats are able to detect distance of prey, background obstacles and difference in the available prey/food in the search path in some magical way using echolocation property.
2. An k^{th} Bat may randomly fly with location as x_k, velocity as v_k, frequency as $f_{\min}$ but with varying wavelength as λ_k and loudness of echo as A^0 to search food/prey. The Micro bats have an ability to adjust frequency (wavelength) of the emitted pulses of echo & rate of pulse emission out of $r \in [0,1]$ according to the distance of their prey/food.
3. The loudness of the echo pulse should be varied as reducing with decreased distance of the food, i.e. from large A^0 to a minimum value $A_{\min}$ (at target/prey location)

Let in an optimization problem; the objective function is represented by Minimization of *F(x)* which is subjected to $x_k \in X_k$, *k = 1, 2, 3 … N.*

Step-1: Initialization

- As an initial step, the bat population is initiated as position x_k and velocity as v_k with *k=1,2,3,…n.*
- Initial pulse frequency is defined as $f_k \in [f_{\min}, f_{\max}]$
- The pulse rates r_k and the loudness A_k are also set as above
- Check number of iterations or $t < T_{max}$

Step-2: Generation of new solutions

- New solutions may be generated by adjusting the pulse frequency and keeping wavelength as constant.
- For each bat (*k*), its position x_k and velocity v_k in a d-dimensional search space should be defined. x_k and v_k should be subsequently updated during the iterations. The new solutions x_k^t and velocities v_k^t at time step 't' can be calculated by:

$$f_k = f_{\min} + (f_{\max} - f_{\min})\beta \tag{1.5}$$

$$v_k^t = v_k^{t-1} + (x_k^{t-1} - x')\, f_k \tag{1.6}$$

$$x_k^t = x_k^{t-1} + v_k^t \tag{1.7}$$

Where, the β is defined for uniform distribution as a vector and selected as $\beta \in [0,1]$. The x' stands as the best location in search space after comparing solutions of all the *n* bats. The product of f_k and λ_k represents the velocity increment. The velocity increment can be adjusted by changing one and keeping fixed another according to a problem. The generally used range of frequency is $0 \leq f \leq 100$ and each bat at initialization step is selected from $f = [f_{\min}, f_{\max}]$.

Step-3: Local Search

Once the best current solution is selected among the available solutions, then a new solution is generated by using local random walk and assigned to each bat as in Eqn. (1.8). If $\varepsilon \in [-1, 1]$ represents a random number range and $A^t = < A_k^t >$ stands for average value of loudness of all initiated *n* bats at time *t*.

$$x_{new} = x_{old} + \varepsilon . A^t \tag{1.8}$$

Step-4: Bat flying & Generation of a new solutions

As the number of iteration increases, the loudness A_k and the rate r_k of pulse emission have to be updated. As a microbat reaches to its target/prey the rate of pulse emission increases while the loudness decreases. The loudness is generally selected from [A^0 , A_{min}] = [1,0]. The A^0 = 1, represents the maximum loudness of emitted pulse by microbat in search of prey, while A_{min} = 0 indicates that the microbat got the target/prey and not emitting any loudness. Thus, the loudness and the rate of pulse emission is updated as.

$$A_k^{t+1} = \alpha A_k^t, \; r_k^{t+1} = r_k^0 \left(1 - e^{-\gamma t}\right) \tag{1.9}$$

Where, α and γ represent the constant values. Here, α is similar to the cooling factor of a cooling schedule in the simulated annealing [181], and the range of these constants is as $0 < \alpha < 1$ and $0 < \gamma$.

$$A_k^t \to 0, \; r_k^t \to r_k^0 \text{ as } t \to \infty \tag{1.10}$$

To make optimization simpler, the value of α and γ should be selected as same, therefore, in this study $\alpha = \gamma = 0.9$. As in Eqn. (1.9) [182], the initial loudness and emission rate may be

represented by A_k^0 and r_k^0, respectively. The value of emission rate at time *t* can be selected from $r_k^0 \in [0, 1]$.

Step 5: Checking the stopping criterion

If the maximum count of iterations is reached as a stopping criterion is satisfied, then the process of computation is terminated. Otherwise, go to steps 3 and 4 to repeat the process. The bat algorithm based conventional power system stabilizer design algorithm is mentioned in Table 1.2, and the flow diagram is presented in Figure 1.2.

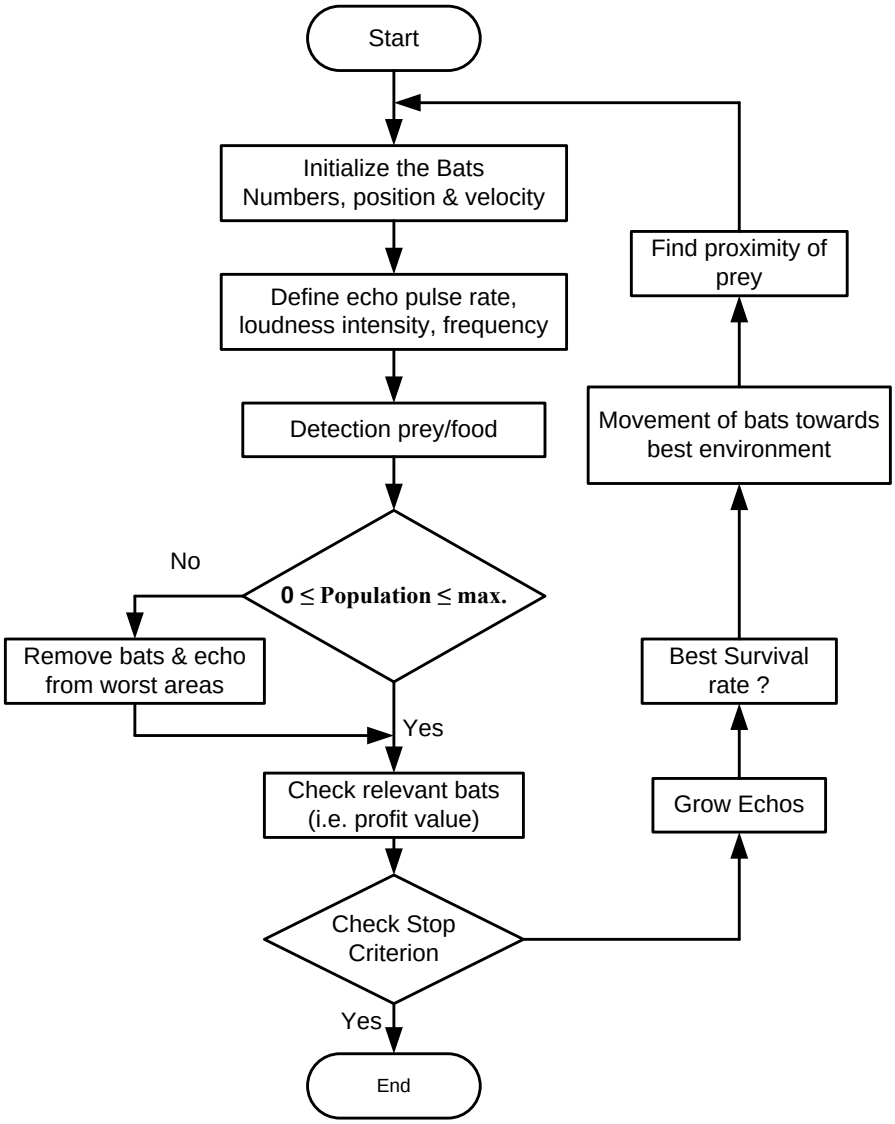

Figure 1.2: Flow chart representation of Bat algorithm

Table 1.2: Pseudo code representation for bat algorithm

Define Objective function f(x), $X=(x_1,x_2, ...,x_d)^T$
Set Initialpopulation of the microbats x_i (i=1, 2, ...,n) and v_i [n=25]
Set the pulse frequency f_i at x_i [f_{min} = 0; f_{max} = 2]
Define lower & upper parameter bound
begin
while *(t < t_{max}) % t_{max} is the maximum number of iterations*
generate new solutions by adjusting frequency and
updating velocities & loudness as in eqn (1.5)-(1.7).
if *(rand > r_i)*
decide & select a best solution among the generated solutions & randomly generate a local solution around the selected best solution by a local random walk as in eqn. (1.5-1.7): F_{new}=f(x),
end *if*
if *(rand < A_i & f(x_i) < f(x_s))*
select the new solutions and increase r_i but reduce A_i
end *if*
rank the bats at each iteration and find their current x_s (best) and minimum objective function value f_{min} corresponding to x_s
Fba(t,:)=f_{min}; save Fba.mat % store f_{min} (minimum fitness function value) for each iteration .
Pba(t,:)=best; save Pba.mat % store best (optimized parameters) for each iteration .
t=t+1; % update i.e. advance the iteration count by 1
end *while*
show last iteration based f_{min} (minimum function value) & best (optimized parameter value

1.3. Review on Objective Functions

The objective function to optimize the parameters of PSS using an optimization algorithm have been designed broadly based on time domain performances and eigenvalue analysis. These objective functions are defined as followings.

1.3.1. Time domain based objective functions

Generally change in speed signal from the generator is sensed and the time-domain based objective functions are designed such as integral of time square weighted squared error (ISTSE) [4, 26, 154], integral of time weighted absolute error (ITAE), integral of squared error (ISE) and integral of absolute error (IAE) . These objective functions generally control the settling time and overshoot of the signal. If the instantaneous change in speed is represented by $\Delta\omega(t)$ and the simulation time is represented by T_{sim} then the time-domain objective functions are introduced in as followings:

1.3.1.1. ISTSE based objective function

In [4, 26, 154], integral square time weighted squared error (ISTSE) based objective function is used of design of PSS and defined as following:

$$J = \int_{t=0}^{T_{sim}} [t\Delta\omega(t)]^2 dt \tag{1.11}$$

1.3.1.2. ITAE based objective function

In [8, 10, 183, 184], an integral of time weighted absolute error (ITAE) based objective function is used to optimize the parameters of PSS as following:

$$J = \int_{t=0}^{t_{sim}} t|\Delta\omega(t)|dt \tag{1.12}$$

1.3.1.3. IAE based objective function

In [30], an integral absolute error based objective function is used and defined as following:

$$J = \int_{t=0}^{T_{sim}} |\Delta\omega(t)|dt \tag{1.13}$$

1.3.1.4. ISE based objective function

In [29, 30, 33, 185], an integral square of error based objective function is used to optimize the parameters of PSS and defined as following:

$$J = \int_{t=0}^{T_{sim}} \Delta\omega(t)^2 dt \tag{1.14}$$

1.3.2. Eigenvalue based objective functions

An eigenvalue analysis of a power system model can be carried out using linmod function in MATLAB Software. An ith eigenvalue is represented as $\lambda_i = \sigma_i + j.\omega_i$, therefore, Real part of λ_i is σ_i and the imaginary is ω_i.

1.3.2.1. Shifting of eigenvalue to the LHS of s-plane

In [2, 22], the maximum value of ith eigenvalue is determined and the objective function is defined as following

$$J = \min(\max(\mathrm{Re}al(\lambda_i))) = \min(\max(\sigma_i)) \quad (1.15)$$

where i corresponds to a set of electromechanical modes. This objective function is subjected to minimization and results as shifting of the eigenvalue to the left-hand side (LHS) of s-plane in order to improve the damping factor and ensure some degree of relative stability.

1.3.2.2. Increase of damping ratio

As the damping ratio to i[th] eigenvalue is defined as $\zeta_i = \frac{-\sigma_i}{\sqrt{\sigma_i^{\,2} + \omega_i^{\,2}}}$, to maximize the lowest damping ratio over a wide range of operating conditions is defined as following [3, 7, 19, 22, 23, 186, 187]:

$$J = \max(\min(\zeta_i)) \quad (1.16)$$

1.3.2.3. Shifting of eigenvalue with threshold to the LHS of s-plane

In [2], the eigenvalue are shifted to left of s-plane without any threshold value, while, in [9, 20, 21, 24], $\sigma_0 = -1$ is a chosen threshold value and the objective function (J) is defined as following

$$J = \sum_{\sigma_i \geq \sigma_0} (\sigma_0 - \sigma_i)^2 \quad (1.17)$$

The value of σ_0 represents the desirable level of system damping. This level can be achieved by shifting the dominant eigenvalue to the left of $s = \sigma_0$ line in the s-plane. This insures some degree of relative stability of the power system. The condition $\sigma_i \geq \sigma_0$ is imposed on J evaluation to consider only the unstable or poorly damped modes which are mainly belonging to the electromechanical ones. The convergence of J in Eqn. (1.17) is able to place the EMOs to the left of a vertical line drawn at σ_0 and is shown in Figure 1.3.

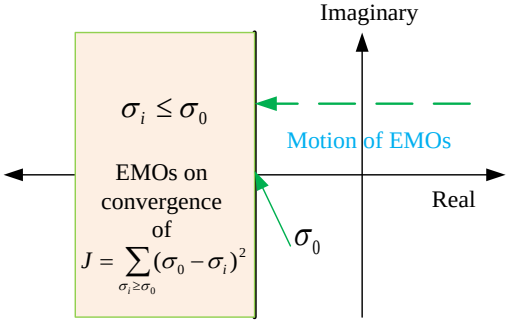

Figure 1.3: Representation for placement of eigenvalue to the left of a vertical line

1.3.2.4. Increasing damping ratio with threshold

In [3, 7, 19, 23, 186], the objective function is designed to increase the damping ratio of the system without any threshold. However, in [24] a threshold value of the damping ratio is introduced as ζ_0 and defined as in Eqn. (1.18), which can place the electromechanical mode eigenvalue in a wedge-shape sector in the left of s-plane as shown in Figure 1.4. The condition $\zeta_i \le \zeta_0$ is imposed on J evaluation to consider only the unstable or poorly damped modes which are mainly belonging to the electromechanical ones. In [65], the value of ζ_0 is selected as 1.0, while it is generally selected within the range of 0.1-0.2 [3, 7, 19, 23, 186].

$$J = \sum_{\zeta_i \le \zeta_0} (\zeta_0 - \zeta_i)^2 \tag{1.18}$$

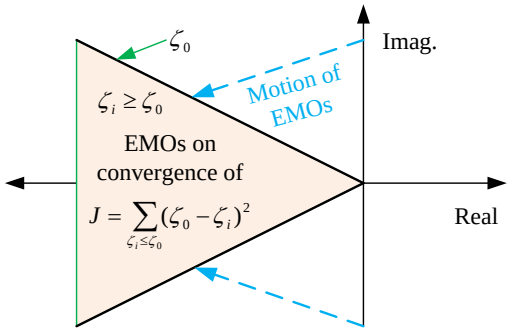

Figure 1.4: Representation for placement of the eigenvalue in a wedge-shape sector in the left of s-plane

1.3.2.5. Damping factor and ratio with threshold: multi-objective approach

In [11, 24, 25, 35, 152, 188, 189], a combination of Eqn. (1.17) and Eqn. (1.18) is carried out to improve both damping factor and damping ratio as following

$$J = J_1 + \alpha . J_2 = \sum_{\sigma_i \ge \sigma_0} (\sigma_0 - \sigma_i)^2 + \alpha . \sum_{\zeta_i \le \zeta_0} (\zeta_0 - \zeta_i)^2 \tag{1.19}$$

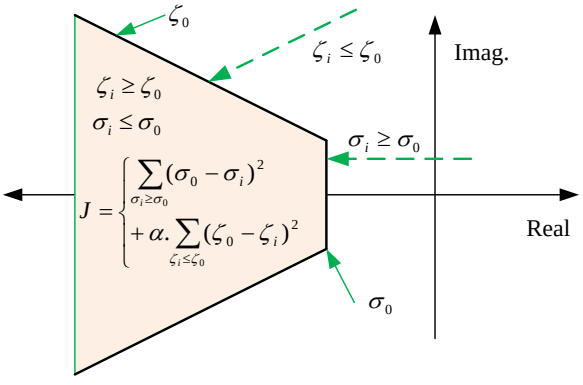

Figure 1.5: Representation for placement of the eigenvalue in a D-shape sector in the left of s-plane

where the value of α is a weight for combining both damping factors and the damping ratios and is considered as 10 [11, 24, 25, 35, 152, 188, 189] but the value of α =1 in [17]. The value of σ_0 determines the relative stability in terms of damping factor margin provided for constraining the placement of eigenvalue during the process of optimization, and the value of ζ_0 is able to shift high-frequency EMOs. The objective function J in Eqn. (1.19) is able to place the electromechanical mode eigenvalue in D-shape sector as shown in Figure 1.5.

1.3.2.6. Weighted sum of damping factor and ratio: multi-objective approach

In [14, 15, 144], the combination of σ_i and ω_i in a different way is used to formulate a multi-objective function. The damping factor σ_i is maximized by considering $J_1 = \min(abs(\sigma_i))$ and the damping ratio is maximized by $J_2 = \min(\zeta_i)$ and the weighted combination of these expressions is considered as multi-objective to place electromechanical mode eigenvalue in D-shape sector on convergence of Eqn. (1.20).

$$J = (J_1 + \alpha . J_2)^{-1} = [\min(abs(\sigma_i)) + \min(\zeta_i)]^{-1} \tag{1.20}$$

1.4. Performance Indices

For completeness and clear perceptiveness about the system response for all the system conditions, three performance indices (PIs) that reflect the settling time and overshoot are introduced. These indices are defined as.

1.4.1. Integral of the time-weighted absolute error

To reduce the contribution of the large initial error to the value of the performance integral, as well as to emphasize errors occurring later in the response. This performance index is designated the integral of time multiplied by absolute error. The performance index ITAE provides the best selectivity of the performance indices; that is, the minimum value of the integral is readily discernible as the system parameters are varied. The speed error corresponding to ith generator, $\Delta\omega_i(t)$ is calculated as the difference between the set point and the output [12, 22, 23, 190].

$$ITAE = \sum_{i=1}^{N} \int_0^{t_{sim}} t \left| \Delta\omega_i(t) \right| dt \tag{1.21}$$

Where t_{sim}; is the simulation time and N refers to the number of generators in power system.

1.4.2. Integral of squared error

Integral square error is an error from an output, squared and added (integrated) over time (in continuous systems) is used to measure system performance in applications to optimal control and estimation. It is used for longer settling time and smaller overshoots as compared to IAE [12, 20, 190] .

$$ISE = \sum_{i=1}^{N} \int_{0}^{t_{sim}} \left|\Delta\omega_i(t)\right|^2 dt \tag{1.22}$$

1.4.3. Integral of absolute error

Integral absolute error is error taken absolute and added over time is used to measure system performance and normal mode control systems. IAE is often used where digital simulation of a system is being employed, but it is inapplicable for analytical work, because the absolute value of an error function is not generally analytic in form. This problem is overcome by the ISE criterion. The ITAE and ITSE have an additional time multiplier of the error function, which emphasizes long-duration errors, and therefore, these criteria are most often applied in systems requiring a fast settling time.

$$IAE = \sum_{i=1}^{N} \int_{0}^{t_{sim}} \left|\Delta\omega_i(t)\right| dt \tag{1.23}$$

where, t_{sim} is the simulation time of the system. Now that large errors penalized by the *ISE* criterion result in the most-aggressive settings and persistent errors penalized by the *ITAE* criterion results in the most-conservative settings, moderate settings are produced between *ISE* and *ITAE* criteria by the *IAE* criterion. It allows larger deviation than ISE [190].

1.5. Main Objectives of Thesis

The main objectives of the proposed research work are as following.

1. Application and comparison of modern heuristic optimization technique in convention PSS design. Performance evaluation of such a designed CPSS in SMIB and multimachine power system scenario.
2. Application of same heuristic optimization technique in the design of PID type PSS for both SMIB and multimachine scenario. Robust performance evaluation and comparison with other techniques.
3. To search and develop an analogy between PD type controller and scaling factors of fuzzy logic based PSS (FPSS). Optimization of scaling factors of FPSS using the heuristic optimization technique in both SMIB and multimachine scenario. To carry

out performance evaluation and comparison of such a designed FPSS with un-tuned FPSS.

4. The application of heuristic optimization technique to tune input-output scaling factors for an FPSS with input signals as speed change, power and output as the voltage signal in both SMIB and multimachine scenario. The performance evaluation and comparison of such a designed FPSS with un-tuned FPSS are carried out.
5. Design of FPSS with a new rule table and comparison of performance in both SMIB and multimachine scenario
6. Design of PSS with newly introduced interval type-2 fuzzy logic in SMIB and multimachine scenario. The performance evaluation and comparison of such a designed interval type-2 FPSS with type-1 based FPSS is carried out.

Comment on performance of these controllers and proving superiority and applicability.

1.6. Modelling of Single-Machine Power System

The phenomenon of small signal or small disturbance stability of a synchronous machine connected to an infinite bus through external reactance has been studied in [75, 191] by means of block diagrams and frequency response analysis. The objective of this analysis is to develop insights into the effects of excitation systems, voltage regulator gain, and stabilizing functions derived from generator speed and working through the voltage reference of the voltage regulator. The analysis based on linearization technique is ideally suitable for investigating problems associated with the small-signal oscillations. In this technique, the characteristics of a power system can be determined through a specific operating point, and the stability of the system is clearly examined by the system eigenvalue.

The following steps have been adopted sequentially to analyze the small-signal stability performance of an SMIB system:

1. The differential equations of the flux-decay model of the synchronous machine are linearized, and a state-space model is constructed considering exciter output E_{fd} as input.
2. From the resulting linearized model, certain constants known as the K constants ($K_1 - K_6$) are derived. They are evaluated by small-perturbation analysis on the fundamental synchronous machine equations and hence are functions of machine and system impedances and operating point.

3. The model so obtained is put in a block diagram form, and a fast-acting exciter between terminal voltage ΔV and exciter output ΔE_{fd} is introduced in the block diagram.
4. The state-space model is then used to examine the eigenvalue and to design supplementary controllers to ensure adequate damping of the dominant modes. The real parts of the electromechanical modes are associated with the damping torque, and the imaginary parts contribute to the synchronizing torque.

1.6.1. Generator dynamics

The single-machine connected to an infinite-bus system is considered as in Figure 1.6 discussed in [75]. For simplicity, we assume a synchronous machine represented by model 1.0, neglecting damper windings both in the d and q axes. It is assumed that the armature resistance of the machine is negligible. The said model is known as the classical model of the synchronous machine. The following assumptions are generally made to analyze the small-signal stability problem in an SMIB power system:

- The mechanical power input remains constant during the period of transient.
- Damping or asynchronous power is negligible.
- Stator resistance is equal to zero.
- The synchronous machine can be represented by a constant voltage source (electrically) behind the transient reactance.
- The mechanical angle of the synchronous machine rotor coincides with the electric phase angle of the voltage behind transient reactance.

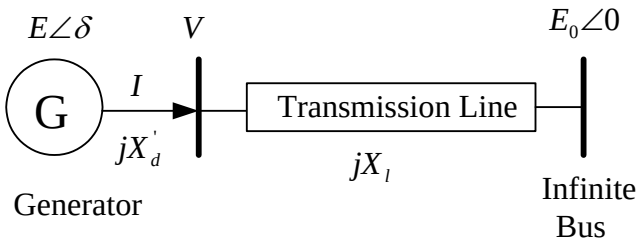

Figure 1.6: Representation of single machine infinite bus power system

The voltage equation

$$E = V_0 + jX_d^{'} I_0 \tag{1.24}$$

where, V_0 and I_0 are pre-fault voltage and current signals

Total reactance of the system

$$jX = jX_d^{'} + jX_l \tag{1.25}$$

Current in the system

$$I = \frac{E\angle\delta - E_0\angle 0^0}{jX} = \frac{E(\cos\delta - j\sin\delta) - E_0}{jX} \tag{1.26}$$

The generated complex power called as the air gap power at the infinite bus is

$$\begin{aligned} S_g &= P_g + jQ_g = E_0\, I^* \\ &= -\frac{|E_0||E|\sin\delta}{|X|} + j\frac{|E|^2 - |E_0||E|\cos\delta}{|X|} \end{aligned} \tag{1.27}$$

For loss less generator, the air gap power is the terminal power of the generator.

$$P_g = \frac{|E||E_0|}{|X|}\sin\delta \tag{1.28}$$

Since, in p.u. system the generated active power P_g is equal to the air gap torque i.e. $T_g = P_g$

$$T_g = P_g = \frac{|E||E_0|}{|X|}\sin\delta \tag{1.29}$$

By linearizing around the operating by taking small perturbation

$$\Delta T_g = \Delta P_g = \frac{|E||E_0|}{|X|}\cos\delta_0\,\Delta\delta \tag{1.30}$$

Now considering the Swing Equation

$$\frac{2H}{\omega_0}\frac{d^2\delta}{dt^2} = P_m - P_e = T_m - T_e \tag{1.31}$$

where, P_m=T_m & P_e=T_e are in p.u. system. Since, the change in P_e is the combination of power due to non-frequency dependent and frequency dependent. The constant in the proportionality is called as damping constant (K_D). Thus, by adding, the damping term proportional to speed in Eqn. (1.30) [191].

$$\frac{2H}{\omega_0}\frac{d^2\delta}{dt^2} = T_m - T - K_D\,\Delta\omega \tag{1.32}$$

Let the angular velocity of rotor is ω_r in rad/sec; then $\delta = \omega_r t - \omega_0 t + \delta_0$ and derivatives $\frac{d\delta}{dt} = \omega_r - \omega_0 = \Delta\omega_r$ and $\frac{d^2\delta}{dt^2} = \omega_r - \omega_0 = \frac{d\Delta\omega_r}{dt}$ and $\omega_r = \omega_0.\omega$, then

$$\frac{d^2\delta}{dt^2} = \frac{d\Delta\omega_r}{dt} = \omega_0\frac{d}{dt}\Delta\omega \tag{1.33}$$

By substituting the value of Eqn. (1.32) in Eqn. (1.33); resulting as following

$$2H\frac{d\Delta\omega}{dt} = T_m - T_e - K_D.\Delta\omega \tag{1.34}$$

$$\frac{d\delta}{dt} = \Delta\omega_r = \omega_0\Delta\omega \tag{1.35}$$

Equation (1.34) and (1.35) are called as rotor dynamic equations. On linearization of Eqn. (1.34) is carried out in Eqn. (1.36).

$$2H\frac{d\Delta\omega}{dt} = \Delta T_m - \Delta T_c - K_D\Delta\omega \tag{1.36}$$

Since, $\Delta T_g = \Delta P_g = \frac{|E||E_0|}{|X|}\cos\delta_0.\Delta\delta = \Delta T_e = T_s.\Delta\delta$; Where $T_s = \frac{|E||E_0|}{|X|}\cos\delta_0$ is called as the synchronizing torque.

$$\dot{\Delta\omega} = \frac{1}{2H}\left(\Delta T_m - T_s\Delta\delta - K_D\Delta\omega\right) \tag{1.37}$$

$$\dot{\delta} = \Delta\omega_r = \omega_0\Delta\omega \tag{1.38}$$

Equation (1.37) and (1.38) are called as the differential equations for rotor dynamics. State Space (SS) Model of rotor dynamics of the synchronous generator is shown in Eqn. (1.39).

$$\begin{bmatrix}\Delta\dot{\omega}\\ \Delta\dot{\delta}\end{bmatrix} = \begin{bmatrix}-\frac{K_D}{2H} & -\frac{T_s}{2H}\\ \omega_0 & 0\end{bmatrix}\begin{bmatrix}\Delta\omega\\ \Delta\delta\end{bmatrix} + \begin{bmatrix}\frac{1}{2H}\\ 0\end{bmatrix}\Delta T_m \tag{1.39}$$

Block Diagram representation from Eqn. (1.37) and Eqn. (1.38) or from SS model in Eqn. (1.39) is shown in Figure 1.7.

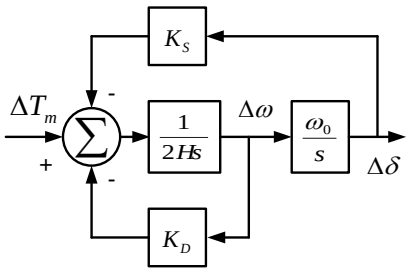

Figure 1.7: Block diagram of SMIB with classical generator

The analysis is to be covered by considering constant flux linkage in field winding, constant field voltage, effect of excitation system and power system stabilizer [75].

1.6.2. Constant flux linkage in field winding

On consideration of the constant flux linkage in the field winding, the generator linear differential Eqn. (1.37) is modified as

$$\dot{\Delta\omega} = \frac{1}{2H}\left(-K_2\,\Delta E_q^{'} - K_1\,\Delta\delta - K_D\,\Delta\omega + \Delta T_m\right) \tag{1.40}$$

The state space model can be given by using Eqn. (2.38) and Eqn. (2.40).

$$\begin{bmatrix} \Delta\dot{\omega} \\ \Delta\dot{\delta} \end{bmatrix} = \begin{bmatrix} -\frac{K_D}{2H} & -\frac{K_1}{2H} \\ \omega_0 & 0 \end{bmatrix} \begin{bmatrix} \Delta\omega \\ \Delta\delta \end{bmatrix} + \begin{bmatrix} -\frac{K_2}{2H} & \frac{1}{2H} \\ 0 & 0 \end{bmatrix} \begin{bmatrix} \Delta E_q^{'} \\ \Delta T_m \end{bmatrix} \tag{1.41}$$

It can be represented by block diagram in Figure 1.8; which is known as torque-angle loop of the generator.

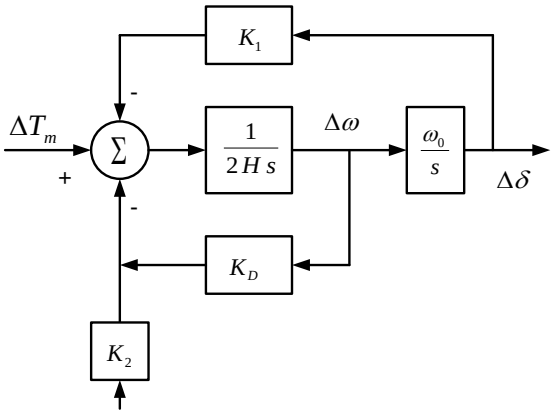

Figure 1.8: Block diagram representation of torque-angle loop

1.6.3. Constant field voltage

The flux decay in the field winding is given by the following linear differential equation

$$\Delta\dot{E}_q^{'} = -\frac{1}{K_3 T_{d0}^{'}} \Delta E_q^{'} - \frac{K_4}{T_{d0}^{'}} \Delta\delta + \frac{1}{T_{d0}^{'}} \Delta E_{fd} \tag{1.42}$$

The flux decay is being represented by the following Figure 1.9.

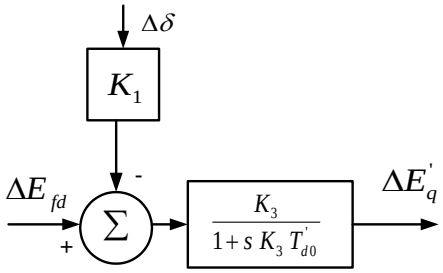

Figure 1.9: Block diagram representation of the flux decay

The new set of states is $[\Delta\omega, \Delta\delta\ \Delta E_q^{'}]$and the state space representation is given by Eqn. (1.38), (1.40) and (1.42). The matrix representation is as in Eqn. (1.43) and the corresponding block diagram representation as in Figure 1.10.

$$\begin{bmatrix} \Delta\dot{\omega} \\ \Delta\dot{\delta} \\ \Delta\dot{E}_q^{'} \end{bmatrix} = \begin{bmatrix} -\frac{K_D}{2H} & -\frac{K_1}{2H} & -\frac{K_2}{2H} \\ \omega_0 & 0 & 0 \\ 0 & -\frac{K_4}{T_{d0}^{'}} & -\frac{1}{K_3 T_{d0}^{'}} \end{bmatrix} \begin{bmatrix} \Delta\omega \\ \Delta\delta \\ \Delta E_q^{'} \end{bmatrix} + \begin{bmatrix} \frac{1}{2H} & 0 \\ 0 & 0 \\ 0 & \frac{1}{T_{d0}^{'}} \end{bmatrix} \begin{bmatrix} \Delta T_m \\ \Delta E_{fd} \end{bmatrix} \tag{1.43}$$

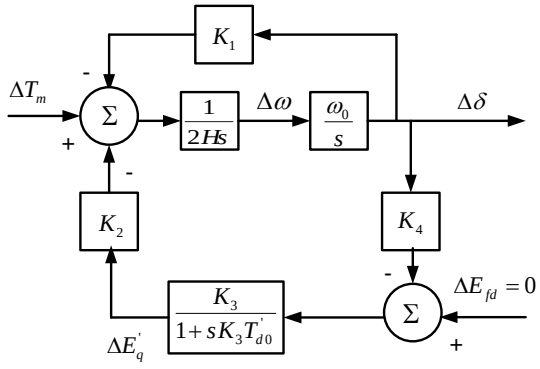

Figure 1.10: Block diagram representation with constant field voltage

1.6.4. Effect of excitation system

The governing linearized differential equation for induced field voltage is given as

$$\Delta\dot{E}_{fd} = \frac{1}{T_A}\left[-E_{fd} + K_A\left(\Delta V_{ref} - \Delta V\right)\right] \tag{1.44}$$

$$\Delta V = K_5\,\Delta\delta + K_6\,\Delta E'_q \tag{1.45}$$

$$\Delta\dot{E}_{fd} = -\frac{K_A K_5}{T_A}\Delta\delta - \frac{K_A K_6}{T_A}E'_q - \frac{1}{T_A}\Delta E_{fd} + \frac{K_A}{T_A}\Delta V_{ref} \tag{1.46}$$

The excitation adds one more state to the system by introducing ΔE_{fd}. The matrix representation is given by considering Eqn. (1.38), (1.40), (1.42) and (1.46) as in Eqn. (1.47) and excitation block diagram is represented in Figure 1.11.

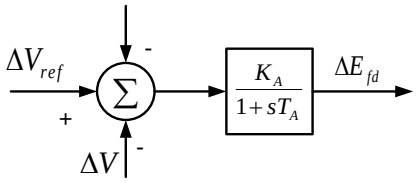

Figure 1.11: Representation of excitation system

$$\begin{bmatrix} \Delta\dot{\omega} \\ \Delta\dot{\delta} \\ \Delta\dot{E}'_q \\ \Delta\dot{E}_{fd} \end{bmatrix} = \begin{bmatrix} -\frac{K_D}{2H} & -\frac{K_1}{2H} & -\frac{K_2}{2H} & 0 \\ \omega_0 & 0 & 0 & 0 \\ 0 & -\frac{K_4}{T'_{d0}} & -\frac{1}{K_3 T'_{d0}} & \frac{1}{T'_{d0}} \\ 0 & -\frac{K_A K_5}{T_A} & -\frac{K_A K_6}{T_A} & -\frac{1}{T_A} \end{bmatrix} \begin{bmatrix} \Delta\omega \\ \Delta\delta \\ \Delta E'_q \\ \Delta E_{fd} \end{bmatrix} + \begin{bmatrix} \frac{1}{2H} & 0 \\ 0 & 0 \\ 0 & 0 \\ 0 & \frac{K_A}{T_A} \end{bmatrix} \begin{bmatrix} \Delta T_m \\ \Delta V_{ref} \end{bmatrix} \tag{1.47}$$

The representation of above equation by block diagram termed as the Heffron Phillip Model [1] and shown in the Figure 1.12.

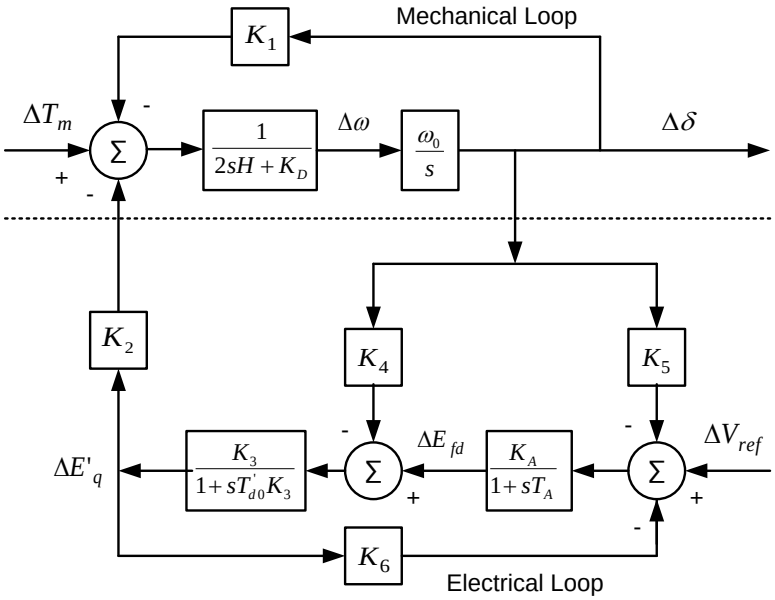

Figure 1.12: Representation of Heffron Phillip model of SMIB power system

$$\begin{bmatrix} \Delta\dot{\omega} \\ \Delta\dot{\delta} \\ \Delta\dot{E}'_q \\ \Delta\dot{E}_{fd} \\ \Delta\dot{V}_{PSS} \end{bmatrix} = \begin{bmatrix} 0 & -\frac{K_1}{2H} & -\frac{K_2}{2H} & 0 & 0 \\ \omega_0 & 0 & 0 & 0 & 0 \\ 0 & -\frac{K_4}{T'_{d0}} & -\frac{1}{K_3 T'_{d0}} & \frac{1}{T'_{d0}} & 0 \\ 0 & -\frac{K_A K_5}{T_A} & -\frac{K_A K_6}{T_A} & -\frac{1}{T_A} & 0 \\ \frac{K_{PSS}}{T_2} & -\frac{K_1 K_{PSS}}{2H}\frac{T_1}{T_2} & -\frac{K_2 K_{PSS}}{2H}\frac{T_1}{T_2} & 0 & -\frac{1}{T_2} \end{bmatrix} \begin{bmatrix} \Delta\omega \\ \Delta\delta \\ \Delta E'_q \\ \Delta E_{fd} \\ \Delta V_{PSS} \end{bmatrix} + \begin{bmatrix} 0 \\ 0 \\ 0 \\ \frac{K_A}{T_A} \\ 0 \end{bmatrix} \begin{bmatrix} \Delta T_m \\ \Delta V_{ref} \end{bmatrix} \quad (1.48)$$

1.7. Calculation of Heffron – Philip Constants

Considering the single-line diagram as shown in Figure 1.6 and terminal voltage as $V\angle\theta$, then calculation of above constants can be carried out by considering the perturbed form of the stator algebraic equations, generator terminal voltage, network equations and the differential equations of Heffron-Philip model [1, 192, 193] and the constants $K_1 - K_6$ are given by.

$$K_1 = E_0 \frac{E_{q0}}{(X_q + X_l)} \cos\delta_0 - E_0 I_{q0} \frac{(X'_d - X_q)}{(X'_d + X_l)} \sin\delta_0 \quad (1.49)$$

$$K_2 = \frac{E_0 \sin\delta_0}{X_l + X'_d} \quad (1.50)$$

$$K_3 = \frac{X_d^{'} + X_l}{X_d + X_l} \tag{1.51}$$

$$K_4 = E_0 \frac{X_d - X_d^{'}}{X_d^{'} + X_l} \sin\delta_0 \tag{1.52}$$

$$K_5 = \frac{X_q}{X_q + X_l}\frac{V_{d0}}{V} E_0 \cos\delta_0 - \frac{X_d^{'}}{X_d^{'} + X_l}\frac{V_{q0}}{V} E_0 \sin\delta_0 \tag{1.53}$$

$$K_6 = \frac{X_l}{X_d^{'} + X_l}\frac{V_{q0}}{V} \tag{1.54}$$

1.8. State Space Representation of SMIB Power System

From the block diagram representation in Figure 1.12, the following state space equations for the entire system can be derived using Heffron-Phillip model, and the analysis made in Eqn. 1.47, considering $\Delta T_m = 0$:

$$\dot{x} = [A]\, x + [B](\Delta V_{ref} + \Delta V) \tag{1.55}$$

Where, $x^T = [\Delta\omega \; \Delta\delta \; \Delta E_q^{'} \; \Delta E_{fd}]$

$$[A] = \begin{bmatrix} -\frac{K_D}{2H} & -\frac{K_1}{2H} & -\frac{K_2}{2H} & 0 \\ \omega_0 & 0 & 0 & 0 \\ 0 & -\frac{K_4}{T_{d0}^{'}} & -\frac{1}{K_3 T_{d0}^{'}} & \frac{1}{T_{d0}^{'}} \\ 0 & -\frac{K_A K_5}{T_A} & -\frac{K_A K_6}{T_A} & -\frac{1}{T_A} \end{bmatrix} \tag{1.56}$$

$$[B]^T = \begin{bmatrix} 0 & 0 & 0 & \frac{K_A}{T_A} \end{bmatrix} \tag{1.57}$$

$$[C] = \begin{bmatrix} 1 & 0 & 0 & 0 \end{bmatrix} \tag{1.58}$$

The damping term K_D is included into the swing equation. The eigenvalue of the matrix should lie in the left-hand side (LHS) in the s-plane for the system to be stable. The effect of various parameters can be examined from eigenvalue analysis. It is to be noted that the elements of [A] are dependent on the operating conditions.

1.9. Representation of Multi-Machine Power System

The dynamic behaviour of a power system can be represented by using ***n*** nonlinear first order differential equations as following [194, 195]:

$$\dot{x} = f(x,u) \tag{1.59}$$

$$y = g(x,u) \tag{1.60}$$

where ***x*** is the state vector with n state variable ***x, u*** the vector of inputs to the system, and ***y*** is the vector of outputs in Eqn.(1.59-1.60).

The linearized incremental model of a power system is needed to analyze small signal stability or to design power system stabilizer around an operating point. Assuming x_0 as the initial state vector at the current operating point and u_0 as the corresponding input vector; the non-linear function f can be expressed in terms of Taylor's series expansion. By using only the first-order terms of Taylor's series expansion, the approximation of the i[th] state variable x_i leads to with *m* number of inputs as following:

$$\dot{x}_i = \dot{x}_{i0} + \Delta\dot{x}_i \tag{1.61}$$

$$\dot{x}_i = f_i(x_0,u_0) + \frac{\partial f_i}{\partial x_i}\Delta x_1 + \cdots + \frac{\partial f_i}{\partial x_n}\Delta x_n + \frac{\partial f_i}{\partial u_i}\Delta u_1 + \cdots + \frac{\partial f_i}{\partial u_m}\Delta u_m \tag{1.62}$$

where, $x_{i0} = f_i(x_0,u_0)$. So, we obtain

$$\Delta\dot{x}_i = \frac{\partial f_i}{\partial x_1}\Delta x_1 + \cdots + \frac{\partial f_i}{\partial x_n}\Delta x_n + \frac{\partial f_i}{\partial u_1}\Delta u_1 + \cdots + \frac{\partial f_i}{\partial u_m}\Delta u_m \tag{1.63}$$

Thus, the linearized system can be written as:

$$\Delta\dot{x} = A\Delta x + B\Delta u \tag{1.64}$$

$$\Delta y = C\Delta x + D\Delta u \tag{1.65}$$

Where, *A* is the state matrix, *B* the control matrix, *C* the output matrix, and *D* is the feed forward matrix. From the stability viewpoint, the state matrix *A* is the most important. This matrix can be represented as:

$$A = \begin{bmatrix} \frac{\partial f_1}{\partial x_1} & \cdots & \frac{\partial f_1}{\partial x_n} \\ \vdots & \vdots & \vdots \\ \frac{\partial f_n}{\partial x_1} & \cdots & \frac{\partial f_n}{\partial x_1} \end{bmatrix} \tag{1.66}$$

It could be better to back referencing Eqn. (1.37, 1.38. 1.42, 1.21, 1.45), which are representing the dynamic behaviour of SMIB power system. In scenario of multimachine power

system, the fourth order model of i[th] machine can be represented by a set of linear differential equations with the small-perturbation variables $\Delta\omega_i$, $\Delta\delta_i$, $\Delta E'_{qi}$, ΔE_{fd} as followings [191].

$$\Delta\dot{\omega}_i = -\frac{K_{Di}}{M_i}\Delta\omega_i - \frac{K_{1i}}{M_i}\Delta\delta_i - \frac{K_{2i}}{M_i}\Delta E'_{qi} + \frac{1}{M_i}\Delta T_{mi} \tag{1.67}$$

$$\Delta\dot{\delta}_i = \omega_0.\omega_i \tag{1.68}$$

$$\Delta\dot{E}'_{qi} = -\frac{K_{4i}}{T'_{d0i}}\Delta\delta_i - \frac{1}{T'_{d0i}.K_{3i}}.E'_{qi} + \frac{1}{T'_{d0i}}.\Delta E_{fdi} \tag{1.69}$$

$$\Delta\dot{E}_{fdi} = -\frac{K_{Ai}.K_{5i}}{T_{Ai}}.\Delta\delta_i - \frac{K_{Ai}.K_{6i}}{T_{Ai}}.\Delta E_{qi} - \frac{1}{T_{Ai}}.\Delta E_{fdi} + \frac{K_{Ai}}{T_{Ai}}.(\Delta V_{refi} + \Delta u_i) \tag{1.70}$$

Where $K_{1i} - K_{6i}$ are the Phillips–Hefferon constants for i[th] machine and $\Delta U_i = \Delta V_{refi} + \Delta u_i$. Figure 1.13, illustrates the transfer function model of a multi-machine power system for small signal stability analysis.

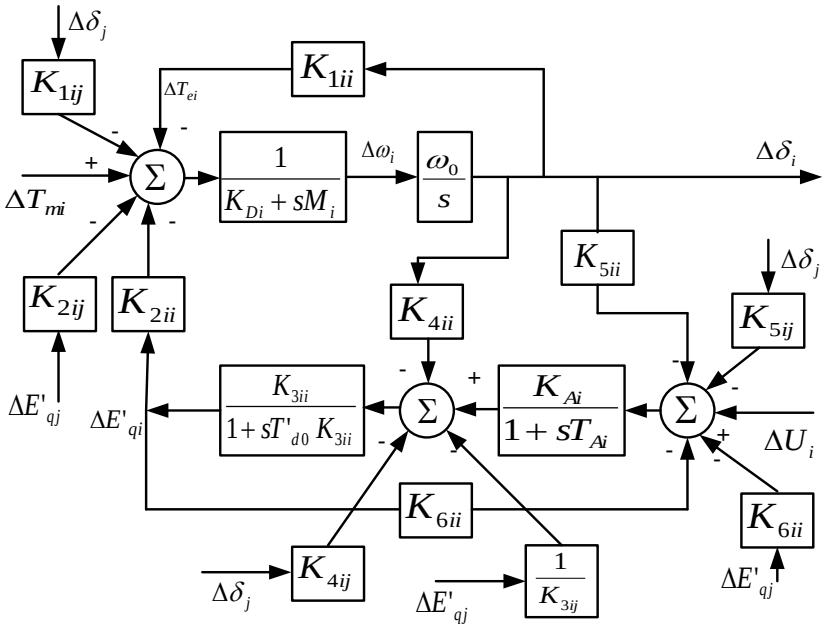

Figure 1.13: Heffron-Philip model representation for multimachine power System

The state space model representation of multimachine power system can be represented for i[th] machine as following:

$$\dot{x}_i = [A_i].x_i + [B_i](\Delta V_{refi} + \Delta u_i) \tag{1.71}$$

$$y_i = [C_i].x_i \tag{1.72}$$

Where, x_i denotes the states of i[th] machine.

1.9.1. Four-machine ten-bus power system

The state space model of the four-machine ten-bus power system shown in Figure 1. 14 can be

obtained using machine data, line data and load flow [75, 191] and the related matrices can be represented as following:

$$\Delta\dot{x} = [\overline{A}]\,\Delta x + [\overline{B}]\,\Delta u \tag{1.73}$$

$$\Delta y = [\overline{C}]\,\Delta x \tag{1.74}$$

Where, $\Delta x = [\Delta x_1\ \Delta x_2\ \Delta x_3\ \Delta x_4]^T = [\Delta\omega\ \Delta\delta\ \Delta E_q^{'}\ \Delta E_{fd}]$

The elements of $\overline{A}$ matrix depend on the network parameters of the power system, and each element represents a sub-matrix of order 4×4. Thus, the diagonal elements of $\overline{A}$ are $A_1, A_2, \cdots A_4$ and off-diagonal elements are $a_1, a_2, \cdots a_{12}$, which depends on the way of interconnection in the power system and of order 4×4.

The state equations of a power system, consisting '*N*' number of generators and N_{pss} number of power system stabilizers can be written as in Eqn. (1.59). Where, $\overline{A}$ is the system matrix with an order as 4N×4 N_{pss} (16×16), while $\overline{B}$ is the input matrix with order 4N×N_{pss} (16×4). The order of state vector $\overline{C}$ is 4N×1 (16×1).

$$\overline{A} = \begin{bmatrix} A_1 & a_1 & a_2 & a_3 \\ a_4 & A_2 & a_5 & a_6 \\ a_7 & a_8 & A_3 & a_9 \\ a_{10} & a_{11} & a_{12} & A_4 \end{bmatrix} \tag{1.75}$$

$$x = [x_1 \quad x_2 \quad x_3 \quad x_4]^T \tag{1.76}$$

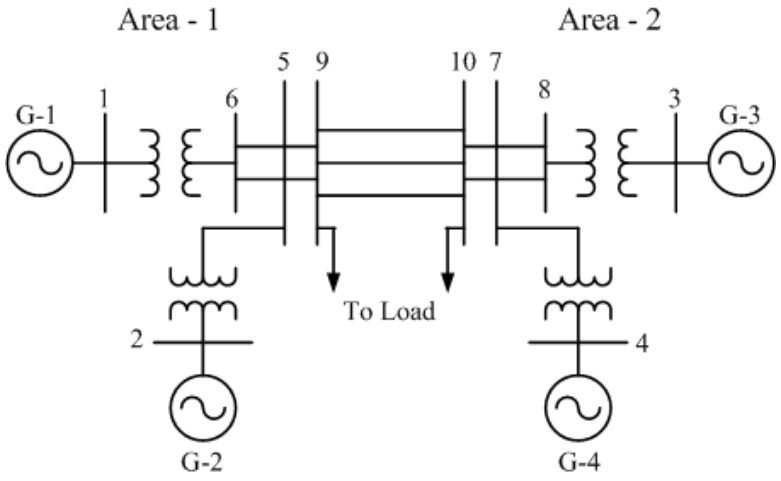

Figure 1.14: Line diagram of two-area four-machine ten-bus power system

1.9.2. New England ten-machine thirty nine-bus power system

The elements of $\overline{A}$ matrix depend on the network parameters of the power system, and each element represents a sub-matrix of order 4 × 4. Thus, the diagonal elements of $\overline{A}$ are $A_1, A_2, \cdots A_{10}$ and off-diagonal elements are $a_1, a_2, \cdots a_{90}$, which depends on the way of interconnection in the

power system and of order 4 × 4.

The state equations of a power system, consisting '*N*' number of generators and N_{pss} number of power system stabilizers can be written as in Eqn. (1.59). Where, $\overline{A}$ is the system matrix with an order as *4N×4N (40×40)* and is given by $\partial f / \partial x$, while *B* is the input matrix with order $4N \times N_{pss}$ *(40×10)* and is given by $\partial f / \partial u$. The order of state vector x (as in Eqn. 1.59) is *4N×1 (40×1)*, the order of Δu is $N_{pss} \times 1$ *(10×1)*. The state space model of the 10-machine 39-bus power system shown in Figure 1. 15 can be obtained using machine data, line data and load flow [191] and the related matrices can be represented as Eqn. (1.77 - 1.78) [196].

$$\overline{A} = \begin{bmatrix} A_1 & a_1 & a_2 & a_3 & a_4 & a_5 & a_6 & a_7 & a_8 & a_9 \\ a_{10} & A_2 & a_{11} & a_{12} & a_{13} & a_{14} & a_{15} & a_{16} & a_{17} & a_{18} \\ a_{19} & a_{20} & A_3 & a_{21} & a_{22} & a_{23} & a_{24} & a_{25} & a_{26} & a_{27} \\ a_{28} & a_{29} & a_{30} & A_4 & a_{31} & a_{32} & a_{33} & a_{34} & a_{35} & a_{36} \\ a_{37} & a_{38} & a_{39} & a_{40} & A_5 & a_{41} & a_{42} & a_{43} & a_{44} & a_{45} \\ a_{46} & a_{47} & a_{48} & a_{49} & a_{50} & A_6 & a_{51} & a_{52} & a_{53} & a_{54} \\ a_{55} & a_{56} & a_{57} & a_{58} & a_{59} & a_{60} & A_7 & a_{61} & a_{62} & a_{63} \\ a_{64} & a_{65} & a_{66} & a_{67} & a_{68} & a_{69} & a_{70} & A_8 & a_{71} & a_{72} \\ a_{73} & a_{74} & a_{75} & a_{76} & a_{77} & a_{78} & a_{79} & a_{80} & A_9 & a_{81} \\ a_{82} & a_{83} & a_{84} & a_{85} & a_{86} & a_{87} & a_{88} & a_{89} & a_{90} & A_{10} \end{bmatrix} \quad (1.77)$$

$$x = [x_1 \quad x_2 \quad x_3 \quad x_4 \quad x_5 \quad x_6 \quad x_7 \quad x_8 \quad x_9 \quad x_{10}]^T \quad (1.78)$$

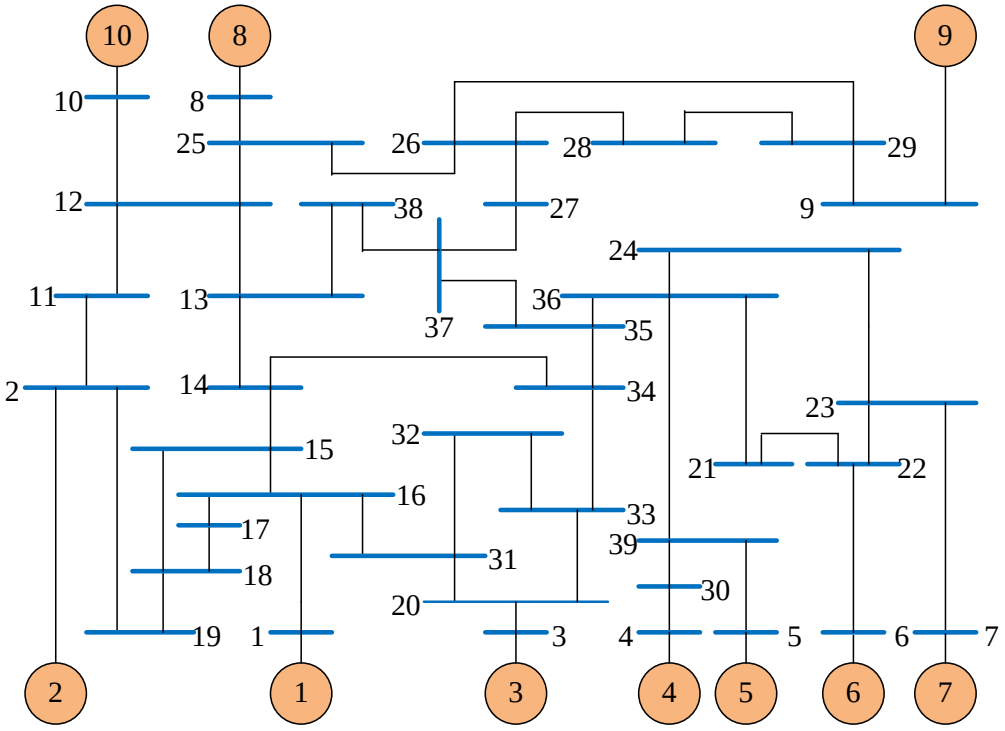

Figure 1.15: Line diagram of New England ten-machine thirty nine-bus power system

1.10. Outline of Thesis

This thesis examines the design of conventional PSS, PID type PSS, Type-1 FPSS (optimized input scaling factors), Type-1 FPSS (optimized input-output scaling factors), Type-1 FPSS (with new rule table) and Interval Type-2 FPSS in order to design globally optimal PSSs that will ensure a stable and robust operation of an SMIB, two-area four-machine ten-bus (TAFMTB) and IEEE New England ten-machine thirty nine-bus power system (NETMTB), for each operating point within a wide range.

This thesis has been organized into seven chapters.

Chapter 1: It presents the problem of small signal stability in power systems, with emphasis on the low-frequency oscillation phenomena occurring due to small disturbances and its mitigation by means of PSS. It presents a brief review of literature discusses the relevant work in this area of tuning PSS and lays down the motivations and objectives of the work. It presents the small-signal modelling of an SMIB power system, including detail of a conventional power system stabilizer. Two multimachine models and relevant representation of a small signal model are presented. The working steps of two algorithms; bat algorithm and the harmony search algorithm have been presented. Brief reviews on objective functions as reported in literature and applied by researchers have been presented. To carry out perspective and complete evaluation of system performance; three types of performance indices are introduced. The outline of the thesis with a brief on chapters is introduced.

Chapter 2: In this chapter, three power system networks are introduced to carry out the performance analysis of different controllers. The different eight plant configurations based on operating conditions and the system configuration for each of these systems have been introduced. The behaviour of these systems without PSS is elaborated by simulation results and eigenvalue analysis. The conventional PSS for SMIB power system is designed using the bat algorithm (BA). The system performance with BA optimized CPSS (BA-CPSS) controller is compared with the CPSSs as reported in literature. The robustness of such a designed BA-CPSS is tested by considering several operating conditions (231 in numbers) to establish the superiority of performance over the other controllers. The application of the bat algorithm (BA) to optimize its gain and pole-zero parameters are extended to multimachine power system. The considered power system models are TAFMTB and IEEE NETMTB power system. The system performance with BA optimized CPSS (BA-CPSS) controller is compared with the CPSSs as reported in literature, which has been

designed by using different optimization algorithms. The system performance with proposed BA-CPSS is compared with that of the CPSSs reported in literature. The close comparison with the speed response of the system with proposed CPSS and that of with reported CPSSs in literature are differentiated by using performance indices. Moreover, the performance enhancement using proposed BA-CPSS is validated by calculating and plotting eigenvalue in s-plane for a wide range of operating conditions and system configuration.

Chapter 3: It presents PID based PSS design using BA to optimize its parameters. The design of proposed PID controller is considered with an objective function based on square error minimization for SMIB, TAFMTB and IEEE NETMTB power system. The designed PSS has applied to these power systems, and the performances have been compared with PID based PSSs designed using different methods in literature.

Chapter 4: It contains a detail on design of a type-1 fuzzy logic power system stabilizer (FPSS). Speed and acceleration are the input signals to FPSS, and the associated normalizing factors (input-scaling factors) are optimized using optimization techniques. A small-signal model of the fuzzy logic power system stabilizer (FPSS) has been derived and proven to be a Proportional Derivative controller to relate its parameters, and the scaling factors associated to input signals of FPSS. These parameters of the PD controller have been tuned using harmony search algorithm and bat algorithm; thereafter considered, as scaling factors of FPSS. The performance of such designed HSA-FPSS and BA-FPSS have been compared against the FPSS performance for a wide range of operating conditions and system configuration on SMIB power system, TAFMTB power system and NETMTB power systems. It also includes design of FPSS by tuning its input-output scaling factors. Two inputs signal to type-1 FPSS has been considered as change of speed and change in power and the output signal as a voltage signal. The normalizing factors of these signals have been considered as an optimization problem with minimization of integral of square error in single-machine and multimachine power systems. These normalizing factors have been tuned using the harmony search algorithm (HSA) and bat algorithm (BA); thereafter considered, as scaling factors of FPSS. The performance of such designed HSA-FPSS and BA-FPSS is compared to the FPSS (without considering scaling factors) performance for a wide range of operating conditions and system configuration on SMIB power system, TAFMTB power system and NETMTB power systems.

Chapter 5: In this chapter, type-1 FPSS has been designed for effective damping using optimal fuzzy rule matrix (FRM). As to achieve impressive performance of a controlled plant,

the rule base/FRM of a fuzzy logic controller (FLC) has been designed using derived empirical relationships from the FPSSs in literature and rule justification on the linguistic phase plane trajectory. A systematic procedure has been introduced to design FRM for acceptable damping of SMIB, TAFMTB and NETMTB power systems. To demonstrate the effectiveness of FPSS based on proposed optimal FRM, over a wide range of operating conditions, nonlinear simulations have been carried out on SMIB System, and the comparison has been made with that of the system response without PSS, with Conventional PSS & with FPSS. Similarly, the application of type-1 FPSS with optimal FRM has been extended to multimachine stability enhancement.

Chapter 6: It includes the evaluation and performance analysis of an interval type-2 fuzzy logic controller (IT2 FLC) as a power system stabilizer (PSS). The evaluation and implementation of IT2 FLC as PSS (IT2-FPSS) have been carried out with an SMIB power system. The input signals to design the FPSS have been considered as speed deviation and acceleration and voltage as an output signal. The evaluation of IT2 FPSS has been considered with 20 separate types of interval type-2 membership functions (MFs) and the performance of each have been evaluated using nonlinear simulations. The performance with IT2 FPSS is compared against the performance of the power system without PSS & with conventional PSS. The application of IT2 FPSS has been extended to TAFMTB and NETMTB power system.

Chapter 7: It high lights the significant contributions of the present work and draws the scope for future work in this area.

1. 11. Conclusions

In this chapter, the PSS has been introduced to enhance the small signal stability. It introduces the relevant literature to draw objectives on heuristic optimization techniques and fuzzy logic control based PSS design. It also introduces the application of performance indices to compare system responses. The modeling of the SMIB power system to develop Heffron-Phillip model, extension to multimachine representation, and calculation of $K_1 - K_6$ have been carried out in this chapter.

Chapter 2

DESIGN AND PERFORMANCE ANALYSIS OF ROBUST CONVENTIONAL PSS USING BAT ALGORITHM

In this chapter, the design of a conventional power system stabilizer (CPSS) is carried out using the bat algorithm (BA). The CPSS design problem is considered for SMIB system as well as multimachine scenario. The problem of tuning CPSS parameters is considered as an optimization with eigenvalue based objective function. The CPSS parameters of SMIB system are tuned by placement of eigenvalue in D-shape sector while that of multimachine in a wedge-shaped sector in s-plane to guaranteeing the stability of nonlinear plant for a wide range of operating conditions power system. The robustness of designed BA-CPSS has been examined by considering large operating conditions (231 in numbers) to establish the effectiveness of performance over the other controllers reported in literature. The considered multimachine power systems are two-area four-machine ten-bus and IEEE New England ten-machine thirty nine-bus power system. The system performance with BA optimized CPSS (BA-CPSS) controller is compared to that of with the CPSSs reported in literature for single-machine and multimachine environment. The performance of proposed BA-CPSS is carried out by considering eight unusual combinations of operating conditions and system configurations with different location of fault in multimachine environment. The close comparison of the speed response of a system with the proposed controller and comparing controllers as reported in literature is validated using performance indices, i.e. ITAE, IAE and ISE. Moreover, the effectiveness and robustness of the proposed BA-CPSS are confirmed by calculating and plotting eigenvalue in s-plane.

2.1. Introduction

Power systems are complex multi-component dynamic systems in which the system characteristics are used to fluctuate with varying loads and varying generation schedules. These power systems suffer by low frequency oscillations on sudden changes in load or occurrence of fault. The transfer of bulk power across weak transmission lines is hindered due to continuous persistence of such a low-frequency oscillation (0.2–3.0 Hz) [197].

In early 1960s, the fast acting, high-gain automatic voltage regulators (AVR) were applied in the generator excitation system which in-turn invites the problem of low frequency electromechanical oscillations in the power system by reducing the damping torque. To reduce the low-frequency oscillations, the PSS adds a stabilizing signal to an automatic voltage regulator

(AVR) that modulates the generator excitation to damping electrical torque component in phase with rotor speed deviation, which increases the generator damping. The uniformly adopted type of PSS is known as conventional PSS (CPSS) [198], which consists of the lead-lag type components. Similar to CPSS a Proportional Integral Derivative (PID) controller [199] may be connected to modulate the signal of the AVR to damp-out the small signal oscillations. The most commonly used input to CPSS is shaft speed of the generator while frequency and acceleration may also be used as input to it. The control and power system engineers made significant contribution to CPSS design after the pioneering work of deMello and Concordia in 1969 [1]. Thereafter, the most designs were developed by using modern control theory like eigenvalue (pole) assignment and optimal control [200], adaptive control [201]. The design and selection of the PSS structure are a complex iterative process which is around an operating point resulting to unsatisfactory operation for another/varying operating point. The effective PSS design, to make adaptive for any changes corresponding to the varying operating conditions can be achieved by self-tuning [201], Lyapunov based adaptive control methods [202] of PSS design. These methods require extensive knowledge of dynamics of the power system and long processing time.

In recent years, artificial intelligence based learning and tuning methods have been introduced to design PSSs such as artificial neural networks (ANNs) as in [203-205], fuzzy logic in [26, 169, 172, 206, 207], adaptive fuzzy in [208, 209], neuro-fuzzy in [195, 210-212] and population based such as Genetic Algorithm in [19, 213, 214]. The applications of these methods enable PSSs design, including the parametric uncertainty as well as nonlinearity. Such designed PSSs are able to provide an optimal and robust [215] stabilizing capability over a wide range of operating conditions of a power system. In case of ANN, the gradient algorithm is being used to learn its parameters using either input/output [193, 204] parameters or online data from different operating points on a power system network.

In 1960 - 70, the classical optimization methods were introduced but not able to converge for non-linear and non-differential engineering problems. Recently, some of the optimization methods such as particle swarm optimization (PSO) [121, 216, 217], genetic algorithm (GA) [213, 218, 219], differential evolution (DE) [208, 220] algorithm and simulated annealing (SA) [221], have been applied to complicated and large dimensional power system problems.

To mitigate these limitations of PSS design, different techniques, including optimization methods are used to design CPSS for nonlinear models of EPSs. However, the CPSS parameter tuning is easy with the help of optimization algorithms. Sequential and simultaneous tunings are two main methods to tune CPSS parameters of EPS. A set of optimal parameters of CPSS are determined for different operating conditions and the performances of EPS with different sets are tested. In simultaneous tuning, the problem of CPSS tuning is formulated as a large nonlinear non-

differentiable optimization [222]. It is difficult to solve such problems by applying traditional differentiable optimization algorithms. The use of an optimization algorithm in literature such as Particle swarm optimization (PSO) [13], small-population-based particle swarm optimization (SPPSO) [13], bacterial foraging algorithm (BFA) [13], genetic algorithm (GA) [14, 24], PSO with passive congregation (PSOPC) [14], Modified PSO (MPSO) [15], combinatorial discrete and continuous action reinforcement learning automata (CDCARLA) [16], modified artificial immune network (MAINet) [17], multiobjective immune algorithm (MOIA) [17], Bacterial foraging optimization algorithm (BFOA) [18], adaptive mutation breeder genetic algorithm (ABGA) [19], strength-pareto evolutionary algorithm (SPEA) [11], differential evolution (DE) [23], fuzzy gravitational search algorithm (FGSA) [26], cultural algorithm (CA) [25], have gained acceptance in CPSS design for multimachine power system because of effectiveness and ability to investigate near-global optimal results in the problem space. It has been established that the GA is satisfactory in finding the optimal set of solutions, but it often yields revisiting the same sub-optimal set of solutions. It needs a long-run time may be up to several hours depending on the size of the system under investigation.

One of the heuristic techniques like Tabu search (TS) is considered to design a CPSS for multimachine system in [20]. It seems to be effective for the design problem, but the efficiency is reduced using highly epistatic objective functions (i.e. large number of parameters with correlations), and it is time consuming method [8].

PSO is a type of random search, which simulates the evolutionary process of nature with excellent complex optimization problems. PSO has some attractive features other evolutionary techniques and GA such as (i) few parameters to adjust, (ii) faster convergent speed because of only two computational formulae for iteration [223]. CPSS design for multimachine system is proposed in [13, 22]. However, PSO causes the less exact at the regulation of its speed and the direction because of the partial optimism and unsuitable for the problems of scattering and optimization. Moreover, it suffers from slow convergence in refined search stage; weak localized search ability and algorithm may lead to possible entrapment in sectional minimum solutions [8].

In [224], a modified PSO algorithm (MPSO) is proposed for optimal placement and tuning of PSSs in power systems. To decrease the possibility of meaningless search by using integrating passive congregation with PSO and the chaotic sequence for improve the global searching capability.

Relatively newer algorithm called as Bacterial foraging is applied to tune the CPSS parameters in multimachine scenario in [18]. It depends on random search directions, which may lead to delay in reaching the global solution [216].

In [21], design is carried out by using an algorithm, inspired by biological and sociological motivations called as differential evolution (DE) which can take care of optimality on rough, discontinuous and multi-modal surfaces. It has three main advantages such as (i) optimal solutions regardless of initial parameter values, (ii) relatively fast convergence, (iii) works with little numbers of control parameters and, (iv) it is simple in coding and easy to use. However, it requires several trials for selection of initializing parameters.

Recently, Yang [100], have proposed a very promising bat algorithm (BA) under the category of meta-heuristic algorithms. BA is a new search algorithm based on the echolocation behaviour of Microbats. Preliminary studies indicate that BA is superior to GA and PSO for solving unconstraint optimization problems [100] because these methods fail to deal with the multimodal optimization problems. In [225], the firefly algorithm (FA) which is based on the flashing characteristics of tropical fireflies. In continuation, cuckoo search (CS) is based on the brooding behaviour of some cuckoo species [226, 227]. As the bat algorithm (BA) uses (i) frequency-tuning technique to increase the diversity of the solutions to the population (ii) the automatic zooming to try to balance exploration and exploitation during the search process by mimicking the variations of pulse emission rates and loudness of bats when searching for prey; It proves to be very efficient with a typical quick start. However, the original version of this algorithm is suitable for continuous problems, so it cannot be applied to binary problems directly. In [228], a binary version of this algorithm is proposed to deal with dimensionality reduction [229] and feature selection [230].

In literature, many CPSS structures are considered like lead-controller (single stage CPSS) as in [6, 24, 211, 231], lead-lag controller (double stage CPSS) as in [25, 213] and normally considering three stages of operation like light loading, nominal and heavy loading operating conditions to tune parameters. The computational time and burden are enlarged with an increase in the size of the controller. Since, the operating condition of a power system tends to vary; therefore, a robust controller examined over a wide range of operating conditions should be designed.

To mitigate these limitations a double-stage controller is considered and tuned at the nominal operating condition of SMIB system using the bat algorithm. Such designed CPSS has been examined over a very wide operating condition (constituting 231 plants). Moreover, the chapter's organization starts with problem formulation in section 2.2. Brief description of representation for SMIB power system, conventional power system stabilizer and objective function for SMIB and multimachine systems based on eigenvalue shifting to guaranteeing the dynamic stability of the system has been introduced in this section. The different eight plant configurations for single-machine and multimachine power system are presented in section 2.3.

The design of CPSS for SMIB system, review on CPSSs reported in literature, time-domain simulation and eigenvalue based comparison is presented in section 2.4. In section 2.5, CPSSs design based on the bat algorithms, a brief review on CPSSs reported in literature, time-domain simulation and eigenvalue analysis based comparison is presented for two-area four-machine ten-bus power system. In section 2.6, CPSSs design based on the bat algorithms, a brief review on CPSSs reported in literature, time-domain simulation and eigenvalue analysis based comparison is presented for 10-machine 39-bus power system. Lastly, the chapter is concluded in section 2.7.

2.2. Problem Formulation

The aim of this chapter is to utilize the Bat algorithm for tuning the CPSS parameters in a power system; therefore, the EPS elements such as generators, excitation system and PSS must be modeled. To complete the tuning process, an objective function to obtain satisfactory results is necessary and should be defined. Accordingly, the system model and an objective function used in PSS parameter tuning in a single-machine and multi machine power system are elaborated.

2.2.1. Test system representation

The systems under consideration are single-machine connected to infinite-bus (SMIB), two-area four-machine ten-bus and IEEE New England ten-machine thirty nine-bus power system. The single-line diagram representation is shown in Figure 1. 6, and the way of connection with AVR is shown in Figure 2.1. The small signal models of the SMIB power system can be represented by Figure 2.2 with connection of CPSS. The output signal of this PSS is added to AVR to modulate the excitation system for enhancing the damping of the small signal oscillations. In SMIB system, an infinite bus can be represented by the Thevenin's equivalent of a large interconnected power system. Synchronous generator control components as schematic are shown in Figure 2.1. The line diagram of a two-area four-machine ten-bus power system is represented in Figure 1.14 and that of the IEEE New England ten-machine thirty nine-bus system, is shown in Figure 1.15. The general representation of Heffron-Phillip model for multimachine system is shown Figure 1.13 [1, 213]. Moreover, the general representation of a complex power system using nonlinear differential equations can be given as.

$$\dot{X} = f(X,U) \tag{2.1}$$

where, X and U represent the vector of state variables and the vector of input variables. As in [22, 213], the power system stabilizers can be designed by use of the linearized incremental

models to a power system around an operating point. The system dynamics is given in section 1.6 - 1.8. The state equations to a power system can be written as.

$$\Delta\dot{x} = A.\Delta x + B.U \tag{2.2}$$

Where, A is the system matrix with order as 4×4 and is given by $\partial f / \partial X$, while B is the input matrix with order 4×1 and is given by $\partial f / \partial U$. The order of state vector Δx is 4×1, the order of ΔU is 1×1.

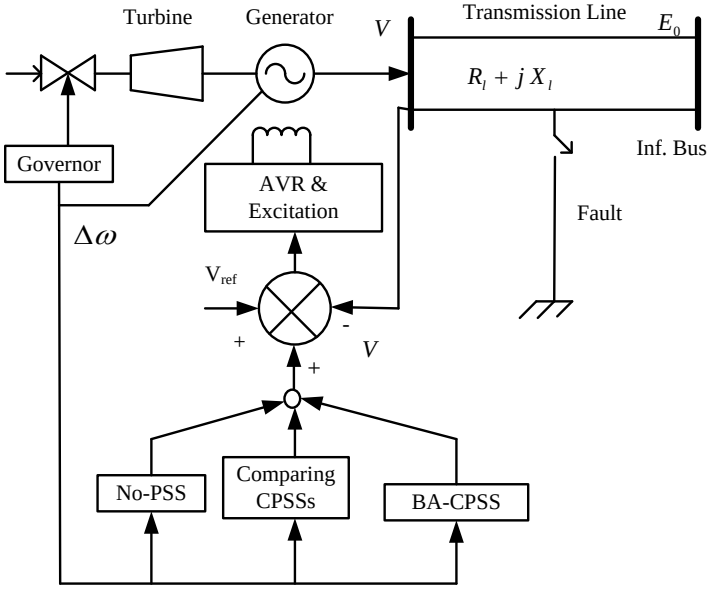

Figure 2.1: Line diagram of SMIB power system and connection of controller

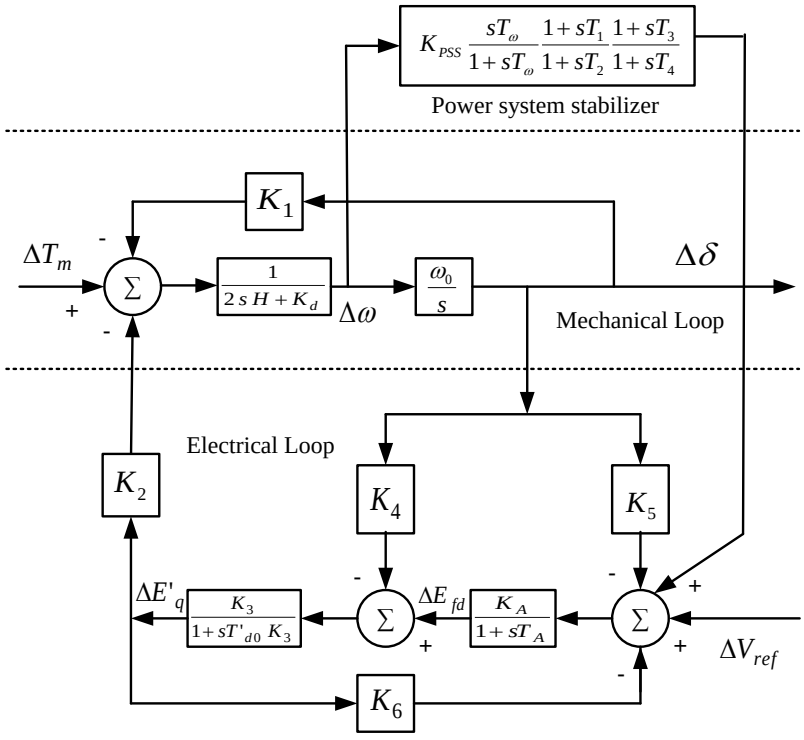

Figure 2.2: Representation of Heffron-Phillip model for SMIB power system with CPSS

The considered synchronous machines of multimachine power system are of the model 1.0 type as discussed in [191]. To cover all operating conditions, the power system with generators, stabilizers, and excitation systems can be modeled by a set of nonlinear differential equations as in Eqn. 2.1 [14]. As the state space model is represented by Eqn. (2.2) and consequently, the system matrix A, therefore, the total electromechanical modes of the system can be evaluated in the form $\lambda = \sigma \pm j.\omega$.

2.2.2. Conventional PSS

Design of conventional PSS is based on a linearized model around a certain operating point. Since the actual power system operates over a wide range of operating conditions and nonlinear characteristics. The tuning of CPSS to cope with most of the operating conditions is very difficult. The change in rotor speed is taken as input to PSS as shown in Figure 2.2. The structure of PSS is mainly composed by a gain, wash out filter and the phase compensator block (Figure 2.2). The gain block determines the damping ratio of PSS, and its value determined by practical considerations [191]. The washout filter behaves as a high-pass filter, therefore, the PSS only responds to the speed deviation of generator and not responds to the steady-state operation of the system. The criterion to select the washout time constant T_ω is to pass required PSS signals intact. The lag compensation between excitation input and electric torque (air-gap torque) is provided by the phase compensator block. The limiting block at the output of PSS is connected to prevent the over excitation [40]. The bounds of limiting block are taken as ±0.02 to ±0.05 p.u. The transfer function of the double-stage conventional PSS (CPSS) is given by Eqn. (2.3), and represented in Figure 2.2.

$$\Delta V_{PSS}(s) = K_{PSS}\frac{sT_\omega}{1+sT_\omega}\frac{1+sT_1}{1+sT_2}\frac{1+sT_3}{1+sT_4} \tag{2.3}$$

2.2.3. Objective function

2.2.3.1. OF for SMIB power system

To increase the system damping over a wide range of operating conditions and configuration throughout the power system, a robust tuning must be incorporated. Therefore, PSS design is formulated as an eigenvalue-based objective function. The two sub-objective functions based on minimization of real part of eigenvalue and maximization of damping ratio are taken into consideration as in [25]. These are represented by Eqn. (2.4) and (2.5).

$$J_1 = \sum_{\sigma_i \geq \sigma_0} (\sigma_0 - \sigma_i)^2 \tag{2.4}$$

$$J_2 = \sum_{\zeta_i \leq \zeta_0} (\zeta_0 - \zeta_i)^2 \tag{2.5}$$

Where, σ_i is the real part of the i^{th} electromechanical mode eigenvalue ($\mathrm{Re}\,al(\lambda_i)$), and ζ_i is damping ratio of the i^{th} electromechanical mode eigenvalue. The aim of optimization of J_1 [139] is to shift the poorly damped eigenvalue to the left in s-plane. The J_2 is maximized such that to increase the damping of electromechanical modes of oscillations. The optimization constraints are the limits/bounds on the optimized parameters such as gain and the time constants (zero-pole). Thus, the optimization problem is subjected to

$$K^{\min} \leq K \leq K^{\max} \tag{2.6}$$

$$T_1^{\min} \leq T_1 \leq T_1^{\max} \tag{2.7}$$

$$T_2^{\min} \leq T_2 \leq T_2^{\max} \tag{2.8}$$

$$T_3^{\min} \leq T_3 \leq T_3^{\max} \tag{2.9}$$

$$T_4^{\min} \leq T_4 \leq T_4^{\max} \tag{2.10}$$

The typical values of the optimized parameters are taken as [0.1 - 50] for K, [0.2 - 1.5] for T_1, T_3 and [0.02 - 0.15] for T_2, T_4 [88]. The time constants T_ω is considered as 10.0 seconds as in [88]. To clarify, the damping ratio of the ith critical mode is given by

$$\zeta_i = \frac{-\sigma_i}{\sqrt{\sigma_i^2 + \omega_i^2}} \tag{2.11}$$

where, considered eigenvalue is given by $\lambda_i = \sigma_i \pm j.\omega_i$. Thus, the objective functions can be represented as

$$J = J_1 + \alpha.J_2 = \sum_{i=1}^{n} (\sigma_0 - \sigma_i)^2 + \alpha.\sum_{i=1}^{n} (\zeta_0 - \zeta_i)^2 \tag{2.12}$$

where, $\sigma_i \leq \sigma_0$ and $\zeta_i \geq \zeta_0$ for *i = 1, 2 …, n* and *n* stands for the number of electromechanical modes which are responsible for instability of the power system. In this system (SMIB), *n* is equal to 4. The effect of J_1 and J_2 are shown in Figure 2.3 (a) - Figure 2.3(b), respectively. While the Combined Objective Function $J = J_1 + \alpha.J_2$ can place the system closed loop eigenvalue in the D-shape sector as shown in Figure 2.3(c). The value of α is considered as 10.

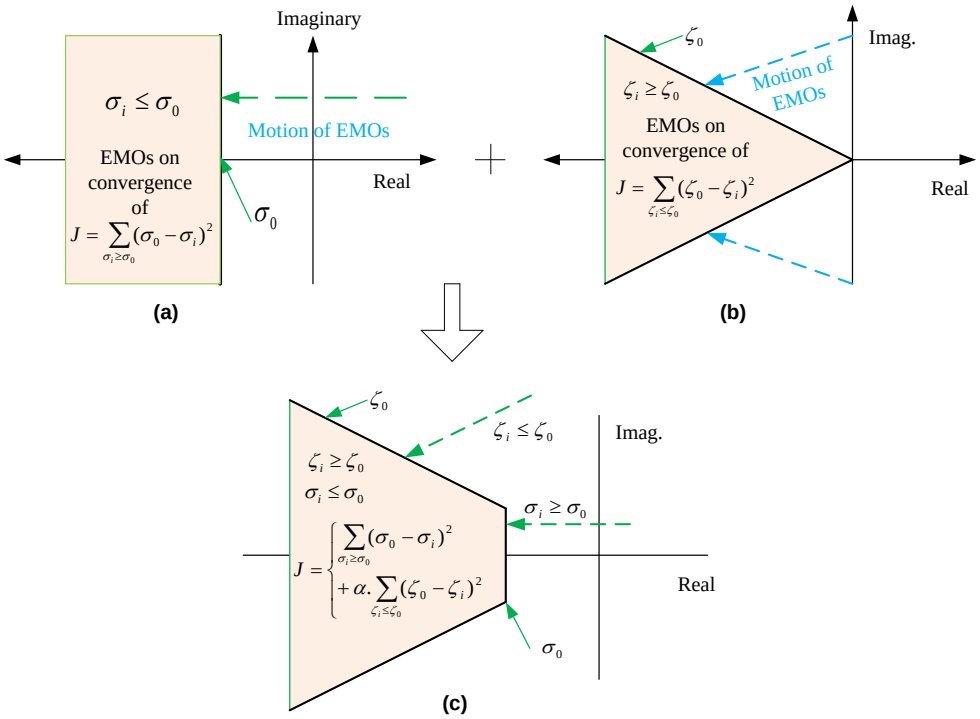

Figure 2.3: Representation of eigenvalue based objective function

2.2.3.2. OF for multimachine systems

In [3, 7, 19, 23, 186], the objective function is designed to increase the damping ratio of the system without any threshold. However, in [24] a threshold value of the damping ratio is introduced as ζ_0 and defined as in Eqn. (2.5), which can place the electromechanical mode eigenvalue in a wedge-shape sector in the left of s-plane as shown in Figure 2.3(b) or in Figure 1.4. The condition $\zeta_i \le \zeta_0$ is imposed on J evaluation to consider only the unstable or poorly damped modes which are mainly belonging to the electromechanical ones. In [65], the value of ζ_0 is exceptionally selected as 1.0, while it is generally selected in the range of 0.1-0.2 [3, 7, 19, 23, 186].

In the optimization process *J* as defined in Eqn. (2.13) is *maximized* in order to increase the damping of electromechanical mode of oscillations. Therefore, the design problem can be formulated as the following optimization problem within the constraints as the optimized parameter bounds.

Maximize J:

$$J = \sum_{\zeta_i \le \zeta_0} (\zeta_0 - \zeta_i)^2 \qquad (2.13)$$

Subjected to:

$$K_j^{\min} \le K_j \le K_j^{\max} \tag{2.14}$$

$$T_{j1}^{\min} \le T_j \le T_{j1}^{\max} \tag{2.15}$$

$$T_{j2}^{\min} \le T_{j2} \le T_{j2}^{\max} \tag{2.16}$$

$$T_{j3}^{\min} \le T_{j3} \le T_{j3}^{\max} \tag{2.17}$$

$$T_{j4}^{\min} \le T_{j4} \le T_{j4}^{\max} \tag{2.18}$$

The typical values of the optimized parameters are taken as [0.1 - 50] for K_j [191, 232] , [0.2 - 1.5] for T_{j1}, T_{j3} and [0.02 - 0.15] for T_{j2}, T_{j4} [23, 88, 191], where in *j* refers to PSS connected to j^{th} generator . The time constants $T_{j\omega}$ is generally not critical and may be in the range of 0.5 to 20 seconds but here in this design is selected as 10.0 seconds as in [88, 232, 233].

2.3. Different Plant Creation and response without PSS

2.3.1. SMIB power system

2.3.1.1. Different plants creation

The necessity of PSS depends upon the operating point of power system and the type of contingencies. In literature, the power system loading conditions has been termed as lightly, nominal and heavy loading for SMIB power system [139]. In [41], three operating conditions have been considered in terms of active power in pu and power factor such as [0.7, 0.85 pf lag], [0.9, 0.85 pf lag] and [0.3, 0.90 pf lead]. In [40], simulation results for operating conditions have been presented for (a) 0.30 pu, 0.90 pf lead, (b) 0.50 pu, 0.90 pf lag (c) 0.90 pu, 0.85 pf lag (d) 0.95 pu., 0.90 pf lag. In [234], the system loading conditions such as nominal loading as 0.7 pu**,** 0.85 pf lag, light loading as 0.20 pu with 0.85 pf lag and heavy 0.3pu with 0.9 pf have been considered for simulation performance analysis. In [39], the SMIB system configurations for which the simulation studies have been considered are such as 0.30 p.u., 0.85 p.f. lag; 0.30 p.u., 0.90 p.f. lead; *P* 0.70 p.u., 0.85 p.f. lag and 0.90 p.u., 0.85 p.f. lag. Some of the operating conditions for SMIB power system as reported in literature have been included in Table 2.1. Clearly, the researchers have used active power variation only up to 1.1 pu either with phase lag or with phase lead [9, 39-41, 234-241].

Table 2.1: Loading conditions in pu of SMIB power system in literature

PSS design in literature	Nominal		Light		Heavy		Leading PF	
	P	Q	P	Q	P	Q	P	Q
Abido, 2000 [139]; Kashki et al., 2010 [235]	1.00	0.015	0.70	0.30	1.10	0.40	--	--
Abido and Abdel-Magid, 1999 [236]; Abido, 1999 [237]	1.00	0.015	--	--	1.10	0.40	0.70	-0.20
Al-Awami, 2006 [238]	1.00	0.015	0.30	0.10	1.10	0.10	--	--
Kashki et al., 2013 [239]	1.00	0.015	0.30	0.10	1.10	0.400	0.70	-0.20
Abido, 2001 [9]	1.00	0.015	--	--	1.10	0.10	0.70	-0.30
Hassan et al.,1991 [240, 241]	0.80	0.20	0.40	0.20	1.10	0.40	0.70	-0.15

The system modelling is described in chapter 1 and the line diagram of the system is shown in Figure 1.6. The nonlinear differential equations governing the behaviour of a power system can be linearized about a particular operating point to obtain a linear model which represents the small signal oscillatory response of a power system. Variations in the operating condition of the system result to changes in the parameters of the small signal model. A given range of variations in the operating conditions of a particular system thus generates a set of linear models each corresponding to one particular operating condition. Since, at any given instant, the actual plant could correspond to any model in this set, a robust controller would have to import an adequate damping to each one of this entire set of linear models. The SMIB power system is configured with SMIB power system data as in Table A.1.

Table 2.2: Plant configuration with different operating conditions: SMIB power system

Power System Model	Active power, P_{g0}	Reactive power, Q_{g0}	Tran. line reactance, X_l (0.2)	K_1	K_2	K_3	K_4	K_5	K_6
Plant-1	0.50	0.0251	0.20	1.2911	1.4849	0.2304	2.4798	0.0771	0.2963
Plant-2	0.50	0.0505	0.40	1.0010	1.1327	0.2954	1.8916	0.0729	0.4318
Plant-3	0.75	0.0566	0.20	1.5801	1.7454	0.2304	2.9148	0.0275	0.2455
Plant-4	0.75	0.1152	0.40	1.1607	1.3142	0.2954	2.1947	-0.0101	0.3714
Plant-5	1.00	0.1010	0.20	1.7110	1.8726	0.2304	3.1272	-0.0293	0.2126
Plant-6	1.00	0.2087	0.40	1.1715	1.3934	0.2954	2.3270	-0.1008	0.3384
Plant-7	1.10	0.2550	0.40	1.1477	1.4099	0.2954	2.3545	-0.1363	0.3309
Plant-8	1.20	0.3068	0.40	1.1106	1.4205	0.2954	2.3723	-0.1711	0.3259

In Table 2.2, there are eight plant conditions based on different values of active power (P_{g0}) ranging from 0.40 pu to 1.20 pu and the transmission line reactance (X_l) from 0.20 to 0.40. The values of Heffron – Phillip constants ($K_1 - K_6$) is calculated and found that the value of K_5 becomes negative after and onwards plant-4 conditions. As per literature, the negative value of K_5

is responsible for reduced damping of the power system and results small signal oscillations. Generally, the SMIB model with operating conditions described in Plant-5 – Plant-6 are referred as nominal operating condition (NOC), Plant-1- Plant-4 as light operating condition (LOC) and Plant-6 – Plant-7 as heavy operating conditions (HOC) [191, 242, 243].

2.3.1.2. Simulation results without PSS

An SIMULINK based block diagram, including all the nonlinear blocks (Generator, Swing equation, AVR, Static excitation, field winding, electrical torque, generator terminal voltage, generator current during fault, PSS, limiter, simulate network during fault) are generated. The speed deviation ($\Delta\omega$) signal is taken as output. The SMIB power system with data in Table A.1 and plants under different operating condition as in Table 2.2 are simulated without controller for eight plants. The speed response due to Plant-1 – Plant-4 is shown in Figure 2.4 and that of with plant configuration Plant-5 – Plant-8 is shown in Figure 2.5.

2.3.1.3. Eigenvalue analysis without PSS

These eight plants are also subjected to evaluate the eigenvalue and only electromechanical modes of oscillations with least damping ratio are mentioned in Table 2.3. This table also includes the associated eigenvalue and the frequency of oscillation. On critical examination of Table 2.3; Plant-1 (P_{g0}=0.5 p.u. and X_l=0.2 p.u.) possesses oscillatory mode in left of s-plane with maximum damping ratio as 0.1213, therefore, its's performance is better with respect to other plant conditions. Similarly, Plant-8 (P_{g0}=1.2 p.u. and X_l=0.4 p.u.) have an oscillatory mode location in positive half of s-plane with damping ratio as -0.1075, which is comparatively least, negative and responsible for the most unstable performance of SMIB power system configuration.

Table 2.3: EMOs with least value of damping ratio and frequency (Hz): SMIB system without PSS

Power System Model	Eigenvalue	Damping ratio	Frequency (Hz)
Plant-1	-0.68385 ± 5.5947i	0.1213	0.8904
Plant-2	-0.34707 ± 4.9073i	0.0706	0.7810
Plant-3	-0.3863 ± 6.4598i	0.0597	1.0281
Plant-4	-0.043136 ± 5.6458i	0.0076	0.8986
Plant-5	-0.0015922 ± 6.8927i	0.0002	1.0970
Plant-6	0.36425 ± 6.0292i	-0.0603	0.9596
Plant-7	0.51961 ± 6.1121i	-0.0847	0.9728
Plant-8	0.66665 ± 6.1639i	-0.1075	0.9810

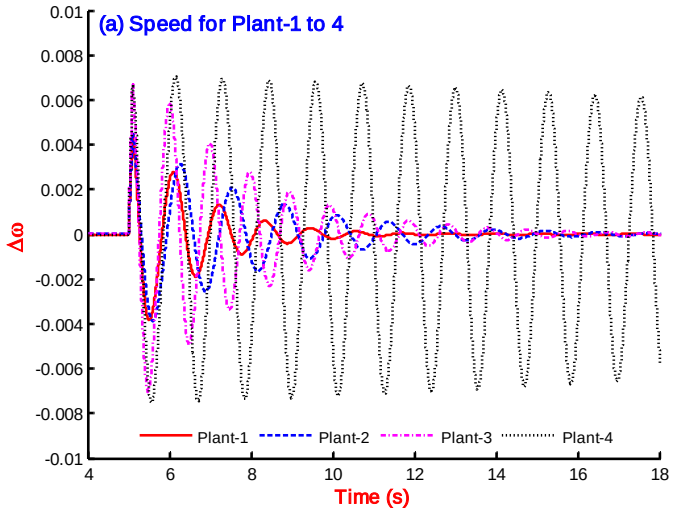

Figure 2.4: Speed response of SMIB systems for plant -1 to plant-4 without PSS

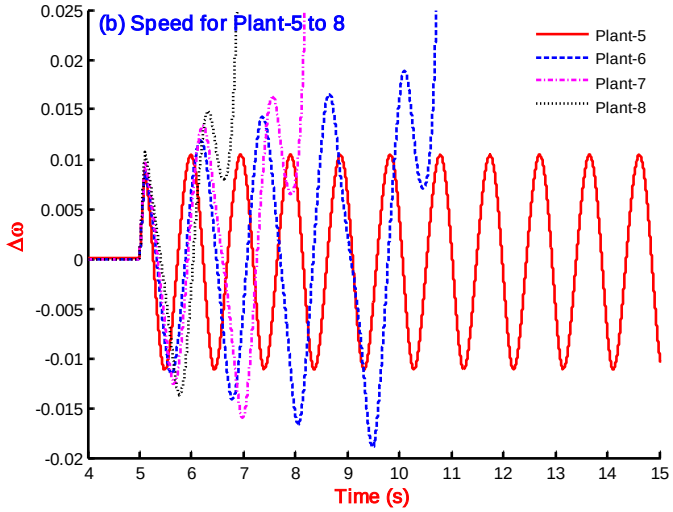

Figure 2.5: Speed response of SMIB systems for plant -5 to plant-8 without PSS

2.3.2. Two-area four-machine ten-bus system

2.3.2.1. Different plants creation

The nonlinear differential equations governing the behaviour of a power system can be linearized about a particular operating point to obtain a linear model which represents the small signal oscillatory response of a power system. Variations in the operating condition of the system result in the variations in the parameters of the small signal model. A given range of variations in the operating conditions of a particular system thus generates a set of linear models each corresponding to one particular operating condition. Since, at any given instant, the actual plant could correspond to any model in this set, a robust controller would have to import an adequate damping to each one of this entire set of linear models.

The single-line diagram of the two-area four-machine ten-bus power system is shown in Figure 1.14, which is a benchmark power system to study small signal oscillations [75, 244]. The line data, load flow and machine data are given Table A.2, Table A.3 and Table A.4, respectively. The above multimachine system is modelled using Simulink Toolbox with machine model 1.0. The test system (four-machine system) is considered with the wide range of operating conditions of power system and system connection configuration. Here, the different test models are created by changing the active power of generation, distributed load, line outage and fault at different bus location as in Table 2.4 and Table A.5, respectively.

In [245], two-area four-machine power system has been considered for small signal stability analysis. The system with same operating conditions with three different contingencies such as (a) short circuit test at the bus 8, (b) line outage between buses 8 and 9, and (c) 3-phase fault at bus 8 followed by a 100 ms transmission line outage between buses 8 and 9. In [14, 15], the system with one operating condition and three distinctive contingencies such as line outages has been considered. The eigenvalue analysis for system without PSS represents only one EMO with negative damping. In [16], the test of robustness has carried out using a different type of disturbances. Three system configurations have been considered in [19], but negative damping ratio is associated to only one condition where in the active power of a generator is changed.

Table 2.4: Plant configuration with different operating conditions and system configurations: Four-machine ten-bus power system

Power system	Active Power	Load	Remarks
Plant – 1	[7, 7, 7.2172, 7]	11.59 + j2.12; 15.75 + j2.88	Bus Structure as per Line diagram
Plant – 2	[7, 7, 7.2172, 7]	11.59 + j2.12; 15.75 + j2.88	Active power and load are same as in case-1 One line out in between bus no.9 and 10.
Plant – 3	[7.2, 7.1, 7.0, 6.9]	11.59 + j2.12; 15.75 + j2.88	Active power changed, Active load is same Bus Structure as per Line diagram
Plant – 4	[7.2, 7.1, 7.0, 6.9]	11.59 + j2.12; 15.75 + j2.88	Active power changed, Active load is same One line out in between bus no.7 and 10.
Plant – 5	[7.2, 7.1, 7.0, 6.9]	11.99 + j2.12; 15.45 + j2.88	Active power changed, Active load is changed, Bus Structure as per Line diagram
Plant – 6	[7.1, 6.9, 7.5, 6.5]	11.19 + j2.12; 15.95 + j2.88	Active power is changed, Active load is changed, Bus Structure as per Line diagram
Plant – 7	[7.1, 6.9, 7.5, 6.5]	11.19 + j2.12; 15.95 + j2.88	Active power is changed, Active load is changed, line out in between bus no.5 and 9.
Plant – 8	[5, 8, 6.2172, 8]	11.59 + j2.12; 15.75 + j2.88	Active power is changed, Active load is same, Bus Structure as per Line diagram

2.3.2.2. Simulation results without PSS

The response due to these eight plant conditions without PSS is required to be introduced; therefore, the plants are simulated and the sample responses for Plant-2 are shown in Figure 2.6. It can be seen that the simulation results of the generators are unstable and same hold for other plant conditions.

2.3.2.3. Eigenvalue analysis without PSS

The system eigenvalue are determined without PSS to verify the unstable behaviour of a system under different plant configurations. The electromechanical modes of oscillations with least damping ratio associated to each generator for each plant condition are shown in Table 2.5. It can be seen that the plants are having negative damping terms, which are responsible for the system (or plant) response to become unstable. In each plant condition, two generators are having negative damping, resulting the inter-area and intra area mode of oscillations to be unstable. Therefore, the configured system can show effective and robust performance of PSS.

Table 2.5: EMOs with least value of damping ratio and frequency (Hz) for each generator of Plant-1 and 2 configurations

Eigenvalue	Damping ratio	Frequency (Hz)	Eigenvalue	Damping ratio	Frequency (Hz)
Plant-1			Plant-2		
-10.091 ± 19.166i	0.46587	3.0503	-10.091 ± 19.155i	0.46608	3.0487
-0.11544 ± 0.92409i	0.12396	0.14707	-0.11033 ± 0.86726i	0.1262	0.13803
0.17831 ± 0.90664i	-0.19298	0.1443	0.1665 ± 0.85619i	-0.19089	0.13627
0.037034 ± 0.87288i	-0.04239	0.13892	0.036963 ± 0.87612i	-0.04215	0.13944
Plant-3			Plant-4		
-10.091 ± 19.164i	0.46591	3.05	-10.093 ± 19.045i	0.46827	3.031
-0.11594 ± 0.92522i	0.12433	0.14725	-0.12103 ± 0.9242i	0.12985	0.14709
0.17894 ± 0.90783i	-0.19338	0.14449	0.18193 ± 0.90757i	-0.19655	0.14444
0.036878 ± 0.87042i	-0.04233	0.13853	0.033524 ± 0.81543i	-0.04108	0.12978
Plant-5			Plant-6		
-10.091 ± 19.16i	0.46599	3.0494	-10.091 ± 19.169i	0.46581	3.0508
-0.11364 ± 0.92765i	0.1216	0.14764	-0.11804 ± 0.91976i	0.1273	0.14638
0.17698 ± 0.91081i	-0.19074	0.14496	0.18003 ± 0.90134i	-0.19587	0.14345
0.037195 ± 0.87207i	-0.04261	0.13879	0.036513 ± 0.86894i	-0.04198	0.1383
Plant-7			Plant-8		
-10.093 ± 19.075i	0.46767	3.0359	-10.09 ± 19.204i	0.46512	3.0563
-0.13539 ± 0.89947i	0.14885	0.14315	-0.076916 ± 0.91241i	0.084002	0.14522
0.19292 ± 0.87705i	-0.21483	0.13959	0.13999 ± 0.90482i	-0.15289	0.14401
0.036335 ± 0.87181i	-0.04164	0.13875	0.038657 ± 0.88314i	-0.04373	0.14056

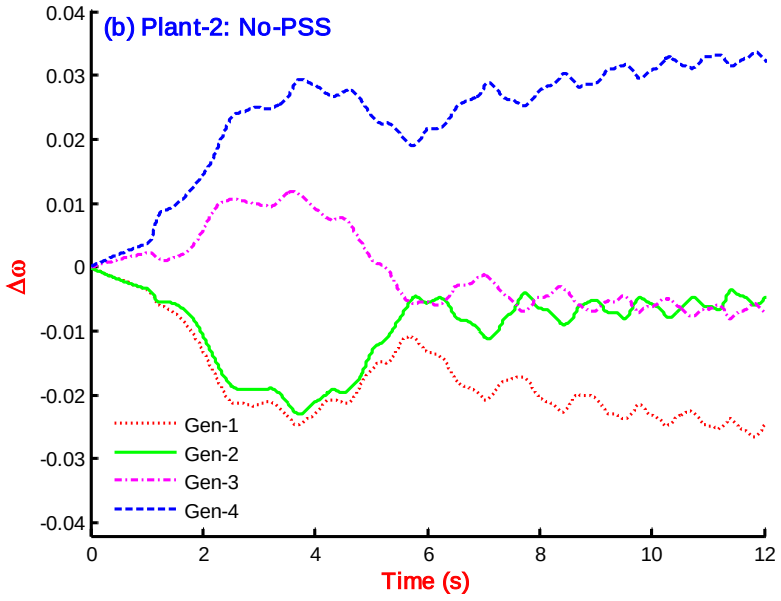

Figure 2.6: Speed response for Plant-2 configuration of four-machine system without PSS

2.3.3. IEEE New England Ten-Machine System

2.3.3.1. Different plant creation

In [142], the stabilization of the ten-machine power system is demonstrated by considering three different loading conditions labelled as nominal, light and heavy. These loading conditions were obtained by varying the load admittances of the system. Generator G_1 has been considered as an equivalent power source representing parts of the U.S.-Canadian interconnection power system. The system response without PSS has been reported as highly oscillatory which in turn represents poor damping of the system [233]. In [20, 21, 23], three system configurations have been considered such as base case and other two with line outages. The base case involves two unstable electromechanical oscillatory modes (EMOs), on the other hand, case-1 and case-2 represents three unstable EMOs of the system without PSSs. The system configuration with base case and with three cases involving line outages have been considered in [138]. The base case, case-1 and case-2 involve EMOs as above without PSS condition, while that of with case-3 four EMOs have been representing an unstable oscillatory response [24, 138]. In [149], the three system configuration such as base case, case-1 and case-2 has been considered; where in the two EMOs to each case resembles non acceptable damping ratios.

Table 2.6: I - Plant configuration with different operating conditions and system configurations: Ten-machine thirty nine-bus power system

Plant	Active Power	Load	Fault Location
1	[5.519816; 10.00; 6.5000; 5.08000; 6.3200; 6.50000; 5.60000; 5.4000; 8.3000; 2.5000]	[(0.0920 + j0.04600), (11.0400 + j2.5000); (3.22000 + j0.02400), (5.000 + j1.84000), (2.3380 + j0.8400); (5.2200 + j1.7600), (2.7400 + j1.1500), (2.74500 + j0.84660); (3.08600 + j0.92200), (2.24000 + j0.47200), (1.3900 + j0.17000); (2.81000 + j0.75500), (2.0600 + j0.27600), (2.83500 + j0.26900); (6.28000 + j1.03000), (.07500 + j0.88000), (3.20000 + j1.5300); (3.29400 + j0.32300), (1.58000 + j0.30000)]	Bus No. – 16 Base case for active power and active load
2	[5.519816; 10.0; *6.6000*; 5.08000; *6.1200*; 6.5000; 5.60000; 5.4000; 8.30000; 2.5000]	[(0.0920 + j0.04600),(*11.2400 + j2.5000*); (*3.02000 + j0.02400*), (5.000 + j1.84000), (2.3380 + j0.8400); (5.2200 + j1.7600), (2.7400 + j1.1500), (2.74500 + j0.84660); (3.08600 + j0.92200), (2.24000 + j0.47200), (1.3900 + j0.17000); (*2.61000 + j0.75500*), (*2.2600 + j0.27600*), (2.83500 + j0.26900); (6.28000 + j1.03000), (.07500 + j0.88000), (3.20000 + j1.5300); (3.29400 + j0.32300), (1.58000 + j0.30000)]	Bus No. – 13 Active power of Gen -3 and 5 are changed. Active load of Gen - 1 and 2 are changed.
3	[*5.419816*; *10.10*; *6.4000*; *5.18000*; 6.32000; 6.5000; 5.60000; 5.4000; 8.3000; 2.50000]	[(0.2920 + j0.04600),(11.0400 + j2.5000); (3.22000 + j0.02400), (5.000 + j1.84000), (*2.1380 + j0.8400*); (5.2200 + j1.7600), (2.7400 + j1.1500), (2.74500 + j0.84660); (*3.28600 + j0.92200*),(2.0400 + j0.47200), (1.3900 + j0.17000); (2.81000 + j0.75500), (2.0600 + j0.27600), (2.83500 + j0.26900); (6.28000 + j1.03000), (.07500 + j0.88000), (3.20000 + j1.5300); (3.29400 + j0.32300), (1.5800 + j0.30000)]	Bus No. – 11 Active power of Gen – 1, 2, 3 and 4 are changed. Active load of Gen - 2 and 4 are changed.
4	[5.519816; 10.00; 6.5000; 5.08000; 6.32000; 6.5000; *5.50000*; *5.5000*; 8.3000; 2.50000]	[(0.0920 + j0.04600),(11.0400 + j2.5000); (3.22000 + j0.02400), (5.000 + j1.84000), (2.3380 + j0.8400); (5.2200 + j1.7600), (2.7400 + j1.1500), (2.74500 + j0.84660); (3.08600 + j0.92200),(2.24000 + j0.47200), (1.3900 + j0.17000); (*2.61000 + j0.75500*), (2.2600 + j0.27600), (2.83500 + j0.26900); (*6.18000 + j1.03000*), (*0.17500 + j0.88000*), (3.20000 + j1.5300); (3.29400 + j0.32300), (1.58000 + j0.30000)]	Bus No. – 9 Active power of Gen – 7 and 8 are changed. Active load of Gen - 5 and 6 are changed.

Table 2.7: II - Plant configuration with different operating conditions and system configurations: Ten-machine thirty nine-bus power system

Plant	Active Power	Active Load	Fault Location
5	[5.519816; *10.10*; 6.50; 5.080; 6.320; 6.500; *5.500*; 5.400; 8.300; 2.500;]	[(0.0920 + j0.0460), (11.040 + j2.50); (3.220 + j0.0240), (5.00 + j1.840), (2.3380 + j0.8400); (5.220 + j1.760), (2.7400 + j1.150), (2.7450 + j0.84660); (3.0860 + j0.9220), (2.240 + j0.4720), (1.390 + j0.170); (2.810 + j0.7550), (2.060 + j0.2760), (2.8350 + j0.2690); (6.380 + j1.030), (.0750 + j0.880), (*3.100 + j1.530*); (*3.1940 + j0.3230*), (*1.680 + j0.30*)]	Bus No. – 7 Active power of Gen – 2 and 7 are changed. Active load of Gen - 6 and 7 are changed.
6	[5.619816; 10.0; *6.40*; 5.080; 6.32; 6.50; 5.60; 5.40; *8.40*; *2.40*]	[(0.0920 + j0.0460),(11.040 + j2.50); (3.220 + j0.0240),(5.0 + j1.840), (2.3380 + j0.840); (5.220 + j1.760), (2.740 + j1.150), (2.7450 + j0.84660); (*3.1860 + j0.9220*), (*2.140 + j0.4720*), (*1.490 + j0.170*); (*2.710 + j0.7550*), (2.060 + j0.2760), (2.8350 + j0.2690); (*6.380 + j1.030*), (.0750 + j0.880), (*3.10 + j1.530*); (*3.1940 + j0.3230*), (*1.680 + j0.30*)]	Bus No. – 17 Active power of Gen – 3, 9 and 10 are changed. Active load of Gen - 4, 5, 6 and 7 are changed.
7	[*5.619816*; 10.00; 6.50; *5.180*; *6.420*; *6.40*; 5.60; 5.40; 8.30; 2.50]	[(0.0920 + j0.0460),(11.040 + j2.50); (*3.120 + j0.0240*),(5.0+j1.840), (2.3380 + j0.840); (5.220 + j1.760), (2.740 + j1.150), (2.7450 + j0.84660); (3.0860 + j0.92200), (*2.340 + j0.4720*), (1.390 + j0.170); (2.810 + j0.7550), (2.060 + j0.2760), (2.8350 + j×.2690); (*6.380 + j1.030*), (.0750 + j0.880), (*3.10 + j1.530*); (3.2940 + j0.3230), (1.580 + j0.30)]	Bus No. – 19 Active power of Gen – 1,4, 5 and 6 are changed. Active load of Gen - 2, 4 and 6 are changed.
8	[5.519816; 10.0; 6.50; *5.180*; *6.220*; *6.40*; *5.60*; 5.50; 8.30; 2.50]	[(0.0920 + j0.0460),(11.040 + j2.50); (3.220 + j0.0240),(5.00 + j1.840), (2.3380 + j0.840); (*5.3200 + j1.760*), (*2.640 + j1.150*), (2.7450 + j0.84660); (3.0860 + j0.9220), (2.240 + j0.4720), (1.390 + j0.170); (*2.710 + j0.7550*), (*2.160 + j0.2760*), (2.8350 + j0.2690); (6.280 + j1.030), (.0750 + j0.880), (3.20000 + j1.5300); (*3.1940 + j0.3230*), (*1.680 + j0.30*)]	Bus No. – 21 Active power of Gen – 4, 5, 6 and 7 are changed. Active load of Gen - 3, 5 and 7 are changed.

The response of three cases of the system in [246], resembles same as in [23] in terms of EMOs without PSS. In [247], the system data have been considered as in [248] and two contingencies as (a) three-phase fault for 0.10s at bus 29 at the end of line 26-29 and (b) three-phase fault for 0.15s at bus 15 at the end of line 14-15. In [25], the system is design using a set of data then to check robustness different short of disturbances have been applied. In the 4-machine 10-bus power system as well in the 10-machine 39-bus power system, a set of varying active power, active load, bus structure and type of faults should be considered to check the robustness test of these systems.

The single-line diagram of the 10-machine 39-bus power system is shown in Figure 1.15. The machine data, load flow data, transformer data and line data are given Table A.6, Table A.7, Table A.9, Table A.10, respectively. The multimachine system is modelled using Simulink Toolbox of MATLAB with machine model 1.0. The test system (ten-machine system) is considered with a wide range of operating conditions of power system and system connection configuration. Here, the different test models are created by a fault at different bus location as in Table A.8. The different plant configurations to cover the wide range of operating conditions by changing the active power of generation, distributed load and fault location are considered as in Table 2.6 - Table 2.7.

2.3.3.2. Simulation results without PSS

The response due to these eight plant conditions without PSS is required to be introduced; therefore, the plants are simulated in MATLAB Software. The speed deviation ($\Delta\omega$) responses of all generators of the plant configurations of the ten-machine power system without PSS are showing unstable behaviour. As a sample due to space limitation, the response of Plant-3 under without PSS is shown in Figure 2.7. The response of each generator is unstable for system without PSS for all eight plant configurations.

2.3.3.3. Eigenvalue analysis without PSS

In this section, the eigenvalue analysis of the system for all plant conditions without PSS is carried out and enlisted in Table 2.8. The eigenvalue plot on s-plane for Plant-3 is shown in Figure 2.8, where in much of EMOs are in the right-hand side (RHS) of s-plane, proving system response to be unstable as in Figure 2.7. Moreover, the EMOs enlisted in Table 2.8 for Plant-3 are with positive real part resulting negative damping to the system. The electromechanical modes of oscillations with least damping ratio associated to each generator for each plant are shown in Table 2. 8; where in the negative value of damping ratio is the responsible factor of unstable speed

responses. In this section 2.3, three power system, have been considered with wide operating range by considering eight plant configurations and contingencies. These are proved to be hard conditions to design and evaluate the performance of PSS to make system stable.

Table 2.8: EMOs with least value of damping ratio and frequency (Hz) for each generator of Plant-1 without PSS

Eigenvalue	Damping ratio	Freq. (Hz)	Eigenvalue	Damping ratio	Freq. (Hz)
Plant-1			Plant-2		
0.026873 ± 11.871i	-0.0022637	1.8894	0.02681 ± 11.875i	-0.0022577	1.8899
0.027162 ± 9.8481i	-0.0027581	1.5674	0.026213 ± 9.8538i	-0.0026602	1.5683
0.03367 ± 9.9563i	-0.0033818	1.5846	0.033567 ± 9.9599i	-0.0033702	1.5852
0.067202 ± 8.6842i	-0.0077382	1.3821	0.067 ± 8.6869i	-0.0077126	1.3826
0.065865 ± 8.161i	-0.0080704	1.2989	0.066103 ± 8.1645i	-0.008096	1.2994
0.10292 ± 7.7315i	-0.013311	1.2305	0.10235 ± 7.7353i	-0.013231	1.2311
0.15237 ± 6.8654i	-0.022188	1.0927	0.15249 ± 6.8685i	-0.022196	1.0932
0.37096 ± 6.3793i	-0.058052	1.0153	0.3728 ± 6.3755i	-0.058375	1.0147
0.17995 ± 4.1924i	-0.042883	0.66724	0.17945 ± 4.1951i	-0.042738	0.66767
Plant-3			Plant-4		
0.027335 ± 9.846i	-0.0027763	1.567	0.027278 ± 11.87i	-0.0022981	1.8892
0.033953 ± 9.9513i	-0.0034119	1.5838	0.026881 ± 9.8538i	-0.0027279	1.5683
0.066858 ± 8.6894i	-0.0076939	1.383	0.033121 ± 9.9597i	-0.0033254	1.5851
0.0651 ± 8.16i	-0.0079777	1.2987	0.067799 ± 8.681i	-0.0078098	1.3816
0.10463 ± 7.7246i	-0.013544	1.2294	0.066158 ± 8.1586i	-0.0081088	1.2985
0.15161 ± 6.8661i	-0.022075	1.0928	0.10207 ± 7.7369i	-0.013191	1.2314
0.37083 ± 6.38i	-0.058025	1.0154	0.15239 ± 6.8653i	-0.022192	1.0926
0.18007 ± 4.1928i	-0.042909	0.6673	0.37332 ± 6.3729i	-0.05848	1.0143
0.027335 ± 9.846i	-0.0027763	1.567	0.18005 ± 4.1929i	-0.042902	0.66731
Plant-5			Plant-6		
0.02686 ± 11.872i	-0.0022626	1.8894	0.026984 ± 11.872i	-0.0022728	1.8895
0.027355 ± 9.8453i	-0.0027785	1.5669	0.027354 ± 9.8451i	-0.0027784	1.5669
0.03313 ± 9.9593i	-0.0033266	1.5851	0.033656 ± 9.9568i	-0.0033802	1.5847
0.067159 ± 8.6844i	-0.007733	1.3822	0.067317 ± 8.6871i	-0.0077488	1.3826
0.065769 ± 8.1623i	-0.0080574	1.2991	0.065789 ± 8.162i	-0.0080602	1.299
0.10269 ± 7.7319i	-0.013281	1.2306	0.10313 ± 7.7301i	-0.01334	1.2303
0.15219 ± 6.8664i	-0.022159	1.0928	0.15213 ± 6.866i	-0.022152	1.0928
0.37103 ± 6.3794i	-0.058062	1.0153	0.37503 ± 6.375i	-0.058726	1.0146
0.17962 ± 4.1937i	-0.042793	0.66745	0.18052 ± 4.1924i	-0.04302	0.66724
Plant-7			Plant-8		
0.02696 ± 11.873i	-0.0022707	1.8896	0.027265 ± 11.869i	-0.0022971	1.8891
0.027666 ± 9.8486i	-0.0028092	1.5675	0.02662 ± 9.8534i	-0.0027016	1.5682
0.033537 ± 9.96i	-0.0033671	1.5852	0.033485 ± 9.96i	-0.0033619	1.5852
0.067204 ± 8.6847i	-0.007738	1.3822	0.067847 ± 8.6811i	-0.0078153	1.3816
0.066083 ± 8.1644i	-0.0080938	1.2994	0.066125 ± 8.158i	-0.0081052	1.2984
0.1034 ± 7.7337i	-0.013369	1.2309	0.10284 ± 7.7349i	-0.013295	1.231
0.15313 ± 6.8664i	-0.022296	1.0928	0.15268 ± 6.864i	-0.022238	1.0924
0.37063 ± 6.3811i	-0.057985	1.0156	0.37206 ± 6.3763i	-0.058251	1.0148
0.18026 ± 4.1931i	-0.042949	0.66736	0.17996 ± 4.1925i	-0.042886	0.66726

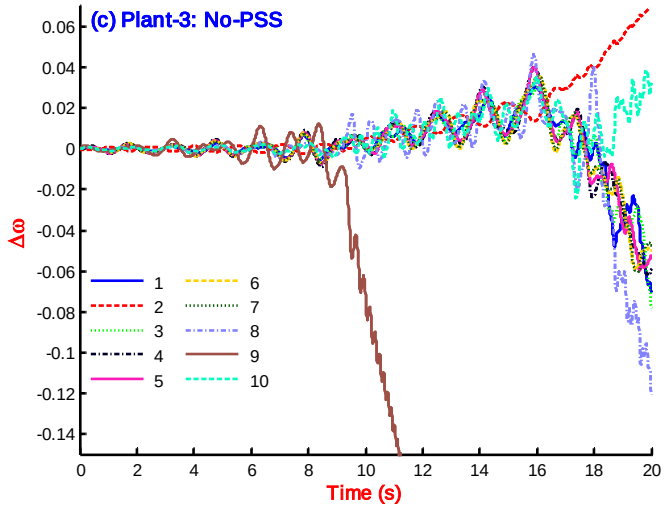

Figure 2.7: Speed response for Plant-3 configuration of ten-machine system without PSS

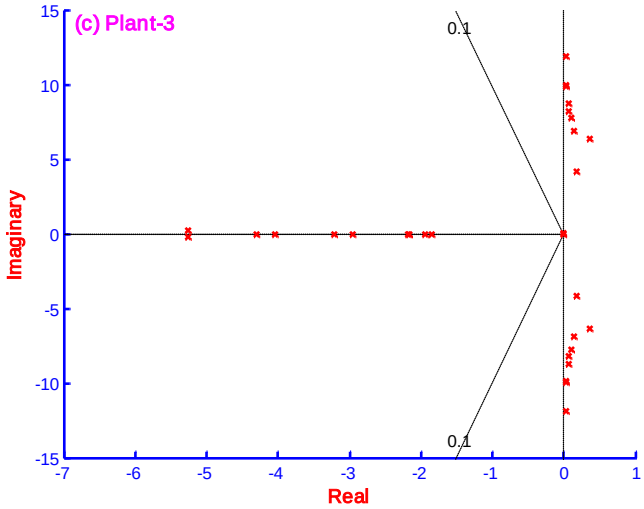

Figure 2.8: Eigenvalue plot for plant-3 configuration of ten-machine system without PSS

2.4. Design and Performance Analysis: SMIB System

2.4.1. Design of CPSS using bat algorithm

In order to assess effectiveness the proposed BA-CPSS algorithm is programmed in MATLAB environment and executed on Intel (R) Core (TM) - 2 Duo CPU T6400 @ 2.00 GHz with 3 GB RAM, 32-bit operating system. Bat algorithm steps necessary to illustrate working in optimization problems is mentioned in section 1.2.2 on page 21. However, the important step for optimization of the CPSS parameters is to select initializing parameters to the algorithm. In [182, 249], the generally opted to initialize parameters for BA are intensity (A) and pulse rate (r) as 0.5 and 0.5, respectively. The both parameters are varied in several combinations; after examine and rejection,

the suitable values to these parameters are selected as A = 0.9 and r = 0.1for CPSS optimization. The other constraint such as initializing population is selected as n = 25 and the bandwidth are considered as $f_{\min} = 0$ and $f_{\max} = 2.0$. The plant (SMIB power system) operating at nominal operating condition (where in X_l = 0.4 pu and P_{g0} = 1.0 pu) is considered for optimal tuning of CPSS parameters as reported in [191]; subjected to the eigenvalue based objective function with the parametric bounds as $0.00 \leq K \leq 50$, $0.2 \leq T_1 \leq 1.5$, $0.02 \leq T_2 \leq 0.15$, $0.2 \leq T_3 \leq 1.5$ and $0.02 \leq T_4 \leq 0.15$. The optimized parameters and the value of objective function for a plant at nominal operating condition are represented in Figure 2.9(a) - Figure 2.11(b) for 200 iterations. It can be seen that the 40 iterations are sufficient because fitness function value is almost constant at 40 and above iterations. The optimized CPSS parameters are enlisted in Table 2.9.

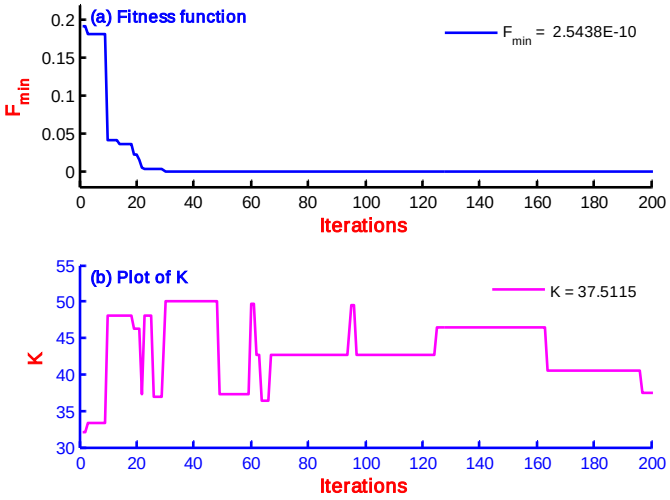

Figure 2.9: Performance of bat algorithm for (a) Fitness function and, (b) Gain, K

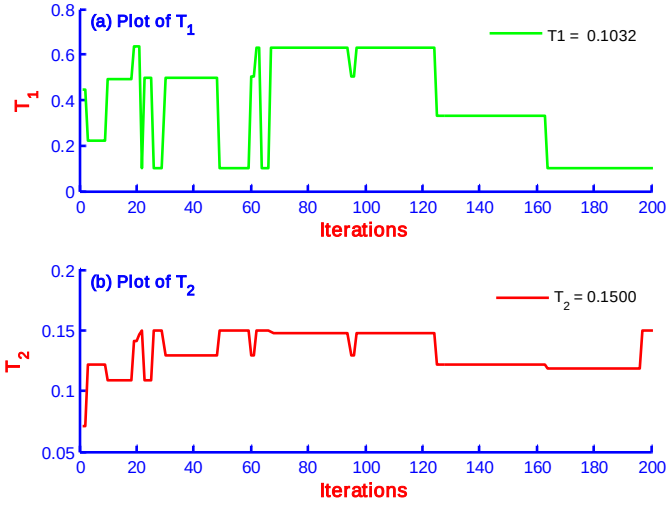

Figure 2.10: Performance of bat algorithm for (a) T_1 and, (b) T_2

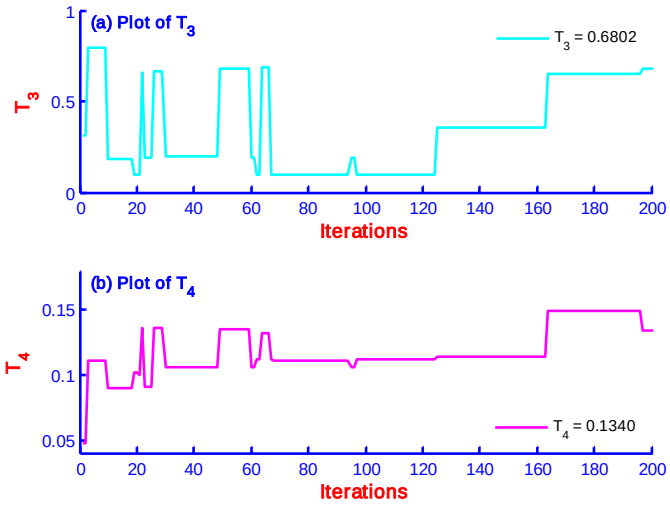

Figure 2.11: Performance of bat algorithm for (a) T_3 and, (b) T_4

Table 2.9: Comparison of controller parameters: CPSSs reported in literature and BA-CPSS

Algorithm	Controller	K	T_1	T_2	T_3	T_4
Tabu search [2]	TS-CPSS	18.247	0.2697	0.100	-	-
RCGA [3]	RCGA-CPSS	17.896	0.2770	0.05	-	-
Genetic Algorithm [4]	GA-CPSS	11.24989	0.14094	0.05	-	-
LMI Approach [5]	LMI-CPSS	28.6	1.0526	0.091743	-	-
Particle swarm opt. [6]	PSO-CPSS	47.95	0.3175	0.077	-	-
Breeder Genetic [7]	BGA-CPSS	18.8838	3.7604	1.7390	-	-
Genetic Algorithm [8]	GA-CPSS	24.3748	0.2671	0.05	0.0679	0.05
Bacteria Foraging [8]	BFA-CPSS	22.0277	0.2527	0.05	0.0784	0.05
Simulated Ann. [9]	SA-CPSS	19.049	0.1393	0.05	0.2634	0.05
Robust SA [9]	RSA-CPSS	33.387	0.1418	0.05	0.2131	0.05
Differential Evolution [10]	DE-CPSS	20.4573	0.2000	0.1500	0.2000	0.0280
Strength Pareto [11]	SPEA-CPSS	70.9	0.36	0.04	0.33	5.81
Bat algorithm (Proposed)	BA-CPSS	37.5115	0.1032	0.1500	0.6802	0.1340

2.4.2. Reported CPSSs in literature

In 1998 - 2013, CPSS parameters in single-stage and double-stage along with a washout block have been tuned using different methods of optimization techniques. The pioneer work of parameter optimization using evolutionary techniques has been carried out by Dr. Abido in 1998 [4]. For ready reference and comparison purposes, the single stage and double stage CPSS parameters are enlisted in Table 2.9. The gain (K) and zero-pole ($T_1 - T_2$) parameters of CPSS are tuned by using Tabu search algorithm [2], Real Coded Genetic Algorithm (RCGA) [3], Genetic Algorithm [4] ,LMI Approach [5], Particle swarm optimization (PSO) [6], and Breeder Genetic algorithm [7]. Similarly, the CPSS parameters of double-stage (lead-lag type) viz. gain (K) and zero-pole ($T_1 - T_4$) have been designed using Genetic Algorithm [8], Bacteria Foraging algorithm

[8], Simulated Annealing [9], Robust Simulated Annealing [9], Differential Evolution [10] and Strength Pareto evolutionary algorithms [11] as in Table 2.9. The detail of objective functions used by with these methods for optimization have been given in section 1.3. The proposed controller parameters have also been included in this table for comparison purpose; while, the detail on optimization have already been given in section 2.4.1.

2.4.3. Response Comparison

In this section, the speed response of the SMIB power system at nominal operating condition (plant-6) is compared for CPSSs reported in literature [2-11] as in Table 2.9 and with the designed BA-CPSS. In Figure 2.12; the speed response with BA-CPSS is compared to the system response with the CPSS designed by Tabu search algorithm [2], Real coded genetic algorithm [3], Genetic Algorithm [4] and LMI Approach[5] and found as superior in terms of improved settling time (Table 2.10) and performance indices (as defined in section 1.4 on page 28). The same speed response with BA-CPSS is also compared with the CPSSs designed using particle swarm optimization [6], Breeder Genetic algorithm [7], Genetic Algorithm [8] and Bacteria Foraging algorithm [8] and found superior in performance as shown in Figure 2.13. It is also compared to the CPSSs designed using Simulated Annealing [9], Robust simulated annealing [9], Differential Evolution [10] and Strength-pareto evolutionary algorithm [11] in Figure 2.14 and also outperformed with a good degree of difference. It can be seen from the Table 2.10 that the performance with BGA-CPSS is worst as compared to others, but it is better to open loop system (without PSS) response. The graphical observation for settling time is always doubtful for its accuracy; therefore, it is better to consider performance indices recorded over the simulation time. The performance indices (ITAE, IAE and ISE) for the system response with CPSSs [2-11] and BA-CPSS is observed for 40 seconds; however, the speed response in Figure 2.12 - Figure 2.14 is scaled only for 10 seconds because of clarity constraint. It should be cleared that the comparatively lesser value of the PIs represents the better performance. On critical examination of Table 2.10, it is clear that the associated PIs (ITAE, IAE and ISE) for the speed response of the system with proposed BA-CPSS are much smaller as compared to CPSSs reported in literature [2-11]. The settling time of the system response with BA-CPSS is recorded as 6.96 seconds, which is lowest to the controllers in subject. In Figure 2.12, the overshoot reported to be minimum in first negative peak, but the settling time is 9.57 seconds. The PI values associated to the system response with BA-CPSS are 0.0195, 0.0036 and 1.6862×10^{-5} for ITAE, IAE and ISE, respectively. These values are comparatively lower in magnitude, proving enhanced performance as compared to other controllers in subject.

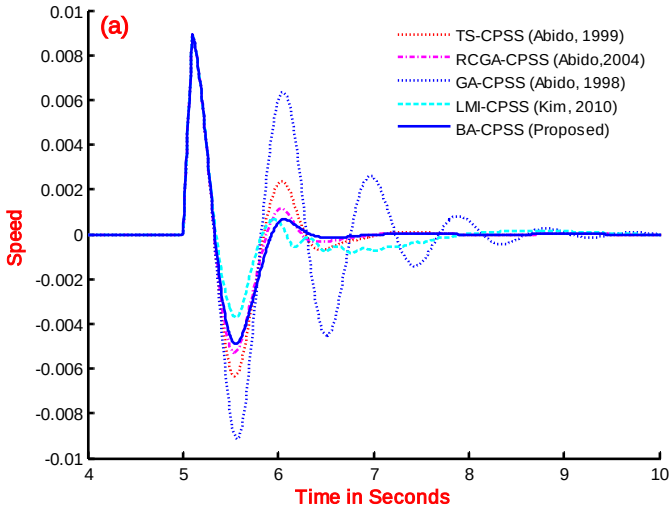

Figure 2.12: Speed response comparison: SMIB system with TS-CPSS, RCGA-CPSS, GA-CPSS, LMI-CPSS and BA-CPSS

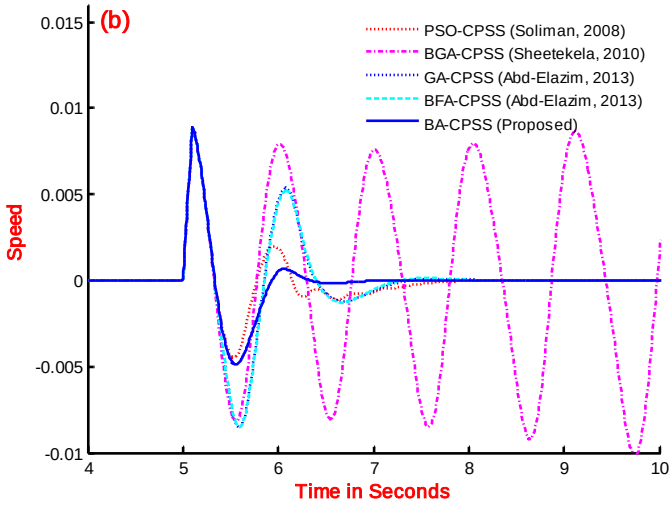

Figure 2.13: Speed response comparison: SMIB system with PSO-CPSS, BGA-CPSS, GA-CPSS, BFA-CPSS and BA-CPSS

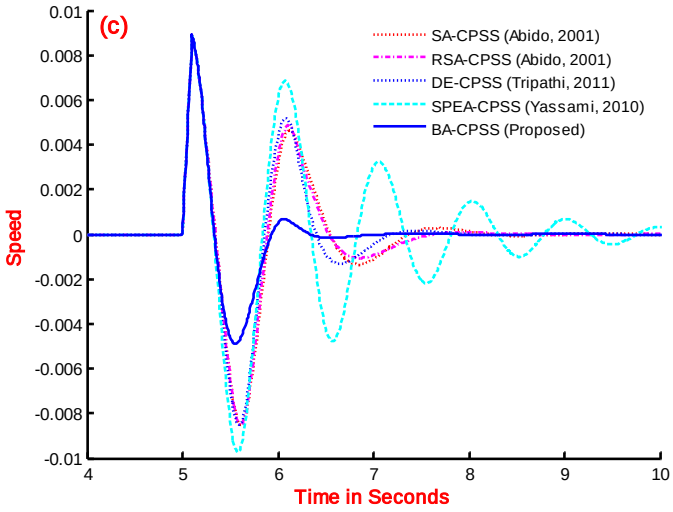

Figure 2.14: Speed response comparison: SMIB system with SA-CPSS, RSA-CPSS, DE-CPSS, SPEA-CPSS and BA-CPSS

Table 2.10: Performance indices based comparison of speed response with CPSSs reported in literature and BA-CPSS

Algorithms	Controller	Settling time (s)	ITAE	IAE	ISE
Tabu search [2]	TS-CPSS	7.71	0.0257	0.0046	2.1425×10^{-05}
RCGA [3]	RCGA-CPSS	7.14	0.0207	0.0038	1.7582×10^{-05}
Genetic Algorithm[4]	GA-CPSS	> 10	0.0569	0.0093	4.6257×10^{-05}
LMI Approach [5]	LMI-CPSS	9.57	0.0230	0.0039	1.3903×10^{-05}
Particle swarm opt. [6]	PSO-CPSS	9.15	0.0243	0.0043	1.6009×10^{-05}
Breeder Genetic [7]	BGA-CPSS	Osc.for > 18	3.6360	0.1942	2.0516×10^{-03}
Genetic Algorithm [8]	GA-CPSS	8.25	0.0384	0.0067	3.5450×10^{-05}
Bacteria Foraging [8]	BFA-CPSS	8.09	0.0382	0.0067	3.5138×10^{-05}
Simulated Anneal. [9]	SA-CPSS	8.75	0.0414	0.0071	3.5773×10^{-05}
Robust SA [9]	RSA-CPSS	7.69	0.0396	0.0068	3.5157×10^{-05}
Differential Evolution [10]	DE-CPSS	7.98	0.0382	0.0067	3.5089×10^{-05}
Strength Pareto [11]	SPEA-CPSS	>10	0.0732	0.0114	5.4897×10^{-05}
BA-CPSS (Proposed)	BA-CPSS	6.96	0.0195	0.0036	1.6862×10^{-05}

2.4.4. Eigenvalue Comparison

In previous section, the effectiveness of system performance with BA-CPSS over other controllers [2-11] has been validated in terms of settling time and performance indices. In this section, the eigenvalue comparison is to be carried out for SMIB power system with nominal operating conditions for all controllers as mentioned in Table 2.9. The power system programmed in MATLAB Software (m-file and Simulink) is run to determine *A, B, C* and *D* matrices using 'linmod' command of the software. To determine eigenvalue of the system 'eig' function of software is used. Some of the resulting eigenvalue have only real parts (negative) with damping ratio as 1.0, therefore, are not of interest. The complex conjugate eigenvalue are responsible for oscillations of the system response, and are enlisted in Table 2.11. As per literature, the desirable damping ratio of the system should be more than 0.1 [3, 7, 19, 23, 186]. The electromechanical eigenvalue of the system without PSS for the operating condition (plant-6 in Table 2.2) is 0.36425 ± 6.0292i, and the associated damping ratio are -0.0603, for which the nonlinear time domain response is unstable. On application of CPSSs in literature [2-11], is increased appreciable as compared to that of the system without PSS. However, the BA-CPSS shift substantially the electromechanical mode eigenvalue to the left of the s-plane as -3.6887 ± 4.0759i and damping ratio as 0.67101. It demonstrates that the BA-CPSS by a considerable amount enhances the system stability and improves the damping characteristics of electromechanical modes greatly as compared with the open-loop system. In addition, the value of minimum damping ratio with the proposed controller (BA-CPSS) is greater compared to CPSSs [2-11]. This illustrates the potential and superiority of the proposed design approach to get optimal set of PSS parameters. The performance if marginally improved with respect to RSA-CPSS and RCGA-CPSS and appreciably as compared to SPEA-CPSS, GA-CPSS and BGA-CPSS.

Table 2.11: Comparison of Eigen value, damping factor and frequency of oscillations of the system with different controllers

Algorithms	Controller	Eigen value	Damping ratio	Frequency (Hz)
Tabu search [2]	TS-CPSS	-4.6839 + 10.008i	0.42388	1.5929
RCGA [3]	RCGA-CPSS	-7.2626 +12.212i	0.51116	1.9436
Genetic Algorithm [4]	GA-CPSS	-1.242 + 6.8422i	0.1786	1.089
LMI Approach [5]	LMI-CPSS	-1.4667 - 24.185i	0.060534	3.8492
Particle swarm opt. [6]	PSO-CPSS	-3.0709 + 19.257i	0.15748	3.0649
Breeder Genetic [7]	BGA-CPSS	-1.0821 - 10.266i	0.10482	1.6339
Genetic Algorithm [8]	GA-CPSS	-8.4677 - 16.808i	0.44991	2.6751
Bacteria Foraging [8]	BFA-CPSS	-9.6089 + 16.73i	0.49805	2.6626
Simulated Anneal. [9]	SA-CPSS	-10.238 - 22.53i	0.41369	3.5858
Robust SA [9]	RSA-CPSS	-8.1326 + 26.018i	0.29834	4.141
Differential Evolution [10]	DE-CPSS	-2.5982 + 3.8795i	0.55646	0.61744
Strength Pareto [11]	SPEA-CPSS	-0.80353 -6.4514i	0.1236	1.0268
BA-CPSS (Proposed)	BA-CPSS	-3.6887 ± 4.0759i	0.67101	0.64871

2.4.5. Speed and other signal behaviour with BA-CPSS

In section 2.4.2 – 2.4.4, the proposed BA-CPSS have been proved to be superior to CPSS in literature [2-11], through nonlinear simulation results and eigenvalue analysis. However, the system operating conditions were restricted to nominal, i.e. plant-6. In this section, the performance of the proposed BA-CPSS is carried out with eight plant conditions, to examine robust operation over the wide range of operating conditions. The speed response, control voltage signals due to CPSS and generator terminal voltages are shown in Figure 2.15, Figure 2.16 and Figure 2.17, respectively. These figures demonstrate the effective and robust performance of proposed BA-CPSS by giving a stable response with all plant conditions. The eigenvalue analysis of the SMIB power system with proposed BA-CPSS for all eight plant conditions is given in Table 2.12. On comparing the damping ratio of the system without PSS, it is greatly improved by BA-CPSS.

Table 2.12: EMOs with least damping ratio and frequency: SMIB system with eight plant configuration with BA-CPSS

Power system model	Eigenvalue	Damping ratio	Frequency in Hz
Plant-1	-8.5807 ± 5.4451i	0.84434	0.86661
Plant-2	-3.0846 ± 2.9525i	0.72241	0.4699
Plant-3	-9.3413 ± 6.9473i	0.80241	1.1057
Plant-4	-3.7863 ± 3.321i	0.75179	0.52855
Plant-5	-9.4109 ± 7.4977i	0.78212	1.1933
Plant-6	-3.6887 ± 4.0759i	0.67101	0.64871
Plant-7	-3.5128 ± 4.346i	0.62862	0.69169
Plant-8	-3.3035 ± 4.5746i	0.58545	0.72808

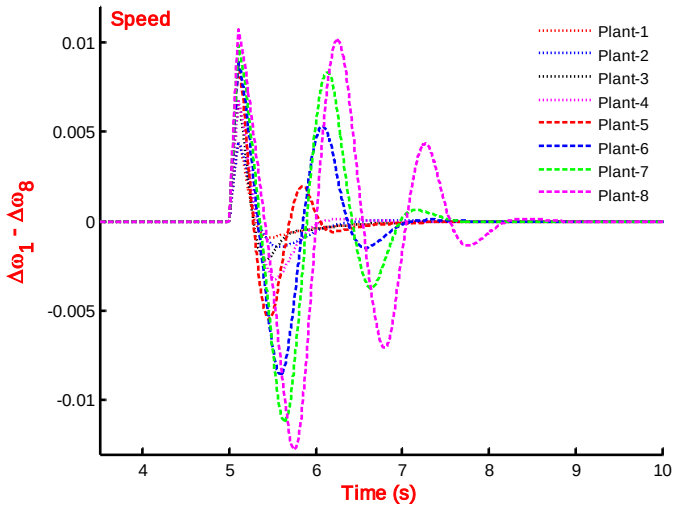

Figure 2.15: Speed response: SMIB system for eight plants with BA-CPSS

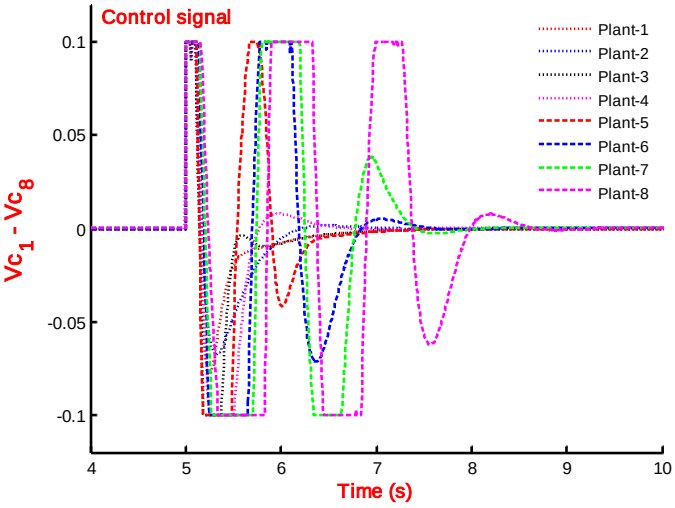

Figure 2.16: Control voltage: SMIB system for eight plants with BA-CPSS

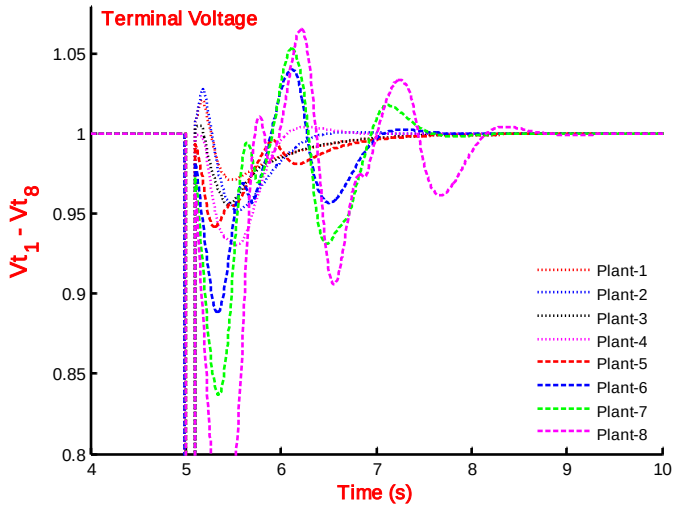

Figure 2.17: Generator terminal voltage: SMIB system for eight plants with BA-CPSS

The damping ratio of SMIB system for plant 6 without PSS is -0.0603 with EMOs as 0.36425 ± 6.02921i (Table 2.3) and is enhanced to 0.67101 with EMOs as -3.6887 ± 4.0759i (Table 2.12). It is highest as compared to CPSSs reported in literature (Table 2.11).

2.4.6. Eigenvalue Plot for 231 Plants

2.4.6.1. Experimental Plant Creation

The line diagram of the SMIB power system is shown in Figure 2.1 with the transmission line connection to an infinite-bus power system. The relevant system data are mentioned in Table A.1. The value of active power (P_{g0}) and the transmission line reactance (X_l) is kept varying to formulate 231 plants of the SMIB power system within the range given in Eqn. (2.19 – 2.20). The value of active power is changed from 0.40 to 1.4 and reactance from 0.20 to 0.7 in the step size of 0.05 in both cases resulting to 21 and 11 combinations respectively and thus constituting 231 plant conditions of the SMIB power system.

$$0.4 \le P_{g0} \le 1.4 \tag{2.19}$$

$$0.2 \le X_l \le 0.7 \tag{2.20}$$

The operating point of power system covered as above encompasses all practical operating conditions and constituting a set of 231 different plants (operating conditions). In section 2.4.5, the designed BA-CPSS is analysed for eight plant conditions, and the performances with other CPSSs [2-11] are compared at nominal operating condition (plant-6) in section 2.4.3 – 2.4.4 out of 231 plants. In this section, the robust performance of SMIB is to be examined for these plant conditions by eigenvalue plot and analysis. The operating conditions covered in Eqn. 2.19 – 2.20 for the SMIB power system, are adequately higher than that of with reported in literature [9, 39-41, 234-241], where in the active power limit is varied over the range of 0.20 - 1.10 pu.

2.4.6.2. Eigenvalue plot for 231 plants without PSS

In this section, the nature of plants (231) of the SMIB power system has to be analysed using eigenvalue plot on s-plane. The algorithm used for calculating and plotting of eigenvalue for 231 plants are mentioned in Table 2.13. The concerned eigenvalue plot for these plants under an open loop (without PSS) is shown in Figure 2.18.

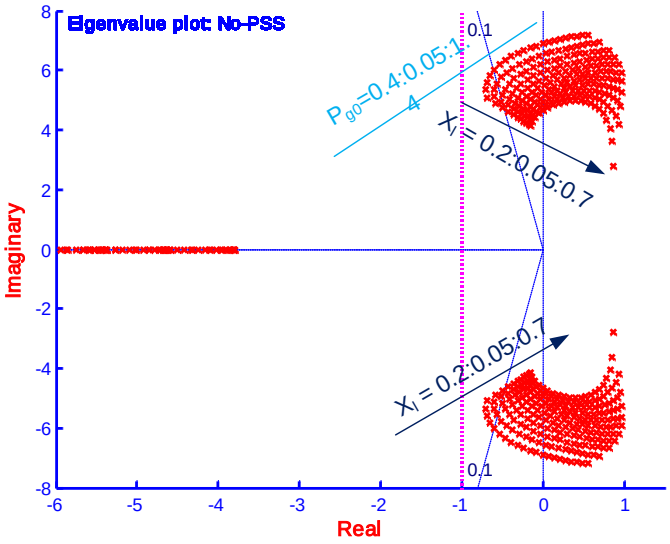

Figure 2.18: Plot of eigenvalue in s-plane: SMIB power system without PSS

Table 2.13: Pseudo code for plot of eigenvalue in s-plane: SMIB power system with 231 plant configurations

Clear all
Define fault and fault clearing time
for i=0.0:0.05:0.4 % first loop
Xe = 0.2+i % as in eq. (2.20)
For ii=0:0.05:1.0 % second loop
P=0.4+ii % as in eq. (2.19)
Load SMIB data with initial conditions
Load BA-CPSS parameters for system with BA-CPSS
Calculate A, B, C, D matrices for SMIB system
Calculate eigenvalue
Plot real and imaginary part of eigenvalue and hold on % to plot each eigenvalue corresponding to operating condition as in eqn. (2.19-2.20)
Define xlabel, ylabel, and title
Create grid for ζ = 0.1 and vertivle line for λ = -1
end for % second loop
end for % first loop

The eigenvalue plot on s-plane, with real part of eigenvalue on x-axis and imaginary part of eigenvalue on y-axis, is drawn in this figure. As the value of X_l is increased the corresponding eigenvalue tends to move towards origin and on the increase in active power, the eigenvalue tends to move towards the right-hand side (RHS) of s-plane. The preferred damping ratio is > 0.1 as in [75] and the eigenvalue plot should be in the left-hand side of the s-plane to meet/guarantee the stability condition. The grid of 0.1 damping ratio is drawn by using 'sgrid' command in MATLAB Software, and the vertical line is drawn to check placement of eigenvalue in the left of s-plane, and the region called as D-shape sector is drawn on left of s-plane. The eigenvalue for a plant condition of SMIB system without PSS is 4, where in two are electromechanical modes

(complex conjugate) and two are having only real part. The eigenvalue with real parts are 2×231=462 and EMOs are 2×231=462, therefore, resulting total eigenvalue as 924 as shown in Figure 2.18. The detail of EMOs in the positive imaginary axis region of s-plane is enlisted in Table 2.14 derived from this figure. It is clear that only 9 EMOs are lying in the wedge-shape sector of s-plane; 76 EMOs are in the region of damping ratio less than 0.10 and 146 EMOs are lying in the right-hand side of s-plane proving necessity of a controller (PSS) to make the system response as stable for these operating conditions.

Table 2.14: The distribution of EMOs in s-plane: SMIB system without PSS for 231 plants

S. No.	Reactance, X_l	$P_{g0} = 0.40 : 0.05 : 1.40$		
		EMOs in Wedge shape sector: $\sigma_i \geq -1, \zeta_i \geq 0.1$	EMOs in region: $0 \leq \zeta_i \leq 0.1$	EMOs in RHS of s-plane: $\sigma_i \geq 0$
1	0.20	4 [0.4:0.05:0.55]	9 [0.60:0.05:1.0]	8 [1.05:0.05:1.4]
2	0.25	3 [0.4:0.05:0.50]	8 [0.55:0.05:0.90]	10 [0.95:0.05:1.4]
3	0.30	2 [0.4, 0.45]	8 [0.50:0.05:0.85]	11 [0.90:0.05:1.4]
4	0.35	-	9 [0.40:0.05:0.80]	12 [0.85:0.05:1.4]
5	0.40	-	8 [0.40:0.05:0.85]	13 [0.90:0.05:1.4]
6	0.45	-	7 [0.40:0.05:0.70]	14 [0.75:0.05:1.4]
7	0.50	-	7 [0.40:0.05:0.70]	14 [0.75:0.05:1.4]
8	0.55	-	6 [0.40:0.05:0.65]	15 [0.70:0.05:1.4]
9	0.60	-	5 [0.40:0.05:0.60]	16 [0.65:0.05:1.4]
10	0.65	-	5 [0.40:0.05:0.60]	16 [0.65:0.05:1.4]
11	0.70	-	4 [0.40:0.05:0.55]	17 [0.60:0.05:1.4]
Total		9	76	146

2.4.6.3. Eigenvalue plot for 231 plants with CPSS

In this section, the robust performance of the BA-CPSS and CPSSs reported in [2-11] were examined over 231 plant conditions using eigenvalue plot. As in Table 2.9, two type of CPSS are considered as single stage CPSSs with 3 - parameters [2-7] and double stage CPSSs with 5 - parameters [8-11] .

In section 2.4.6.2, the eigenvalue plot for SMIB power system is carried out over the 231 plant conditions (operating conditions) with total eigenvalue as 4× 231 = 462. On connecting single stage CPSS to a SMIB power system on extra state, i.e. eigenvalue is added and two additional eigenvalue are added, thus resulting five and six eigenvalue, respectively. Therefore, total eigenvalue of a system with 231 plants with single-stage CPSS is 5×231 = 1155 and with double-stage CPSS is 6×231 = 1386. Entire number of EMOs is 4×231 = 924 with both types of CPSSs while eigenvalue with only real part are 1×231 =231 with single state, and it is as 2×232 = 462 with double stage CPSSs. Since the small signal stability is affected by the placement of EMOs in s-plane, therefore, the eigenvalue plot for SMIB system for 231 plant conditions is

plotted on s-plane by using each controller as per detail in Table 2.9. The placement of EMOs due to each controller in s-plane is summarized in Table 2.15. As per the detail of EMOs in Table 2.15, none of CPSSs except proposed BA-CPSS can place all EMOs in D-shape sector of s-plane. The one probable region of failure to controllers in literature may be because of extended range of operating conditions. The eigenvalue plots of BFA-CPSS and BA-CPSS are shown in Figure 2.19 and Figure 2.20, respectively. The plot because of other controllers is not shown because of space constraint. The plot of EMOs in Figure 2.20 shows that all EMOs are in D-shape sector and fully complying with the provisions of objective function as mentioned in section 2.2.3.1.

Table 2.15: Placement of EMOs in s-plane: CPSSs in literature and BA-CPSS for 231 plants

Controller	Total Eigen-value	Total EMOs	Eigenvalue with real part only	Placement of EMOs			
				D-shape sector	Wedge-shape sector	EMOs in region: $0 \le \zeta_i \le 0.1$	EMOs in RHS of s-plane: $\sigma_i \ge 0$
TS-CPSS [2]	1155	924	231	852	60	10	2
RCGA-CPSS [3]	1155	924	231	904	20	-	-
GA-CPSS [4]	1155	924	231	742	86	84	12
LMI-CPSS [5]	1155	924	231	220	462	208	34
PSO-CPSS [6]	1155	924	231	868	-	56	-
BGA-CPSS [7]	1155	924	231	334	462	126	2
GA-CPSS [8]	1386	924	462	916	8	-	-
BFA-CPSS [8]	1386	924	462	910	14	-	-
SA-CPSS [9]	1386	924	462	872	52	-	-
RSA-CPSS [9]	1386	924	462	920	4	-	-
DE-CPSS [10]	1386	924	462	902	22	-	-
SPEA-CPSS [11]	1386	924	462	630	126	118	50
BA-CPSS (Prop.)	1386	924	462	924	-	-	-

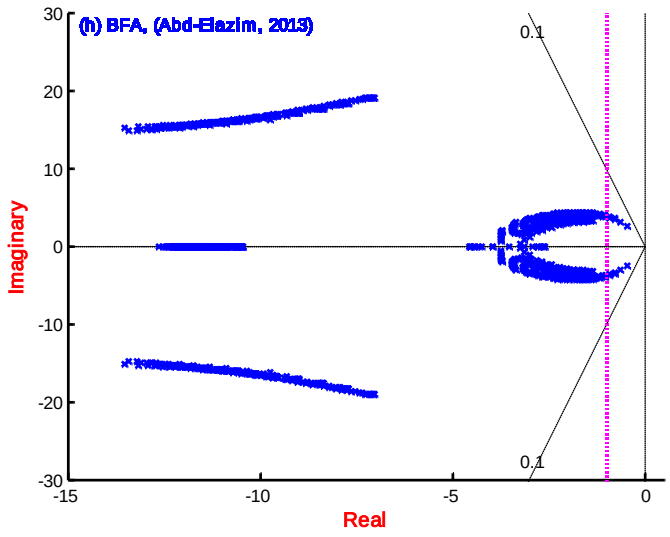

Figure 2.19: Eigen value plot of system with BFA-CPSS for 231 plant conditions

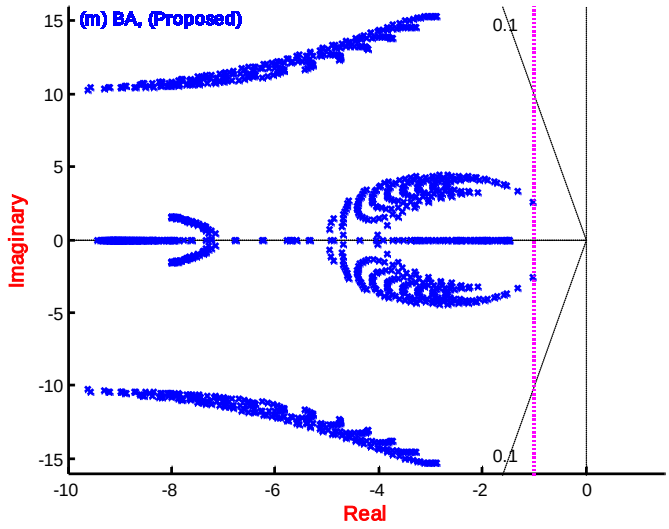

Figure 2.20: Eigenvalue plot of system with BA-CPSS (proposed) for 231 plant conditions

2.5. Design and Performance Analysis: Four-Machine System

2.5.1. Design of CPSS using bat algorithm

In this section, the bat algorithm is used to design CPSS parameters for 4-machine 10-bus power system. All four generators are equipped with CPSSs and the optimization problem is considered with an eigenvalue based objective function as described in section 2.2.3.2, to place eigenvalue in the wedge-shaped sector in the left side of s-plane. The computer configurations are considered as in section 2.4.1 with same initializing parameters of the bat algorithm. As the creations of experimental plants for two-area four-machine ten-bus power system are well explained in section 2.3.2.1, where in the line data (Table A.2), load flow data (Table A.3) and machine data (Table A.4) are given for the system configuration without PSS. The optimization of CPSSs parameter is carried out with parameter bounds as $10 \le K_j \le 50$, $0.001 \le T_{j1} \le 0.50$, $0.001 \le T_{j2} \le 0.80$, $0.001 \le T_{j3} \le 2.0$, $0.001 \le T_{j4} \le 0.05$. The termination criterion is considered as maximum iteration count as 200. The fitness function variation for 200 iterations is shown in Figure 2.21. The value of fitness function is constantly minimum at and above 150 iterations. The plots for gain parameters of four CPSSs as $K_1 - K_4$ are shown not included because of space limitation. The optimized values of 4-CPSSs parameters using the bat algorithm are enlisted in Table 2.16.

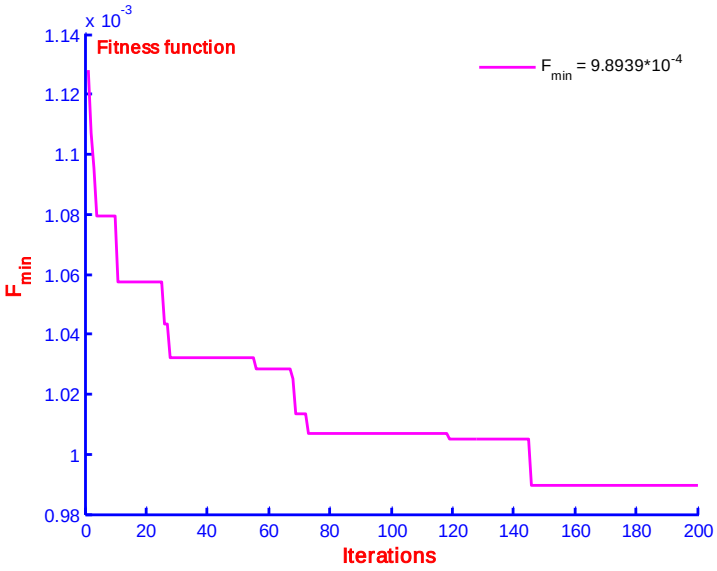

Figure 2.21: Plot of fitness function variation with iterations

2.5.2. Reported CPSSs in literature

As per literature survey, twelve different optimization based designs of CPSSs for two-area four-machine ten-bus power system are considered and enlisted in Table 2.16 to make a comparison of CPSSs performance with that of the Bat algorithm based designed CPSSs for this system.

In [13], the BFA, PSO, SPPSO has been applied to tune CPSSs parameters. The performance of BFA-CPSS outperforms the performance of the system with that of PSO, SPPSO and CPSS [250]. In [14], the problem of optimization is formulated by considering shifting of eigenvalue in the wedge-shaped sector with threshold damping ratio as 0.2 using GA, SPSO and PSOPC. The performance with PSOPC-PSS reported as better as compared to CPSS, GAPSS, and SPSOPSS. In [15] multiobjective optimization is employed and reported as best fitness value obtained by MPSO is 0.7998 and is slightly lower than those obtained by PSOPC (0.8347), PSO (0.8710) and GA (0.9145). In [16], the design of CPSSs has been carried out using CDCARLA. The effectiveness of the CDCARLA based CPSSs is proved to be better in performance as compared to that of with IEEE MB-PSS [251] and CPSS [252]. In [17], MOIA and MAINet approaches are used for multiobjective simultaneous coordinated tuning of damping controllers. The performance of the system is better with MOIA as compared to MAINet based PSS design. In [11], the SPEA and GA are used to tune the CPSS parameters. The performances of the system with SPEA outperform the GA. In [19]; the design of CPSSs is carried out using ABGA and GA. The performance of the system is compared with ABGA-CPSS, GA-CPSS and CPSS [252] and reported as better with ABGA-CPSS.

Table 2.16: CPSSs parameters optimized with different algorithms for four-machine system

S. No.	Controller	Generators	K_j	T_{j1}	T_{j2}	T_{j3}	T_{j4}
1	PSO-CPSS [13]	Gen-1	30.0	1.17	0.39	5.77	15
		Gen-2	30.0	1.21	0.34	4.36	14.66
		Gen-3	17.71	0.83	0.36	10	15
		Gen-4	29.77	0.90	0.55	4.10	15
2	SPPSO-CPSS [13]	Gen-1	23.71	1.28	0.50	3.77	7.03
		Gen-2	22.76	1.54	0.49	3.61	8.45
		Gen-3	23.88	1.25	0.75	5.35	8.57
		Gen-4	27.31	1.17	1.00	2.96	8.18
3	BFA-CPSS [13]	Gen-1	23.84	2.00	1.00	6.16	8.25
		Gen-2	21.48	2.00	1.00	4.93	8.19
		Gen-3	18.22	2.00	1.00	4.87	7.24
		Gen-4	20.71	2.00	1.00	4.74	8.92
4	GA-CPSS [14]	Gen-1	11.934	0.0512	0.0241	0.0500	0.0567
		Gen-2	17.033	0.1907	0.0161	0.1021	0.0348
		Gen-3	26.308	0.0675	0.0231	0.0731	0.0364
		Gen-4	15.099	0.0356	0.0151	0.0715	0.0384
5	PSOPC-CPSS [14]	Gen-1	24.4382	0.0834	0.0153	0.0500	0.1670
		Gen-2	15.8664	0.5070	0.0440	0.0487	0.0650
		Gen-3	26.3067	0.0675	0.0160	0.0541	0.0158
		Gen-4	23.4433	0.0356	0.0100	0.0389	0.0100
6	MPSO-CPSS [15]	Gen-1	38.15	0.450	0.711	0.970	0.213
		Gen-2	30.14	0.481	0.210	0.386	0.613
		Gen-3	43.07	0.646	0.310	0.080	0.010
		Gen-4	23.32	0.760	0.317	0.081	0.416
7	CDCARLA-CPSS [16]	Gen-1	14.79	18.98	3.17	10.71	18.07
		Gen-2	13.98	9.70	17.80	11.46	1.45
		Gen-3	14.28	4.57	5.09	19.36	22.72
		Gen-4	18.91	8.66	19.22	15.59	16.23
8	MAINet-CPSS [17]	Gen-1	-	-	-	-	-
		Gen-2	36.12	1.515	1.458	1.835	0.056
		Gen-3	26.00	2.01	0.861	1.08	0.429
		Gen-4	-	-	-	-	-
9	MOIA-CPSS[17]	Gen-1	-	-	-	-	-
		Gen-2	29.12	1.525	0.094	0.651	1.53
		Gen-3	49.76	1.426	0.622	0.996	0.786
		Gen-4	-	-	-	-	-
10	BFOA-CPSS [18]	Gen-1	-	-	-	-	-
		Gen-2	30.80	0.62	0.16	0.84	2.44
		Gen-3	48.1960	0.81214	0.66123	1.25786	1.57184
		Gen-4	-	-	-	-	-
11	ABGA-CPSS [19]	Gen-1	-	-	-	-	-
		Gen-2	21.87	0.4876	0.3657	0.1523	0.1100
		Gen-3	39.63	0.6567	0.4554	0.1301	0.1048
		Gen-4	-	-	-	-	-
12	SPEA-CPSS [11]	Gen-1	42.0	0.26	0.01	4.5	9.7
		Gen-2	-	-	-	-	-
		Gen-3	-	-	-	-	-
		Gen-4	42.0	0.26	0.01	4.5	9.7
13	BA-CPSS (Proposed)	Gen-1	46.3554	0.1058	0.2277	0.2228	0.0364
		Gen-2	48.9279	0.0402	0.2912	0.4924	0.0323
		Gen-3	48.0119	0.0095	0.7856	1.4301	0.0224
		Gen-4	49.9690	0.0855	0.5883	0.2430	0.0013

2.5.3. Response Comparison

The two-area four-machine ten-bus power system is described in section 2.3.2 without PSS, and the creations of system models based on operating conditions are elaborated in section 2.3.2.1. The CPSSs designed in previous section are connected to the system. In each plant condition as listed in Table 2.4 are considered with fault location as given in Table A.5. The disturbance is considered as self-clearing at different buses at 1.0 second and cleared after 0.05 second. Referring to section 2.3.2.2 and section 2.3.2.3, wherein the simulation and eigenvalue analysis with eight plant conditions under an open loop are described and found that none of the generators of plants are showing stable operation; therefore, not needed to compare in the simulation results.

In this section, the response with proposed BA-CPSS is compared to the responses with different controllers as in Table 2.16. The speed response of the four-machine system with BA-CPSSs for all four generators is compared with the system response for plant-1 using PSO-CPSS [13], SPPSO-CPSS [13], BFA-CPSS [13], GA-CPSS [14], PSOPC-CPSS [14], MPSO-CPSS [15], CDCARLA-CPSS [16], MAINet-CPSS [17], MOIA-CPSS [17], BFOA-CPSS [18], ABGA-CPSS [19], SPEA-CPSS [11]. The response comparison with each controller for all eight plant conditions is recorded in terms of performance indices. Relatively, best-performing CPSSs are selected as CDCARLA-CPSS [16], MOIA-CPSS [17], BFOA-CPSS [18], ABGA-CPSS [19], SPEA-CPSS [11] and are compared with the speed response by BA-CPSS (proposed) on plant-1 of the power system in Figure 2.22 - Figure 2.25 for Gen-1 – Gen-4, respectively. Clearly, the response of the system is comparatively better with BA-CPSS. To check robust operation of BA-CPSS over the wide range of operating conditions, the simulation is carried out with all plant conditions as in Table 2.4. The speed response of the system with all CPSSs as in Table 2.4 are carried out for all eight plant conditions, but the responses with other plants except plant-1 are not shown because of space constraint. Therefore, the performance indices as ITAE, IAE and ISE are recorded for all plant conditions with all CPSSs and BA-CPSS for better comparison for a common simulation time of 30 seconds. The detail on the performance indices may be referred in section 1.4. The value of performance indices of speed response with different methods based CPSSs are incorporated in Table 2.17 for Plant-1 – Plant-4. As the smaller value of PI refers to a better performance, the close comparison of the performance indices reveals that the performance with BA-CPSS as compared to others is best, even for all plant conditions.

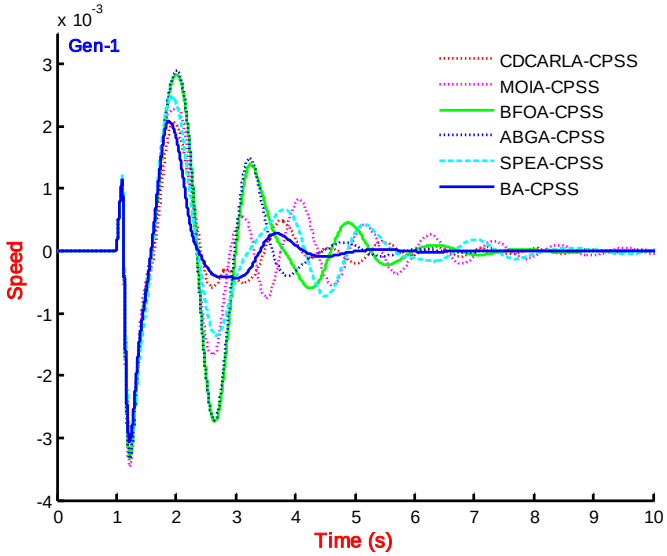

Figure 2.22: Speed response for Gen-1 of Plant-1 with CDCARLA, MOIA, BFOA, ABGA, SPEA and BA based CPSSs with four-machine system

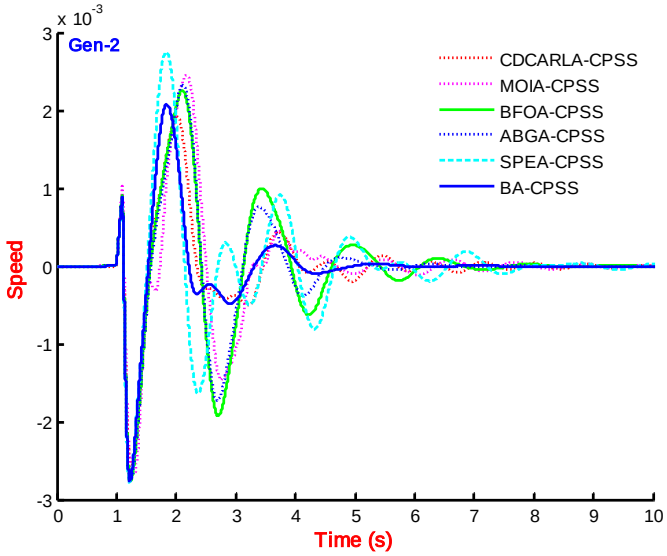

Figure 2.23: Speed response for Gen-2 of Plant-1 with CDCARLA, MOIA, BFOA, ABGA, SPEA and BA based CPSSs with four-machine system

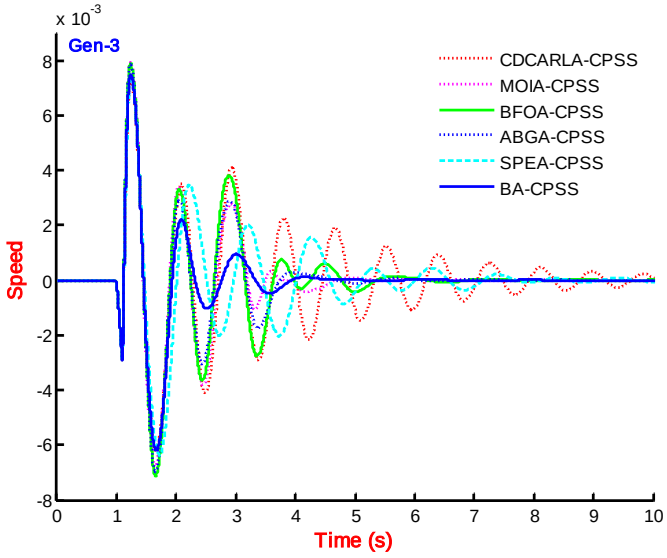

Figure 2.24: Speed response for Gen-3 of Plant-1 with CDCARLA, MOIA, BFOA, ABGA, SPEA and BA based CPSSs with four-machine system

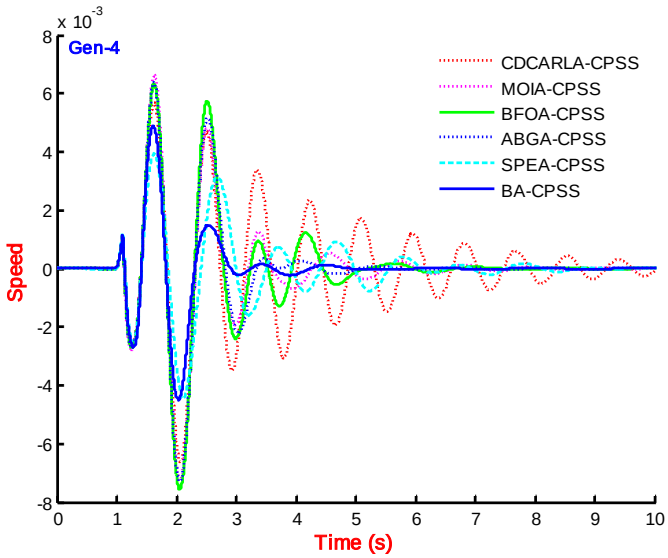

Figure 2.25: Speed response for Gen-4 of Plant-1 with CDCARLA, MOIA, BFOA, ABGA, SPEA and BA based CPSSs with four-machine system

Table 2.17: Performance of speed response of four-machine system with different controllers for plant-1 – plant-4

Controllers	ITAE	IAE	ISE	ITAE	IAE	ISE
	Plant-1			Plant-2		
PSO-CPSS [13]	0.0385	0.0176	5.0513×10^{-05}	0.0589	0.0255	8.7133×10^{-05}
SPPSO-CPSS [13]	0.0447	0.0193	5.5812×10^{-05}	0.0657	0.0274	9.4165×10^{-05}
BFA-CPSS [13]	0.0320	0.0156	4.6263×10^{-05}	0.0506	0.0237	8.7960×10^{-05}
GA-CPSS [14]	0.0376	0.0166	4.3719×10^{-05}	0.0599	0.0254	8.6105×10^{-05}
PSOPC-CPSS [14]	0.0278	0.0138	3.8312×10^{-05}	0.0506	0.0234	8.6007×10^{-05}
MPSO-CPSS [15]	0.0312	0.0154	4.5491×10^{-05}	0.0577	0.0263	1.0759×10^{-04}
CDCARLA-CPSS [16]	0.1030	0.0293	7.5104×10^{-05}	0.1436	0.0410	1.3458×10^{-04}
MAINet-CPSS [17]	0.1072	0.0268	6.8136×10^{-05}	0.1260	0.0348	1.1411×10^{-04}
MOIA-CPSS [17]	0.0558	0.0223	6.9309×10^{-05}	0.0755	0.0310	1.1828×10^{-04}
BFOA-CPSS [18]	0.0628	0.0251	7.9276×10^{-05}	0.0981	0.0363	1.3088×10^{-04}
ABGA-CPSS [19]	0.0488	0.0217	7.1284×10^{-05}	0.0764	0.0316	1.1966×10^{-04}
SPEA-CPSS [11]	0.0649	0.0226	5.2086×10^{-05}	0.1638	0.0495	1.8194×10^{-04}
BA-CPSS (Proposed)	0.0265	0.0135	3.8266×10^{-05}	0.0426	0.0215	8.5632×10^{-05}
	Plant-3			Plant-4		
PSO-CPSS[13]	0.0176	0.0085	1.1963×10^{-05}	0.0190	0.0089	1.0992×10^{-05}
SPPSO-CPSS[13]	0.0169	0.0084	1.2202×10^{-05}	0.0183	0.0088	1.1429×10^{-05}
BFA-CPSS[13]	0.0148	0.0077	1.1579×10^{-05}	0.0182	0.0087	1.1945×10^{-05}
GA-CPSS[14]	0.0292	0.0122	1.7629×10^{-05}	0.0213	0.0095	1.1034×10^{-05}
PSOPC-CPSS[14]	0.0194	0.0091	1.2071×10^{-05}	0.0170	0.0082	1.0832×10^{-05}
MPSO-CPSS[15]	0.0115	0.0062	9.3547×10^{-06}	0.0150	0.0073	9.9786×10^{-06}
CDCARLA-CPSS[16]	0.0205	0.0093	1.3300×10^{-05}	0.0246	0.0106	1.3684×10^{-05}
MAINet-CPSS[17]	0.0958	0.0197	2.3169×10^{-05}	0.0866	0.0185	1.9534×10^{-05}
MOIA-CPSS[17]	0.0501	0.0166	2.5575×10^{-05}	0.0328	0.0127	1.6108×10^{-05}
BFOA-CPSS[18]	0.0300	0.0130	2.1832×10^{-05}	0.0232	0.0105	1.3618×10^{-05}
ABGA-CPSS[19]	0.0259	0.0121	2.1340×10^{-05}	0.0213	0.0102	1.4002×10^{-05}
SPEA-CPSS[11]	0.0334	0.0122	1.4477×10^{-05}	0.0357	0.0121	1.0218×10^{-05}
BA-CPSS (Proposed)	0.0114	0.0062	1.0045×10^{-05}	0.0133	0.0067	9.5846×10^{-06}

Table 2.18: Performance of speed response of four-machine system with different controllers for plant-5 – plant-8

Controllers	ITAE	IAE	ISE	ITAE	IAE	ISE
	Plant-5			Plant-6		
PSO-CPSS [13]	0.0184	0.0085	1.0775×10^{-05}	0.0182	0.0087	1.1109×10^{-05}
SPPSO-CPSS [13]	0.0194	0.0088	1.0973×10^{-05}	0.0206	0.0094	1.2361×10^{-05}
BFA-CPSS [13]	0.0153	0.0076	1.0310×10^{-05}	0.0148	0.0077	1.0556×10^{-05}
GA-CPSS [14]	0.0207	0.0089	1.0744×10^{-05}	0.0188	0.0084	9.4774×10^{-06}
PSOPC-CPSS [14]	0.0169	0.0079	1.0274×10^{-05}	0.0139	0.0069	8.2686×10^{-06}
MPSO-CPSS [15]	0.0131	0.0067	9.4346×10^{-06}	0.0119	0.0063	7.5290×10^{-06}
CDCARLA-CPSS [16]	0.0467	0.0141	1.6790×10^{-05}	0.0436	0.0133	1.4893×10^{-05}
MAINet-CPSS [17]	0.0747	0.0145	1.3753×10^{-05}	0.0702	0.0138	1.3636×10^{-05}
MOIA-CPSS [17]	0.0290	0.0107	1.2663×10^{-05}	0.0210	0.0094	1.2446×10^{-05}
BFOA-CPSS [18]	0.0246	0.0106	1.3668×10^{-05}	0.0256	0.0112	1.5258×10^{-05}
ABGA-CPSS [19]	0.0205	0.0096	1.2913×10^{-05}	0.0217	0.0101	1.3415×10^{-05}
SPEA-CPSS [11]	0.0549	0.0181	2.7013×10^{-05}	0.0334	0.0119	1.3203×10^{-05}
BA-CPSS (Proposed)	0.0092	0.0052	6.8402×10^{-06}	0.0109	0.0063	1.0200×10^{-06}
	Plant-7			Plant-8		
PSO-CPSS [13]	0.0153	0.0066	4.2653×10^{-06}	0.0118	0.0058	4.3577×10^{-06}
SPPSO-CPSS [13]	0.0148	0.0063	4.0338×10^{-06}	0.0133	0.0063	4.6012×10^{-06}
BFA-CPSS [13]	0.0132	0.0058	3.7274×10^{-06}	0.0110	0.0057	4.9542×10^{-06}
GA-CPSS [14]	0.0195	0.0080	5.0634×10^{-06}	0.0109	0.0054	3.6669×10^{-06}
PSOPC-CPSS [14]	0.0152	0.0064	4.0234×10^{-06}	0.0094	0.0048	3.3567×10^{-06}
MPSO-CPSS [15]	0.0123	0.0051	3.1051×10^{-06}	0.0093	0.0047	3.6450×10^{-06}
CDCARLA-CPSS [16]	0.0170	0.0068	4.1174×10^{-06}	0.0286	0.0092	6.5905×10^{-06}
MAINet-CPSS [17]	0.0650	0.0135	9.0065×10^{-06}	0.0657	0.0099	3.6995×10^{-06}
MOIA-CPSS [17]	0.0210	0.0088	6.6208×10^{-06}	0.0158	0.0063	3.2916×10^{-06}
BFOA-CPSS [18]	0.0218	0.0094	7.5560×10^{-06}	0.0119	0.0060	3.6712×10^{-06}
ABGA-CPSS [19]	0.0198	0.0089	7.4761×10^{-06}	0.0115	0.0059	3.6160×10^{-06}
SPEA-CPSS [11]	0.0315	0.0110	7.0607×10^{-06}	0.0366	0.0128	1.2077×10^{-05}
BA-CPSS (Proposed)	0.0121	0.0048	2.8141×10^{-06}	0.0061	0.0031	1.9943×10^{-06}

2.5.4. Eigenvalue Comparison

In previous section, the speed response and its performance indices based analysis has been carried out and proved the superior performance of the proposed BA-CPSS over the other controllers. In this section, the eigenvalue analysis is carried through the system without PSS, with BA-CPSS and with other controllers as in Table 2.9 for plant-1. The electromechanical modes with least value of damping ratio have been recorded in Table 2.5. The eigenvalue analysis with plant-1 of the system without PSS, with BA-CPSS and PSS are recorded in Table 2.19. The eigenvalue plot of the system for plant-1 without PSS, with BA-CPSS is compared with CDCARLA-CPSS[16] and with MPSO-CPSS[15] in Figure 2.26 and Figure 2.27, respectively. In each plot, the eigenvalue of the system with BA-CPSS is satisfying the condition of the wedge-

shape sector, i.e. none of EMOs are lying out of the wedge-shape sector on s-plane. The eigenvalue analysis for remaining plant-2 –plant-8 and respective eigenvalue plots have not shown because of similar behaviour of BA-CPSS and space constraint.

Table 2.19: Eigenvalue, damping factor and frequency of oscillations with different controllers for least damped electromechanical oscillations for plant-1: Four-machine system

Eigenvalue	Damping Factor	Freq. (Hz)	Eigenvalue	Damping Factor	Freq. (Hz)
No-PSS			PSO-CPSS[13]		
0.037034 ± 0.87288i	-0.04239	0.13892	-1.1483 ± 7.6591i	0.14827	1.219
0.17831 ± 0.90664i	-0.19298	0.1443	-2.1889 ± 10.186i	0.2101	1.6211
-0.11544 ± 0.92409i	0.12396	0.14707	-0.96718 ± 3.6502i	0.25612	0.58095
-10.091 ± 19.166i	0.46587	3.0503	-8.0889 ± 18.536i	0.39996	2.9501
SPPSO-CPSS[13]			BFA-CPSS[13]		
-0.91195 ± 7.695i	0.11769	1.2247	-1.5625 ± 9.8412i	0.15681	1.5663
-1.8992 ± 10.014i	0.18634	1.5937	-1.3378 ± 8.1621i	0.16175	1.299
-1.0653 ± 3.8306i	0.26793	0.60966	-1.3633 ± 3.928i	0.32788	0.62516
-8.2725 ± 18.481i	0.40856	2.9413	-8.1719 ± 18.466i	0.40469	2.9389
GA-CPSS[14]			PSOPC-CPSS[14]		
-9.8765 ± 24.917i	0.36848	3.9657	-1.6508 ± 6.9763i	0.23027	1.1103
-1.0547 ± 6.888i	0.15136	1.0963	-0.9772 ± 3.5434i	0.26585	0.56395
-1.6177 ± 7.0673i	0.22313	1.1248	-5.6333 ± 19.725i	0.27461	3.1393
-0.75167 ± 3.7713i	0.19547	0.60022	-2.0891 ± 6.9517i	0.28781	1.1064
MPSO-CPSS[15]			CDCARLA-CPSS[16]		
-2.1411 ± 13.257i	0.15945	2.1099	-1.2054 ± 12.577i	0.095402	2.0017
-1.4643 ± 7.4601i	0.1926	1.1873	-0.39715 ± 7.2828i	0.054451	1.1591
-4.3933 ± 17.985i	0.2373	2.8624	-0.98145 ± 3.4101i	0.27658	0.54274
-6.278 ± 22.589i	0.26777	3.5952	-6.5722 ± 17.425i	0.3529	2.7733
MAINet-CPSS[17]			MOIA-CPSS[17]		
5.7467 ± 35.023i	-0.16192	5.5741	-1.5463 ± 21.155i	0.072897	3.367
-0.20157 ± 5.7046i	0.035313	0.90791	-0.47077 ± 5.7978i	0.080932	0.92275
-2.3752 ± 17.852i	0.13189	2.8412	-2.2871 ± 17.223i	0.13164	2.7412
-1.0348 ± 4.8607i	0.20823	0.77361	-1.0918 ± 4.9642i	0.21481	0.79008
BFOA-CPSS[18]			ABGA-CPSS[19]		
-0.85935 ± 4.283i	0.19672	0.68166	-1.8575 ± 7.2055i	0.24963	1.1468
-1.5514 ± 6.8295i	0.22151	1.0869	-1.2765 ± 4.5134i	0.27216	0.71833
-1.7749 ± 7.4842i	0.23075	1.1911	-2.3474 ± 5.6489i	0.38374	0.89906
-8.6383 ± 18.469i	0.42366	2.9395	-8.3438 ± 18.157i	0.41755	2.8898
SPEA-CPSS[11]			BA-CPSS (Proposed)		
-0.59205 ± 6.1041i	0.096538	0.97151	-1.5806 ± 9.5491i	0.1633	1.5198
-0.8024 ± 6.755i	0.11796	1.0751	-1.6478 ± 6.2955i	0.25321	1.002
-0.51302 ± 3.7701i	0.13483	0.60003	-1.1833 ± 3.6678i	0.30705	0.58374
-8.3764 ± 22.972i	0.34258	3.656	-7.4439 ± 18.55i	0.37242	2.9523

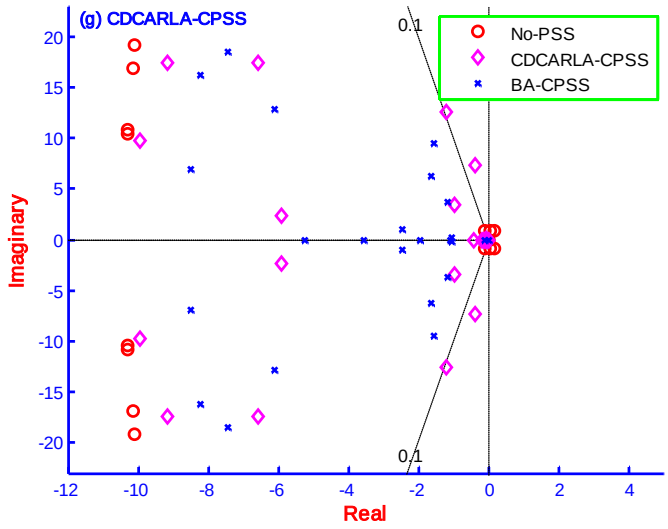

Figure 2.26: Eigenvalue plot of plant-1 without PSS, with CDCARLA-CPSS and BA-CPSS

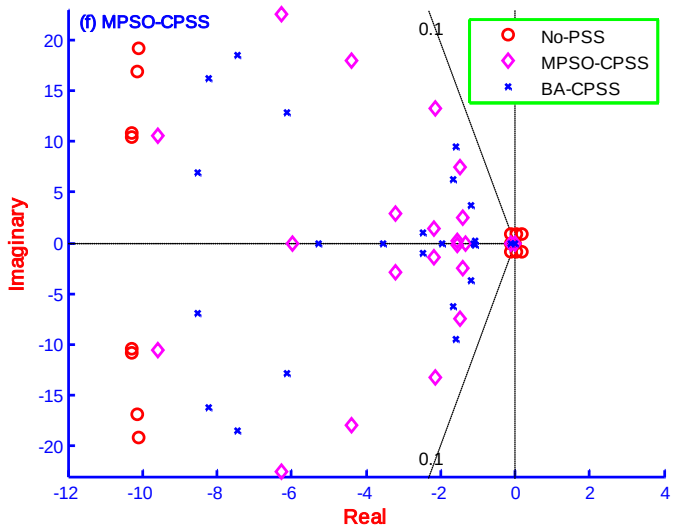

Figure 2.27: Eigenvalue plot of plant-1 without PSS, with MPSO-CPSS and BA-CPSS

2.6. Design and Performance Analysis: Ten-Machine System

2.6.1. Design of CPSS using bat algorithm

As the creation of experimental plants for IEEE New England ten-machine thirty nine-bus power system are well explained in section 2.3.3.1, where in the machine data, load flow data, transformer data and line data are considered as in Table A.6 - Table A.10, for the system configuration without PSS. The system model referring to plant-1 configuration as in Table 2.6-Table 2.7, is equipped with CPSSs to all nine-machines (named as Gen-1 to Gen-9) except Gen-10, which is considered as the slack and subjected to CPSSs design using the bat algorithm as described section 1.2.2. As the eigenvalue in Table 2.8 are referring negative damping for the

generators, resulting system conditions as sufficiently hard from the stability point of view [23]. The CPSSs parameter bounds are selected to cover the parameter range as enlisted in Table 2.20 - Table 2.21 and considered as $0 \le K_j \le 50$, $0.1 \le T_{j1} \le 0.2$, $0.1 \le T_{j2} \le 0.8$, $0.5 \le T_{j3} \le 2.0$, $0.01 \le T_{j4} \le 0.02$. With the initializing parameters as above of Bat algorithm are simulated for an iteration count as 200. The fitness function variation for 200 iterations is shown in Figure 2.28. The plots for gain and pole-zero parameters of nine CPSSs are not shown because of space constraints, but the numeral value found at the end of iteration count 200 is enlisted in Table 2.21.

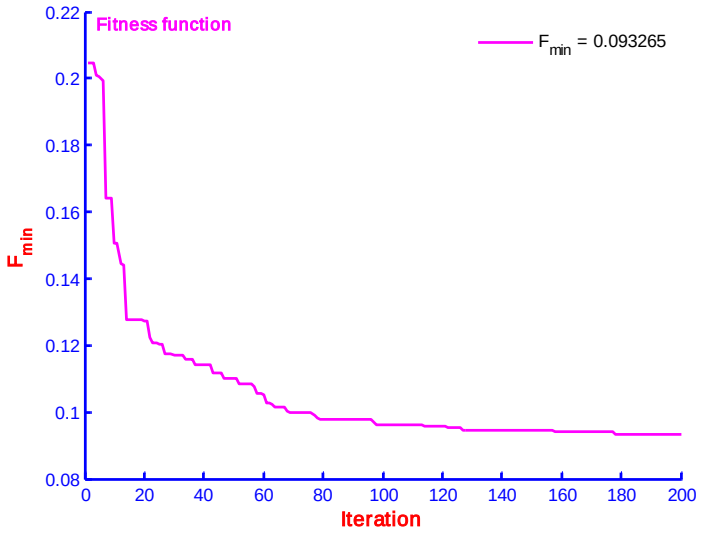

Figure 2.28: Performance of BA in terms of fitness function variation in ten-machine system

2.6.2. Reported CPSSs in literature

The nine different optimization based designs of CPSSs for New England ten-machine thirty nine-bus power system are considered and enlisted in Table 2.6 - Table 2.7 to make a comparison of CPSSs performance with that of the bat algorithm based designed CPSSs for this system. As per the requirement of the power system model, one machine is considered as the slack generator who is not equipped with the PSS, therefore, only nine controllers are designed in literature connected to nine machines. The machine/ generator -1 is considered as the slack, therefore, nomenclature of the PSS is made accordingly [23]. In this study, author has considered 10th machine as the slack generator.

In [20], the problem of optimization is to minimize the square of damping factor with threshold (-1), and the performance is compared with [140]. The ISE based performance index has been reported proposed PSS and PSS [140] in the range of 0.6989-5.8645 and 1.0491-1118.6, respectively. In [21], the performance is compared to the controller in [140], where in the ISE is reported in the range 1.0491-1.1032, and with that of proposed EP based PSS is in the range of

0.5631-0.6297. In [22], the performance of speed response has been compared in terms of performance index as ISE and reported in range 1.05-1.06 with gradient based design [140], in range 1.09-8.64 [142] with GA based PSS, and as 0.56-7.25 with PSO based PSS [22].

Table 2.20: I - CPSSs parameters optimized with different algorithms for ten-machine system

S. No.	Controller	Generators	K_j	T_{j1}	T_{j2}	T_{j3}	T_{j4}
		Gen-1	23.447	0.693	0.05	0.960	0.05
		Gen-2	41.581	0.663	0.05	0.960	0.05
		Gen-3	22.074	0.361	0.05	0.884	0.05
		Gen-4	2.612	0.888	0.05	0.223	0.05
1	TS-CPSS [20]	Gen-5	49.208	0.659	0.05	0.643	0.05
		Gen-6	26.249	0.088	0.05	0.609	0.05
		Gen-7	32.417	0.604	0.05	0.680	0.05
		Gen-8	2.738	0.674	0.05	0.272	0.05
		Gen-9	10.576	0.968	0.05	0.961	0.05
		Gen-1	23.162	0.368	0.05	0.365	0.05
		Gen-2	47.485	0.496	0.05	0.502	0.05
		Gen-3	46.826	0.508	0.05	0.986	0.05
		Gen-4	9.472	0.158	0.05	0.381	0.05
2	EP-CPSS [21]	Gen-5	45.417	0.430	0.05	0.939	0.05
		Gen-6	18.755	0.268	0.05	0.102	0.05
		Gen-7	39.767	0.889	0.05	0.914	0.05
		Gen-8	45.728	0.214	0.05	0.124	0.05
		Gen-9	26.870	0.999	0.05	0.749	0.05
		Gen-1	38.462	0.728	0.05	0.603	0.05
		Gen-2	21.538	0.719	0.05	0.785	0.05
		Gen-3	19.716	0.953	0.05	0.592	0.05
		Gen-4	38.040	0.131	0.05	0.251	0.05
3	PSO-CPSS [22]	Gen-5	46.057	0.477	0.05	0.857	0.05
		Gen-6	5.1928	0.294	0.05	0.199	0.05
		Gen-7	23.418	1.000	0.05	1.000	0.05
		Gen-8	49.998	0.176	0.05	0.136	0.05
		Gen-9	31.462	1.000	0.05	0.992	0.05
		Gen-1	48.430	0.336	0.045	0.546	0.027
		Gen-2	22.915	0.915	0.038	0.556	0.052
		Gen-3	47.778	0.682	0.019	0.397	0.042
		Gen-4	48.795	0.132	0.030	0.241	0.036
4	DE-CPSS [23]	Gen-5	49.346	0.157	0.059	0.690	0.063
		Gen-6	7.254	0.186	0.058	0.194	0.035
		Gen-7	13.329	0.662	0.035	1.272	0.025
		Gen-8	21.098	0.314	0.049	0.159	0.079
		Gen-9	17.019	1.054	0.024	1.049	0.015
		Gen-1	48.8622	0.3686	0.0137	0.4450	0.0159
		Gen-2	28.6638	0.7259	0.0252	0.6528	0.0370
		Gen-3	42.9380	0.7016	0.0426	0.5638	0.0403
		Gen-4	49.4392	0.1211	0.0619	0.3043	0.0228
5	GA-CPSS [24]	Gen-5	48.4517	0.6944	0.0156	1.4158	0.0793
		Gen-6	1.2414	0.3564	0.0275	0.5639	0.1211
		Gen-7	26.9913	0.8148	0.0164	0.7331	0.0177
		Gen-8	5.7991	0.2522	0.0494	0.2892	0.0285
		Gen-9	20.5553	1.2483	0.0371	1.1991	0.0305

Table 2.21: II - CPSSs parameters optimized with different algorithms for ten-machine system

S. No.	Controller	Generators	K_j	T_{j1}	T_{j2}	T_{j3}	T_{j4}
6	CA-CPSS [25]	Gen-1	3.18530	0.3238	0.6832	0.010	0.010
		Gen-2	197.066	0.0208	0.3194	0.010	0.010
		Gen-3	153.636	0.0954	0.1828	0.010	0.010
		Gen-4	168.189	0.0791	0.0653	0.010	0.010
		Gen-5	194.514	0.0492	0.0590	0.010	0.010
		Gen-6	189.157	0.0915	0.2446	0.010	0.010
		Gen-7	195.226	0.1499	0.0603	0.010	0.010
		Gen-8	173.634	0.0715	0.0803	0.010	0.010
		Gen-9	154.570	0.1384	0.0463	0.010	0.010
7	ABGA-CPSS [19]	Gen-1	49.0065	0.4325	0.0234	0.5455	0.0146
		Gen-2	31.9876	0.7878	0.0281	0.6764	0.0456
		Gen-3	43.4535	0.6576	0.0523	0.5678	0.5421
		Gen-4	45.9876	0.2434	0.0654	0.3545	0.0345
		Gen-5	49.5775	0.7665	0.0214	1.5456	0.0675
		Gen-6	1.2478	0.4566	0.0227	0.5346	0.2314
		Gen-7	26.8757	0.8766	0.0154	0.6875	0.2130
		Gen-8	5.7895	0.2456	0.0567	0.2768	0.3045
		Gen-9	20.9941	1.6465	0.0453	1.2331	0.3213
8	SPEA-CPSS [11]	Gen-1	13	0.090	1.500	0.100	0.050
		Gen-2	35.3	0.100	0.240	0.100	0.050
		Gen-3	22.9	0.090	0.900	0.100	0.050
		Gen-4	8	0.030	1.400	0.100	0.050
		Gen-5	70	0.070	0.660	0.100	0.050
		Gen-6	62.6	0.090	1.400	0.100	0.050
		Gen-7	7.9	0.060	0.900	0.100	0.050
		Gen-8	20.4	0.090	0.600	0.100	0.050
		Gen-9	47.7	0.010	0.460	0.100	0.050
9	FGSA-CPSS [26]	Gen-1	22.1092	0.1103	0.2923	0.9287	0.0193
		Gen-2	21.9056	0.1272	0.1317	0.9941	0.0173
		Gen-3	29.5315	0.1374	0.1101	1.6566	0.0105
		Gen-4	27.6296	0.1183	0.2912	0.9326	0.0101
		Gen-5	21.2167	0.1837	0.6327	1.5139	0.0134
		Gen-6	21.8760	0.1003	0.1239	0.8865	0.0112
		Gen-7	22.0239	0.1119	0.1017	0.9643	0.0112
		Gen-8	25.2960	0.1212	0.3135	0.9853	0.0193
		Gen-9	21.1787	0.1410	0.4121	1.5230	0.0103
10	BA-CPSS (Proposed)	Gen-1	49.9420	0.1251	0.1117	1.8619	0.0175
		Gen-2	50.0000	0.2000	0.1000	1.9413	0.0150
		Gen-3	49.9740	0.1011	0.1082	1.5388	0.0107
		Gen-4	50.0000	0.1562	0.1411	1.1974	0.0115
		Gen-5	50.0000	0.1363	0.3534	1.8870	0.0175
		Gen-6	49.8710	0.1625	0.3417	1.9317	0.0200
		Gen-7	50.0000	0.1839	0.5834	1.5104	0.0130
		Gen-8	49.9750	0.1821	0.2143	0.7853	0.0134
		Gen-9	49.9730	0.1577	0.7372	1.0921	0.0100

In [23], CPSSs have been designed using DE. The termination criterion considered is reach of 5000 iterations. However, the fitness function reaches to a constant value at around 1000 iterations. The performance with DE-CPSSs is compared to that of with GA [142] and PSO [22] and ISE based performance is reported as 1.056, 1.062 and 1.011, respectively. In [24], the 45

parameters of CPSSs in the 10-machine system are designed using GA with a multiobjective function to place eigenvalue in D-shape sector.

In [25], the problem of optimization is formulated as to shift eigenvalue in the d-shape sector using CA and GA. The performance comparison has been reported among CA, GA and CPSS [253]. In [19], the problem of optimization is formulated to maximize a minimum of damping ratio to tune the CPSSs parameters using ABGA and GA. The ABGA-PSS outperforms GA and CPSS [140] performance for a wide range of operating conditions. In [26], the PSS designed using FGSA with ITAE based objective function for tuning 9-CPSSs and compared with CPSS [140] and SPEA based PSS. The performance (ITAE) variations of the system with FGSA, SPEA and CPSS [140] are as 0.6527-5.3984, 0.7823-5.4011 and 1.5683 - 10.276, respectively.

2.6.3. Response Comparison

The IEEE New England ten-machine thirty nine-bus power system is described in section 2.3.3 without PSS, and the creations of system models based on operating conditions are elaborated in section 2.3.3.1. The CPSSs designed in section 2.6.1 are connected to the system. In each plant condition as listed in Table 2.6 - Table 2.7 are considered with fault location as given in Table A.8. The disturbance is considered as self-clearing at different buses at 1.0 second and cleared after 0.05 second. Referring to section 2.3.3.2 and section 2.3.3.3, wherein the simulation and eigenvalue analysis with eight plant conditions are considered under the open loop (without PSS or no-PSS) is described and found that none of the generators of plants are showing stable operation; therefore, not needed to compare to the simulation results.

In this section, the speed response with CPSSs reported in literatures by nine different methods are considered and compared to BA-CPSS. It is impossible to show results of all generators for all plant conditions and with all reported CPSSs because of space limitation. The system response with EP-CPSS, PSO-CPSS and DE-CPSS is shown in Figure 2.29 - Figure 2.31, respectively. The speed response of the system with BA-CPSSs for all ten generators for plant-1 condition is shown in Figure 2.32, which reveals the effectiveness of the proposed controller as compared to above. The response comparison in terms of performance indices (as ITAE, IAE and ISE) is shown in Table 2.22 and found best with BA-CPSS (Proposed) and relatively good for CA-CPSS [25], FGSA-CPSS [26] and SPEA-CPSS [11] among the other controllers reported in literature. Therefore, it is better to compare the speed responses of the system for plant-1 configuration with BA-CPSS, CA-CPSS [25], FGSA-CPSS [26] and SPEA-CPSS [11]. The responses for Gen-1, Gen-2, Gen-4 and Gen-8 are shown in Figure 2.33 - Figure 2.37, respectively. It is clear from the responses that the performance of the system equipped with BA-CPSS (Proposed) is much better than as compared to others.

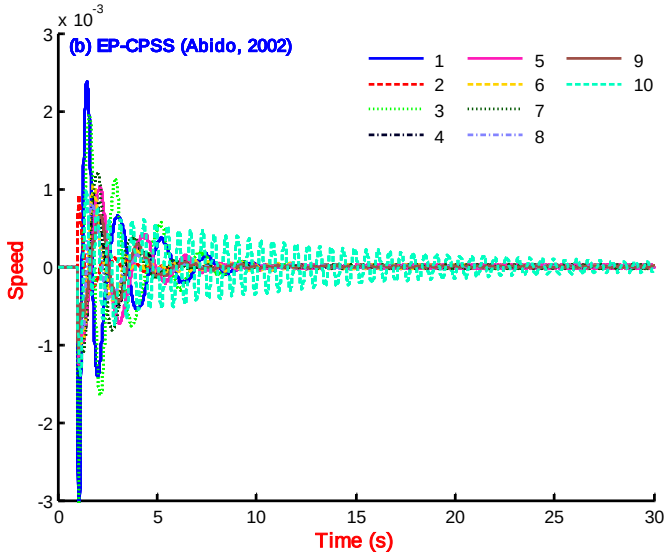

Figure 2.29: Speed variation for ten-generators of plant -1 configuration with EP-CPSS

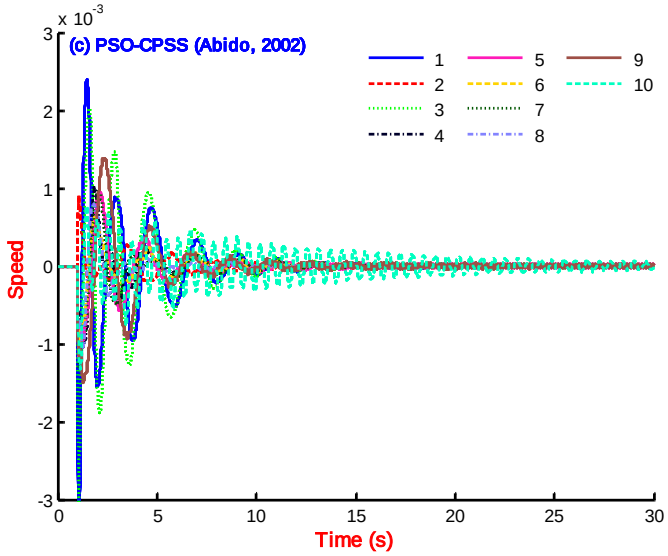

Figure 2.30: Speed variation for ten-generators of plant -1 configuration with PSO-CPSS

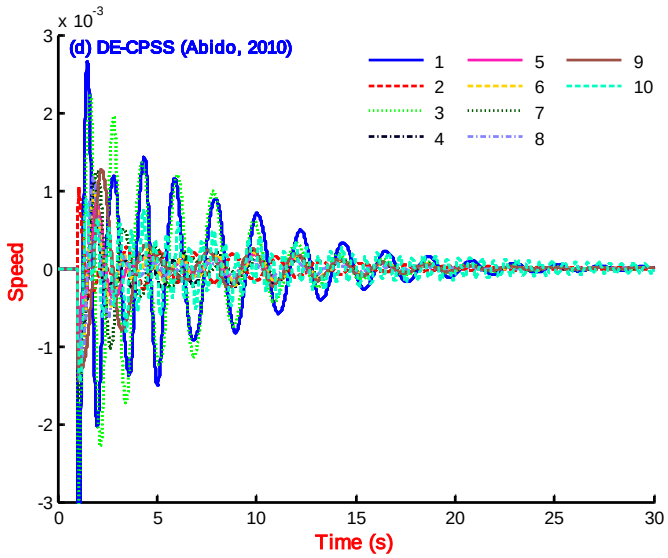

Figure 2.31: Speed variation for ten-generators of plant -1 configuration with DE-CPSS

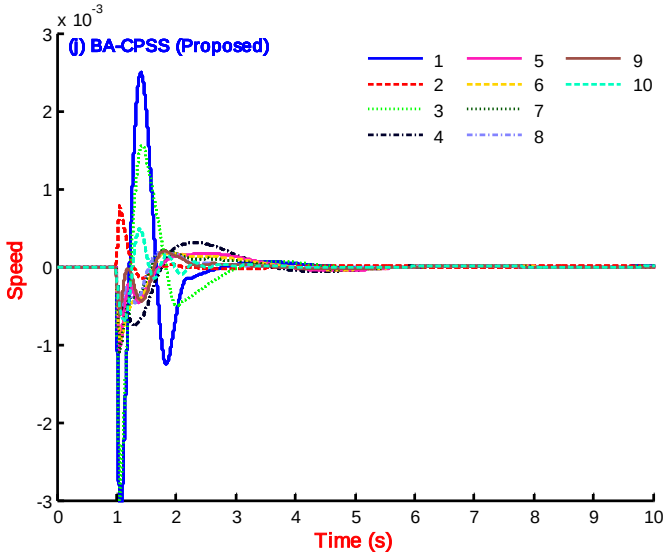

Figure 2.32: Speed variation for ten-generators of plant -1 configuration with BA-CPSS (Proposed)

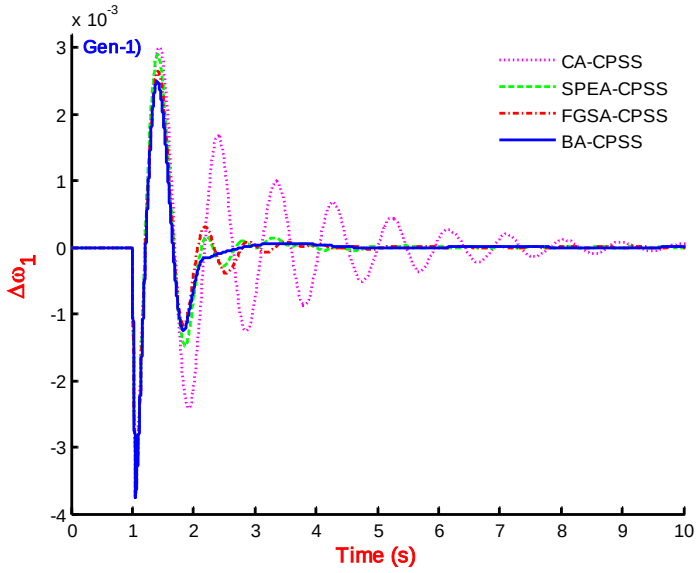

Figure 2.33: Speed response for generator-1 of plant-1 with CA-CPSS, SPEA-CPSS, FGSA-CPSS and BA-CPSS

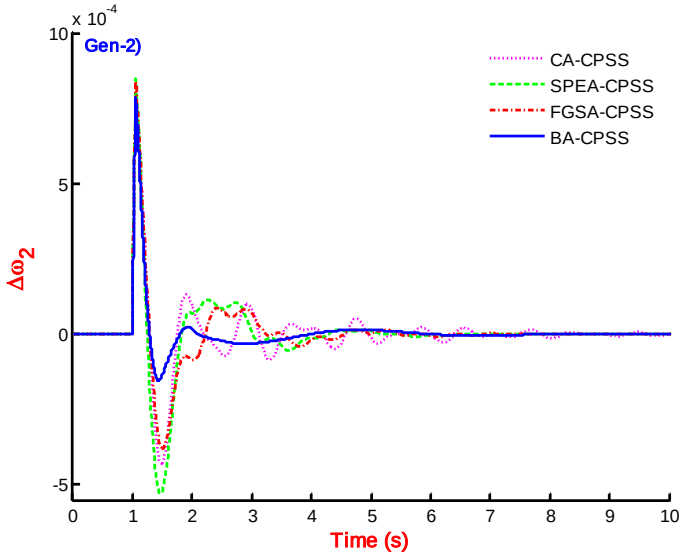

Figure 2.34: Speed response for generator-2 of plant-1 with CA-CPSS, SPEA-CPSS, FGSA-CPSS and BA-CPSS

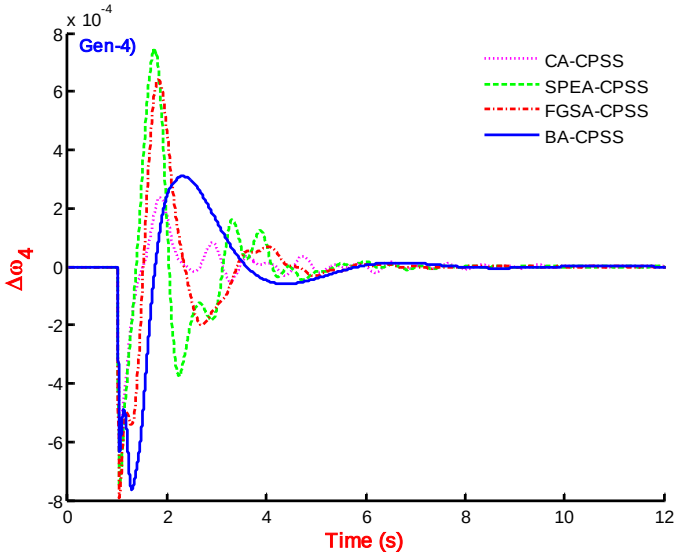

Figure 2.35: Speed response for generator-4 of plant-1 with CA-CPSS, SPEA-CPSS, FGSA-CPSS and BA-CPSS

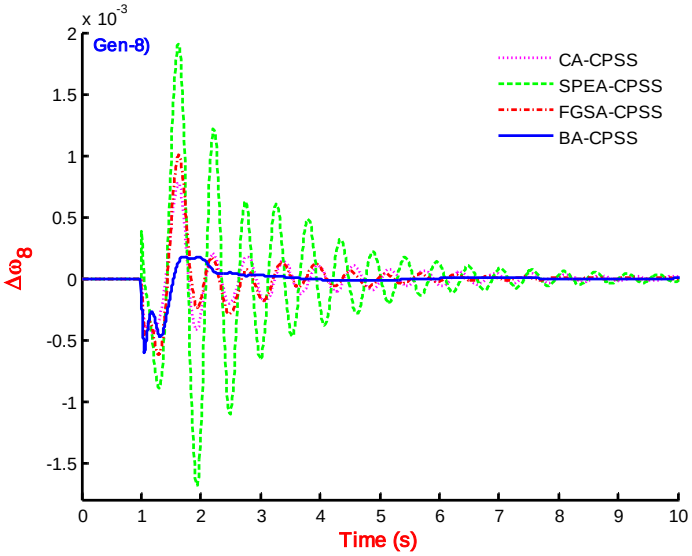

Figure 2.36: Speed response for generator-8 of plant-1 with CA-CPSS, SPEA-CPSS, FGSA-CPSS and BA-CPSS

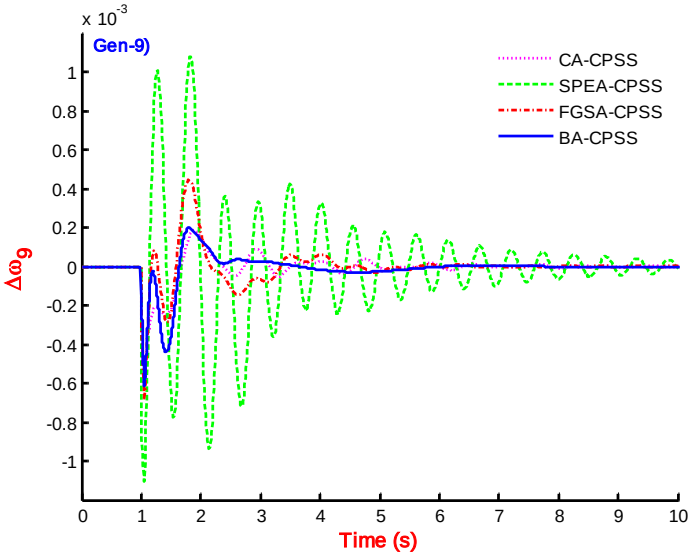

Figure 2.37: Speed response for generator-9 of plant-1 with CA-CPSS, SPEA-CPSS, FGSA-CPSS and BA-CPSS

Table 2.22: PIs for speed response with plant-1 – plant-8 of ten-machine system

Controllers	ITAE	IAE	ISE	ITAE	IAE	ISE
	Plant-1			Plant-2		
TS-CPSS [20]	0.4951	0.0621	4.6719×10^{-05}	0.1809	0.0348	2.1623×10^{-05}
EP-CPSS [21]	0.1365	0.0273	1.6775×10^{-05}	0.1681	0.0289	1.5046×10^{-05}
PSO-CPSS [22]	0.1578	0.0315	2.0336×10^{-05}	0.1608	0.0284	1.4595×10^{-05}
DE-CPSS [23]	0.2983	0.0459	3.1803×10^{-05}	0.2641	0.0409	2.2700×10^{-05}
GA-CPSS [24]	0.7176	0.0794	5.8893×10^{-05}	0.7645	0.0841	5.3184×10^{-05}
CA-CPSS [25]	0.0357	0.0139	1.1636×10^{-05}	0.0339	0.0127	7.5570×10^{-06}
ABGA-CPSS [19]	0.2550	0.0427	2.7732×10^{-05}	0.3413	0.0513	3.0041×10^{-05}
SPEA-CPSS [11]	0.0358	0.0164	1.3156×10^{-05}	0.0371	0.0175	1.4232×10^{-05}
FGSA-CPSS [26]	0.0208	0.0118	8.6749×10^{-06}	0.0251	0.0127	7.5094×10^{-06}
BA-CPSS (Proposed)	0.0138	0.0080	5.9342×10^{-06}	0.0148	0.0078	3.8796×10^{-06}
	Plant-3			Plant-4		
TS-CPSS[20]	0.1804	0.0250	8.0904×10^{-06}	2.0819	0.1425	2.2078×10^{-04}
EP-CPSS[21]	0.1681	0.0289	1.5046×10^{-05}	0.1462	0.0267	2.2120×10^{-05}
PSO-CPSS[22]	0.1145	0.0186	5.5668×10^{-06}	0.2999	0.0468	4.9061×10^{-05}
DE-CPSS[23]	0.1605	0.0258	9.2001×10^{-06}	0.2945	0.0466	4.0727×10^{-05}
GA-CPSS[24]	0.4316	0.0484	1.7528×10^{-05}	0.7216	0.0846	7.8384×10^{-05}
CA-CPSS[25]	0.0202	0.0073	2.5068×10^{-06}	0.0200	0.0098	1.0399×10^{-05}
ABGA-CPSS[19]	0.2042	0.0314	1.1968×10^{-05}	0.5749	0.0759	6.8650×10^{-05}
SPEA-CPSS[11]	0.0214	0.0094	4.0660×10^{-06}	0.0614	0.0242	3.8760×10^{-05}
FGSA-CPSS[26]	0.0120	0.0065	2.1052×10^{-06}	0.0190	0.0112	1.3383×10^{-05}
BA-CPSS (Proposed)	0.0060	0.0038	7.5086×10^{-07}	0.0115	0.0072	9.3028×10^{-06}
	Plant-5			Plant-6		
TS-CPSS[20]	0.1859	0.0305	1.7517×10^{-05}	0.3228	0.0446	2.4855×10^{-05}
EP-CPSS[21]	0.1132	0.0212	1.1646×10^{-05}	0.1378	0.0262	1.4255×10^{-05}
PSO-CPSS[22]	0.1137	0.0223	1.2449×10^{-05}	0.1390	0.0273	1.4938×10^{-05}
DE-CPSS[23]	0.1778	0.0321	1.8140×10^{-05}	0.2393	0.0382	2.2500×10^{-05}
GA-CPSS[24]	0.4405	0.0540	2.8344×10^{-05}	0.6389	0.0708	4.5463×10^{-05}
CA-CPSS[25]	0.0235	0.0101	7.8741×10^{-06}	0.0317	0.0122	8.5154×10^{-06}
ABGA-CPSS[19]	0.2498	0.0403	2.4133×10^{-05}	0.2227	0.0382	2.1782×10^{-05}
SPEA-CPSS[11]	0.0320	0.0144	1.1481×10^{-05}	0.0328	0.0144	9.5331×10^{-06}
FGSA-CPSS[26]	0.0154	0.0097	8.2015×10^{-06}	0.0176	0.0101	6.0931×10^{-06}
BA-CPSS (Proposed)	0.0109	0.0069	6.8971×10^{-06}	0.0107	0.0066	3.9466×10^{-06}
	Plant-7			Plant-8		
TS-CPSS[20]	0.2390	0.0304	1.1968×10^{-05}	0.5819	0.0688	4.8479×10^{-05}
EP-CPSS[21]	0.1138	0.0183	5.7842×10^{-06}	0.1228	0.0236	1.2338×10^{-05}
PSO-CPSS[22]	0.1241	0.0209	7.0208×10^{-06}	0.1204	0.0239	1.3114×10^{-05}
DE-CPSS[23]	0.1464	0.0241	8.7068×10^{-06}	0.2666	0.0424	2.6581×10^{-05}
GA-CPSS[24]	0.2798	0.0379	1.5966×10^{-05}	0.5755	0.0662	3.7217×10^{-05}
CA-CPSS[25]	0.0216	0.0080	3.0716×10^{-06}	0.0282	0.0112	7.4942×10^{-05}
ABGA-CPSS[19]	0.1909	0.0312	1.2801×10^{-05}	0.2537	0.0442	2.9079×10^{-05}
SPEA-CPSS[11]	0.0220	0.0096	4.1197×10^{-06}	0.0384	0.0172	1.3420×10^{-05}
FGSA-CPSS[26]	0.0114	0.0066	2.2490×10^{-06}	0.0237	0.0124	8.3173×10^{-06}
BA-CPSS (Proposed)	0.0043	0.0033	9.6798×10^{-07}	0.0149	0.0080	5.0021×10^{-06}

The robust performance analysis is carried out by creating the simulation with eight plant conditions and system contingencies. Since total controllers are ten including proposed BA-CPSS and considered eight plants, therefore, simulation has to be carried out for eighty times and each time the performance indices (ITAE, IAE and ISE) for the speed response are recorded and shown in Table 2.22. It can be seen from the PI values that the comparatively lower value with BA-CPSS proves its superiority over the other methods even for the wide range of operating conditions and system configurations. As an example, the ITAE, IAE and ISE values with proposed BA-CPSS for plant-7 are as 0.0043, 0.0033 and 9.6798×10^{-7}, respectively and comparatively lesses in magnitude, proving the superiority of the performance.

2.6.4. Eigenvalue Comparison

As per literature, PSS performance is generally checked by nonlinear simulation analysis and with eigenvalue analysis. Therefore, as an example the system with plant-1 configuration is initialized, and state space model is obtained by using 'linmod' function in MATLAB Software with all considered controllers and the eigenvalue, damping ratio and frequency is determined and enlisted in Table 2.23 - Table 2.24. All generators with least damping ratio are showing negative value without PSS, which proves the necessity of PSS to improve damping. It can be observed that the three generators are showing negative value of damping ratio with TS-CPSS; therefore, the performance with TS-CPSS is not satisfactory under said operating conditions and system configurations. The eigenvalue analysis of the system without PSS, and with other controllers as reported in literature for plant-1 configuration throughout the ten-machine system is enlisted in Table 2.23, while that of with BA-CPSS is mentioned in Table 2.24. The eigenvalue analysis of the system in Table 2.24 with BA-CPSS, reveals that the generators are not only having a positive value of damping ratio but also having a higher value as compared to other controllers proving superior performance.

Since, it is impossible to show eigenvalue analysis with all plant conditions because of space constraints, therefore, it is limited to plant-1. To show the location of eigenvalue on s-plane, three controllers PSO-CPSS, DE-CPSS and FGSA-CPSS are compared of the system without PSS and with BA-CPSS in Figure 2.38 - Figure 2.40. The PSO-CPSS [22], have four EMOs in the right-hand side of s-plane, making system response unsatisfactory, on the other hand, BA-CPSS provides the stable response in Figure 2.38. In Figure 2.39, DE - CPSS [23] represents some EMOs with < 0.1 damping ratio, resulting degraded response as compared to BA-CPSS. The eigenvalue plot of FGSA - CPSS [26], is also representing one-pair of EMO with < 0.1 damping ratio, resulting poor response as compared to BA-CPSS in Figure 2.40.

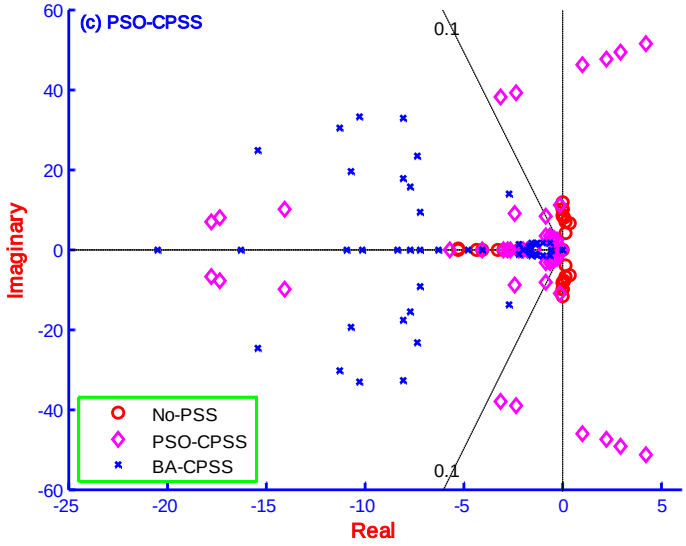

Figure 2.38: Eigenvalue plot of plant-1 without PSS, PSO-CPSS and BA-CPSS

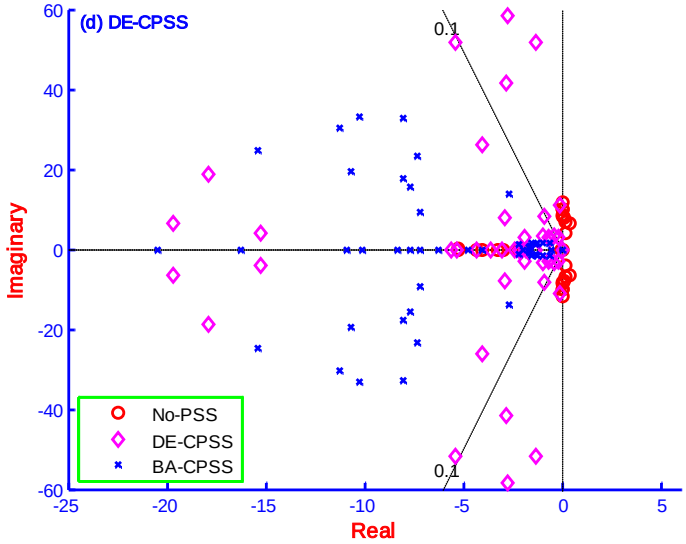

Figure 2.39: Eigenvalue plot of plant-1 without PSS, DE-CPSS and BA-CPSS

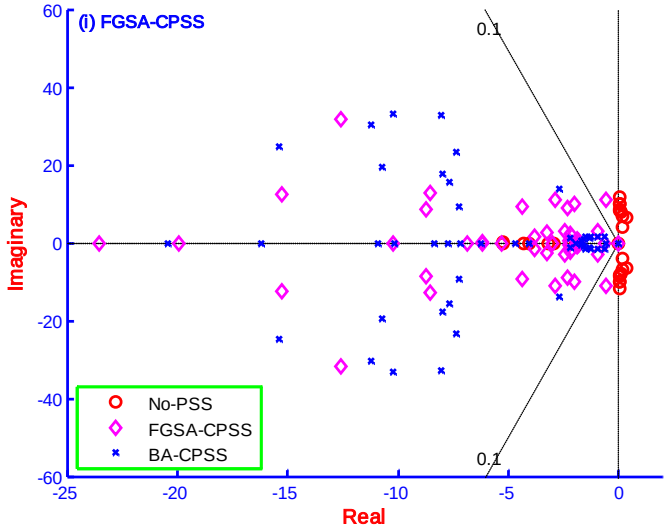

Figure 2.40: Eigenvalue plot of plant-1 without PSS, FGSA-CPSS and BA-CPSS system

Table 2.23: Eigenvalue, damping factor and freq. of oscillations (Hz) of system for plant-1.

Eigenvalue	Damping ratio	Freq. (Hz)	Eigenvalue	Damping ratio	Freq. (Hz)
No-PSS			TS-CPSS [20]		
0.0269 ± 11.8712i	-0.0023	1.8894	4.4434 ± 51.8270i	-0.0854	8.2485
0.0272 ± 9.8481i	-0.0028	1.5674	3.3552 ± 49.7055i	-0.0673	7.9109
0.0337 ± 9.9563i	-0.0034	1.5846	2.6668 ± 48.8047i	-0.0546	7.7675
0.0672 ± 8.6842i	-0.0077	1.3821	-2.6829 ± 38.4475i	0.0696	6.1191
0.0659 ± 8.1610i	-0.0081	1.2989	-0.0489 ± 10.9662i	0.0045	1.7453
0.1029 ± 7.7315i	-0.0133	1.2305	-0.8888 ± 8.3505i	0.1058	1.3290
0.1524 ± 6.8654i	-0.0222	1.0927	-0.3788 ± 2.9687i	0.1266	0.4725
0.3710 ± 6.3793i	-0.0581	1.0153	-0.1738 ± 2.3327i	0.0743	0.3713
0.1799 ± 4.1924i	-0.0429	0.6672	-0.4506 ± 2.6556i	0.1673	0.4227
EP-CPSS [21]			PSO-CPSS [22]		
4.7502 ± 52.5746i	-0.0900	8.3675	4.2180 ± 51.3808i	-0.0818	8.1775
3.1009 ± 49.3163i	-0.0628	7.8489	2.9718 ± 49.2594i	-0.0602	7.8399
2.0518 ± 47.1126i	-0.0435	7.4982	2.2444 ± 47.6889i	-0.0470	7.5899
-0.0871 ± 10.9808i	0.0079	1.7476	1.0236 ± 45.9724i	-0.0223	7.3167
-1.1374 ± 1.6415i	0.0273	6.6274	-2.3343 ± 39.1372i	0.0595	6.2289
-2.0744 ± 38.5212i	0.0538	6.1308	-3.0955 ± 38.0191i	0.0812	6.0509
-1.0486 ± 8.6106i	0.1209	1.3704	-0.0878 ± 10.9645i	0.0080	1.7451
-0.3585 ± 2.2471i	0.1575	0.3576	-0.8257 ± 8.1048i	0.1014	1.2899
-1.5694 ± 8.5176i	0.1812	1.3556	-0.2757 ± 2.1257i	0.1286	0.3383
DE-CPSS [23]			GA-CPSS [24]		
-0.0871 ± 10.969i	0.0079	1.7457	10.605 ± 81.844i	-0.1285	13.026
-1.2945 ± 51.817i	0.0250	8.2470	3.5842 ± 63.325i	-0.0565	10.078
-2.8007 ± 78.222i	0.0358	12.449	0.5364 ± 49.935i	-0.0107	7.9475
-2.7388 ± 58.327i	0.0469	9.2830	-0.0624 ± 10.976i	0.0057	1.7468
-0.1987 ± 2.9827i	0.0665	0.4747	-2.514 ± 84.261i	0.0298	13.411
-2.8168 ± 41.691i	0.0674	6.6354	-1.7306 ± 56.56i	0.0306	9.0018
-5.4278 ± 51.76i	0.1043	8.2378	-4.4752 ± 88.003i	0.0508	14.006
-0.9275 ± 8.2165i	0.1122	1.3077	-0.1712 ± 2.8836i	0.0593	0.45894
-0.4203 ± 3.3561i	0.1243	0.5341	-0.4797 ± 8.0258i	0.0597	1.2774
CA-CPSS [25]			ABGA-CPSS [19]		
-0.3285 ± 10.861i	0.0302	1.7286	15.842 ± 84.329i	-0.1846	13.421
-0.4947 ± 6.8178i	0.0724	1.0851	1.7032 ± 86.089i	-0.0198	13.701
-4.5151 ± 13.31i	0.3212	2.1184	0.36251 ± 54.852i	-0.0066	8.7299
-4.9499 ± 11.148i	0.4058	1.7743	-2.2534 ± 28.196i	0.0797	4.4876
-31.717 ± 62.49i	0.4526	9.9456	-3.7093 ± 16.525i	0.2190	2.63
-5.6634 ± 9.8976i	0.4966	1.5753	-0.0739 ± 10.954i	0.0067	1.7435
-35.421 ± 55.556i	0.5376	8.842	-0.3978 ± 8.1127i	0.0490	1.2912
-36.980 ± 45.49i	0.6308	7.2399	-0.3030 ± 2.8788i	0.1047	0.45817
-6.779 ± 7.8346i	0.6543	1.2469	-0.2090 ± 1.8832i	0.1103	0.29972
SPEA-CPSS [11]			FGSA-CPSS [26]		
-0.1751 ± 12.245i	0.0143	1.9489	-0.5578 ± 11.07i	0.050323	1.7619
-0.9727 ± 12.39i	0.0783	1.9719	-2.0126 ± 9.9144i	0.19894	1.5779
-1.0334 ± 10.174i	0.1011	1.6192	-2.3070 ± 9.0928i	0.24593	1.4472
-2.0324 ± 18.968i	0.1065	3.0189	-2.8675 ± 11.226i	0.2475	1.7866
-1.1371 ± 10.071i	0.1122	1.6029	-0.9760 ± 2.8309i	0.32596	0.45055
-2.6440 ± 21.33i	0.1230	3.3947	-12.607 ± 31.847i	0.36806	5.0687
-1.5950 ± 9.6791i	0.1626	1.5405	-4.3961 ± 9.2117i	0.4307	1.4661
-3.2698 ± 10.892i	0.2875	1.7336	-8.5668 ± 12.663i	0.56033	2.0154
-0.9733 ± 2.9036i	0.3178	0.46213	-2.4411 ± 2.9483i	0.63774	0.46924

Table 2.24: Eigenvalue, damping factor and freq. (Hz) with BA-CPSS

Eigenvalue	Damping Factor	Frequency of oscillations (Hz)
-2.6829 ± 13.938i	0.18901	2.2184
-8.0468 ± 32.959i	0.23718	5.2457
-10.246 ± 33.207i	0.29484	5.2851
-7.3467 ± 23.377i	0.29982	3.7205
-11.239 ± 30.438i	0.34637	4.8443
-0.6199 ± 1.6773i	0.3467	0.26695
-8.0104 ± 17.868i	0.40908	2.8438
-7.6582 ± 15.489i	0.44322	2.4651
-10.696 ± 19.403i	0.48277	3.0881

2.7. Conclusions

In this chapter, a double stage conventional power system stabilizer is designed and investigated for small signal stability enhancement on a single-machine infinite-bus power system. The gain and time constants (zero and pole) of CPSS are optimized by using the bat algorithm with an eigenvalue based objective function as to place electromechanical mode oscillations in D-shape sector on s-plane. The speed response of a synchronous generator for the SMIB power system without PSS, with CPSSs reported in literature [2-11] and with the bat algorithm based optimized CPSS is compared for power system models with different operating conditions.

It is found that the response with CPSSs [2-11] can stabilize the system for some plant conditions but with prolonged settling time as compared against reduced settling time with BA-CPSS for all plant conditions. The superior performance of BA-CPSS is further illustrated by using performance indices as the value is least as compared to the system with CPSSs [2-11] and without PSS. The small signal stability is guaranteed by use of BA-CPSS because all electromechanical mode eigenvalue (for 231 plants) are shifted to LHS of s-plane under the D-shape sector while with other CPSSs [2-11], some plant conditions are proved to be either unstable or not in desired D-shape sector of s-plane. Probable reasons of better performance with BA-CPSS could be as (i) Powerful and quick-start characteristics of the bat algorithm are able to search globally optimal PSS parameter settings without trapping in local minima, (ii) Another important reason could be the operating point selected for tuning PSS parameters. The operating point in terms of active power and reactive power is 1.0 pu and 0.2087 pu for proposed BA-CPSS, as compared to 1.0 pu and 0.015 pu as reported in literature [9, 39-41, 234-241].

The proposed approach is applied to two multimachine power systems as two-area four-machine ten-bus power system and IEEE New England ten-bus thirty nine-bus power system models with different loading conditions, disturbances and contingencies. The problem of CPSSs parameter's selection is treated as an optimization problem which is solved by the Bat algorithm using an eigenvalue based objective function. Maximization of the minimum damping ratio of

dominant oscillatory modes is employed as an objective to optimize the PSS parameters and designed simultaneously with consideration of interaction among them. The stabilizers are tuned to simultaneously shift the lightly damped electromechanical modes of plant to a prescribed zone in the s-plane, called as the wedge-shaped sector. The proposed CPSSs are considered as decentralized in nature because only local measurements are employed as the stabilizer inputs; easy to tune and install.

In performance analysis of the both systems, eight plants of each system are considered with different fault locations and operating conditions. The simulation results as the speed response are observed and the performance indices are recorded to see the comparison with CPSSs designed by BA and with different techniques as reported in literature. Eigenvalue analysis of both systems provides acceptable damping of electromechanical modes, particularly of the low-frequency local as well as inter-area modes, of the system equipped with BA-CPSSs. It is established that the both systems with proposed BA-CPSSs in the decentralized way can rapidly damp local and inter-area modes of oscillations over the range of different operating conditions and contingencies. The effectiveness and robustness of BA-CPSS is validated by performance indices and the eigenvalue analysis.

The CPSSs designed using BA has been examined for eight plant conditions of the four-machine power system. The performance of nonlinear time-domain simulation with BA-CPSS is examined and compared with CPSSs reported in literature and found to be with reduced overshoot and settling time. The observed PIs of speed response with proposed BA-CPSS for eight plant conditions are found to be lesser as compared against the performance that of with CPSSs as reported in literature. The eigenvalue analysis with BA-CPSS proves stable operation because of EMOs recorded with positive damping and more than 0.1. The damping ratio with BA-CPSS (0.1633, 0.25321, 0.30705, 0.37242) is greatly enhanced as compared to that of the system without PSS (-0.04239, -0.19298, 0.12396, 0.46587) and with CPSSs reported in literature.

The CPSSs designed using BA has been examined for eight plant conditions of the IEEE ten-machine power system. The performance of nonlinear time-domain simulation with BA-CPSS is examined and compared with CPSSs reported in literature and found to be with reduced overshoot and settling time. The observed PIs of speed response with proposed BA-CPSS for eight plant conditions are found to be lesser as compared against the performance that of with CPSSs as reported in literature. The eigenvalue analysis proves stable operation because of EMOs recorded with positive damping and more than 0.1. The damping ratio with BA-CPSS is greatly enhanced as compared to that of the system without PSS and with CPSSs reported in literature. The eigenvalue plot reveals that all EMOs of the system with BA-CPSS moved to LHS or more specifically to the wedge-shaped sector on s-plane.

Chapter 3

DESIGN OF OPTIMALLY TUNED PID BASED POWER SYSTEM STABILIZER USING BAT ALGORITHM

In this chapter, the design of a proportional, derivative and integral (PID) based power system stabilizer (PSS) is carried out using the bat algorithm (BA) to optimize the parameters. The design of proposed PID controller is considered with an objective function based on square error minimization to enhance the small signal stability of nonlinear plant for a wide range of operating conditions of single-machine infinite-bus power system, two-area four-machine ten-bus power system and IEEE New England ten-machine thirty nine-bus power system. The BA optimized PID based PSS (BA-PID-PSS) controller is applied to these test power system models and the performance is compared with PID based PSSs designed by distinct methods in literature. The robustness is tested by considering eight plant conditions representing the wide range of operating conditions, unlike loading conditions and system configurations to establish the superior performance with BA-PID-PSS over the counter controllers.

3.1. Introduction

Power system stability is an ability to regain synchronism on occurrence of disturbance. In general, an electric power system (EPS) is large, complex in nature and interconnected and prone to small signal oscillation on occurrence of disturbances. These low-frequency electromechanical oscillations (EMOs) persist because of insufficient damping torque caused by high/adverse operating conditions. In the absence of sufficient damping, such EMOs may persist for longer time resulting to limitations on power transfer capability of EPSs. In multimachine EPS model, two distinct types of EMOs are recognized [75]. The oscillations associated to generators at a generating station, swinging with respect to the rest of the power system are called as intra-area mode oscillations. Similarly, the swinging of many machines in an area of EPS against machines in another area is called as inter-area oscillations. Thus, a supplementary control signal is added to the excitation system to damp out these oscillations, and the system is called as power system stabilizer (PSS) [191]. The widely used PSS is conventional PSS, which is designed by phase compensation in the frequency domain and are introduced as lead lag compensator. It is necessary to have a linearized model of EPS to design CPSS parameters by using modern control techniques, such as to provide well damping for both types of oscillations. The CPSS parameters are tuned to an operating point which may fail to give satisfactory damping to other operating

conditions of the power system. The use adaptive control techniques to design CPSS may eliminate this limitation but are complex in nature and costly [23].

In recent years, many optimization methods based on random search are suitable for solving suitable for solving complex problems, which are impossible to be solved by mathematical methods such as the gradient. Application of new optimization methods, fuzzy and intelligent method is the focus of researchers to design a good quality controller for enhancement of small signal stability of a power system [254].

In [73], the fuzzy logic based power system stabilizer is designed for single-machine infinite-bus power system model and extended it to multimachine power system in [72, 255]. To mitigate the shortcomings of conventional methods much optimization based algorithms have been proposed. The methods available in literature are as the Tabu search [256], evolutionary algorithm [257], the differential evolution (DE) algorithm [258], simulated annealing [11], Genetic Algorithm [259], Fuzzy logic with genetic algorithm [211], Artificial Bee Colony (ABC) [6], Particle swarm optimization [206, 260], an iterative linear matrix inequalities algorithm [34, 261, 262].

The different controller structures are always the field of interest for researchers. The proportional integral derivative (PID) type PSS is used for improving damping of EPSs. This is generally accepted in the industries for various applications. In literature PID based PSSs are designed for SMIB power system such as using genetic algorithm (GA) [27, 263], harmony search algorithm (HSA) [27], bacterial foraging algorithm (BFA) [28, 29], real coded genetic algorithm (RCGA) [30], Ziegler-Nichols (ZN) [31], hybrid particle swarm-bacteria foraging optimization (PSO-BFA) [29], artificial bee colony (ABC) [32], bio-geographical based optimization (BBO) [33], and for two-area four-machine ten-bus power system such as iterative linear matrix inequality (ILMI) [34] based PID based PSS is successfully employed. The application of GA has been reported to tune the PI and PID based PSS design for multimachine power systems [263, 264]

To mitigate the drawbacks of above optimization methods for PSS design, a relatively new optimization scheme known as the bat algorithm (BA) is used for the PID type PSS parameter design. It appeared as a promising one for handling the optimization problems even with epistatic objective functions as in ten-machine power systems where the number of variables is ranging up to 27. It is not largely affected by the size and nonlinearity of the problem and can converge to the optimal solution in many cases where many analytical methods fail to converge. Considering the strength of this algorithm, it is employed in the present work for the optimal PID tuning for stability enhancement in SMIB, four-machine and ten-machine power system power system.

In the organization of chapter, the problem is formulated in section 3.2 with information

about power system models, on PID and about the objective function used in optimization. Section 3.3, includes the detail on design, performance comparison of PID based PSS with the SMIB power system. The design and performance comparison of PID based PSS for four-machine system is considered in section 3.4. The PID based PSSs are designed and compared for ten-machine power system in section 3.5. Lastly, the analysis is concluded in section 3.6.

3.2. Problem Formulation

The aim of the chapter is to utilize the Bat algorithm for tuning the PID parameters to the power system; therefore, the EPS elements such as generators, excitation system and PSS must be modeled. To complete the tuning process, an objective function to obtain satisfactory results is necessary and should be defined. Consequently, the system model and an objective function used in PSS parameter tuning in a multi machine power system are elaborated.

3.2.1. Test system configuration

The systems under consideration are single-machine connected to infinite-bus (SMIB), two-area four-machine ten-bus and IEEE New England ten-machine thirty nine-bus power system. The single-line diagram representation is shown in Figure 1.6, and the way of connection with AVR is shown in Figure 3.1. The small signal model of the SMIB power system can be represented by Figure 3.2 with connection of PID based PSS. The output signal of this PSS is added to AVR to modulate the excitation system for enhancing the damping of the small signal oscillations.

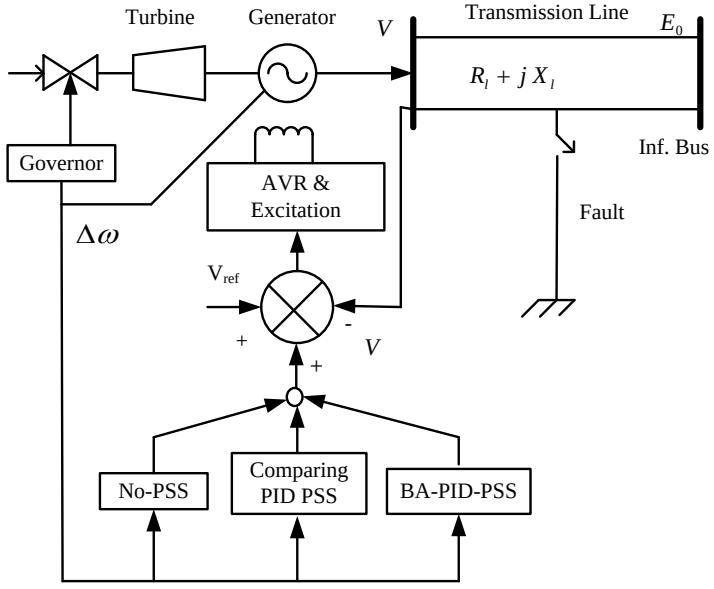

Figure 3.1: Line diagram of SMIB power system with PID controller

The single-line diagram representation of four-machine and ten-machine models is shown in Figure 1.14 and Figure 1.15, respectively. Moreover, a general Heffron-Philip representation is shown in Figure 1.13 [1, 99, 213]. The considered synchronous machines of SMIB and multimachine power systems are of the model 1.0 type as discussed in [191]. To cover all operating conditions, the power system with generators, stabilizers, and excitation systems can be modeled by a set of nonlinear differential equations as in Eqn. (1.59) and (1.60) [14].

It is necessary to have linearized model to a power system around an operating point to analyze the small signal stability and consequently, to design power system stabilizer. The power system represented by Eqn. (1.59 - 1.60), is linearized around an equilibrium operating point of the power system, and represented by Eqn. (1.64 -1.65) [14, 23]. As the state space model is represented by Eqn. (1.64), and consequently, the system matrix A, therefore, the total electromechanical modes within the system can be evaluated in the form $\lambda = \sigma \pm j.\omega$.

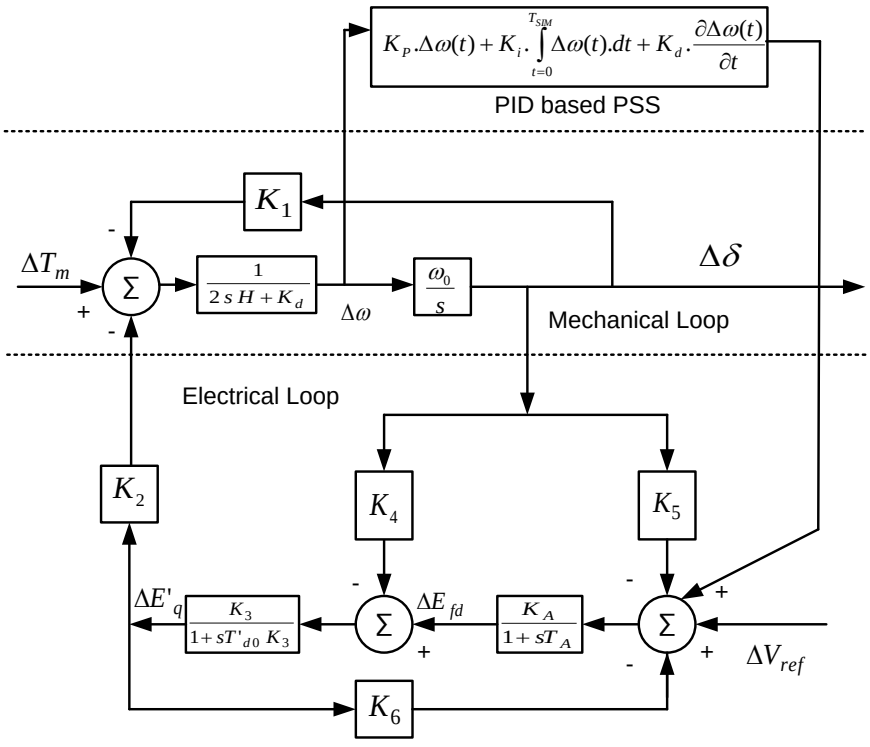

Figure 3.2: Representation of Heffron-Philip model with PID type PSS

The state equations of a power system, consisting '*N*' number of generators and N_{pss} number of power system stabilizers can be written as in Eqn. (1.68). Where, *A* is the system matrix of an order as *4N×4N* and is given by $\partial f / \partial X$, while *B* is the input matrix with order $4N \times N_{pss}$ and is given by $\partial f / \partial U$. The order of state vector ΔX is *4N×1*, the order of ΔU is $N_{pss} \times 1$.

3.2.2. On proportional integral derivative PSS

The proportional-integral-derivate (PID) controller is most popularly known and used as a feedback controller in the field of complex process industries. It can provide excellent robust control performance over a wide range of operating conditions of a power system because of its three different modes of operation. The proportional controller mode can reduce the rise time but unable to reduce the steady-state error of the response. The higher value of proportional gain may cause a system to become an unstable but lower value make in-sensitive or lesser sensitive to even large value of error. The derivative control mode enhances the system stability by reducing overshoot & improving transient response. The integral control mode of operation may eliminate the steady-state error but may worsen the transient response of a system. The lower value of integral gain value makes a system sluggish while the higher value causes a random increase in the overshoot. Therefore, to design the PID controller, all three gains require special attention to get the control signal by the trial-and-error method based on the experience and plant behaviour. The block diagram representation of PID controller for a closed-loop system is shown in Figure 3.3 and mathematically represented by Eqn. (3.1).

$$U_{pid} = K_P.\Delta\omega(t) + K_i.\int_{t=0}^{T_{SIM}} \Delta\omega(t).dt + K_d.\frac{\partial\Delta\omega(t)}{\partial t} \tag{3.1}$$

3.2.3. Objective function

To optimize the PID parameters (K_p , K_d and K_i) an objective function is formulated, where in the damping is maximized in terms of reduced overshoots and settling time in system oscillations. As in integral square error (ISE), the error is heavily reduced / penalized in beginning (during large errors) and low for light errors. Since, the speed deviation $\Delta\omega$ of the generator is sensed from the shaft of the generator. As an objective function, the ISE based cost function is represented for SMIB, four-machine and ten-machine power system by Eqn. (3.2 - 3.4), respectively.

$$J = \int_0^{T_{SIM}} \left|\Delta\omega(t)\right|^2 dt \tag{3.2}$$

$$J = \sum_{j=1}^{4} \int_0^{T_{SIM}} \left|\Delta\omega_j(t)\right|^2 dt \tag{3.3}$$

$$J = \sum_{j=1}^{10} \int_{0}^{T_{SIM}} \left|\Delta\omega_j(t)\right|^2 .dt \tag{3.4}$$

Subjected to parameter bounds for SMIB power system as in Eqn. (3.5)

$$\begin{cases} K_p^{\min} \le K_p \le K_p^{\max} \\ K_d^{\min} \le K_d \le K_d^{\max} \\ K_i^{\min} \le K_i \le K_i^{\max} \end{cases} \tag{3.5}$$

Subjected to parameter bounds for two-area four-machine power system as in Eqn. (3.6)

$$\begin{cases} K_{jp}^{\min} \le K_{jp} \le K_{jp}^{\max} \\ K_{jd}^{\min} \le K_{jd} \le K_{jd}^{\max} \quad j = 1,\cdots,4 \\ K_{ji}^{\min} \le K_{ji} \le K_{ji}^{\max} \end{cases} \tag{3.6}$$

Subjected to parameter bounds for New England ten-machine power system as in Eqn. (3.7)

$$\begin{cases} K_{jp}^{\min} \le K_{jp} \le K_{jp}^{\max} \\ K_{jd}^{\min} \le K_{jd} \le K_{jd}^{\max} \quad j = 1,\cdots,9 \\ K_{ji}^{\min} \le K_{ji} \le K_{ji}^{\max} \end{cases} \tag{3.7}$$

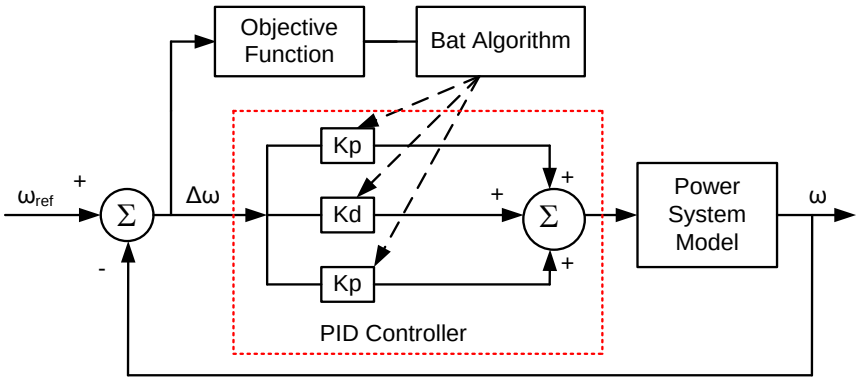

Figure 3.3: Scheme of PID controller tuning using Bat Algorithm

Typical ranges of the optimizing parameters as selected are mentioned in preceding sections for respective power system models. Considering one of the above objectives, the proposed approach employs BA to solve this optimization problem for an optimal set of PSS parameters. The process of optimization of PID parameters is carried out according to the arrangement as in Figure 3.3, where in generators of the test system is equipped with PID controllers with input as change in speed at the generator shaft. The used bat algorithm is introduced in section 1.2.2.

3.3. Design and Performance Evaluation: SMIB System

3.3.1. Design of PID-PSS using bat algorithm

In this section, the design of PID based PSS parameters are designed by the proposed bat algorithm; the problem is formulated in MATLAB environment and executed on Intel (R) Core (TM) - 2 Duo CPU T6400 @ 2.00 GHz with 3 GB RAM, 32-bit operating system. The initializing parameters to the bat algorithm are considered as in section 2.4.1. The plant (SMIB power system) operating at nominal operating condition (where in X_l = 0.4 pu and P_{g0} = 1.0 pu) is considered for optimal tuning of PID-PSS parameters; subjected to the time domain based simple ISE minimization based objective function with the parametric bounds as $0.001 \le K_p \le 70$, $0.001 \le K_d \le 20$, $-20.0 \le K_i \le 10$ are considered for the optimization of PID parameters. The plot of fitness function for 50 iterations is shown in Figure 3.4. The plot for BA-PID-PSS optimized parameter is shown in Figure 3.5 for same 50 iterations. It can be seen that the 40 iterations are sufficient because all three parameters are almost constant at 40 and above iterations. The values of PID parameters optimized using the bat algorithm is included in Table 3.1 for comparison of values with that of reported in literature.

3.3.2. PID-PSS reported in literature

In literature PID based PSSs are designed for SMIB power system such as using genetic algorithm (GA) [27], harmony search algorithm (HSA) [27], bacterial foraging algorithm (BFA) [28, 29], real coded genetic algorithm (RCGA) [30], Ziegler-Nichols (ZN) [31], hybrid particle swarm-bacteria foraging optimization (PSO-BFA) [29] , artificial bee colony (ABC) [32], bio-geographical based optimization (BBO) [33] , and the parameters of the controller are enlisted in Table 3.1.

Table 3.1: Comparison of PID based PSS parameters: SMIB power system

S. No.	Controller	K_p	K_d	K_i
1	GA-PID-PSS [27]	9.984	8.784	1.722
2	HS-PID-PSS [27]	26.758	15.479	3.1202
3	BFA-PID-PSS [28]	31.58	32.32	6.3202
4	RCGA-PID-PSS [30]	49.9740	7.8802	5.6789
5	ZN-PID-PSS [31]	30.0	2.8	3.226
6	BFA-PID-PSS [29]	36.1976	5.2715	1.2732
7	PSBFA-PID-PSS [29]	190.4623	11.2516	2.4753
8	ABC-PID-PSS [32]	26.03226	0.8354	14.7003
9	BBO-PID-PSS [33]	51.4655	9.6729	20.3237
10	BA-PID-PSO (Proposed)	23.8668	5.0211	-19.6162

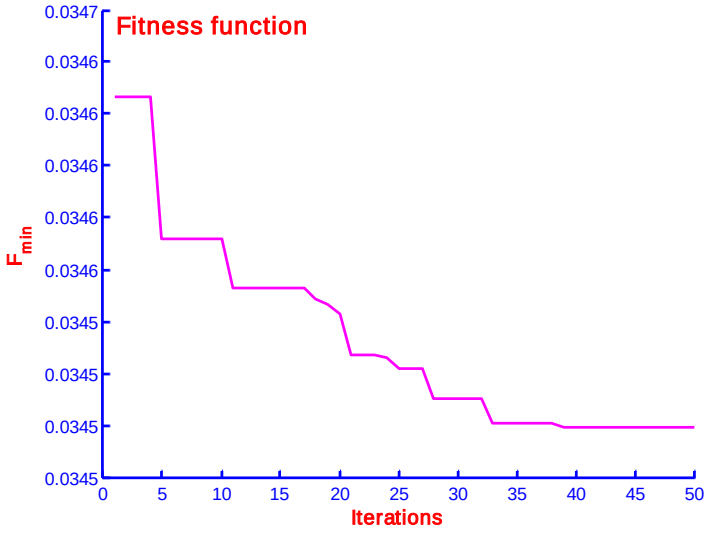

Figure 3.4: Fitness function plot of PID design: SMIB power system

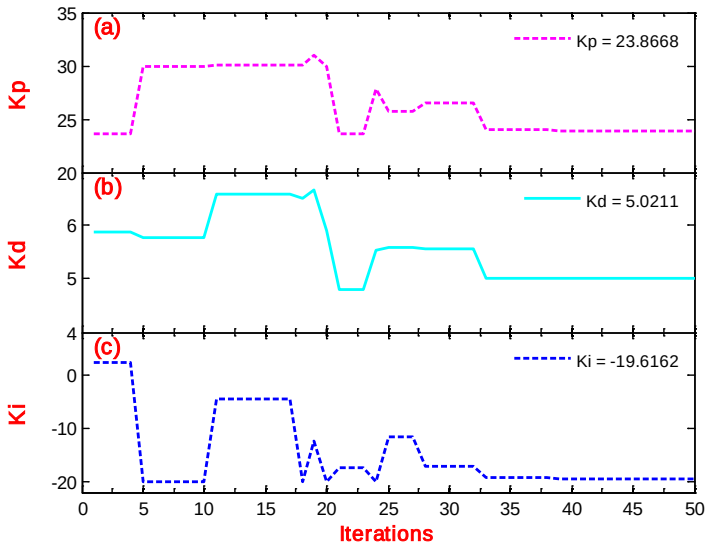

Figure 3.5: Plot of PID parameters (a) K_p , (b) K_d and (c) K_i

3.3.3. Simulation result comparison

To examine performance of the SMIB power system under nonlinear mode by creating fault at time 5 seconds and persistent for 0.1 seconds is carried out with a wide range of operating conditions, resulting different plants. The system with distinct combinations of different active power and transmission line reactance as in Table 2.2 (eight different plants) and system data as in Table A.1 are considered for nonlinear simulations. Such obtained eight-plants are examined for the speed response with PID based PSSs reported in literature. An SIMULINK based block diagram, including all the nonlinear blocks is generated in MATLAB Software. The speed signal is taken as output. Initially, the speed response of the SMIB power system with nominal operating condition (plant-6) is compared and shown in Figure 3.6, using BA-PID-PSS (Proposed) and the

GA-PID-PSS [27], HS-PID-PSS [27], BFA-PID-PSS [28] and RCGA-PID-PSS [30] as mentioned in Table 3.1. The speed response of ZN-PID-PSS [31], BFA-PID-PSS [29], PSBFA-PID-PSS [29], ABC-PID-PSS [32], BBO-PID-PSS [33] and BA-PID-PSS (Proposed) is compared in Figure 3.7. To observe the robustness of the BA-PID-PSS, the SMIB power system is simulated with the eight plants conditions as in Table 2.2. The different signals of the synchronous generator viz. speed response, generator terminal voltage, and control voltage as output of BA-PID-PSS are shown in Figure 3.8, Figure 3.9 and Figure 3.10, respectively. It is easily concluded that the SMIB power system with BA-PID-PSS produces a stable response even with adverse operating conditions (Plant-7 and Plant-8) of the power system. To prove superiority of the BA-PID-PSS, the SMIB system is simulated one by one with other controllers as reported in literature (Table 3.1) and the performance indices (ITAE, IAE and ISE as introduced in section 1.4) of speed response are recorded for the simulation time as 40 seconds and produced in Table 3.2. As the lower value of PI, represents the superior performance of the system with reduced settling time and overshoots. In Table 3.2, the value of PIs (i.e. ITAE, IAE and ISE are 0.0371, 0.0065, and 3.4499×10^{-05}, respectively) with BA-PID-PSS is lesser as compared to others, resulting good performance, i.e. the small signal stability is greatly enhanced as compared to others.

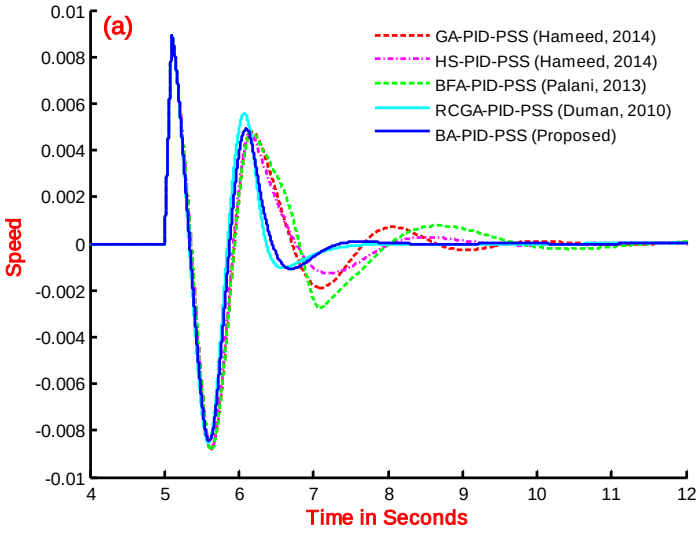

Figure 3.6: Speed response comparison of GA, HS, BFA, RCGA and BA (Proposed) based PID type PSS for SMIB power system with nominal operating conditions

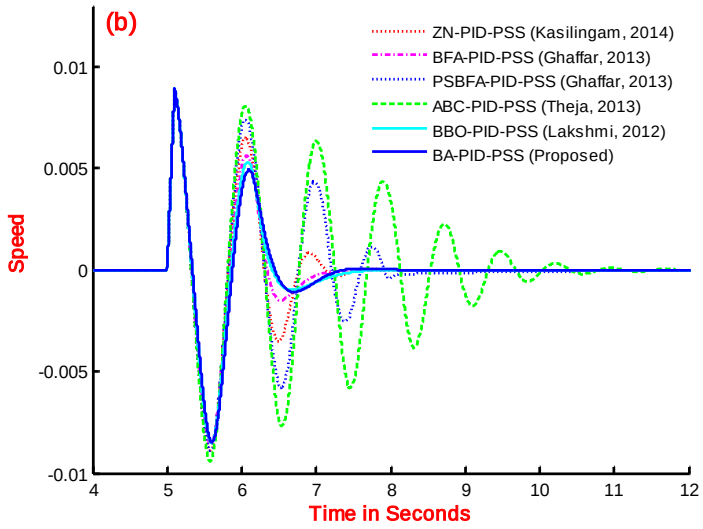

Figure 3.7: Speed response comparison of ZN, BFA, PSBFA, ABC, BBO and BA (Proposed) based PID type PSS for SMIB power system

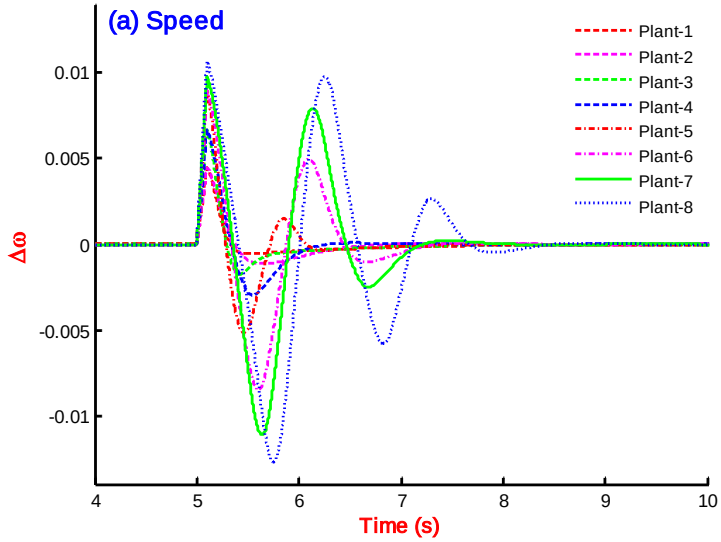

Figure 3.8: Speed response using BA-PID-PSS with eight nonlinear plants

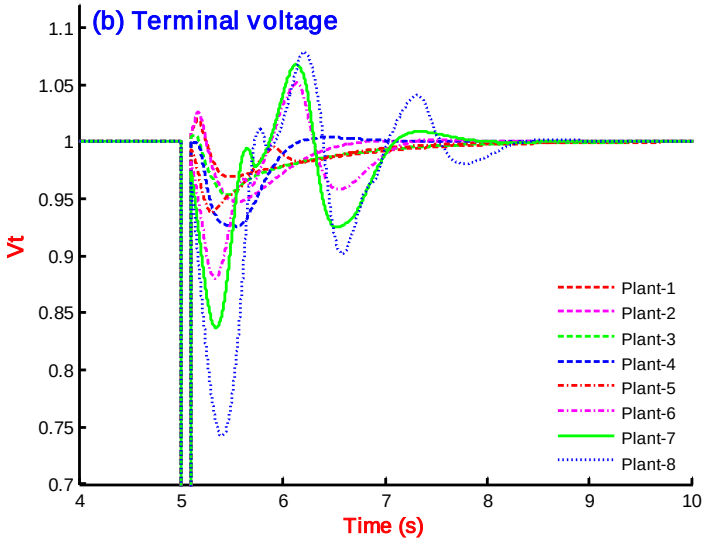

Figure 3.9: Terminal voltage using BA-PID-PSS with eight nonlinear plants

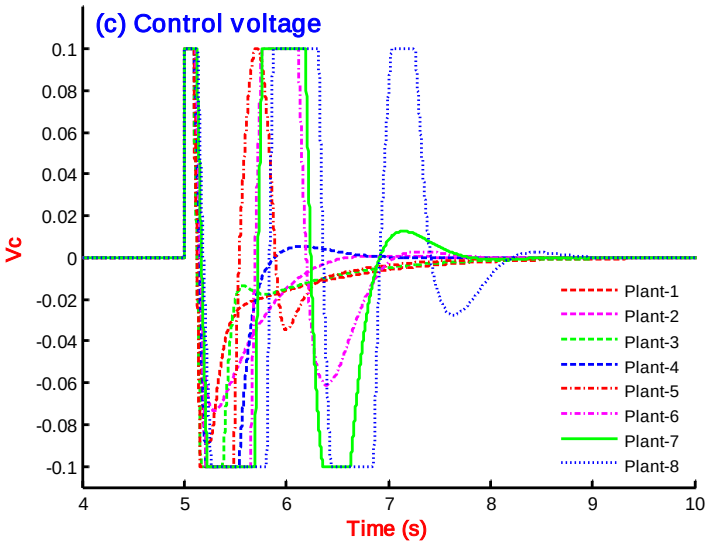

Figure 3.10: Control voltage using BA-PID-PSS with eight nonlinear plants

Table 3.2: Performance indices based comparison of speed response with PID-PSS and BA-PID-PSS

S. No.	Controller	ITAE	IAE	ISE
1	GA-PID-PSS [27]	0.0541	0.0088	4.1610×10^{-05}
2	HS-PID-PSS [27]	0.0490	0.0081	3.9365×10^{-05}
3	BFA-PID-PSS [28]	0.0668	0.0103	4.4853×10^{-05}
4	RCGA-PID-PSS [30]	0.0382	0.0067	3.5710×10^{-05}
5	ZN-PID-PSS [31]	0.0441	0.0076	4.2167×10^{-05}
6	BFA-PID-PSS [29]	0.0382	0.0067	3.6350×10^{-05}
7	PSBFA-PID-PSS [29]	0.0675	0.0108	5.6106×10^{-05}
8	ABC-PID-PSS [32]	0.1120	0.0165	8.6844×10^{-05}
9	BBO-PID-PSS [33]	0.0378	0.0066	3.5029×10^{-05}
10	BA-PID-PSO (Proposed)	0.0371	0.0065	3.4499×10^{-05}

3.3.4. Eigenvalue comparison

In previous section, the speed response of nonlinear simulation with the PSSs is compared, and superiority of the BA-PID-PSS is established in terms of settling time and performance indices. In this section, the eigenvalue comparison is to be carried out for SMIB power system with nominal operating conditions for all controllers in Table 3.1. The power system, programmed in MATLAB Software (m-file and Simulink) is run to determine *A*, *B*, *C* and *D* matrices using 'linmod' command of the software. To determine eigenvalue of the system 'eig' function of software is used. The resulting eigenvalue have only real parts (negative) with damping ratio as 1.0, therefore, are not of interest. The complex conjugate eigenvalue are responsible for oscillations of the system response, and are enlisted in Table 3.3. As per literature, the desirable damping ratio of the system should be more than 0.1. On critical examination of the 4^{th} column of Table 3.3, the maximum damping ratio of the system is associated to the proposed controller as 0.125400,

proving its superiority among the other controllers.

Table 3.3: EMOs having least damping factor for SMIB system with nominal operating conditions with PID-PSS reported in literature and BA-PID-PSS

S. No.	Controller	Eigenvalue	Damping factor	Frequency (Hz)
1	GA-PID-PSS [27]	-0.24386 ± 6.9823i	0.034905	1.1113
2	HS-PID-PSS [27]	-0.82746 ± 8.8267i	0.093336	1.4048
3	BFA-PID-PSS [28]	-0.85728 ± 9.3378i	0.091423	1.4862
4	RCGA-PID-PSS [30]	-0.8924 ± 11.083i	0.080258	1.764
5	ZN-PID-PSS [31]	-0.8741 ± 9.1725i	0.094865	1.4599
6	BFA-PID-PSS [29]	-0.94423 ± 9.8075i	0.095833	1.5609
7	PSBFA-PID-PSS [29]	0.86605 ± 19.065i	-0.045381	3.0342
8	ABC-PID-PSS [32]	-0.67126 ± 8.7627i	0.076381	1.3946
9	BBO-PID-PSS [33]	-0.77408 ± 11.198i	0.068964	1.7822
10	BA-PID-PSO (Proposed)	-1.0733 ± 8.4915i	0.125400	1.3515

3.3.5. Robustness test using eigenvalue plot for 231 plants

The line diagram of the SMIB power system is shown in Figure 3.1 with the configuration of system modes like without PSS, with comparing PID-PSS reported in literature (Table 3.1) and the transmission line connection to the infinite-bus with fault location. The relevant system data are mentioned in Table A.1. The value of active power (P_{g0}) and the transmission line reactance (X_l) is kept varying to formulate 231 plants of the SMIB power system within the range given in Eqn. (2.19 – 2.20). The value of active power is changed from 0.4 to 1.4 and reactance from 0.2 to 0.7 in the step size of 0.05 in both cases resulting to 21 and 11 combinations respectively and thus constituting 231 plant conditions within the SMIB power system.

The operating point of power system covered as above encompasses all practical operating conditions and constituting a set of 231 different plants (operating conditions). In previous section, the nonlinear simulation is carried out and the superiority of the proposed BA-PID-PSS is proved. In this section, the robust performance of SMIB is to be checked for 231 plant conditions (covering very heavy loading conditions) by eigenvalue plot. The eigenvalue plots for 231 plants (as defined by Eqn. 2.19 – 2.20) are drawn for all controllers in Table 3.1 including BA-PID-PSS (proposed), and the robust operation of the proposed controller is to be established. In this section, the eigenvalue of the system are not expected to be in d-shape sector or wedge-shaped sector with the proposed BA-PID-PSS, because the objective function is a time domain based minimization of ISE of the speed error signal. Therefore, the robustness would be checked by having all eigenvalue for the wide operating conditions in the left half of s-plane (LHS). The eigenvalue detail of the system without PSS is given in Table 3.4, where in 146 EMOs are in the right-hand side (RHS) of s-plane.

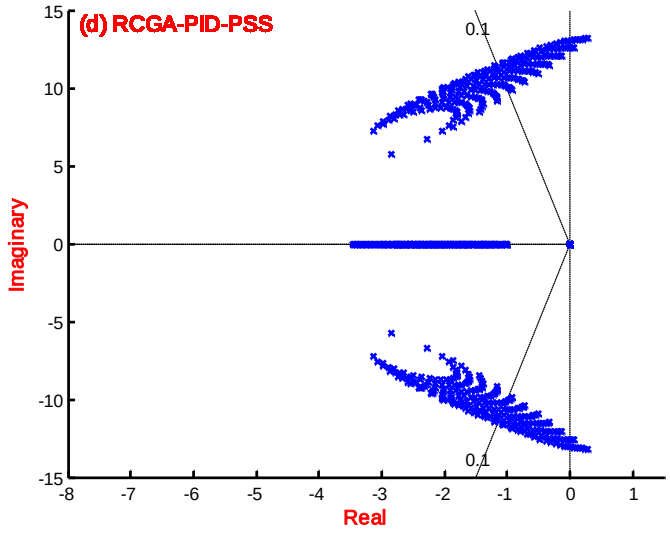

Figure 3.11: Eigenvalue plot for 231 plants with RCGA-PID-PSS: SMIB system

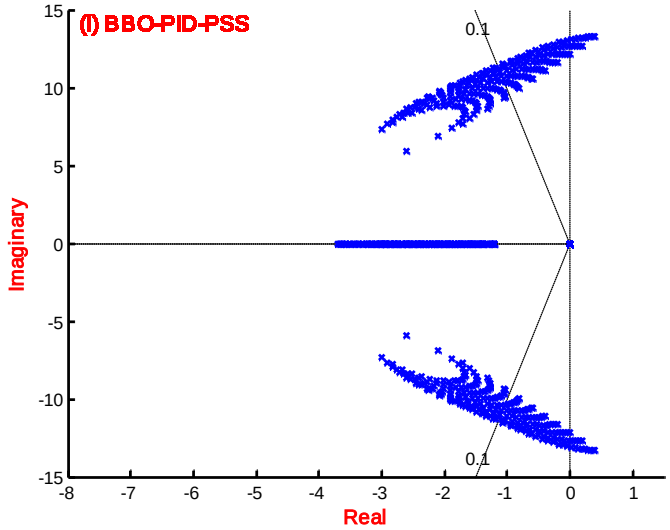

Figure 3.12: Eigenvalue plot for 231 plants with BBO-PID-PSS: SMIB system

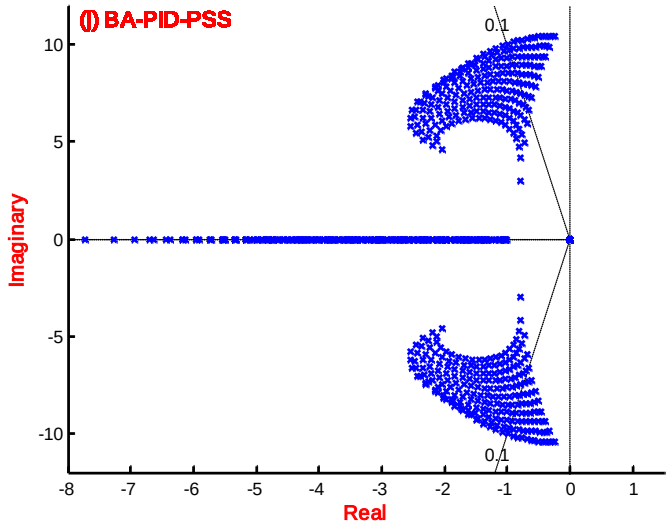

Figure 3.13: Eigenvalue plot for 231 plants with BA-PID-PSS (Proposed)

The SMIB system equipped with different PID based PSS (as in Table 3.1) is simulated to get eigenvalue plot and the EMOs lying in RHS are enlisted in Table 3.4. The eigenvalue plots with all controllers are carried out but shown only with RCGA-PID-PSS [30], BBO-PID-PSS [33] and proposed BA-PID-PSS in Figure 3.11, Figure 3.12 and Figure 3.13, respectively. It can be seen that the EMOs in RHS of s-plane with BA-PID-PSS is zero proving robust operation over the wide range of operating conditions (over 231 plants) of the power system.

Table 3.4: Detail of the number of EMOs in RHS of s-plane for SMIB power system with 231 plant configurations

S. No.	Controller	EMOs in RHS of s-plane: $\sigma_i \geq 0$
1	Without PSS	146
2	GA-PID-PSS [27]	138
3	HS-PID-PSS [27]	4
4	BFA-PID-PSS [28]	6
5	RCGA-PID-PSS [30]	20
6	ZN-PID-PSS [31]	4
7	BFA-PID-PSS [29]	6
8	PSBFA-PID-PSS [29]	276
9	ABC-PID-PSS [32]	16
10	BBO-PID-PSS [33]	30
11	BA-PID-PSS (Proposed)	Nill

3.4. Design and Performance Evaluation: 4-Machine System

3.4.1. Design of PID-PSS using bat algorithm

As the creations of experimental plants for two-area four-machine ten-bus power system are well explained in section 2.3.2.1, where in the line data (Table A.2), load flow data (Table A.3) and machine data (Table A.4) are given to the system configuration without PSS. The system model referring to plant-1 configuration as in Table 2.4; is equipped with PID type PSSs to all four-machines (named as Gen-1 to Gen-4) and subjected to PSSs design using the bat algorithm with a simple time domain based minimization of ISE as an objective function (Eqn. 3.3). The speed signal from each generator is sensed and the value of sum of ISE of the error signal is minimized to tune PID parameters of four PSSs. By a trial-and-error method, it is found that the suitable values of loudness and pulse rate for PID-PSS optimization using the bat algorithm are as A = 0.9 and r = 0.1. The termination criterion of the tuning process is considered as the maximum number of iterations and set as 200. The parameter bounds are selected by using a trial-and-error method; therefore, several attempts are required and considered as $20 \leq K_{pj} \leq 60$, $5 \leq K_{dj} \leq 20$, $0.01 \leq K_{ij} \leq 25$. The optimized PID based PSSs parameters are shown in Table 3.5 to compare with that of reported in literature. The behavior of BA during optimization in terms of fitness

function is shown in Figure 3.14. Clearly, the 90 iterations are sufficient to have constant value of fitness function.

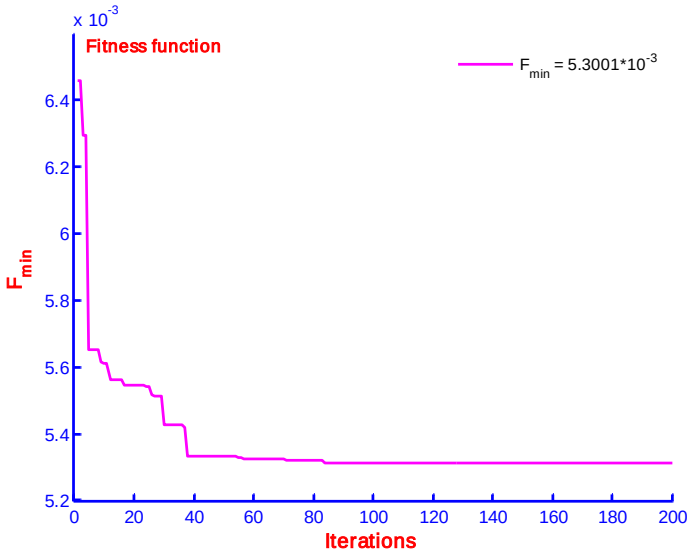

Figure 3.14: Fitness function plot of during PID design: Four-machine power system

3.4.2. PID-PSS reported in literature

In literature, the PID type controller design for four-machine power system is only designed using iterative linear matrix inequality (ILMI) [24], and the parameters of four PID type PSS parameters connected to four-machines are enlisted in Table 3.5.

Table 3.5: Comparison of PID type PSSs parameters: Four-machine power system

S. No.	Controller	Generators	K_{pj}	K_{dj}	K_{ij}
1	ILMI-PID-PSS [34]	Gen-1	47.311	-0.0267	53.077
		Gen-2	39.426	0.0697	139.84
		Gen-3	23.285	-0.0312	-17.477
		Gen-4	21.689	-0.0796	54.573
2	BA-PID-PSS (Proposed)	Gen-1	60.0000	5.2592	25.0000
		Gen-2	59.9900	19.9890	24.9990
		Gen-3	59.9980	10.4790	25.0000
		Gen-4	54.2700	5.0000	25.0000

3.4.3. Simulation result comparison

An SIMULINK based block diagram, including all the nonlinear blocks is generated [191]. The speed signals of the machines are considered as output and the initial value of the change in speed is taken as zero. The output signals of CPSSs are added to V_{ref} via limiters. It is used to damp out the small signal disturbances via modulating the generator excitation. The output must be limited to preventing the PSS acting to counter action of AVR. Different operating points are taken as the distinctive plants for both systems. The limits of PSS outputs are taken as ± 0.05. In decentralized

PSSs, to activate the proposed controller at same instant, proper synchronization signal is required to be sent to all machines. All PSSs can be applied simultaneously to the respective machines for both power system models.

The two-area four-machine ten-bus power system is described in section 2.3.2 without PSS, and the creations of system models based on operating conditions are elaborated in section 2.3.2.1. The PID based PSSs designed in section 3.4.1 are connected with the system. In each plant condition as listed in Table 2.4 is considered with fault location as given in Table A.5. The disturbance is considered as self-clearing at different buses at 1.0 second and cleared after 0.05 second. Referring to section 2.3.2.2 and section 2.3.2.3, wherein the simulation and eigenvalue analysis with eight plant conditions without PSS are described and found that none of the generators of plants are showing stable operation; therefore, not needed to compare to the simulation results.

In this section, the speed response with proposed BA-PID-PSS is compared to the response of the system with only controller available in literature, i.e. ILMI-PID-PSS[34] and conventional PSSs designed in [13]. The parametric comparison of PID based PSS is incorporated in Table 3.5. The speed response of the four-machine system of plant-1configuration with CPSSs [13], ILMI-PID-PSSs [34] and proposed BA-PID-PSSs for all four generators is compared with the system response in Figure 3.15 - Figure 3.18. It can be clearly said that the speed response of plant-1with the use of BA-PID-PSS is greatly improved. To have the robust performance study of the proposed BA-PID-PSS, the system configuration (as eight plants) is simulated for eight times and the speed responses for each generator (Gen-1 to Gen-4) are presented in Figure 3.19 - Figure 3.22. The system response with proposed controller gives a stable response for each generator with each plant configuration (Table 3.6).

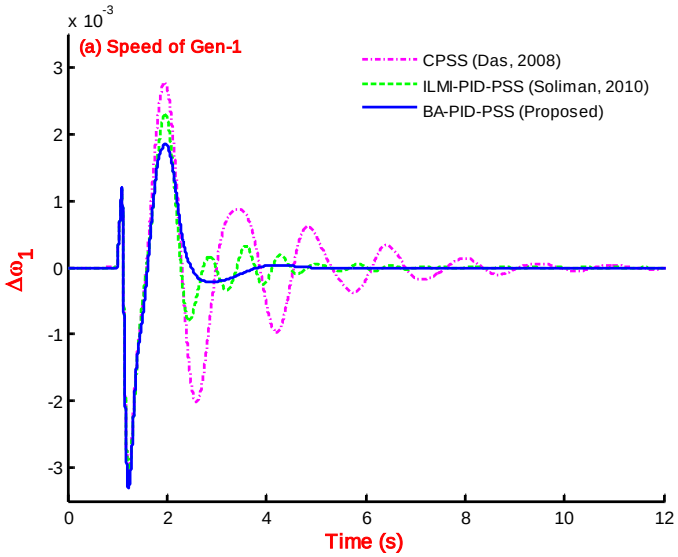

Figure 3.15: Speed response comparison for Gen-1 of Plant-1 with CPSS, ILMI-PID-PSS and BA-PID-PSS (Proposed)

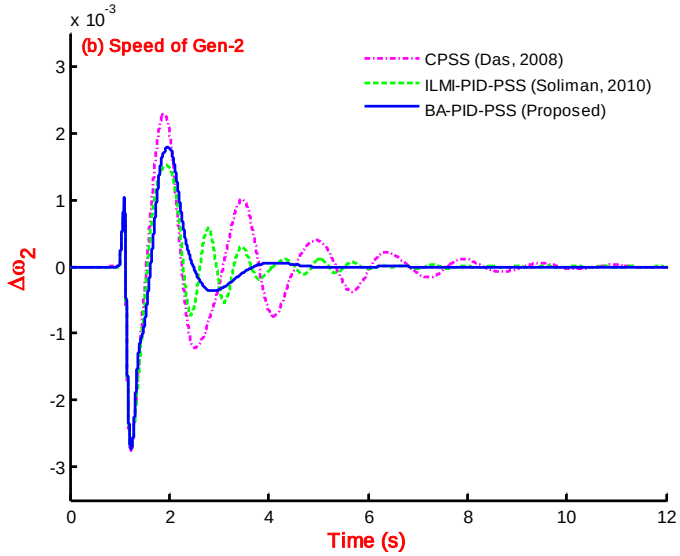

Figure 3.16: Speed response comparison for Gen-2 of Plant-1 with CPSS, ILMI-PID-PSS and BA-PID-PSS (Proposed)

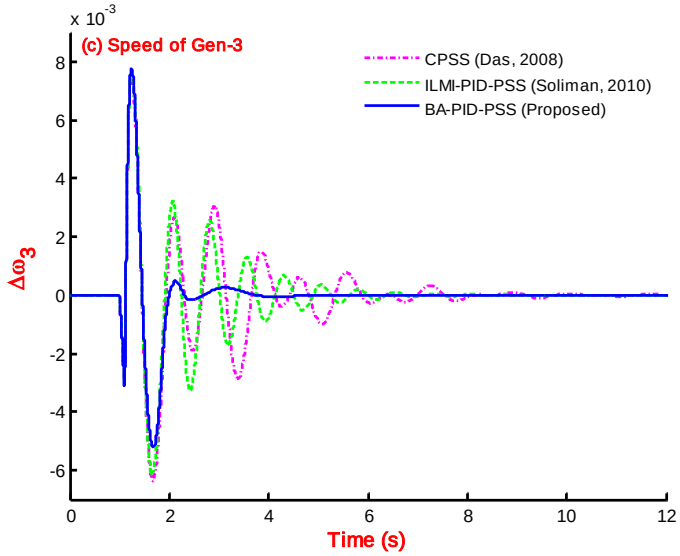

Figure 3.17: Speed response comparison for Gen-3 of Plant-1 with CPSS, ILMI-PID-PSS and BA-PID-PSS (Proposed)

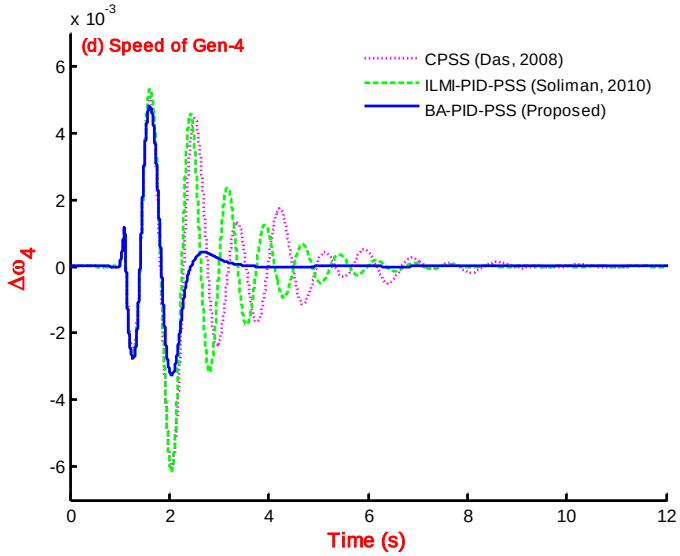

Figure 3.18: Speed response comparison for Gen-4 of Plant-1 with CPSS, ILMI-PID-PSS and BA-PID-PSS (Proposed)

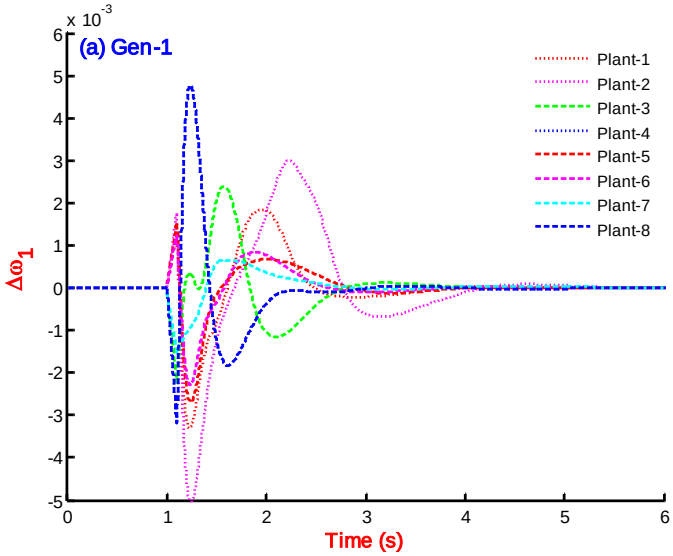

Figure 3.19: Speed response for Gen-1 of eight nonlinear plants with BA-PID-PSS

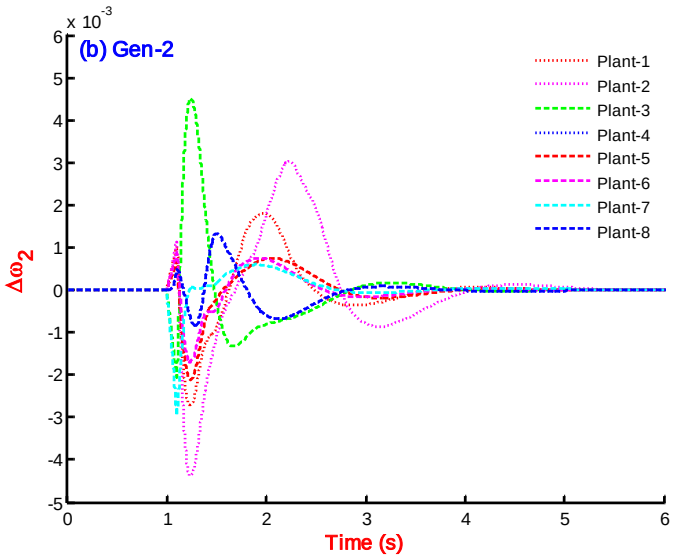

Figure 3.20: Speed response for Gen-2 of eight nonlinear plants with BA-PID-PSS

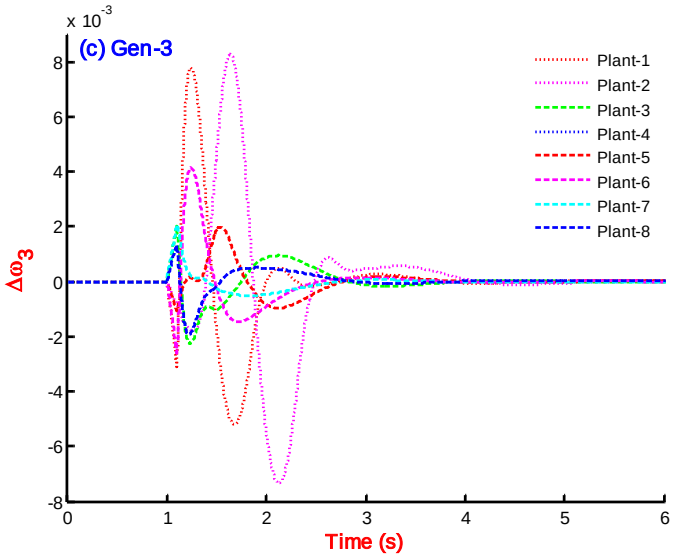

Figure 3.21: Speed response for Gen-3 of eight nonlinear plants with BA-PID-PSS

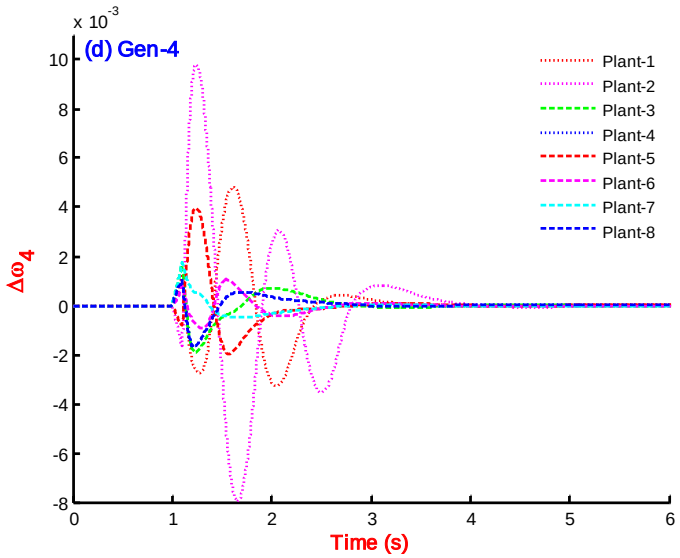

Figure 3.22: Speed response for Gen-4 of eight nonlinear plants with BA-PID-PSS

To have a complete comparison of the system over a wide range of operating conditions with different system configuration with CPSSs [13], ILMI-PID-PSSs [34] and BA-PID-PSSs (proposed) controllers is simulated. Since, the system plants are eight and controllers are three, therefore, the system is simulated for 24 times and each time the performance's indices (ITAE, IAE and ISE) are recorded as in Table 3.6. On comparison of PIs, the minimum value is presented by the proposed BA-PID-PSS for all plant conditions, proving its superior performance over the CPSSs [13] and ILMI-PID-PSSs [34].

Table 3.6: Performance indices based comparison of speed response for plant-1 – plant-8 with CPSS, ILMI-PID-PSS and BA-PID-PSS (Proposed)

Controller	ITAE	IAE	ISE	ITAE	IAE	ISE
	Plant-1			Plant-2		
CPSS [13]	0.0752	0.0251	6.0598×10^{-05}	0.1042	0.0351	1.0987×10^{-04}
ILMI-PID-PSS [34]	0.0469	0.0194	5.4053×10^{-05}	0.0808	0.0317	1.2326×10^{-04}
BA-PID-PSS (Prop.)	0.0201	0.0112	3.2318×10^{-05}	0.0434	0.0214	8.4797×10^{-05}
	Plant-3			Plant-4		
CPSS [13]	0.0442	0.0150	1.9582×10^{-05}	0.0384	0.0137	1.5681×10^{-05}
ILMI-PID-PSS [34]	0.0363	0.0130	1.9048×10^{-05}	0.0398	0.0141	1.9356×10^{-05}
BA-PID-PSS (Prop.)	0.0134	0.0068	9.0028×10^{-06}	0.0119	0.0058	6.9224×10^{-06}
	Plant-5			Plant-6		
CPSS [13]	0.0460	0.0151	1.8749×10^{-05}	0.0379	0.0128	1.3858×10^{-05}
ILMI-PID-PSS [34]	0.0228	0.0096	1.3308×10^{-05}	0.0183	0.0084	1.0583×10^{-05}
BA-PID-PSS (Prop.)	0.0112	0.0057	7.2262×10^{-06}	0.0093	0.0052	6.2257×10^{-06}
	Plant-7			Plant-8		
CPSS [13]	0.0282	0.0103	7.0640×10^{-06}	0.0257	0.0096	7.0855×10^{-06}
ILMI-PID-PSS [34]	0.0123	0.0054	2.9837×10^{-06}	0.0195	0.0084	7.8744×10^{-06}
BA-PID-PSS (Prop.)	0.0119	0.0049	2.7070×10^{-06}	0.0061	0.0030	1.9644×10^{-06}

3.4.4. Eigenvalue comparison

In previous section, the speed response and its performance indices analysis carried out and proved the superior performance of the proposed BA-PID-PSS over the comparing controllers. In this section, the eigenvalue analysis is carried with the system for plant-1 configuration when equipped with CPSSs [13], ILMI-PID-PSSs [34] and BA-PID-PSSs (proposed) controllers. The electromechanical modes with least value of damping ratio are recorded for each generator as in Table 3.7. The eigenvalue analysis reveals that the damping ratio with BA-PID-PSS is improved as compared to other controllers (CPSSs [13], ILMI-PID-PSSs [34]).

Table 3.7: EMOs with least damping factor for plant-1 with CPSS, ILMI-PID-PSS and BA-PID-PSS

S. No.	Controller	Eigenvalue	Damping Factor	Frequency (Hz)
1	CPSS [13]	-0.63261 ± 7.241i	0.087033	1.1524
		-0.69844 ± 7.8906i	0.08817	1.2558
		-0.47113 ± 4.1411i	0.11304	0.65907
		-9.1938 ± 19.344i	0.42927	3.0786
2	ILMI-PID-PSS [34]	-0.45173 ± 11.077i	0.040747	1.763
		-0.87931 ± 8.3531i	0.10469	1.3294
		-2.0076 ± 4.629i	0.39789	0.73673
		-7.9106 ± 17.918i	0.40387	2.8518
3	BA-PID-PSS (Prop.)	-0.78886 ± 12.602i	0.062476	2.0056
		-1.2327 ± 11.513i	0.10647	1.8323
		-5.6764 ± 18.295i	0.29633	2.9118
		-6.3388 ± 15.563i	0.37722	2.4769

3.5. Design and Performance Evaluation: 10-Machine System

3.5.1. Design of PID-PSS using bat algorithm

As the creation of experimental plants for IEEE New England ten-machine thirty nine-bus power system are well explained in section 2.3.3, where in the machine data, load flow data, transformer data and line data are given Table A.6 - Table A.10 for the system configuration without PSS. The system model referring to plant-1 configuration as in Table 2.6, is equipped with PID type PSSs to all nine-machines (named as Gen-1 to Gen-9) except Gen-10, which is considered as the slack and subjected to PSSs design using the bat algorithm as described in section 1.2.2 with parameter bounds as $0.001 \le K_{pj} \le 50.0$, $0.001 \le K_{dj} \le 50.0$, $0.001 \le K_{ij} \le 50.0$. With the initializing parameters as above of Bat algorithm, the power system is simulated to tune the CPSSs parameters for an iteration count as 200. The problem of optimization is considered with minimization of ISE of speed response with parameter bounds. The fitness function variation for 200 iterations is shown in Figure 3.23, where in the fitness value becomes constant at around 180

iterations. The plots of K_p, K_d and K_i (PID parameters) for ten generators (Gen-1 – Gen-9) are not shown because of space constraints, therefore, the values are enlisted in Table 3.8.

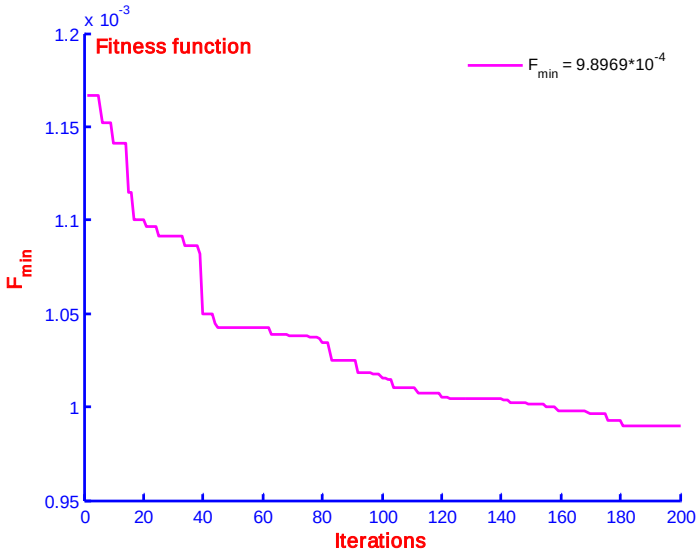

Figure 3.23: Fitness function plot of PID design: Ten-machine power system

Table 3.8: BA-PID-PSS parameters by Bat algorithm: Ten-machine power system

PSS at Generator	K_{pj}	K_{dj}	K_{ij}
Gen-1	0.69040	50.0000	6.09810
Gen-2	49.5740	9.9091	23.9860
Gen-3	12.2050	25.0880	25.0000
Gen-4	50.0000	23.9720	23.9370
Gen-5	46.7900	39.2490	24.8720
Gen-6	50.0000	15.5030	24.9040
Gen-7	46.8710	24.4330	24.3130
Gen-8	18.0610	40.7080	23.7110
Gen-9	49.5310	10.3740	22.8630

3.5.2. Simulation result comparison

It is found that there is no PID type PSSs for the IEEE New England system is available within the literature; therefore, some conventional PSSs are considered for comparison purpose. In this section genetic algorithm (GA) [24], ant colony optimization (ACO) [35], strength-pareto evolutionary algorithm (SPEA) [11] based CPSSs are used to compare the response with proposed BA-PID-PSS.

The simulation study with nonlinear plant-1 configuration is carried out four times because of 3-CPSS controllers and one proposed BA-PID-PSS. It is impossible to show responses comparison of all generators to all plant conditions; therefore, responses of Gen-1, Gen-2, Gen-4, Gen-7 and Gen-10 of plant-1 are shown in Figure 3.24, Figure 3.25, Figure 3.26, Figure 3.27 and Figure 3.28, respectively. Clearly, the application of BA-PID-PSS improves the speed response in terms of settling time and overshoots as compared to CPSSs.

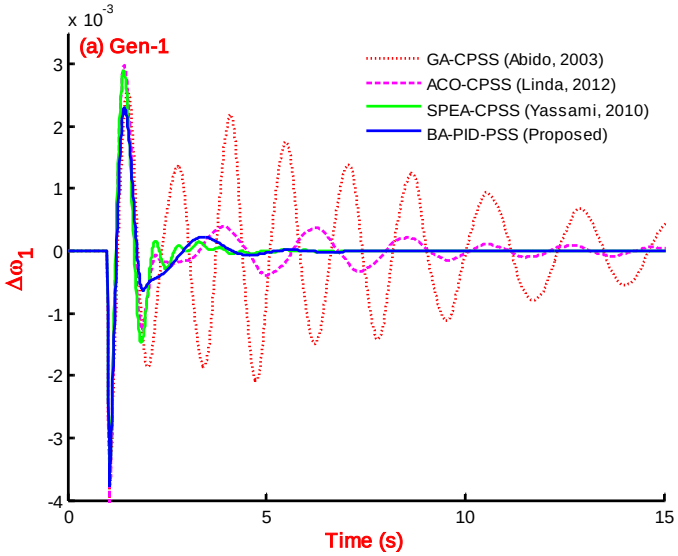

Figure 3.24: Speed response for Gen-1 of plant-1 with GA-CPSS, ACO-CPSS, SPEA-CPSS and BA-PID-PSS

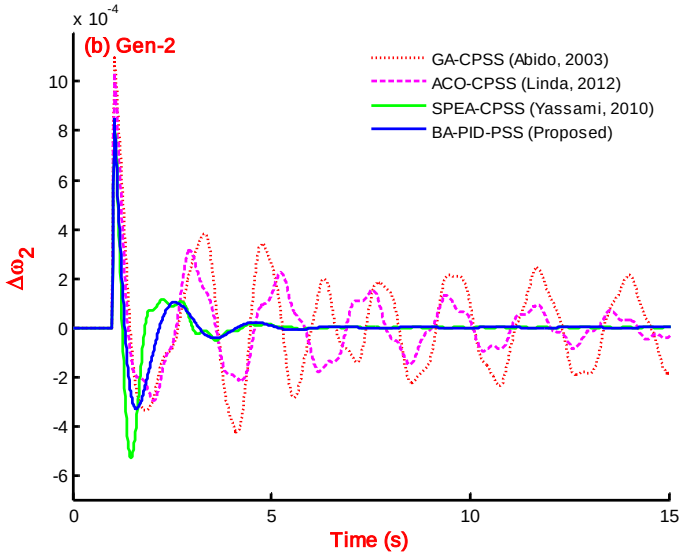

Figure 3.25: Speed response for Gen-2 of plant-1 with GA-CPSS, ACO-CPSS, SPEA-CPSS and BA-PID-PSS

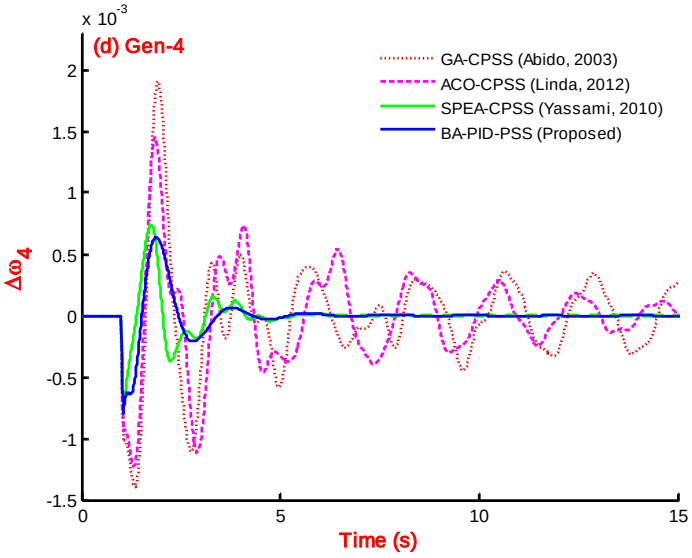

Figure 3.26: Speed response for Gen-4 of plant-1 with GA-CPSS, ACO-CPSS, SPEA-CPSS and BA-PID-PSS

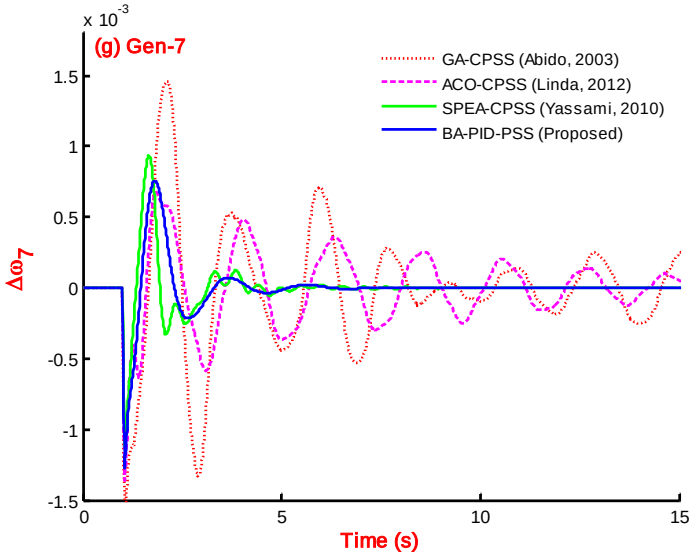

Figure 3.27: Speed response for Gen-7 of plant-1 with GA-CPSS, ACO-CPSS, SPEA-CPSS and BA-PID-PSS

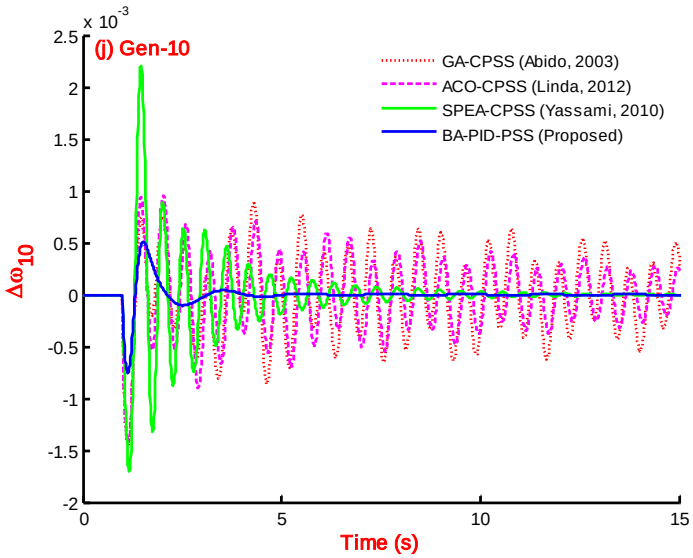

Figure 3.28: Speed response for Gen-10 of plant-1 with GA-CPSS, ACO-CPSS, SPEA-CPSS and BA-PID-PSS

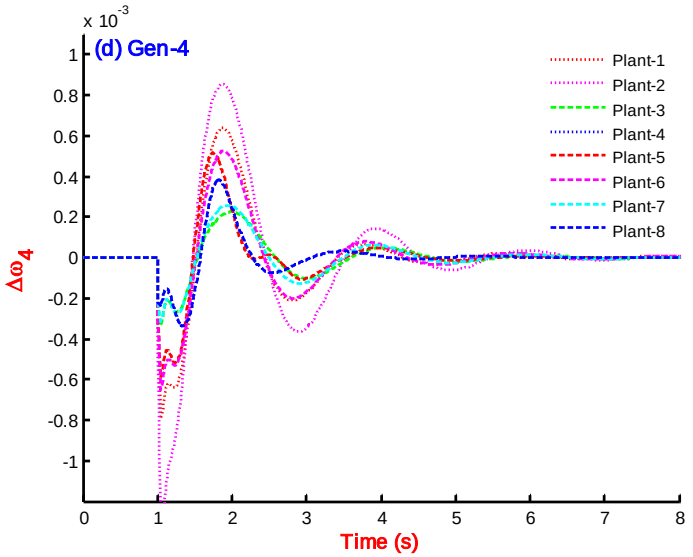

Figure 3.29: Speed response of Gen-4 over eight nonlinear plants with BA-PID-PSS

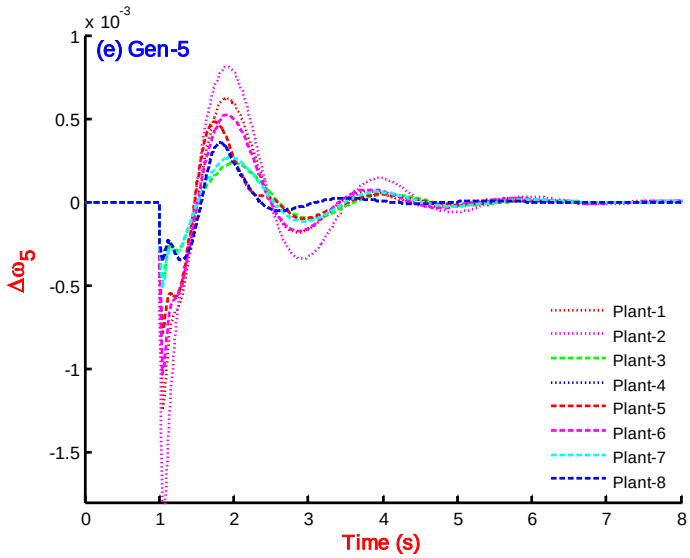

Figure 3.30: Speed response of Gen-5 over eight nonlinear plants with BA-PID-PSS

To check robustness of the proposed PID type PSS, the simulation is again carried out with eight plants (referring wide range of operating conditions with different system configurations) and the speed response is recorded. The plot of speed response for Gen-4 and Gen-5 with eight plants is shown in Figure 3.29 and Figure 3.30, respectively. It is easy to say that the system is stable for all eight plant conditions with BA-PID-PSS.

Table 3.9: PI based comparison of speed response with GA-CPSS, ACO-CPSS, SPEA-CPSS and BA-PID-PSS (Proposed) for plant-1 – plant-8.

Controller	ITAE	IAE	ISE	ITAE	IAE	ISE
	Plant-1			Plant-2		
GA-CPSS [24]	0.5058	0.0706	5.7778×10^{-05}	0.5465	0.0751	5.1958×10^{-05}
ACO-CPSS [35]	0.2191	0.0412	2.7658×10^{-05}	0.2893	0.0492	2.9828×10^{-05}
SPEA-CPSS [11]	0.0357	0.0164	1.3156×10^{-05}	0.0371	0.0175	1.4232×10^{-05}
BA-PID-PSS (Proposed)	0.0184	0.0106	7.3609×10^{-06}	0.0245	0.0123	6.7891×10^{-06}
	Plant-3			Plant-4		
GA-CPSS [24]	0.3058	0.0432	1.7065×10^{-05}	0.5308	0.0767	7.7482×10^{-05}
ACO-CPSS [35]	0.1661	0.0299	1.1854×10^{-05}	0.4977	0.0726	6.8426×10^{-05}
SPEA-CPSS [11]	0.0213	0.0094	4.0660×10^{-06}	0.0612	0.0242	3.8760×10^{-05}
BA-PID-PSS (Proposed)	0.0087	0.0054	1.2355×10^{-06}	0.0119	0.0082	9.8820×10^{-06}
	Plant-5			Plant-6		
GA-CPSS [24]	0.3175	0.0490	2.7905×10^{-05}	0.4491	0.0629	4.4569×10^{-05}
ACO-CPSS [35]	0.2065	0.0385	2.3980×10^{-05}	0.1884	0.0368	2.1708×10^{-05}
SPEA-CPSS [11]	0.0319	0.0144	1.1481×10^{-05}	0.0326	0.0144	9.5331×10^{-06}
BA-PID-PSS (Proposed)	0.0125	0.0081	7.1431×10^{-06}	0.0169	0.0095	5.2514×10^{-06}
	Plant-7			Plant-8		
GA-CPSS [24]	0.2040	0.0348	1.5736×10^{-05}	0.4115	0.0595	3.6522×10^{-05}
ACO-CPSS [35]	0.1596	0.0299	1.2726×10^{-05}	0.2160	0.0427	2.8966×10^{-05}
SPEA-CPSS [11]	0.0219	0.0096	4.1197×10^{-06}	0.0383	0.0172	1.3420×10^{-05}
BA-PID-PSS (Proposed)	0.0105	0.0060	1.6533×10^{-06}	0.0219	0.0115	7.3241×10^{-06}

3.5.3. PI based analysis

As in previous section the comparing CPSSs are GA-CPSS [24], ACO-CPSS [35], SPEA-CPSS [11], therefore, the performance of proposed BA-PID-PSS should also be compared to system responses for all eight plant configurations of Table 2.6 - Table 2.7 with these CPSSs. The simulation is carried out for 32 times and each time the performance indices (ITAE, IAE and ISE) of speed response are recorded for simulation time as 30 seconds. The values of these PIs are enlisted in Table 3.9 for all considered plant conditions. The comparatively lower values of PIs with BA-PID-PSS prove its superiority over other controllers [11, 24, 35].

3.6. Conclusion

In this chapter, the application of the bat algorithm is used to tune the parameters of PID based PSS for three systems such as single-machine infinite-bus power system (SMIB), two-area four-machine ten-bus power system and IEEE New England ten-machine thirty nine-bus power systems.

The designed BA tuned PID based PSS is connected to SMIB power system and simulation study is carried out with the eight nonlinear plant conditions, the speed response is compared to the PID based PSSs reported in [27-33] . The speed response of the system with BA-PID-PSS is compared to that of with reported in literature and found with reduced overshoot and settling time. The lesser value of performance indices of speed response with the proposed controller proves the superior performance as compared to that of with the controllers in [27-33]. The eigenvalue analysis gives information of damping ratio as better with BA-PID-PSS as compared to others. The eigenvalue plot for 231 plant conditions determines the robustness and applicability of the proposed controller.

The bat algorithm based BA–PID-PSS are connected to the four-machine power system in decentralized manner and simulation study is carried out with the eight nonlinear plant conditions. The speed response of the system with proposed BA-PID-PSSs is compared to that of with CPSSs [13] and ILMI-PID-PSSs [34] . The nonlinear simulation results and the eigenvalue analysis reveal the superiority of the BA-PID-PSS as compared to that of with others with reduced settling time and overshoot in terms of performance indices. The superiority of the proposed controller is proved by performance indices (relatively lesser value) recorded for speed response and the eigenvalue analysis (relatively greater value of damping ratio) as compared to that of with the controllers reported in literature [13, 34].

The application of the bat algorithm is extended to the standard IEEE ten-machine power system network to tune the PID based PSS parameters with minimization of ISE. The nonlinear

time-domain simulation results of the system with proposed BA-PID-PSS and that of with CPSSs as reported in literature [11, 24, 35] are compared. The speed response of the system with proposed controller can stabilize more quickly with reduced overshoot as compared to that of with others in subject. The recorded performance indices of speed response with proposed BA-PID-PSS appeared with lesser value as compared to CPSSs in [11, 24, 35]. The eigenvalue analysis proves the superiority of the performance with higher value of damping ratio as compared to that of with CPSSs in [11, 24, 35].

The performance of the systems with proposed BA-PID-PSS is proved to be better as compared with PID-PSSs [27-33], ILMI-PID-PSS [34] and CPSSs [11, 24, 35]. However, the performance of BA-PID-PSS is not comparable to that of with BA-CPSSs. It has been observed that the PID parameter tuning using an eigenvalue based objective function is unable to provide acceptable solutions; therefore, simple time-domain based objective function has been used. It could be one of the reasons that the performance of systems with BA-PID-PSS is not more effective than that of with BA-CPSSs.

Chapter 4

DESIGN OF OPTIMALLY TUNED SCALING FACTORS BASED FUZZY LOGIC POWER SYSTEM STABILIZER USING BAT ALGORITHM

In this chapter, a Type-1 fuzzy logic power system stabilizer (FPSS) is designed by tuning its scaling factors for single-machine and two multimachine power systems. The scaling factors are designed using heuristic optimization techniques. The problem of tuning scaling factors is condered as optimization under an ISE based objective function and solved y using harmony search algorithm and bat algorithm. Two schemes of scaling factors is condered; in (a) scenario-1, the input signals to the fuzzy logic controller (FLC) are considered as speed deviation and acceleration with normalizing coefficients, (b) scenario-2, the input signals to FLC are considered as speed deviation and electric power. In both schemes, the output signal from FLC is considered as output, but normalizing coefficient is considered only in scheme-2. In scenario-1, a small-signal model of the fuzzy logic power system stabilizer (FPSS) is derived to relate proportional derivative (PD) controller parameters, and the scaling factors associated to input signals of FPSS. The derived such a small signal model of FPSS is proven to be a proportional derivative controller. The parameters of the PD controller are tuned using harmony search algorithm and bat algorithm and used as scaling factors of FPSS. In scenario-2, the normalizing factors of input-output are tuned using harmony search algorithm and bat algorithm and used as scaling factors of FPSS. In both cases, the performance of such designed HSA-FPSS and BA-FPSS is compared to the FPSS (without considering scaling factors) performance for a wide range of operating conditions and system configuration on SMIB power system, four-machine ten-bus power system and ten-machine thirty nine-bus power systems. The comparison is carried out in terms of performance indices (ITAE, IAE and ISE) of speed response for systems with FPSS, HSA-FPSS and BA-FPSS. The superior performance of systems with BA-FPSS is established by considering eight plant conditions of each system, which represents the wide range of operating conditions and system configurations.

4.1. Introduction

Electromechanical oscillations (EMOs) are becoming a critical problem in large, complex and interconnected electrical power systems (EPSs). The use of fast acting automatic voltage regulators (AVRs) in the excitation system of synchronous generators causes low frequency oscillations (LFOs) in the range of 0.2-3.0 Hz. The other reasons for these LFOs are bulk power

transfer across weak transmission line, sudden changes in loads, changes in transmission line parameters, changes in turbine output parameters and the faults under different operating points and configuration of a power system. Some of these LFOs could fade away; not affecting the EPS but some of them might stay for a while, grow gradually and result to system separations.

The widely accepted solution to get rid of these LFOs is the use of a power system stabilizer, which adds a stabilizing signal to AVR for modulating the excitation signal of the generator. An electrical damping torque is being added in phase with the rotor speed deviations to enhance damping of a system. Conventional power system stabilizer (CPSS) is the most accepted type of controller with fixed structure of lead-lag type. The CPSSs are designed based on linear control theory by phase compensation technique for EPSs with a specific operating condition. Performance of EPS with such a designed CPSS is not satisfactory over the wide range of operating conditions (OCs).

To mitigate these difficulties of CPSS, adaptive stabilizers have been proposed using different adaptable control techniques [81, 82, 84, 265, 266]. However, the performances of EPS with adaptive stabilizers are good enough over a wide range of OCs but suffer from the major drawback of requiring online based model identification, parameter tuning, state observation and feedback signals. On erroneous parameter identification, these stabilizers lead to incorrect control signals resulting to reduced robustness. H_∞ optimization technique has been applied to design robust PSS [194, 267]. The selection of weighting functions in the H_∞ optimization synthesis is an important and difficult task along with the order of a designed stabilizer as high as that of the plant. It gives rise to complex structure of such a stabilizers and reduces their applicability [92].

Gradient based optimization is used to tune the PSS parameters at different operating conditions of EPS in [91], which requires computations of sensitivity factors and eigenvalue at each iteration, results to heavy computational burden and slow convergence. It is reported that the search process is susceptible to be trapped in local minima, and the parameters of PSS are not optimal [92]. Thus the conventional techniques which are using derivatives, and gradients are not able to locate or identify global desirable solutions, but for real-world applications, one may often content a good solution, even if it is not the best. To remove these limitations of conventional optimization techniques, heuristic methods are widely used for global optimization problems.

Much of modern optimization techniques like Tabu search [233], genetic algorithms (GA) [24, 142, 268, 269], evolutionary programming [21], simulated annealing [138], and rule based bacteria foraging [270] have been applied for PSS parameter optimization. These methods give good solution of PSS parameters and able to enhance stability of EPS. However, the system having highly epistatic objective function gives degraded efficiency to obtain global optimum solution and takes a lot of computing time. Moreover, in [21, 142, 233, 268] the robust PSS design

was formulated as a single objective function problem, and not all PSS parameters were considered adjustable. Genetic algorithm (GA), simulated annealing are some of the algorithms, which suffer from settings of its parameters and give rise to repeated revisiting of the same suboptimal solutions [119].

Fuzzy logic controllers (FLCs) have attracted considerable attention because of the variety of the advantages they offer over the conventional computational systems [103, 104]. These are model-free controllers having rapidity and robustness as their most profound and interesting properties in comparison to the other classical schemes [113]. These have been successfully applied to the control of non-linear dynamical systems [36, 43] especially in the field of adaptive control by making use of on-line training. The flexibility and subjectivity of knowledge representation are a distinct feature of fuzzy logic, which allows the technique to be a notable candidate for PSS design, as reported in [106]. A FLC designed with appropriate membership functions works like a PD or PID controller with variable gains. The equivalence between the scaling factor of a fuzzy controller and linear PID controller coefficients is examined in [114]. FLCs are reported to provide superior performance in terms of nonlinear control because of the variable gains [271]. In the design of fuzzy logic based PSS, it is necessary to define membership functions for all the input and output variables of the controller. Moreover, a rule table should be selected to relate the input and output variables to each other. The control rule table and membership functions are chosen by the time consuming trial and error procedure. To overcome this drawback, some researchers have designed the FLPSS with the aid of searching algorithms such as genetic algorithms, particle swarm optimization, bacteria foraging optimization, chaotic optimization algorithms and so forth [65, 113, 115-123].

The Harmony Search (HS) Algorithm is proposed by Geem et al in 2001 [272], is inspired from the process of the improvisation used by musicians to achieve the harmony. The HS algorithm [177] is a meta-heuristic optimization algorithm which is similar to the PSO [216] and GA [213]. It has been implemented extensively in the fields of engineering optimization [273], in recent years. It became an alternative to other heuristic algorithms like PSO [216] and simulated annealing (SA) [221]. It is a derivative free, meta-heuristic optimization (which doesn't use Friedlander), inspired by the way; musicians improvise new harmonies [21], and it uses higher-level techniques to solve problems efficiently [180]. HS can be classified as a population-based evolutionary algorithm such as GA and the PSO algorithm [274].

It has a cheap running cost but has strong ability of exploration [180]. The classical harmony search algorithm suffers from low-precision value and slow convergence speed in solving large-scale problems [180]. Therefore, improved HS algorithms is proposed in [275], which generating new solution vectors to enhance convergence speed and accuracy.

The use of the HS as an optimization in the field of a power system is a few except, to search the optimal control parameters to improve the dynamic control in [265], transmission network expansion planning with security constraints in [276], to select the optimal size & location of static synchronous compensators (STATCOMs) and static Var compensators (SVCs) in a transmission network in [277]. The small signal stability analysis is not carried out by use of Harmony search algorithm. In this chapter, a mathematical analogy in between proportional derivative (PD) controller parameters and the scaling factors of the fuzzy logic based power system stabilizer (FPSS) is developed. The scaling factors in terms of the pd controller parameters are optimized by Harmony Search Algorithm.

Recently, Yang [100], have proposed a very promising bat algorithm (BA) under the category of meta-heuristic algorithms. BA is a new search algorithm based on the echolocation behaviour of Microbats. Preliminary studies indicate that BA is superior to GA and PSO for solving unconstraint optimization problems [100] because these methods fail to deal with the multimodal optimization problems. In [225], the firefly algorithm (FA) which is based on the flashing characteristics of tropical fireflies. In continuation, cuckoo search (CS) is based on the brooding behaviour of some cuckoo species [226, 227]. As the bat algorithm (BA) uses (i) frequency-tuning technique to increase the diversity of the solutions to the population (ii) the automatic zooming to try to balance exploration and exploitation during the search process by mimicking the variations of pulse emission rates and loudness of bats when searching for prey; It proves to be very efficient with a typical quick start. However, the original version of this algorithm is suitable for continuous problems, so it cannot be applied to binary problems directly. In [228], a binary version of this algorithm is proposed to deal with dimensionality reduction [229] and feature selection [230]. Therefore, scaling factors in terms of the pd controller parameters are optimized by Bat Algorithm.

Tuning of a fuzzy power system stabilizer (PSSs) is formulated with a nonlinear model of a single-machine infinite-bus (SMIB) power system, two-area four-machine ten-bus power system and IEEE New England ten-machine thirty nine-bus power system. The optimization problem is dealt with parameter bounds, and an objective function based on integral square error (ISE) minimization. The combination of FPSS and scaling factors tuned using HS algorithm and BA would be called as HS-FPSS and BA-FPSS, respectively.

In the organization of this chapter, the problem is formulated in section 4.2; where in the detail on considered power systems, fuzzy logic based PSS, small signal model of FPSS to relate pd controller parameters is developed. The optimization of input scaling factors for SMIB, four-machine and ten-machine power system are carried out using HS algorithm and bat algorithm. The performance comparisons with three systems with such a tuned FPSSs are carried out. In section

4.4, the input-output scaling factors with different input signals are optimized using HS algorithm and BA. The design and performance evaluation is considered for all three systems. Lastly, the analysis is concluded in section 4.5.

4.2. Problem Formulation

The aim of this chapter is to utilize the superior performance of Bat algorithm for tuning the PD controller parameters or in turn scaling factors of FPSS in connection with power systems; therefore, the EPS elements such as generators, excitation system and PSS must be modeled. To complete the tuning process, an objective function to obtain satisfactory results is necessary and should be defined. Thereby, the system model and an objective function used in PSS parameter tuning in SMIB, and multi machine power system are elaborated.

4.2.1. Scenario - 1: Input scaling factors of FPSS

4.2.1.1. Power system representation

The systems under consideration are single-machine connected to infinite-bus (SMIB), two-area four-machine ten-bus and IEEE New England ten-machine thirty nine-bus power system. The single-line diagram is shown in Figure 1.6 The small signal models of the SMIB power system can be represented by Figure 4.1 with connection of FPSS with scaling factors. The output signal of this PSS is added to AVR to modulate the excitation system for enhancing the damping of the small signal oscillations.

The single-line diagram representation of four-machine and ten-machine models is shown in Figure 1.14 and Figure 1.15, respectively. Moreover, a general Heffron-Philip representation is shown in Figure 1.13 [1, 99, 213]. The considered synchronous machines of SMIB and multimachine power systems are of the model 1.0 type as discussed in [191]. To cover all operating conditions, the power system with generators, stabilizers, and excitation systems can be modeled by a set of nonlinear differential equations as in Eqn. (1.59 - 1.60) [14].

It is necessary to have linearized model of the power system around an operating point to analyze the small signal stability of a power system and consequently, to design power system stabilizer. The power system represented by Eqn. (1.59 - 1.60) is linearized around an equilibrium operating point of the power system and is represented by Eqn. (1.64 - 1.65) [14, 23].

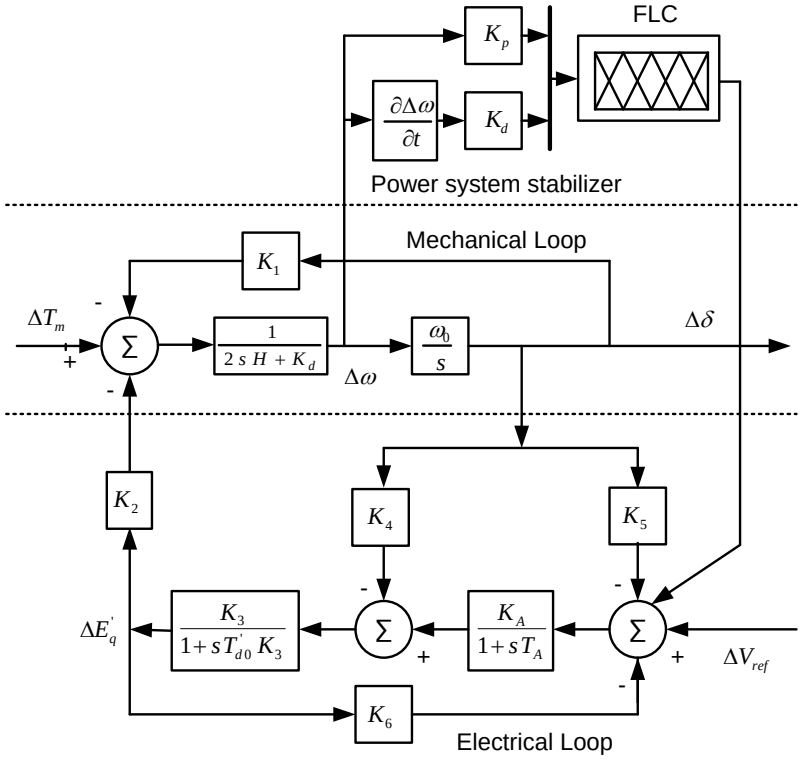

Figure 4.1: Representation of SMIB system: FPSS with input scaling factors (Scenario-1)

The state equations of a power system, consisting '*N*' number of generators and N_{pss} number of power system stabilizers can be written as in Eqn. (1.64). Where, *A* is the system matrix of an order as $4N \times 4N$ and is given by $\partial f / \partial X$, while *B* is the input matrix with order $4N \times N_{pss}$ *and* is given by $\partial f / \partial U$. The order of state vector ΔX is $4N \times 1$, the order of ΔU is $N_{pss} \times 1$.

4.2.1.2. Fuzzy logic power system stabilizer

The fuzzy logic controller is considered as the fuzzy logic based power system stabilizer (FPSS). The main parts of FPSS are fuzzification, knowledge base, inference and defuzzification process. The knowledge base consists the storage of the linguistic variables (LVs), membership functions (MFs) and the fuzzy rules defined by the user. The number of MFs is equal to the number of LVs. The increased number of LVs improves the performance of the FPSS but simultaneously increases the computational time and computational burden. Therefore, a compromise is taken over the selection of the number of LVs and MFs. The selected number of LVs is three and named as N (negative), Z (zero) and P (positive) while the selected MFs is a triangular type. The number of rules in the knowledge base is square with the number of LVs i.e. nine in this case. The main objective of FPSS is to map crisp input signal to the crisp output control signal, which is applied to the excitation system to modulate the excitation control and to

increase the damping of the system.

The FPSS is a two input and one output device as speed deviation ($\Delta\omega$) , acceleration ($\Delta\dot{\omega} = \Delta a$) and voltage (ΔV_{pss}) respectively. The selected input signal $\Delta\omega$ is sensed from the rotor shaft of the generator while the acceleration is computed as $\Delta\dot{\omega} = \Delta a = \{\Delta\omega(kT) - \Delta\omega(k-1)T\}/T$, where T is the sampling time.

The sensed crisp signals are applied as input to the fuzzification system and is mapped to the MFs to fuzzify it. The triangular MF is shown in Figure 4.2. The output of fuzzification process is applied to the inference process to get fuzzy control output signal according to the fuzzy rules. In defuzzification process, the fuzzy control signal is applied to defuzzification process to get crisp control signal. The crisp control signal is added to modulate the excitation signal to increase the damping of the system. The universe of discourse as in Figure 4.2 for both input signals is selected in between X_{min} and $X_{max.}$ If X_{min} = -X_{max}, this discourse can be normalized between -1 and +1 by introducing a set of scaling factors to represent the actual signal. Let the scaling factors for speed deviation, acceleration and voltages are $k_{\omega,}$, k_a and k_v respectively can be represented as $k_\omega = 1/\Delta\omega_{max}$, $k_a = 1/\Delta a_{max}$ and $k_v = 1/v_{max}$. These maximum values can be determined by simulation of system under severe conditions. Each fuzzy rule takes the general form of "IF Antecedent THEN Consequent", e.g. IF $\Delta\omega$ is *P* AND Δa is *Z* THEN *v* is β_8 as in Figure 4.1. The firing strength of the i^{th} rule consequent is a scalar value (s_i) which is equal to the product of the two antecedent conjunction values. The defuzzification method used is centroid. As in Figure 4.2, β_i, $i = 1, \ldots N$ represent the centroid of *N* MFs that are assigned to V_{pss}. Therefore, the crisp output [278] of an FLPSS is computed as follows.

$$V_{pss} = K_v \times \frac{\sum_{n=1}^{N} s_i \beta_i}{\sum_{n=1}^{N} s_i} = K_v \ \alpha_i \ \beta_i \tag{4.1}$$

$$\alpha_i = \frac{s_i}{\sum_{n=1}^{N} s_i} \tag{4.2}$$

$$\alpha = [\alpha_1 \ \alpha_2 \ \ldots \alpha_N] \tag{4.3}$$

$$\beta = [\beta_1 \ \beta_2 \ \ldots \beta_N]^T \tag{4.4}$$

The firing strength of the i^{th} rule (s_i) is calculated based on interpreting the conjunction "and" as a product of the values of the MFs corresponding to the measured quantities $\Delta\omega$ and Δa. For example, the firing strength of the shaded rule in Table 4.1 is given by $s_8 = \mu_p(\Delta\tilde{\omega}) \times \mu_z(\Delta\tilde{a})$) where $\Delta\tilde{\omega}$ and $\Delta\tilde{a}$ are the normalized values of $\Delta\omega$ and Δa respectively, i.e., $\Delta\tilde{\omega} = K_\omega \Delta\omega$ and

$\Delta\tilde{a} = K_a \Delta a = K_a \Delta\dot{\omega}$. In an FLPSS, the values of β_i, i = 1. 2, …, N is set once and are kept constant afterwards. As a common practice, the values of β_i, i = 1, ..., 9 are set so that $\beta_1 = \beta_2 = \beta_4 = \beta^-$, $\beta_3 = \beta_5 = \beta_7 = \beta^0$ and $\beta_6 = \beta_8 = \beta_9 = \beta^+$.As a result, the output of an FLPSS turns out to have only three MFs whose centroids are β^-, β^0 and β^+. In the following subsection, the FLPSS output MFs are assumed to be singletons.

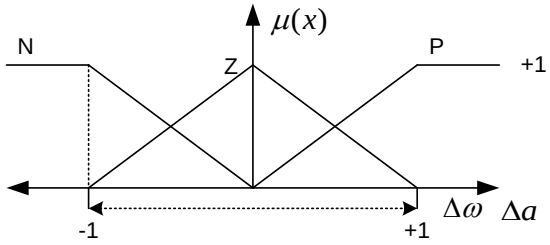

Figure 4.2: Triangular MFs used for FLPSS as input variables

Table 4.1: Fuzzy rules with singleton output

Acceleration: $\Delta a \rightarrow$ Speed Devn.: $\Delta\omega \downarrow$	N	Z	P
N	β_1	β_2	β_3
Z	β_4	β_5	β_6
P	β_7	β_8	β_9

4.2.1.3. Small signal perturbed model of fuzzy PSS

The crisp control output of an FLPSS is given as following

$$V_{pss} = K_v \begin{pmatrix} \mu_N(\Delta\tilde{\omega}) \times \mu_N(\Delta\tilde{a}) \times \beta^- + \mu_N(\Delta\tilde{\omega}) \times \mu_Z(\Delta\tilde{a}) \times \beta^- + \cdots \\ \mu_N(\Delta\tilde{\omega}) \times \mu_P(\Delta\tilde{a}) \times \beta^0 + \mu_Z(\Delta\tilde{\omega}) \times \mu_N(\Delta\tilde{a}) \times \beta^- + \cdots \\ \mu_Z(\Delta\tilde{\omega}) \times \mu_Z(\Delta\tilde{a}) \times \beta^0 + \mu_Z(\Delta\tilde{\omega}) \times \mu_P(\Delta\tilde{a}) \times \beta^+ + \cdots \\ \mu_P(\Delta\tilde{\omega}) \times \mu_N(\Delta\tilde{a}) \times \beta^0 + \mu_P(\Delta\tilde{\omega}) \times \mu_Z(\Delta\tilde{a}) \times \beta^+ + \cdots \\ \mu_P(\Delta\tilde{\omega}) \times \mu_P(\Delta\tilde{a}) \times \beta^+ \end{pmatrix} \tag{4.5}$$

Considering the dynamic stability (i.e. small signal stability) of the power system, where the speed deviation is $|\Delta\omega| > \varepsilon \rightarrow 0^+$, therefore the input MFs can be computed as

$$\left.\begin{aligned} \mu_N^{(0)}(\Delta\tilde{\omega}) = \mu_N^{(0)}(\Delta\tilde{a}) = 0 \\ \mu_Z^{(0)}(\Delta\tilde{\omega}) = \mu_Z^{(0)}(\Delta\tilde{a}) = 1 \\ \mu_P^{(0)}(\Delta\tilde{\omega}) = \mu_P^{(0)}(\Delta\tilde{a}) = 0 \end{aligned}\right\} \tag{4.6}$$

Thus, the small signal perturbed output control is given by

$$\Delta V_{pss} = K_v \begin{pmatrix} \Delta\mu_N(\Delta\tilde{\omega}) \times \beta^- + \Delta\mu_Z(\Delta\tilde{\omega}) \times \beta^0 + \cdots \\ \Delta\mu_P(\Delta\tilde{\omega}) \times \beta^+ + \Delta\mu_N(\Delta\tilde{a}) \times \beta^- + \cdots \\ \Delta\mu_Z(\Delta\tilde{a}) \times \beta^0 + \Delta\mu_P(\Delta\tilde{a}) \times \beta^+ \end{pmatrix} \tag{4.7}$$

The perturbed values may be taken as following

$$\left.\begin{aligned} \Delta\mu_N(\Delta\tilde{\omega}) &= -K_\omega \Delta\omega \\ \Delta\mu_Z(\Delta\tilde{\omega}) &= 0 \\ \Delta\mu_P(\Delta\tilde{\omega}) &= K_\omega \Delta\omega \end{aligned}\right\} \tag{4.8}$$

$$\left.\begin{aligned} \Delta\mu_N(\Delta\tilde{a}) &= -K_a \Delta a \\ \Delta\mu_Z(\Delta\tilde{a}) &= 0 \\ \Delta\mu_P(\Delta\tilde{a}) &= K_a \Delta a \end{aligned}\right\} \tag{4.9}$$

The output of FPSS is given as

$$\Delta V_{pss} = K_v\left(-K_\omega \Delta\omega \times \beta^- + K_\omega \Delta\omega \times \beta^+ - K_a \Delta a \times \beta^- + K_a \Delta a \times \beta^+\right) \tag{4.10}$$

$$\Delta V_{pss} = \underbrace{K_v K_\omega (\beta^+ - \beta^-)}_{K_p} \Delta\omega + \underbrace{K_v K_a (\beta^+ - \beta^-)}_{K_d} \Delta a \tag{4.11}$$

$$\Delta V_{pss} = K_p \Delta\omega + K_d \Delta a \tag{4.12}$$

Since the value of $\beta^+ = 1$ and $\beta^- = -1$, thus

$$\left.\begin{aligned} K_p &= (2K_v) K_\omega \propto K_\omega \\ K_d &= (2K_v) K_a \propto K_a \end{aligned}\right\} \tag{4.13}$$

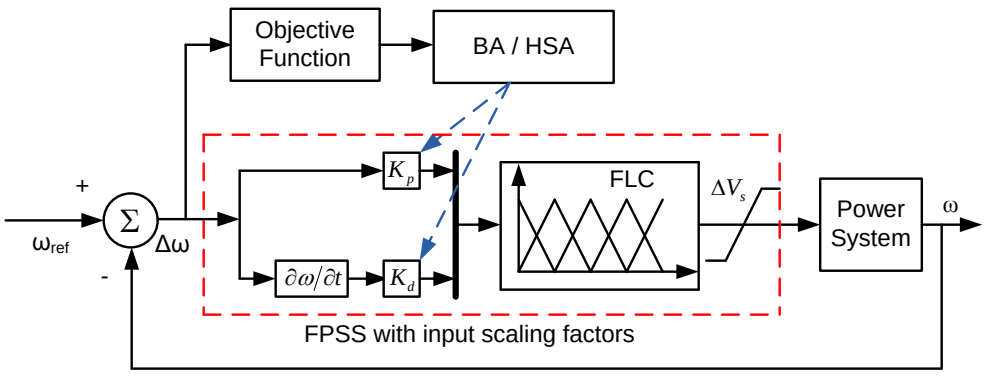

Figure 4.3: PD controller tuned by Harmony Search and Bat algorithm

Thus, the problem of tuning scaling factors of the FPSS is transformed to tune the PD controller. The tuning of these scaling factors is carried out by using harmony search algorithm and bat Algorithm by using an objective function is described in following section.

4.2.1.4. Objective Function

Here, the Harmony Search Algorithm (HSA) is used to optimize the scaling factors of Fuzzy PSS as developed in terms of PD controller as in Eqn. 4.13. To optimize these parameters (K_p and K_d) an objective function is formulated, where in the integral of squared error is minimized in terms of reduced overshoots and settling time in system oscillations. As in integral square error (ISE), the error is heavily reduced / penalized in beginning (during large errors) and low for light errors. Since, the speed deviation $\Delta\omega$ of the generator is sensed from the shaft of the generator. As an objective function, the ISE based cost function is represented for SMIB, four-machine and ten-machine power system by Eqn. (4.14 - 4.16), respectively. The Eqn. (4.19) includes parameter bounds only for nine FPSSs because the 10^{th} generator is considered as the slack, not needed to be equipped with controller.

$$J = \int_0^{T_{SIM}} \left|\Delta\omega(t)\right|^2 .dt \tag{4.14}$$

$$J = \sum_{i=1}^{4} \int_0^{T_{SIM}} \left|\Delta\omega_i(t)\right|^2 .dt \tag{4.15}$$

$$J = \sum_{i=1}^{10} \int_0^{T_{SIM}} \left|\Delta\omega_i(t)\right|^2 .dt \tag{4.16}$$

Subjected to parameter bounds for SMIB power system as in Eqn. (4.17)

$$\left.\begin{aligned} K_p^{\min} \le K_p \le K_p^{\max} \\ K_d^{\min} \le K_d \le K_d^{\max} \end{aligned}\right\} \tag{4.17}$$

Subjected to parameter bounds for two-area four-machine power system as in Eqn. (4.18)

$$\begin{cases} K_{pi}^{\min} \le K_{pi} \le K_{pi}^{\max} \\ K_{di}^{\min} \le K_{di} \le K_{di}^{\max} \end{cases} \quad i = 1,\cdots,4 \tag{4.18}$$

Subjected to parameter bounds for New England ten-machine power system as in Eqn. (4.19)

$$\begin{cases} K_{pi}^{\min} \le K_{pi} \le K_{pi}^{\max} \\ K_{di}^{\min} \le K_{di} \le K_{di}^{\max} \end{cases} \quad i = 1, \cdots, 9 \tag{4.19}$$

where, i stands for i^{th} generator in multimachine power system and T_{SIM} refers to simulation time during optimization process and specified as 100 seconds.

Typical ranges of the optimized parameters are selected as 0.00 to 50.00 for both K_p and K_d in SMIB as well as in multimachine (four machine and ten-machine) power system. Considering one of the above objectives corresponding to the system under investigation, the proposed approach employs the harmony search algorithm (HSA) and bat algorithm (BA) to solve this optimization problem for an optimal set of PD controller parameters or the scaling factors of FPSS.

4.2.2. Scenario - 2: Input-output scaling factors of FPSS

4.2.2.1. System representation

The systems under consideration are single-machine connected to infinite-bus (SMIB), two-area four-machine ten-bus and IEEE New England ten-machine thirty nine-bus power system. The small signal models of the SMIB power system can be represented by Figure 4.4 with connection of FPSS with input-output scaling factors. The output signal of this PSS is added to AVR to modulate the excitation system for enhancing the damping of the small signal oscillations.

The single-line diagram representation of four-machine and ten-machine models is shown in Figure 1.14 and Figure 1.15, respectively. Moreover, a general Heffron-Philip representation is shown in Figure 1.13 [1, 99, 213]. The considered synchronous machines of SMIB and multimachine power systems are of the model 1.0 type as discussed in [191]. To cover all operating conditions, the power system with generators, stabilizers, and excitation systems can be modeled by a set of nonlinear differential equations as in Eqn. (1.59 - 1.60) [39].

It is necessary to have linearized model of the power system around an operating point to analyze the small signal stability of a power system and consequently, to design power system stabilizer. Thus, power system represented by Eqn. (1.59 - 1.60) is linearized around an equilibrium operating point of the power system and represented by Eqn. (1.64 – 1.65) [14, 23].

The state equations of a power system, consisting '*N*' number of generators and N_{pss} number of power system stabilizers can be written as in Eqn. (1.64). Where, *A* is the system

matrix of an order as $4N \times 4N$ and is given by $\partial f / \partial X$, while B is the input matrix with order $4N \times N_{pss}$ *and* is given by $\partial f / \partial U$. The order of state vector ΔX is $4N \times 1$, the order of ΔU is $N_{pss} \times 1$.

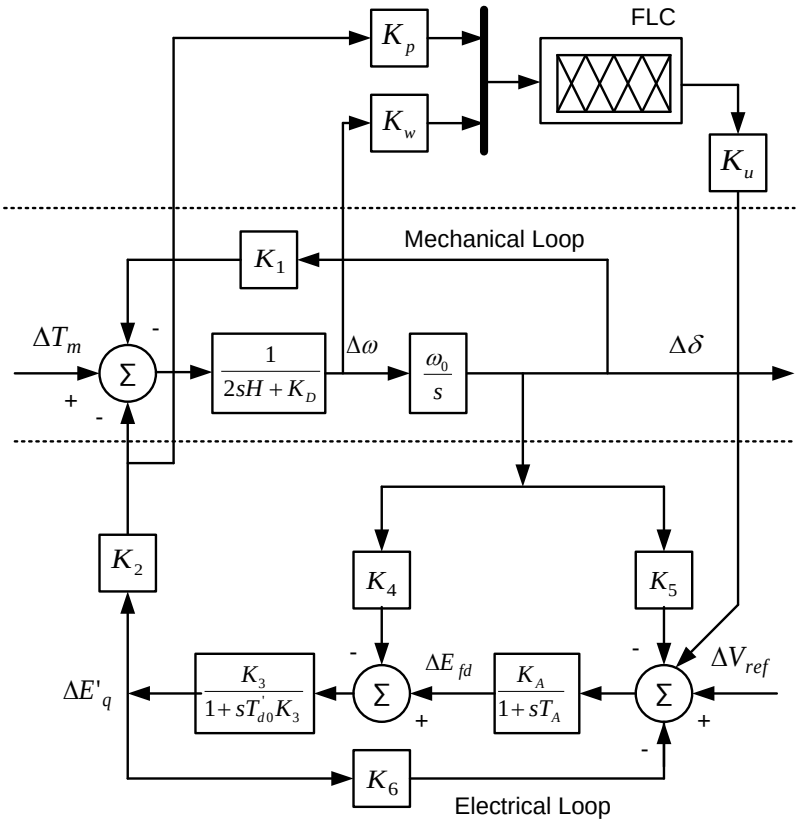

Figure 4.4: Representation of SMIB system: FPSS with input-output scaling factors (Scenario-2)

4.2.2.2. Objective function

Here, the harmony search algorithm (HSA) and bat algorithm (BA) are used to optimize the input-output scaling factors of Fuzzy PSS as developed in [65]. The input signals to FPSS are considered as change in speed ($\Delta\omega$), change in power (Δp) and the output as (Δu). The corresponding normalizing factors, i.e. scaling factors to inputs and output are K_ω, K_p and K_u, respectively. To optimize these parameters (K_ω, K_p and K_u) using BA and HSA; an objective function is formulated, where in the integral of squared error is minimized in terms of reduced overshoots and settling time in system oscillations. As in integral square error (ISE), the error is heavily reduced / penalized in beginning (during large errors) and low for light errors. Since, the speed deviation $\Delta\omega$ of the generator is sensed from the shaft of the generator. As an objective function, the ISE based cost function is represented for SMIB, four-machine and ten-machine power system by Eqn. (4.20 – 4.22), respectively. Eqn. (4.25) includes parameter bounds only for nine FPSSs because the 10th generator is considered as the slack, not needed to be equipped with controller.

$$J = \int_0^{T_{SIM}} \left|\Delta\omega(t)\right|^2 .dt \tag{4.20}$$

$$J = \sum_{i=1}^{4} \int_0^{T_{SIM}} \left|\Delta\omega_i(t)\right|^2 .dt \tag{4.21}$$

$$J = \sum_{i=1}^{10} \int_0^{T_{SIM}} \left|\Delta\omega_i(t)\right|^2 .dt \tag{4.22}$$

Subjected to parameter bounds for SMIB power system as in Eqn. (4.23)

$$\begin{cases} K_p^{\min} \le K_p \le K_p^{\max} \\ K_\omega^{\min} \le K_\omega \le K_\omega^{\max} \\ K_u^{\min} \le K_u \le K_u^{\max} \end{cases} \tag{4.23}$$

Subjected to parameter bounds for two-area four-machine power system as in Eqn. (4.24)

$$\begin{cases} K_{pi}^{\min} \le K_{pi} \le K_{pi}^{\max} \\ K_{\omega i}^{\min} \le K_{\omega i} \le K_{\omega i}^{\max} \quad i = 1,\cdots,4 \\ K_{ui}^{\min} \le K_{ui} \le K_{ui}^{\max} \end{cases} \tag{4.24}$$

Subjected to parameter bounds for New England ten-machine power system as in Eqn. (4.25)

$$\begin{cases} K_{pi}^{\min} \le K_{pi} \le K_{pi}^{\max} \\ K_{\omega i}^{\min} \le K_{\omega i} \le K_{\omega i}^{\max} \quad i = 1,\cdots,9 \\ K_{ui}^{\min} \le K_{ui} \le K_{ui}^{\max} \end{cases} \tag{4.25}$$

where, i stands for i^{th} generator in multimachine power system and T_{SIM} refers to simulation time during optimization process and specified as 100 seconds.

Considering one of the above objectives corresponding to the system under investigation, the proposed approach employs HS and Bat algorithm with parameter bounds to solve this optimization problem for an optimal set of scaling factors of FPSS.

4.3. Design and Performance Evaluation: Scenario - 1

4.3.1. Optimal FPSS for SMIB system

4.3.1.1. Design of input scaling factors

In order to assess effectiveness of the proposed Bat and Harmony search algorithm in optimizing the PD controller for tuning scaling factors of FPSS; the problem is formulated in MATLAB environment and executed on Intel (R) Core (TM) - 2 Duo CPU T6400 @ 2.00 GHz with 3 GB RAM, 32-bit operating system. Bat algorithm and its main steps for optimization are mentioned in section 2.4.1. In [182, 249], the generally opted to initialize as intensity (*A*) and pulse rate (*r*) as 0.5 and 0.5 respectively. By the trial-and-error method, it is found that the suitable values of loudness and pulse rate for PD controller optimization using a bat algorithm are as $A = 0.9$ and $r = 0.1$. The other constraint such as initializing population is selected as $n = 25$ and the bandwidth are considered as $f_{\min} = 0$ and $f_{\max} = 2.0$. The plant (SMIB power system) operating at nominal operating condition (where in $X_l = 0.4$ pu and $P_{g0} = 1.0$ pu) is considered for optimal tuning of PD controller parameters; subjected to the time domain based simple ISE minimization type objective functions with the parametric bounds are considered for the optimization. The plot of fitness function for 100 iterations is shown in Figure 4.5.

With same configuration of the system, the harmony search algorithm (as described in section 1.2.1) is applied to tune the PD controller parameters. The detail of the initializing parameters used with HSA is given in Table 4.2 and resulting behaviour of HSA in terms of fitness function is given in Figure 4.5. The optimized PD controller parameters using HSA and BA for SMIB power system are enlisted in Table 4.3. The behaviour of K_p and K_d parameters as the iteration count increases with SMIB power system using HSA and BA is represented in Figure 4.6(a) and Figure 4.6(b), respectively. As the optimization process with both algorithms is set to terminate with maximum iteration counts as 100. The minimum value of fitness function with HSA and BA is 7.0166×10^{-4} and 6.9919×10^{-4}, respectively. These values concerns to 25 and 30 iteration counts with HSA and BA, respectively. However, the convergence rate with HSA is relatively higher but with higher value of fitness function. Therefore, the bat algorithm is better than the harmony search algorithm.

Table 4.2: Initializing Parameters of Harmony Search Algorithm

HS Parameter	Specified Value
Number of Variables (NVAR)	18
Maximum number of iterations	100
Harmony memory size (HMS)	54
Harmony consideration rate (HMCR)	0.9
Minimum pitch adjusting rate (PARmin)	0.2
Maximum pitch adjusting rate (PARmax)	0.5
Minumum bandwidth (bwmin)	0.0001
Maxiumum bandwidth (bwmax)	1.0
Range of variables (PVB): PDPSS parameter range	[0 50; 0 50]

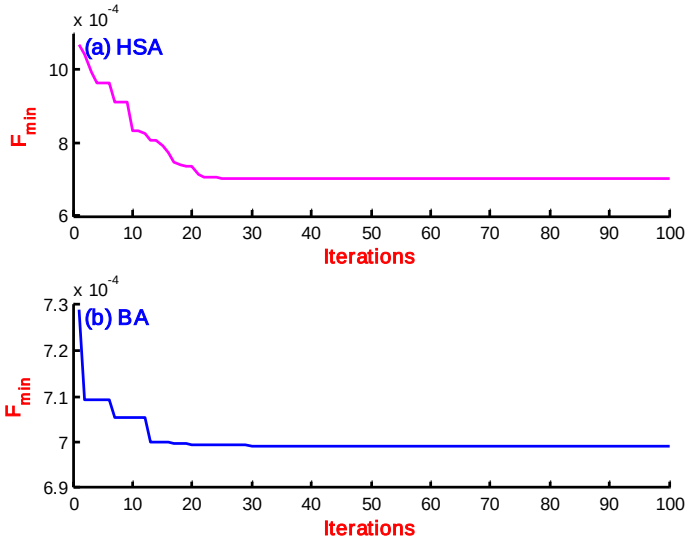

Figure 4.5: Fitness function plot with (a) Harmony search and (b) Bat algorithm for SMIB system

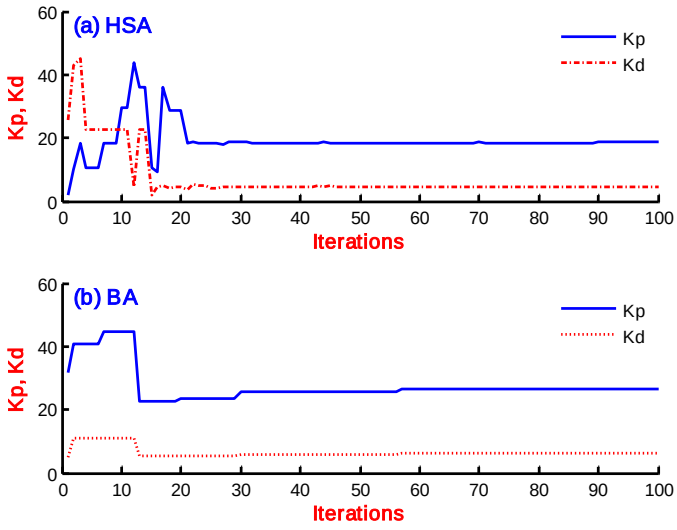

Figure 4.6: Plot of scaling factors of FPSS with (a) Harmony search and (b) Bat algorithm

Table 4.3: Harmony search and Bat algorithm based optimized scaling factors for SMIB system

Particulars	Harmony search algorithms		Bat algorithm	
Value of Scaling factors	K_p	K_d	K_p	K_d
	18.7239	4.5718	26.6184	6.1121
Value of Objective function	7.0166×10^{-4}		6.9919×10^{-4}	

4.3.1.2. Speed response comparison

To examine performance of the SMIB power system under nonlinear mode by creating fault at time 5 seconds and persistent for 0.1 seconds is carried out with a wide range of operating conditions, resulting different plant configurations. The system with distinct combinations of different active power and transmission line reactance as in Table 2.2 (eight different plants) and system data as in Table A.1 are considered for nonlinear simulations. Such obtained eight-plants (covering wide range of operating conditions) are examined for the speed response with FPSS, HSA-FPSS and BA-FPSS in this section. An SIMULINK based block diagram, including all the nonlinear blocks is generated in MATLAB Software.

The comparing Fuzzy logic based PSS (FPSS) is considered as in [72, 73]. The numbers of linguistic variables are five as LN (large negative), MN (medium negative), Z (zero), MP (medium positive) and LP (large positive). The input signals to FLC are considered as change in speed ($\Delta\omega$) and acceleration (Δa), while that the output signal is considered as correction voltage (ΔV_{pss}). The corresponding 25 rule base is represented in Table 4.4. The triangular type membership function is considered for both input and output signals. The crisp value is obtained using centroid type defuzzification method.

Table 4.4: Decision table for PSS output [72, 73]

Acceleration → Speed deviation ↓	LN	MN	Z	MP	LP
LP	Z	Z	MP	MP	LP
MP	MN	Z	Z	MP	MP
Z	MN	Z	Z	Z	MP
MN	MN	MN	Z	Z	MP
LN	LN	MN	MN	Z	Z

The Simulink model of SMIB system is prepared in MATLAB Software with FPSS, BA-FPSS and HSA-FPSS and simulation are carried out for all eight plants as created in Table 2.2. The comparison of speed response of SMIB system with FPSS, BA-FPSS and HSA-FPSS is

carried out for each plant configuration but represented only for Plant-6, Plant-7 and Plant-8, in Figure 4.7, Figure 4.8 and Figure 4.9, respectively because of space constraint. The performance at lower loading conditions (Plant 1- 4) is almost similar, but for nominal and heavy loading conditions (Plant 5 - 8), the performance with BA-FPSS is greatly improved. The speed response of the SMIB power system without PSS is not included in these figures (Figure 4.7 - Figure 4.9) as already discussed in section 2.3.1.2. The speed response of the system without PSS, with FPSS, with HSA-FPSS and with BA-FPSS, in terms of settling time is shown in Table 4.5. As an example, considering the plant-6 condition where in the SMIB system is unstable under an open loop, i.e. without PSS. The system equipped with FPSS, HSA-FPSS and BA-FPSS representing stable with settling time 14.52 seconds, 8.53 seconds and 7.41 seconds, respectively. Clearly, the settling time with BA-FPSS is better as compared to HSA-FPSS and greatly improved with respect to FPSS [72]. The speed response of the SMIB system with BA-FPSS for all eight plant conditions is represented in Figure 4.10. The results show the greater enhancement in small signal stability on application of BA-FPSS.

Table 4.5: Settling time with different controllers for different plants of SMIB power system

Power system model	No-PSS	FPSS	HSA-FPSS	BA-FPSS
Plant-1	11.56	8.37	6.44	6.14
Plant-2	>15	10.44	8.29	7.28
Plant-3	18.1	8.85	7.49	6.14
Plant-4	Oscillatory	10.73	7.76	6.66
Plant-5	Oscillatory	10.27	6.39	6.07
Plant-6	Unstable	14.52	8.53	7.41
Plant-7	Unstable	>15.60	9.82	8.42
Plant-8	Unstable	>15.00	8.42	7.31

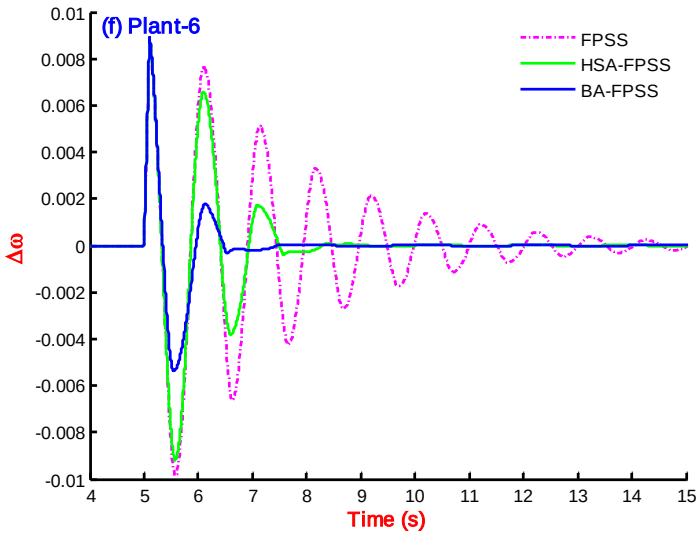

Figure 4.7: Speed response comparison of SMIB system for plant-6 with fuzzy PSS, HSA-FPSS and BA-FPSS

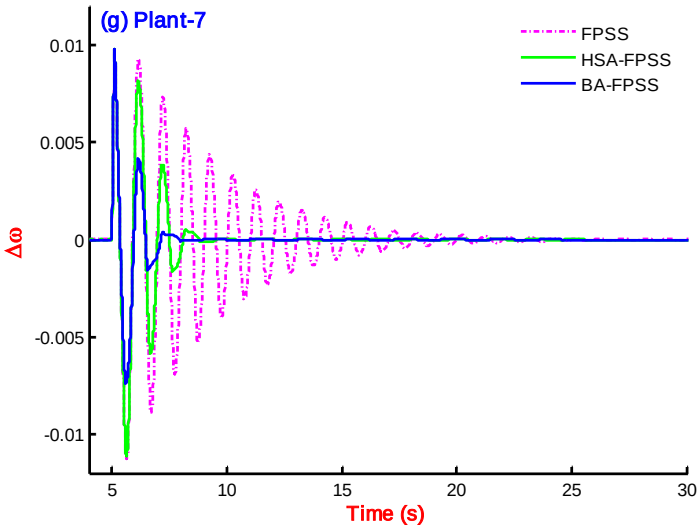

Figure 4.8: Speed response comparison of SMIB system for plant-7 with fuzzy PSS, HSA-FPSS and BA-FPSS

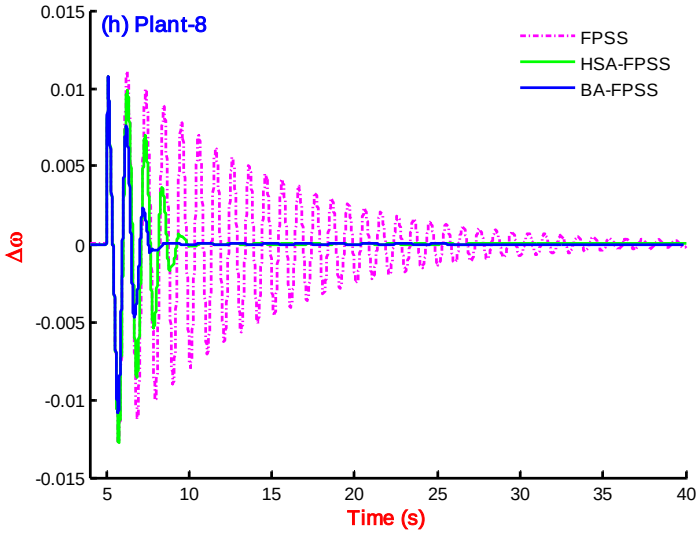

Figure 4.9: Speed response comparison of SMIB system for plant-8 with fuzzy PSS, HSA-FPSS and BA-FPSS

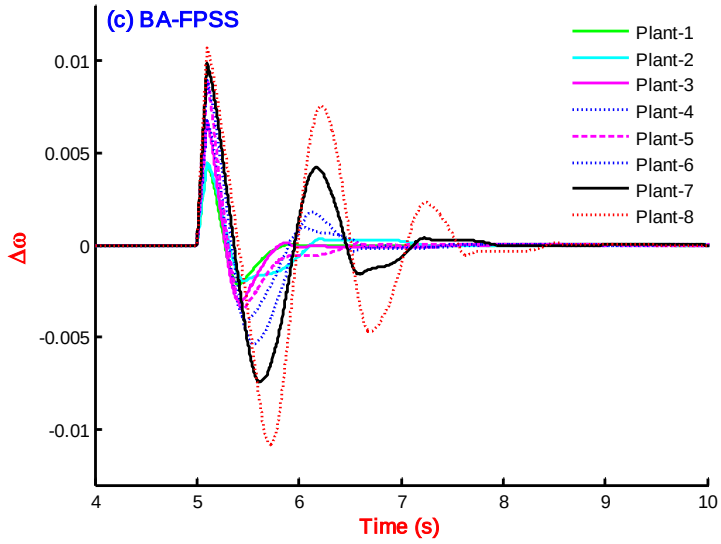

Figure 4.10: Speed response with BA-FPSS (Proposed) on eight plants

4.3.1.3. PI based performance comparison

To prove superiority of the BA-FPSS, the SMIB system is simulated one by one with all three controllers (FPSS, HSA-FPSS and BA-FPSS) and the performance indices (ITAE, IAE and ISE as presented in section 1.4) of speed response are recorded for the simulation time as 40 seconds and produced in Table 4.6. As the lower value of PI, represents the superior performance of the system with reduced settling time and overshoots. In this table, the value of PIs with BA-FPSS is lesser as compared to others, resulting good performance, i.e. the small signal stability enhancement as compared to others.

Table 4.6: Performance indices with different controllers for different plants of SMIB power system

Controller	ITAE	IAE	ISE	ITAE	IAE	ISE
	Plant-1			Plant-2		
FPSS [72, 73]	0.0140	0.0025	5.1939×10^{-06}	0.0221	0.0036	7.0078×10^{-06}
HSA-FPSS	0.0073	0.0014	3.1948×10^{-06}	0.0127	0.0022	4.2708×10^{-06}
BA-PSS	0.0073	0.0014	3.0517×10^{-06}	0.0118	0.0021	3.9931×10^{-06}
	Plant-3			Plant-4		
FPSS [72, 73]	0.0259	0.0044	1.4628×10^{-05}	0.0454	0.0072	2.2946×10^{-05}
HSA-FPSS	0.0141	0.0026	9.2914×10^{-06}	0.0221	0.0039	1.3194×10^{-05}
BA-PSS	0.0108	0.0020	6.5631×10^{-06}	0.0172	0.0031	1.0192×10^{-05}
	Plant-5			Plant-6		
FPSS [72, 73]	0.0529	0.0086	3.9531×10^{-05}	0.1364	0.0182	8.1390×10^{-05}
HSA-FPSS	0.0207	0.0038	1.6835×10^{-05}	0.0544	0.0091	4.8721×10^{-05}
BA-PSS	0.0153	0.0028	1.1397×10^{-05}	0.0248	0.0045	1.9732×10^{-05}
	Plant-7			Plant-8		
FPSS [72, 73]	0.2791	0.0313	1.5210×10^{-04}	0.97088	0.07295	3.7782×10^{-04}
HSA-FPSS	0.0793	0.0128	7.7939×10^{-05}	0.13059	0.01957	1.3159×10^{-04}
BA-PSS	0.0401	0.0069	3.4476×10^{-05}	0.06778	0.01120	6.9541×10^{-05}

4.3.2. Optimal FPSS for 4-machine system

4.3.2.1. Design of input scaling factors

As the creations of experimental plants for two-area four-machine ten-bus power system are well explained in section 2.3.2.1, where in the line data (Table A.2), load flow data (Table A.3) and machine data (Table A.4) are considered for the system configuration without PSS. The system model referring to plant-1 configuration as in Table 2.4, is equipped with PD controller to all four-machines (named as Gen-1 to Gen-4) and subjected to design using the harmony search algorithm (as described in section 1.2.1) and the bat algorithms (as described in section 1.2.2) and with a simple time domain based minimization of ISE as an objective function (Eqn. 4.18). The speed

signal from each generator is sensed and minimum value of sum of ISE of the error signal is minimized to tune PD parameters of four PSSs with parameter bounds as considered as 0.0 – 50.0 for K_{pi} and K_{di}. The initializing parameter for HS algorithm and BA is considered same as in previous section. The termination criterion of the tuning process is considered as the maximum number of iterations and set as 100. The parameter bounds are selected by using the trial-and-error method; therefore, several attempts are required. The optimized PD controller parameters are shown in Table 4.7. The behavior of HSA and BA during optimization in terms of fitness function is shown in Figure 4.11(a) and Figure 4.11(b), respectively.

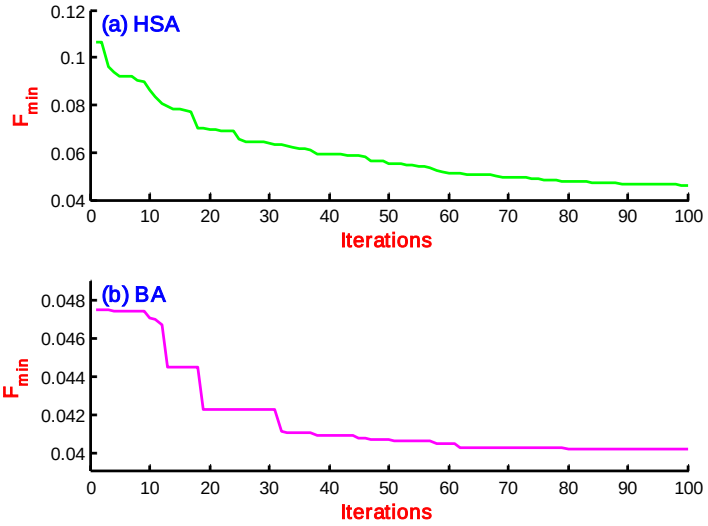

Figure 4.11: Fitness function plot with (a) Harmony search and (b) Bat algorithm for four-machine system

Table 4.7: Harmony search and Bat algorithm based optimized scaling factors for four-machine power system

Generators	Harmony search algorithms		Bat algorithm	
	K_p	K_d	K_p	K_d
Gen-1	41.2760	4.1190	49.9989	4.3498
Gen-2	37.2683	27.9770	39.0156	1.4612
Gen-3	42.5774	12.6510	11.0533	0.5686
Gen-4	48.2562	10.2401	44.8146	6.8195

4.3.2.2. Speed response comparison

The two-area four-machine ten-bus power system is described in section 2.3.2 without PSS, and the creations of system models based on operating conditions are elaborated in section 2.3.2.1. The FPSS [72] ; HSA-FPSS and BA-FPSS designed in section 4.3.2.1 are connected to the system

and simulation carried out for the speed response. In each plant condition as listed in Table 2.4 is considered with fault location as given in Table A.5. The disturbance is considered as self-clearing at different buses at 1.0 second and cleared after 0.05 second. Referring to section 2.3.2.2 and section 2.3.2.3, wherein the simulation and eigenvalue analysis with eight plant conditions without PSS are described and found that none of the generators of plants are showing stable operation; therefore, not needed to compare to the simulation results. As a sample, the speed response of Gen-1 to Gen-4 for plant-1 is compared with FPSS [72], HSA-FPSS and BA-FPSS in Figure 4.12 - Figure 4.15. It can be seen that the settling time with FPSS [72] is about 20 seconds, while it is around 7.5-8.0 seconds with HSA-FPSS and greatly improved with BA-FPSS by reporting as approximately 5 seconds. It is observable that the overshoot of the speed response is also highly reduced with BA-FPSS as compared to HSA-FPSS and FPSS [72].

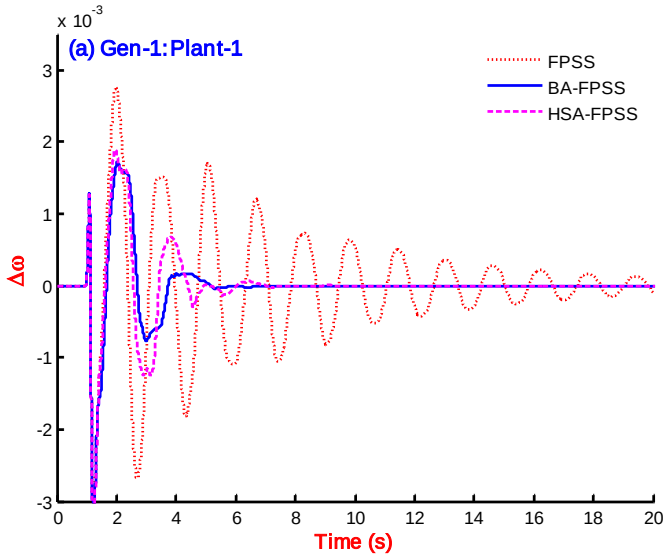

Figure 4.12: Speed response of Gen-1 of plant-1 with FPSS, HSA-FPSS and BA-FPSS

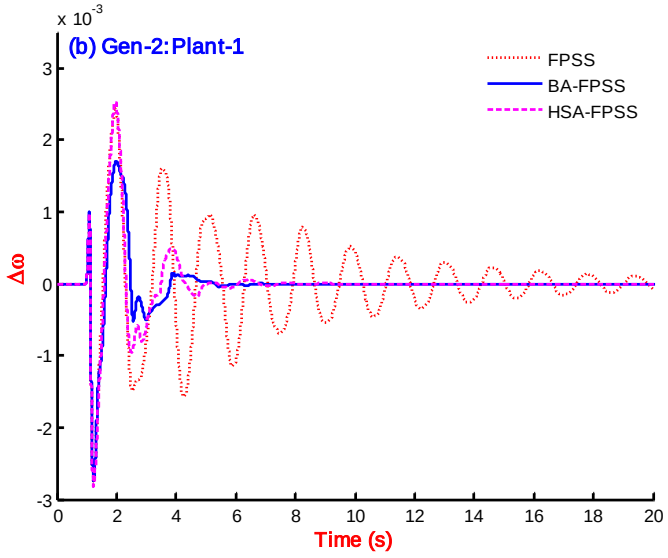

Figure 4.13: Speed response of Gen-2 of plant-1 with FPSS, HSA-FPSS and BA-FPSS

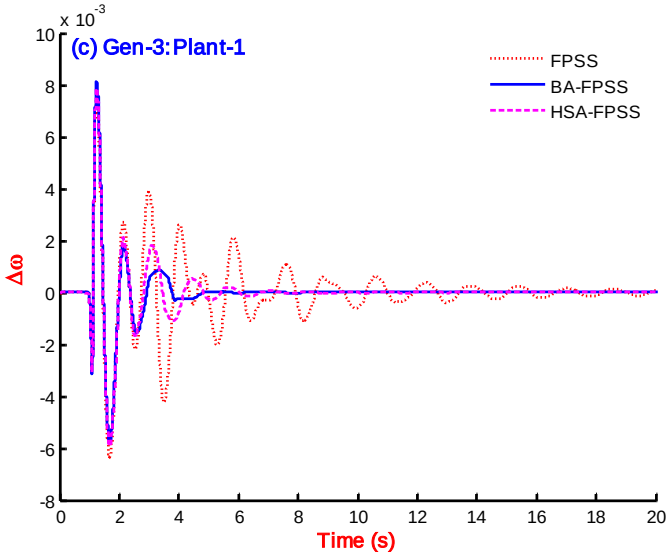

Figure 4.14: Speed response of Gen-3 of plant-1 with FPSS, HSA-FPSS and BA-FPSS

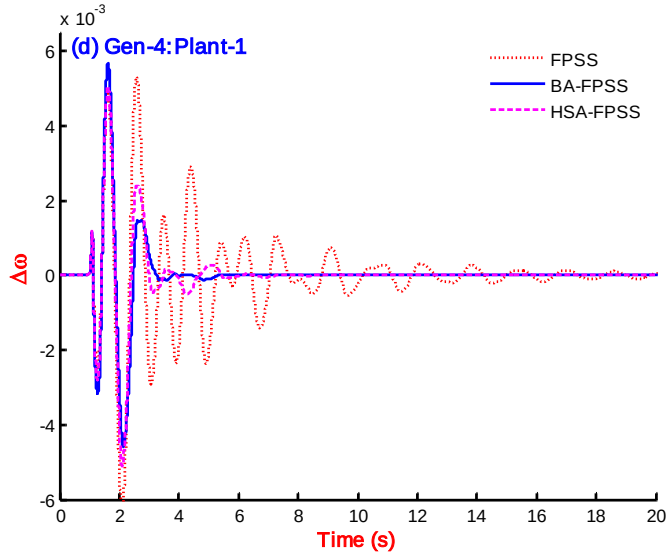

Figure 4.15: Speed response of Gen-4 of plant-1 with FPSS, HSA-FPSS and BA-FPSS

4.3.2.3. PI based performance comparison

To evaluate the robustness of the proposed BA-FPSS, simulation is carried out for all eight plant configurations which represent the wide range of operating conditions and system configurations. The system is simulated without PSS, with FPSS and with HSA-FPSS for comparison purpose with eight plant conditions. Each time the performance indices (ITAE, IAE and ISE) are recorded and enlisted in Table 4.8. Since the system possesses four generators, therefore, the PI values in this table are the sum of PIs of four generators. Comparatively lower value of PI refers to better performance. The performance indices recorded for 30 seconds of speed response is found as the minimum with proposed BA-FPSS. As an example, the values of ITAE for plant-1 with FPSS, with HSA-FPSS and with BA-FPSS are 0.1822, 0.0519 and 0.0471, respectively. The difference in ITAE with HSA-FPSS and BA-FPSS is not so far, but it matters in comparison. It is clear from

this table, that the performance of the system is enhanced by using proposed BA-FPSS as compared to others.

Table 4.8: PIs with different controllers for different plants of four-machine power system

Controllers	ITAE	IAE	ISE	ITAE	IAE	ISE
	Plant-1			Plant-2		
No-PSS	81.3215	3.402	1.2805×10^{-01}	76.5615	3.3049	1.0983×10^{-01}
FPSS [72, 73]	0.2959	0.0488	9.3138×10^{-05}	0.9025	0.0883	1.9058×10^{-04}
HSA-FPSS	0.0444	0.0187	4.8605×10^{-05}	0.209	0.04	1.3472×10^{-04}
BA-FPSS	0.0339	0.0159	4.4957×10^{-05}	0.1748	0.0362	1.2570×10^{-04}
	Plant-3			Plant-4		
No-PSS	125.279	5.3401	2.4912×10^{-01}	119.239	5.0362	2.2529×10^{-01}
FPSS [72, 73]	0.2352	0.0343	3.6603×10^{-05}	1.8959	0.0937	7.6246×10^{-05}
HSA-FPSS	0.0297	0.0096	1.3064×10^{-05}	0.4645	0.0274	1.3273×10^{-05}
BA-FPSS	0.0237	0.0091	1.1494×10^{-05}	0.2122	0.021	1.1174×10^{-05}
	Plant-5			Plant-6		
No-PSS	80.5643	3.4607	1.2891×10^{-01}	131.297	5.5711	3.0880×10^{-01}
FPSS [72, 73]	0.4077	0.0399	3.6438×10^{-05}	0.1822	0.0266	2.2424×10^{-05}
HSA-FPSS	0.0641	0.0125	1.5750×10^{-05}	0.0254	0.0084	1.1203×10^{-05}
BA-FPSS	0.057	0.0111	1.3590×10^{-05}	0.0214	0.0081	1.0175×10^{-05}
	Plant-7			Plant-8		
No-PSS	132.451	5.594	3.1287×10^{-01}	253.529	10.8127	9.3746×10^{-01}
FPSS [72, 73]	2.7333	0.1358	1.4411×10^{-04}	0.6667	0.0422	1.7748×10^{-05}
HSA-FPSS	0.4207	0.0304	1.2906×10^{-05}	0.4041	0.0219	9.7789×10^{-06}
BA-FPSS	0.4018	0.027	1.1625×10^{-05}	0.1589	0.0181	7.8399×10^{-06}

4.3.3. Optimal FPSS for 10-machine system

4.3.3.1. Design of input scaling factors

As the creations of experimental plants for IEEE New England ten-machine thirty nine-bus power system are well explained in section 2.3.3, where in the machine data, load flow data, transformer data and line data are given Table A.6 - Table A.10 for the system configuration without PSS. The system model referring to plant-1 configuration as in Table 2.20, is equipped with PD controller to all nine-machines (named as Gen-1 to Gen-9) except Gen-10, which is considered as the slack and subjected to controller design using the harmony search algorithm (as described in section 1.2.1) and the bat algorithms (as described in section 1.2.2) with all parameter's bounds within 0.001 – 50.00. With the initializing parameters as above for HSA and BA; the systems are simulated for the iteration count as 100. The fitness function variation for 100 iterations with HSA and BA is shown in Figure 4.16(a) and Figure 4.16(b), respectively. The plots of K_p, K_d and K_i (PID parameters) for ten generators (Gen-1 – Gen-9) are not shown because of space constraints, therefore, the values are enlisted in Table 4.9.

Table 4.9: Harmony search and Bat algorithm based optimized scaling factors for ten-machine power system

Generators	Harmony search algorithms		Bat algorithm	
	K_p	K_d	K_p	K_d
Gen-1	18.3912	45.5000	49.9970	27.9344
Gen-2	47.3821	46.4248	49.9865	37.2260
Gen-3	44.9837	11.1413	49.2967	31.5004
Gen-4	39.4896	29.9330	49.0089	16.9278
Gen-5	43.2640	42.9599	49.9967	30.8271
Gen-6	35.6375	40.5484	49.6088	48.5895
Gen-7	26.6901	49.3825	49.7307	9.2717
Gen-8	24.0119	25.1981	49.9805	45.8716
Gen-9	26.5061	47.7962	49.1970	28.8038

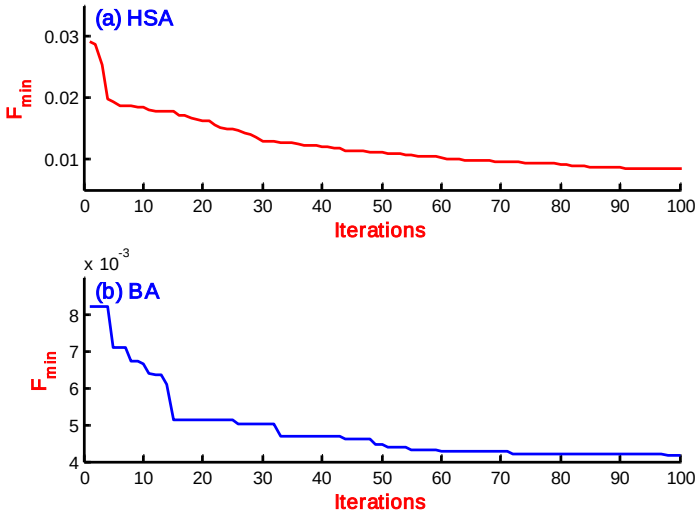

Figure 4.16: Fitness function plot with (a) Harmony search and (b) Bat algorithm for ten-machine system

4.3.3.2. Speed response comparison

The IEEE New England ten-machine thirty nine-bus power system is described in section 2.3.3 without PSS, and the creations of system models based on operating conditions are elaborated in section 2.3.3.1. In each plant condition as listed in Table 2.6 - Table 2.7 are considered with fault location as given in Table A.8. The disturbance is considered as self-clearing at different buses at 1.0 second and cleared after 0.05 second. Referring to section 2.3.3.2 and section 2.3.3.3, wherein the simulation and eigenvalue analysis with eight plant conditions are considered under no-PSS is described and found that none of the generators of plants are showing stable operation; therefore, not needed to compare to the simulation results.

An SIMULINK based block diagram, including all the nonlinear blocks is generated [191]. The speed signals of the machines are considered as output and the initial value of the speed is taken as zero. The output signals of CPSSs are added to V_{ref} via limiters. It is used to damp out the small signal disturbances via modulating the generator excitation. The output must be limited to preventing the PSS acting to counter action of AVR. Different operating points are taken as the unlike plants for both systems. The limits of PSS outputs are taken as ± 0.05. In decentralized PSS, to activate the proposed controller at same instant, proper synchronization signal is required to be sent to all machines. All PSSs can be applied simultaneously to the respective machines for both power system models [279, 280].

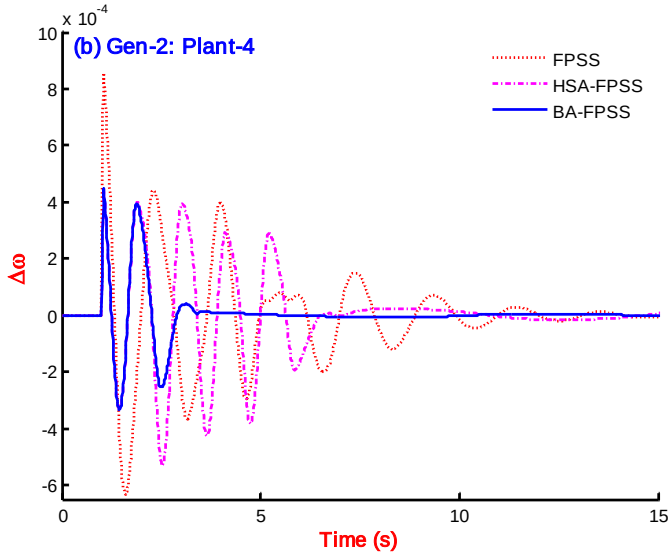

Figure 4.17: Speed response of Gen-2 of plant-4 with FPSS, HSA-FPSS and BA-FPSS on ten-machine system

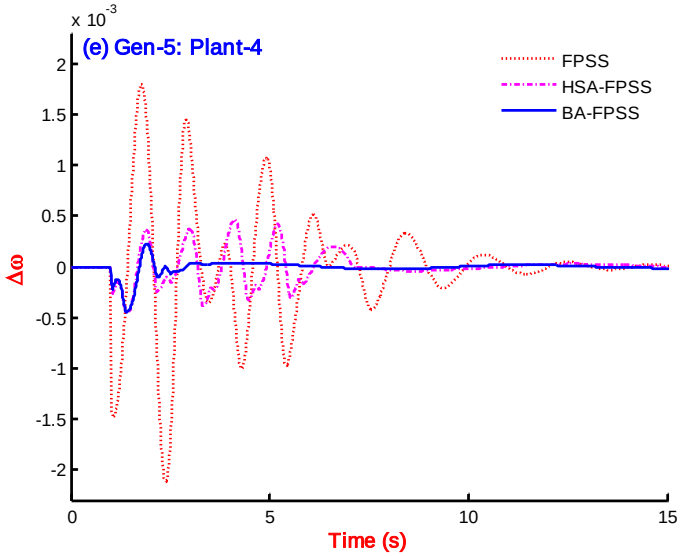

Figure 4.18: Speed response of Gen-5 of plant-4 with FPSS, HSA-FPSS and BA-FPSS on ten-machine system

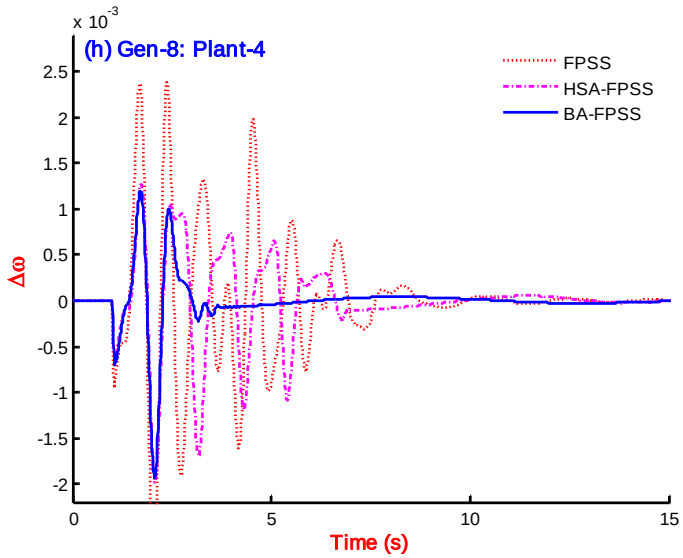

Figure 4. 19: Speed response of Gen-8 of plant-4 with FPSS, HSA-FPSS and BA-FPSS on ten-machine system

Graphical representation of speed response of New England system with FPSS, HSA-FPSS and BA-FPSS is carried out by simulation of nonlinear plant-4 configurations (Table 2.6 - Table 2.7). As a sample, speed responsefor Gen-2, Gen-5 and Gen-8 are compared in Figure 4.17, Figure 4.18 and Figure 4.19, respectively for system plant-4 configuration. The response of system with BA-FPSS shows better performance as compared to the response with FPSS [72] and HSA-FPSS. The simulation study of the system with all plant conditions has been carried out with these controllers and found BA-FPSS as best performers as compared to others, however, not shown because of space limitation.

4.3.3.3. PI based performance comparison

To evaluate the robustness of the proposed BA-FPSS, simulation is carried out for all eight plant configurations which represent the wide range of operating conditions and system configurations. The system is simulated without PSS, with FPSS and with HSA-FPSS for comparison purpose with eight plant conditions. Each time the performance indices (ITAE, IAE and ISE) are recorded and enlisted in Table 4.10. Since the system possesses ten generators, therefore, the PI values in this table show the sum of PIs of ten generators. Comparatively lower value of PI refers to better performance. It is clear from this table, that the performance of the system is enhanced by using proposed BA-FPSS as compared to performance with FPSS and with HSA-FPSS. Considering ITAE value for plant-3 for FPSS, HSA-FPSS and BA-FPSS as 0.0667, 0.0455 and 0.0379, respectively. The performance improvement using BA-FPSS with respect to HSA-FPSS and FPSS are enhanced by 20.05% and 75.98%, correspondingly.

Table 4.10: Performance indices with different controllers for different plants of ten-machine system

Controller	ITAE	IAE	ISE	ITAE	IAE	ISE
	Plant-1			Plant-2		
No-PSS	4240.765	137.6347	$1.0275\times10^{+02}$	3705.798	121.1653	$8.4972\times10^{+01}$
FPSS [72, 73]	0.1822	0.0515	5.5684×10^{-05}	0.1752	0.0496	4.9798×10^{-05}
HSA-FPSS	0.0519	0.0122	8.7900×10^{-06}	0.0583	0.0119	5.3000×10^{-06}
BA-FPSS	0.0471	0.0107	5.9800×10^{-06}	0.0572	0.0115	5.2800×10^{-06}
	Plant-3			Plant-4		
No-PSS	2913.119	92.7685	$6.2458\times10^{+01}$	4474.842	152.0426	$1.1454\times10^{+02}$
FPSS [72, 73]	0.0667	0.0236	1.3278×10^{-05}	0.2187	0.0591	9.1527×10^{-05}
HSA-FPSS	0.0455	0.0066	9.7400×10^{-07}	0.1815	0.038	8.3000×10^{-05}
BA-FPSS	0.0379	0.0062	9.6400×10^{-07}	0.0603	0.0148	2.2700×10^{-05}
	Plant-5			Plant-6		
No-PSS	3507.641	113.914	$8.0111\times10^{+01}$	3655.633	120.1519	$8.5115\times10^{+01}$
FPSS [72, 73]	0.1258	0.0395	4.0099×10^{-05}	0.1494	0.0438	4.0533×10^{-05}
HSA-FPSS	0.0668	0.0138	1.2100×10^{-05}	0.054	0.011	5.8000×10^{-06}
BA-FPSS	0.0544	0.0112	7.5900×10^{-06}	0.04	0.0087	3.9900×10^{-06}
	Plant-7			Plant-8		
No-PSS	3794.343	121.3309	$8.8423\times10^{+01}$	4089.768	134.6285	$9.7553\times10^{+01}$
FPSS [72, 73]	0.0764	0.0259	1.6134×10^{-05}	0.1878	0.0519	5.4968×10^{-05}
HSA-FPSS	0.0313	0.0054	1.4000×10^{-06}	0.067	0.0137	7.6700×10^{-06}
BA-FPSS	0.0189	0.0047	1.1900×10^{-06}	0.0441	0.0099	5.7900×10^{-06}

4.4. Design and Performance Evaluation: Scenario - 2

4.4.1. Optimal FPSS for SMIB system

4.4.1.1. Design of input – output scaling factors

In order to assess effectiveness of the proposed Bat and Harmony search algorithm in optimizing the input-output scaling factors of FPSS; the problem is formulated in MATLAB environment and executed on Intel (R) Core (TM) - 2 Duo CPU T6400 @ 2.00 GHz with 3 GB RAM, 32-bit operating system. Bat algorithm and its main steps for optimization are mentioned in section 1.2.2. In [182, 249], the generally opted to initialize as intensity (A) and pulse rate (r) as 0.5 and 0.5 respectively. By the trial-and-error method, it is found that the suitable values of loudness and pulse rate in optimization of input-output scaling factors of FPSS using the bat algorithm are as A = 0.9 and r = 0.1. The other constraint such as initializing population is selected as n = 25 and the bandwidth are considered as $f_{\min} = 0$ and $f_{\max} = 2.0$. The plant (SMIB power system) operating at nominal operating condition (where in X_l = 0.4 pu and P_{g0} = 1.0 pu) is considered for optimal tuning of input-output scaling factors of FPSS; subjected to the time domain based

simple ISE minimization type objective function with the way of the parametric bounds as in section 4.2.2.2 are considered for the optimization.

With same configuration of the system, the harmony search algorithm (as described in section 1.2.1) is applied to tune the input-output scaling factors of FPSS. The detail of the initializing parameters used with HSA is given in Table 4.2 and parameter bounds as $0.001 \le K_{\omega} \le 70$, $0.001 \le K_{p} \le 10$, $0.001 \le K_{u} \le 5.0$ and resulting behaviour of HSA in terms of fitness function is given in Figure 4.20. The optimized input-output scaling factors of FPSS; using HSA and BA for SMIB power system is enlisted in Table 4.11. As the optimization process with both algorithms is set to terminate with maximum iteration counts as 200. However, the convergence rate with HSA is almost same to BA but with higher value of fitness function. Therefore, the bat algorithm is better than the harmony search algorithm.

Table 4.11: Comparison of input-output scaling factors of FPSS by PSO-FPSS, HSA-FPSS and BA-FPSS: SMIB power system

S. No.	Controller	K_{ω}	K_{p}	K_{u}
1	PSO-FPSS[65]	59.800	4.000	1.000
2	HSA-FPSS	24.9845	5.6648	2.1173
3	BA-FPSS	13.2238	3.0358	2.0128

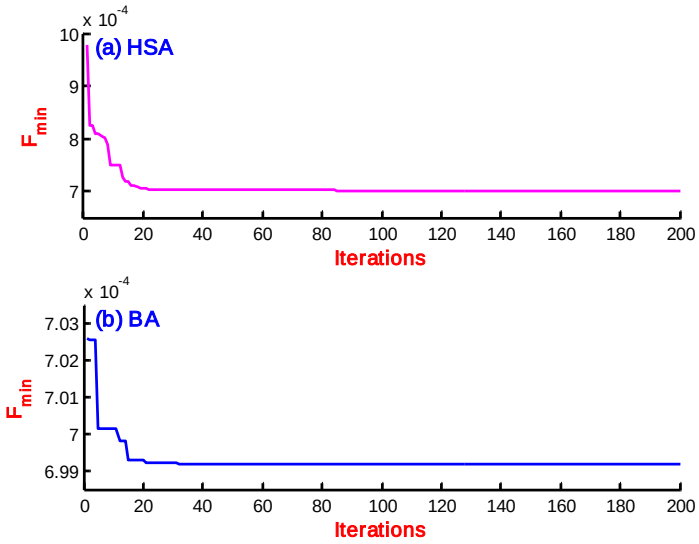

Figure 4.20: Plot of fitness function using (a) HSA and (b) BA: SMIB power system

4.4.1.2. Speed response comparison

The SMIB power system performance under nonlinear mode is carried out by creating fault at time 5 seconds and persistent for 0.1 second with the wide range of operating conditions and plant configurations. The system with unlike combinations of different active power and transmission

line reactance as in Table 2.2 (eight different plants) and system data as in Table A.1 is considered for nonlinear simulations. Such obtained eight-plants (covering wide range of operating conditions) are examined for the speed response with FPSS, HSA-FPSS and BA-FPSS in this section. An SIMULINK based block diagram, including all the nonlinear blocks is generated in MATLAB Software.

The fuzzy logic based PSS (FPSS) reported in [72] is considered for comparison purpose. The numbers of linguistic variables are five as LN (large negative), MN (medium negative), Z (zero), MP (medium positive) and LP (large positive). The input signals to FLC have been considered as change in speed ($\Delta\omega$) and change in power (Δp), while that of the output signal is considered as correction voltage (ΔV_{pss}). The corresponding 25 rule base is represented in Table 4.4. The triangular type membership function is considered for both input and output signals. The crisp value is obtained using centroid type defuzzification method.

The Simulink model of SMIB system is prepared in MATLAB Software equipped with FPSS, BA-FPSS and HSA-FPSS controllers. These systems are simulated for all eight plants as created in Table 2.2. The comparison of speed response of SMIB system with FPSS, with PSO-FPSS [65], with HSA-FPSS and with BA-FPSS is carried out for each plant configuration but presented only for Plant-3, Plant-6 and Plant-8 in Figure 4.21, Figure 4.22 and Figure 4.23, respectively. The performance at lower loading conditions (Plant 1- 4) is almost similar, but for nominal and heavy loading conditions (Plant 5 - 8), the performance with BA-FPSS is greatly improved in comparison to others. The speed response of the SMIB power system without PSS is not included in these figures as already discussed in section 2.3.1. Clearly, the settling time with BA-FPSS is better as compared to HSA-FPSS, PSO-FPSS [65] and greatly improved with respect to FPSS [72]. Considering the speed response of the system these controllers for Plant-8 in Figure 4.23, where in, the response with PSO-FPSS [65] is unstable while with FPSS [72], HSA-FPSS and BA-FPSS is stable. The response with HSA-FPSS and BA-FPSS are comparable, but the response with FPSS [72] settles in more than 25 seconds. The closely related responses with HSA-FPSS and BA-FPSS are to be differentiated by recording performance indices in next section.

4.4.1.3. PI based performance comparison

To prove superiority of the BA-FPSS, the SMIB system is simulated one by one with all four controllers (FPSS [72], PSO-FPSS [65], HSA-FPSS and BA-FPSS) and the performance indices (ITAE, IAE and ISE as introduced in section 1.4) of speed response are recorded for the simulation time as 40 seconds and enlisted in Table 4.12.

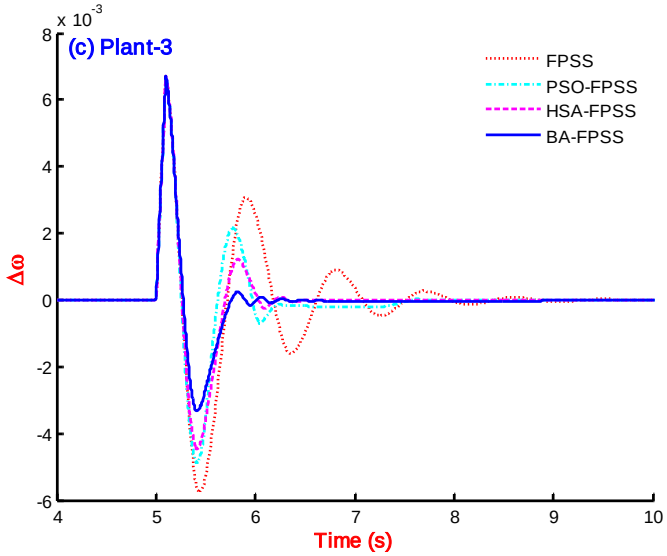

Figure 4.21: Speed response for Plant-3with FPSS, PSO-FPSS, HSA-FPSS and BA-FPSS

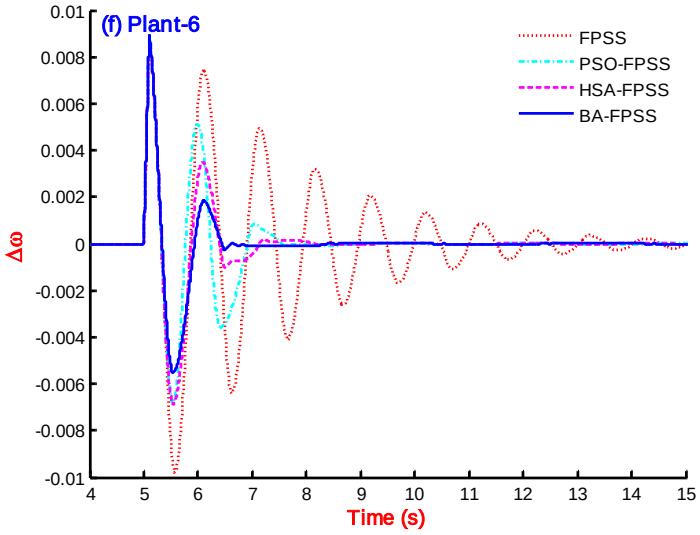

Figure 4.22: Speed response for Plant-6with FPSS, PSO-FPSS, HSA-FPSS and BA-FPSS

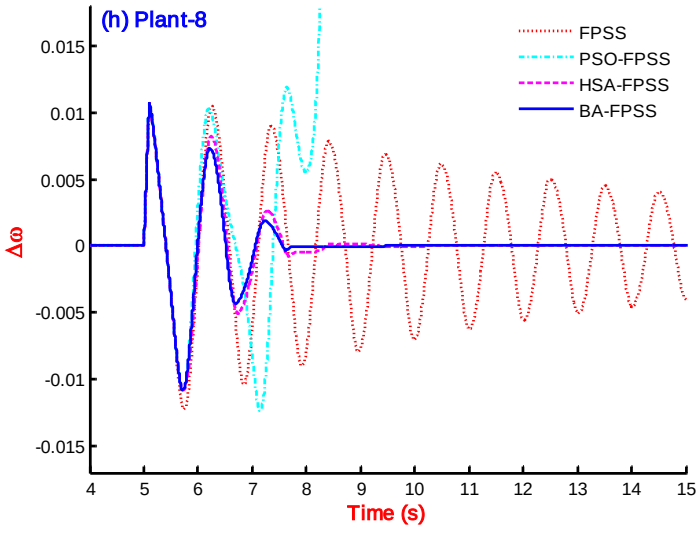

Figure 4. 23: Speed response for Plant-8with FPSS, PSO-FPSS, HSA-FPSS and BA-FPSS

The closely related responses with HSA-FPSS and BA-FPSS are well differentiated by distinct values of performance indices. As the lower value of PI, represents the superior performance of the system with reduced settling time and overshoots. In Table 4.12, the value of PIs with BA-FPSS is lesser as compared to others, resulting good performance. Due to unstable behaviour of the system with PSO-FPSS [65] for plant-7 and plant-8; the recorded PI values are highest in magnitude.

Table 4.12: Performance of speed response comparison with FPSS, PSO-FPSS, HSA-FPSS and BA-FPSS: SMIB power system

Controller	ITAE	IAE	ISE	ITAE	IAE	ISE
	Plant-1			Plant-2		
FPSS [72, 73]	0.0140	0.0025	5.1939×10^{-06}	0.0221	0.0036	7.0078×10^{-06}
PSO-FPSS [65]	0.0072	0.0013	3.0359×10^{-06}	0.0119	0.0021	3.9812×10^{-06}
HSA-FPSS	0.0073	0.0013	3.0437×10^{-06}	0.0117	0.0039	3.9599×10^{-06}
BA-FPSS	0.0073	0.0013	2.9941×10^{-06}	0.0115	0.0020	3.8997×10^{-06}
	Plant-3			Plant-4		
FPSS [72, 73]	0.0259	0.0044	1.4628×10^{-05}	0.0453	0.0071	2.2915×10^{-05}
PSO-FPSS [65]	0.0159	0.0029	9.5283×10^{-06}	0.0162	0.0029	1.0369×10^{-05}
HSA-FPSS	0.0131	0.0024	8.6405×10^{-06}	0.0181	0.0032	1.0954×10^{-05}
BA-FPSS	0.0110	0.0020	6.7405×10^{-06}	0.0177	0.0032	1.0785×10^{-05}
	Plant-5			Plant-6		
FPSS [72, 73]	0.0529	0.0086	3.9531×10^{-05}	0.1364	0.0182	8.1390×10^{-05}
PSO-FPSS [65]	0.0229	0.0041	1.6368×10^{-05}	0.0411	0.0070	3.1181×10^{-05}
HSA-FPSS	0.0245	0.0044	2.1180×10^{-05}	0.0328	0.0057	2.6481×10^{-05}
BA-FPSS	0.0150	0.0028	1.1477×10^{-05}	0.0247	0.0044	1.9924×10^{-05}
	Plant-7			Plant-8		
FPSS [72, 73]	0.2791	0.0313	1.5210×10^{-04}	0.97088	0.07295	3.7782×10^{-04}
PSO-FPSS [65]	0.0821	0.0129	6.7567×10^{-05}	124.26	7.7840	6.6780
HSA-FPSS	0.0448	0.0077	4.0846×10^{-05}	0.0733	0.0120	7.6007×10^{-05}
BA-FPSS	0.0398	0.0069	3.4579×10^{-05}	0.0644	0.0107	6.7486×10^{-05}

4.4.2. Optimal FPSS for 4-machine system

4.4.2.1. Design of input – output scaling factors

As the creations of experimental plants for two-area four-machine ten-bus power system are well explained in section 2.3.2, where in the line data (Table A.2), load flow data (Table A.3) and machine data (Table A.4) are given to the system configuration without PSS. The system model referring to plant-1 configuration as in Table 2.4, is equipped with FPSS to all four-machines (named as Gen-1 to Gen-4) and subjected to design using Harmony search algorithm (as described in section 1.2.1) and the bat algorithms (as described in section 1.2.2), with a simple time domain

based minimization of ISE as an objective function (Eqn. 4.21) with bounds as defined in Eqn. (4.24).

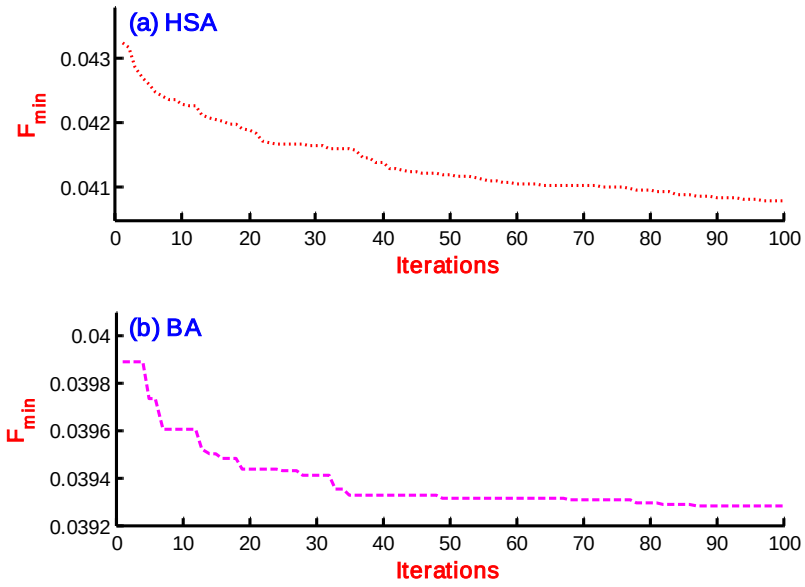

Figure 4.24: Plot of fitness function using (a) HSA and (b) BA: Four-machine power system

Table 4.13: Comparison of input-output scaling factors of FPSS using PSO-FPSS, HSA-FPSS and BA-FPSS: Four-machine power system

Controller	Generator	$K_{\omega i}$	K_{pi}	K_{ui}
PSO-FPSS[65]	Gen-1	59.8000	4.0000	1.0000
	Gen-2	59.8000	4.0000	1.0000
	Gen-3	59.8000	4.0000	1.0000
	Gen-4	59.8000	4.0000	1.0000
HSA-FPSS	Gen-1	61.8533	3.6269	0.8851
	Gen-2	60.2417	4.2179	0.8534
	Gen-3	62.3934	4.0654	0.1086
	Gen-4	62.8035	3.5687	0.9963
BA-FPSS	Gen-1	58.6538	4.0109	1.8991
	Gen-2	56.0157	4.0016	1.0021
	Gen-3	59.3950	6.4531	4.0501
	Gen-4	40.0012	7.997	3.9996

The speed signal from each generator is sensed and minimum value of sum of ISE of the error signal is minimized to tune input-output scaling factors of four FPSSs with parameter bounds as $40 \le K_{\omega} \le 70$, $1.0 \le K_{p} \le 10$, $1.0 \le K_{u} \le 5.0$. The initializing parameters for HSA and BA is considered same as in previous section. The termination criterion of the tuning process is considered as the maximum number of iterations and set as 100. The parameter bounds are selected by using the trial-and-error method; therefore, several attempts are required. The optimized scaling factors are shown in Table 4.13. The behavior of HSA and BA during

optimization in terms of fitness function is plotted in Figure 4.24(a) and Figure 4.24(b), respectively.

4.4.2.2. Speed response comparison

The two-area four-machine ten-bus power system is described in section 2.3.2 without PSS, and the creations of system models based on operating conditions are elaborated in section 2.3.2.1. The FPSS [40, 41], PSO-FPSS [65]; HSA-FPSS and BA-FPSS designed in section 4.4.2.1 are connected to the system and simulation carried out for the speed response. In each plant condition as listed in Table 2.4 is considered with fault location as given in Table A.5. The disturbance is considered as self-clearing at different buses at 1.0 second and cleared after 0.05 second. Referring to section 2.3.2.2 and section 2.3.2.3, wherein the simulation and eigenvalue analysis with eight plant conditions without PSS are described and found that none of the generators of plants are showing stable operation; therefore, not needed to compare to the simulation results. As a sample, the speed response of Gen-1 to Gen-4 for plant-3 is compared with FPSS [40, 41], PSO-FPSS [65], HSA-FPSS and BA-FPSS in Figure 4.25 - Figure 4.28. These graphical representations of the simulation results reveal that the performance of the system with PSO-FPSS [65], HSA-FPSS and BA-FPSS is greatly improved as compared to FPSS [40, 41]. As the responses of the system with FPSS [40, 41], PSO-FPSS [65], HSA-FPSS and BA-FPSS are closely related, therefore, to differentiate the associated performance indices is to be carried in next section.

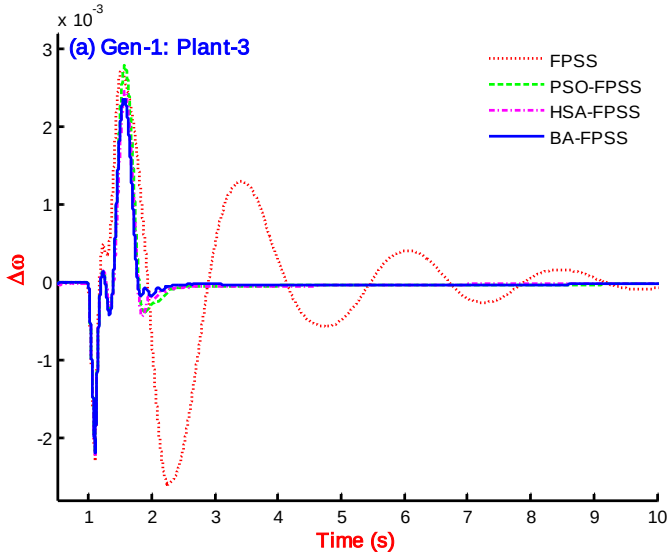

Figure 4.25: Speed response for Gen-1 of Plant-3 with FPSS, PSO-FPSS, HSA-FPSS and BA-FPSS

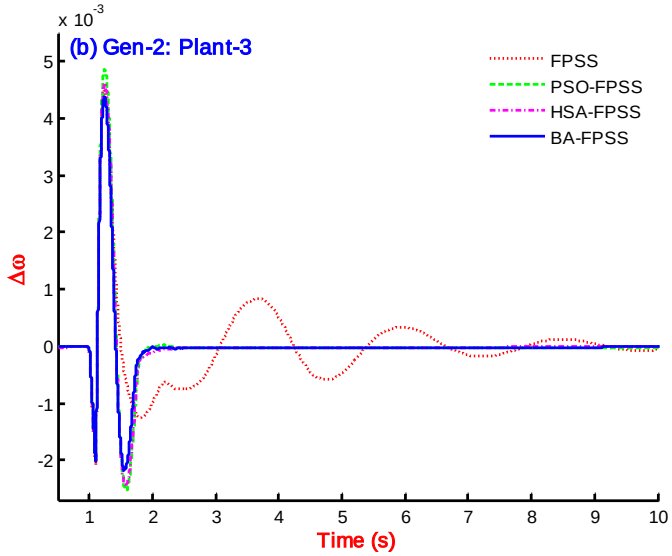

Figure 4.26: Speed response for Gen-2 of Plant-3 with FPSS, PSO-FPSS, HSA-FPSS and BA-FPSS

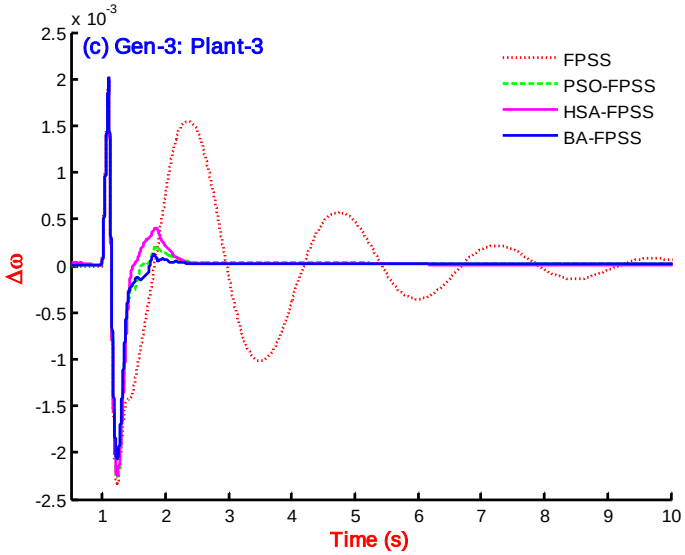

Figure 4.27: Speed response for Gen-3 of Plant-3 with FPSS, PSO-FPSS, HSA-FPSS and BA-FPSS

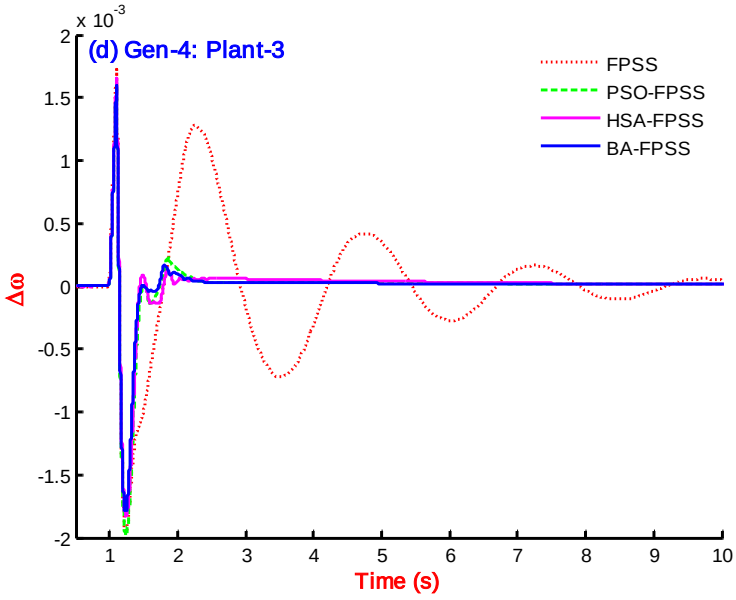

Figure 4.28: Speed response for Gen-4 of Plant-3 with FPSS, PSO-FPSS, HSA-FPSS and BA-FPSS

4.4.2.3. PI based performance comparison

To evaluate the robustness of the proposed BA-FPSS, simulation is carried out for all eight plant configurations which represent the wide range of operating conditions and system configurations. The system is simulated FPSS [40, 41], PSO-FPSS [65], HSA-FPSS and BA-FPSS for comparison purpose with eight plant conditions. Each time the performance indices (ITAE, IAE and ISE) are recorded and enlisted in Table 4.14. Since the system possesses four generators, therefore, the PI values in Table 4.14 are the sum of PIs of four generators. Comparatively lower value of PI refers to better performance. It is clear from this table, that the performance of the system is enhanced by using proposed BA-FPSS as compared to other controllers.

Table 4.14: Performance of speed response comparison with FPSS, PSO-FPSS, HSA-FPSS and BA-FPSS: Four-machine power system

Controller	ITAE	IAE	ISE	ITAE	IAE	ISE
	Plant-1			Plant-2		
FPSS [40, 41]	0.0763	0.0231	4.5996×10^{-05}	0.1823	0.0473	1.4331×10^{-04}
PSO-FPSS [65]	0.0308	0.0128	4.0754×10^{-05}	0.0828	0.0322	1.6105×10^{-04}
HSA-FPSS	0.0356	0.0135	4.2913×10^{-05}	0.0846	0.0354	1.8268×10^{-04}
BA-FPSS	0.0285	0.0133	3.9055×10^{-05}	0.0775	0.0302	1.4252×10^{-04}
	Plant-3			Plant-4		
FPSS [40, 41]	0.0596	0.0169	1.4331×10^{-04}	0.0497	0.0132	1.1295×10^{-05}
PSO-FPSS [65]	0.0191	0.0053	8.3550×10^{-06}	0.0301	0.0062	9.0234×10^{-06}
HSA-FPSS	0.0169	0.0050	7.4998×10^{-06}	0.0262	0.0059	8.2087×10^{-06}
BA-FPSS	0.0155	0.0046	6.4506×10^{-06}	0.0183	0.0055	7.6245×10^{-06}
	Plant-5			Plant-6		
FPSS [40, 41]	0.0625	0.0167	1.7306×10^{-05}	0.0362	0.0111	1.0156×10^{-05}
PSO-FPSS [65]	0.0224	0.0052	6.5374×10^{-06}	0.0206	0.0050	6.1350×10^{-06}
HSA-FPSS	0.0280	0.0064	7.6419×10^{-06}	0.0270	0.0058	6.7488×10^{-06}
BA-FPSS	0.0171	0.0048	5.7325×10^{-06}	0.0132	0.0046	5.8600×10^{-06}
	Plant-7			Plant-8		
FPSS [40, 41]	0.0613	0.0149	9.2326×10^{-06}	0.0428	0.0111	6.8407×10^{-06}
PSO-FPSS [65]	0.0320	0.0038	1.7054×10^{-06}	0.0082	0.0021	1.2035×10^{-06}
HSA-FPSS	0.0309	0.0037	1.7049×10^{-06}	0.0168	0.0037	2.0258×10^{-06}
BA-FPSS	0.0195	0.0036	1.6846×10^{-06}	0.0094	0.0027	1.5931×10^{-06}

4.4.3. Optimal FPSS for 10 - machine system

4.4.3.1. Design of input – output scaling factors

As the creation of experimental plants for IEEE New England ten-machine thirty nine-bus power system are well explained in section 2.3.3, where in the machine data, load flow data, transformer data and line data are given Table A.6 - Table A.10 for the system configuration without PSS. The system model referring to plant-1 configuration as in Table 2.6 - Table 2.7, is equipped with FPSS

at all nine-machines (named as Gen-1 to Gen-9) except Gen-10, which is considered as the slack and subjected to controller design using Harmony search algorithm (as described in section 1.2.1) Bat algorithm (as described in section 1.2.2) with parameter bounds as $0.001 \le K_{\omega} \le 60$, $0.001 \le K_p \le 8.0$, $0.001 \le K_u \le 5.0$. With the initializing parameters as above for HSA and BA; the systems are simulated for an iteration count as 200. The fitness function variation for 200 iterations with HSA and BA is shown in Figure 4.29(a) and Figure 4.29(b), respectively. The plots of K_p, K_d and K_i (PID parameters) for ten generators (Gen-1 – Gen-9) are not shown because of space constraints, therefore, the values are enlisted in Table 4.15.

Table 4.15: Comparison of input-output scaling factors of FPSS using HSA-FPSS and BA-FPSS: Ten-machine system

Generators	HSA-FPSS			BA-FPSS		
	$K_{\omega i}$	K_{pi}	K_{ui}	$K_{\omega i}$	K_{pi}	K_{ui}
Gen-1	10.0000	9.7770	9.9991	19.6546	4.7485	3.0247
Gen-2	56.8062	6.8892	9.9382	59.7079	8.4225	4.8785
Gen-3	10.0899	9.9099	10.0000	13.1155	8.4256	3.9920
Gen-4	59.8892	5.8811	10.0000	59.4908	7.1621	3.1274
Gen-5	55.5804	8.9766	9.7362	25.9536	2.9191	4.6584
Gen-6	59.5663	9.8928	10.0000	17.4769	4.2649	4.8460
Gen-7	60.0000	6.5596	8.9733	44.3857	9.0319	3.6861
Gen-8	52.9681	9.0131	8.7615	45.5560	4.6530	3.9345
Gen-9	56.4434	7.9649	6.4976	27.4008	7.8812	4.7202

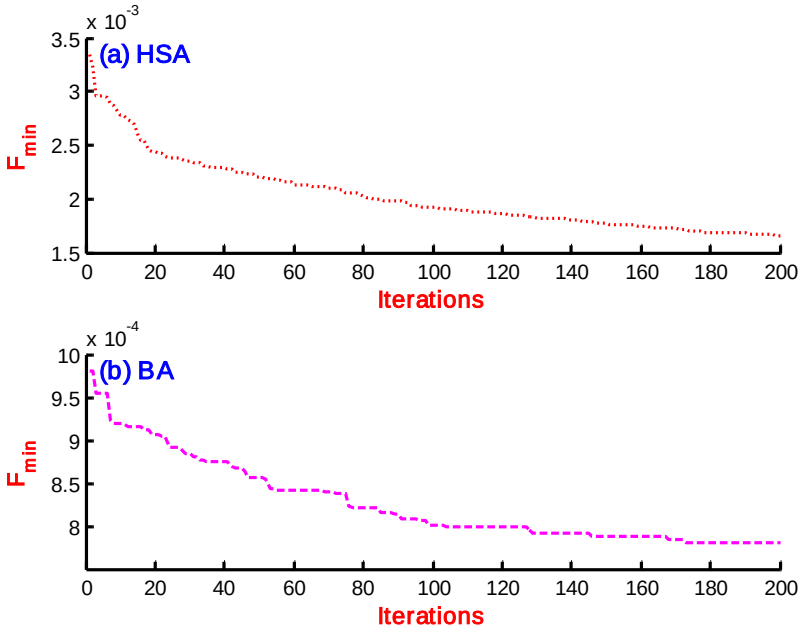

Figure 4.29: Plot of fitness function using (a) HSA and (b) BA: Ten-machine power system

4.4.3.2. Speed response comparison

The IEEE New England ten-machine thirty nine-bus power system is described in section 2.3.3

without PSS, and the creations of system models based on operating conditions are elaborated in section 2.3.3.1. In each plant condition as listed in Table 2.6 - Table 2.7 are considered with fault location as given in Table A.8. The disturbance is considered as self-clearing at different buses at 1.0 second and cleared after 0.05 second. Referring to section 2.3.3.2 and section 2.3.3.3, wherein the simulation and eigenvalue analysis with eight plant conditions are considered under no-PSS is described and found that none of the generators of plants are showing stable operation; therefore, not needed to compare to the simulation results.

An SIMULINK based block diagram, including all the nonlinear blocks is generated [191] as in section 2.6.3. The speed signals of the machines are considered as output and the initial value of the speed is taken as zero. The output signals of FPSSs are added to V_{ref} via limiters. It is used to damp out the small signal disturbances via modulating the generator excitation. The output must be limited to preventing the PSS acting to counter action of AVR. Different operating points are taken as the unlike plants for both systems. The limits of PSS outputs are taken as ± 0.05. In decentralized PSS, to activate the proposed controller at same instant, proper synchronization signal is required to be sent to all machines. All PSSs can be applied simultaneously to the respective machines for both power system models [215].

Graphical representation of speed response of New England system with FPSS [40, 41], HSA-FPSS and BA-FPSS is carried out by simulation of nonlinear plant-5 configurations (Table 2.6 - Table 2.7). The generators associated to a plant configuration are 10, but because of space constraints, speed response is compared for Gen-1, Gen-3, Gen-5, Gen-8 and Gen-9 in Figure 4.30, Figure 4.31, Figure 4.32, Figure 4.33 and Figure 4.34, respectively. In each response in these figures, the response with BA-FPSS is superior as compared to the response with FPSS [40, 41] and HSA-FPSS.

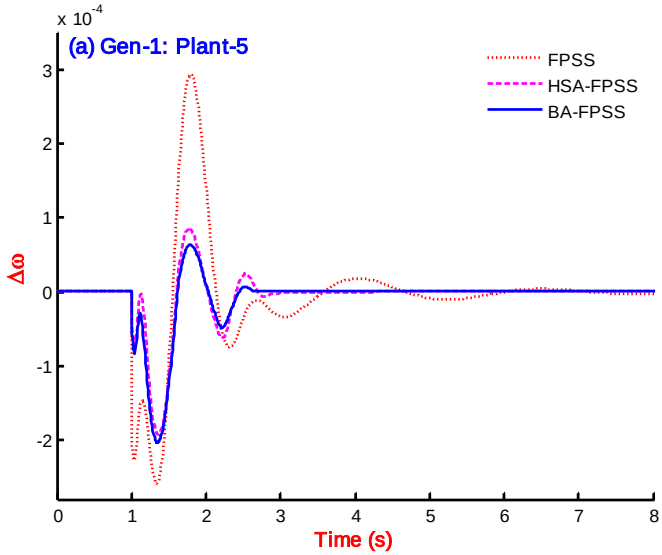

Figure 4.30: Speed response of Gen-1 for palnt-5 with FPSS, HSA-FPSS and BA-FPSS

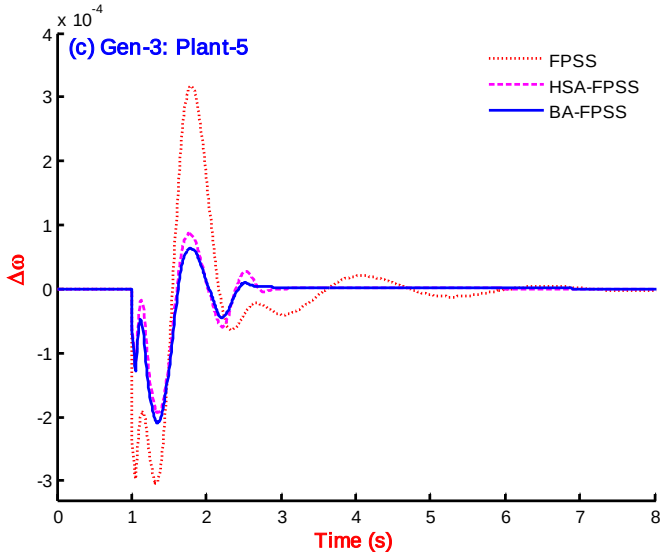

Figure 4.31: Speed response of Gen-3 for palnt-5 with FPSS, HSA-FPSS and BA-FPSS

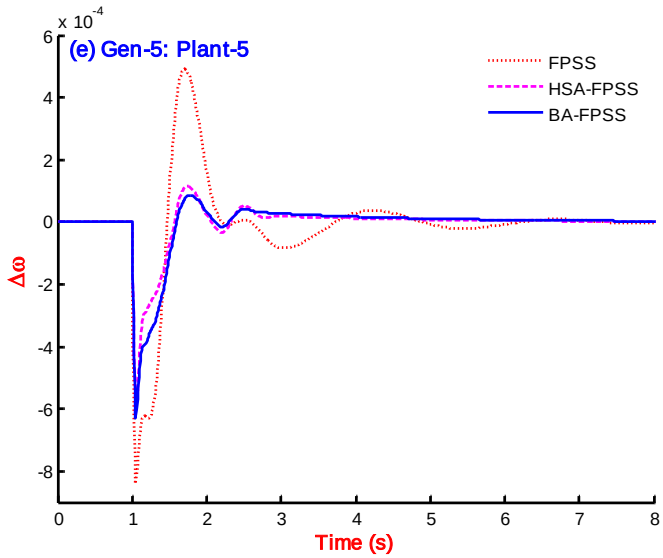

Figure 4.32: Speed response of Gen-5 for palnt-5 with FPSS, HSA-FPSS and BA-FPSS

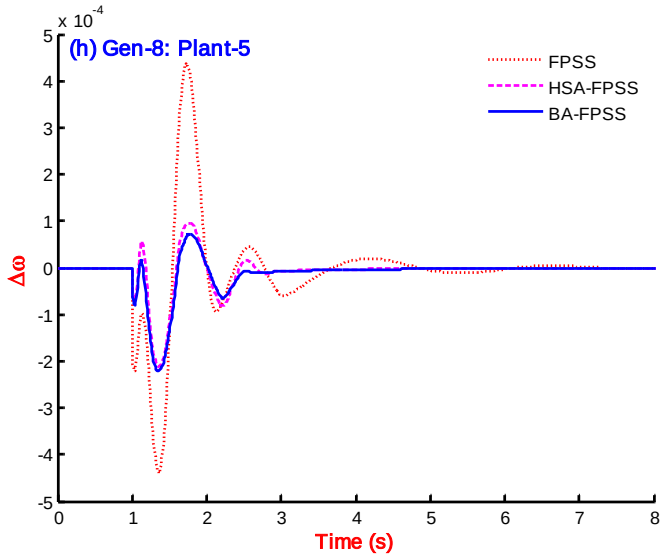

Figure 4.33: Speed response of Gen-8 for palnt-5 with FPSS, HSA-FPSS and BA-FPSS

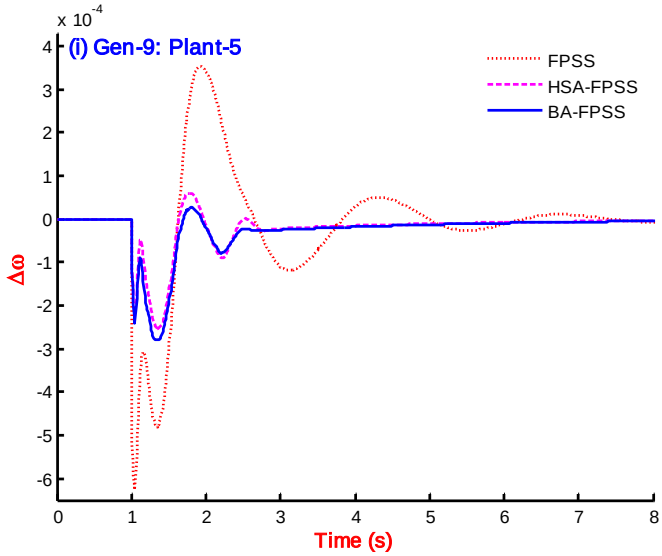

Figure 4.34: Speed response of Gen-9 for palnt-5 with FPSS, HSA-FPSS and BA-FPSS

The graphical representation of the response due to these controllers is quite clear to interpret best performance with BA-FPSS and worst as with FPSS [40, 41]. It can be seen that the overshoot as well as the settling time with BA-FPSS is greatly improved as compared to that of with FPSS [40, 41]. However, the response with BA-FPSS is closely related to that of with HSA-FPSS; therefore, the performance indices based analysis is needed to differentiate the degree of performance.

Table 4. 16: Performance of speed response comparison with FPSS, HSA-FPSS and BA-FPSS: Ten-machine power system

Controller	ITAE	IAE	ISE	ITAE	IAE	ISE
	Plant-1			Plant-2		
FPSS [40, 41]	0.0236	0.0122	8.3233×10^{-06}	0.0339	0.0149	8.4324×10^{-06}
HSA-FPSS	0.0104	0.0064	5.8288×10^{-06}	0.0097	0.0056	3.1842×10^{-06}
BA-FPSS	0.0099	0.0063	5.3339×10^{-06}	0.0080	0.0051	3.0877×10^{-06}
	Plant-3			Plant-4		
FPSS [40, 41]	0.0115	0.0063	1.5598×10^{-06}	0.0185	0.0104	1.0332×10^{-05}
HSA-FPSS	0.0021	0.0022	5.5395×10^{-07}	0.0066	0.0048	6.3518×10^{-06}
BA-FPSS	0.0017	0.0019	5.0791×10^{-07}	0.0063	0.0048	5.6729×10^{-06}
	Plant-5			Plant-6		
FPSS [40, 41]	0.0132	0.0086	7.0048×10^{-06}	0.0204	0.0107	5.8676×10^{-06}
HSA-FPSS	0.0082	0.0056	6.3767×10^{-06}	0.0081	0.0052	3.4451×10^{-06}
BA-FPSS	0.0079	0.0054	5.7404×10^{-06}	0.0076	0.0049	3.6366×10^{-06}
	Plant-7			Plant-8		
FPSS [40, 41]	0.0120	0.0066	1.9293×10^{-06}	0.0291	0.0135	8.2817×10^{-06}
HSA-FPSS	0.0030	0.0025	8.0286×10^{-07}	0.0084	0.0056	4.3251×10^{-06}
BA-FPSS	0.0027	0.0023	7.7544×10^{-07}	0.0075	0.0052	4.3215×10^{-06}

4.4.3.3. PI based performance comparison

To evaluate the robustness of the proposed BA-FPSS, simulation is carried out for all eight plant configurations which represent the wide range of operating conditions and system configurations. The system is simulated with FPSS and with HSA-FPSS for comparison purpose with eight plant conditions. Each time the performance indices (ITAE, IAE and ISE) are recorded and enlisted in Table 4. 16. Since the system possesses ten generators, therefore, the PI values in Table 4. 16 are the sum of PIs of ten generators. Comparatively lower value of PI refers to better performance. It is clear from this table, that the performance of the system is enhanced by using proposed BA-FPSS as compared to performance with FPSS and with HSA-FPSS.

4.5. Conclusion

In this chapter, the application of two different optimization techniques such as harmony search algorithm and bat algorithm is used to tune the scaling factors of fuzzy logic based power system stabilizer for three systems such as single-machine infinite-bus power system (SMIB), two-area four-machine ten-bus power system and IEEE New England ten-machine thirty nine-bus power systems.

The two schemes of optimization for scaling factors are considered as (a) Scenario-1: Normalizing factors of two input signals ($\Delta\omega, \Delta a$) are optimized with HSA and BA, and (b) Scenario-2: Normalizing factors of two input signals ($\Delta\omega, \Delta p$) and output (ΔV_{PSS}) are optimized with HSA and BA.

In scenario-1, the designed BA-FPSS and HSA-FPSS with tuned input signal scaling factors are connected to SMIB system, 4-machine 10-bus system and 10-machine 39-bus power system. The simulation study has been carried out with the eight nonlinear plant conditions, and response performance is compared. The effectiveness and superiority of the proposed controller (BA-FPSS) are proved in terms of performance indices (ITAE, IAE and ISE).

In scenario-2, the designed BA-FPSS and HSA-FPSS with tuned input-output signal scaling factors are connected to SMIB system, 4-machine 10-bus system and 10-machine 39-bus power system. The simulation study has been carried out with the eight nonlinear plant conditions, and response performance is compared. The effectiveness and superiority of the proposed controller (BA-FPSS) is proved in terms of performance indices (ITAE, IAE and ISE).

Clearly, the BA-FPSS in scenario-2 outperforms the BA-FPSS in scenario-1and proved by performance indices based analysis.

Chapter 5

DESIGN OF NEW RULE TABLE BASED FUZZY LOGIC POWER SYSTEM STABILIZER

In this chapter, fuzzy logic based power system stabilizer (FPSS) is designed to have effective and robust damping of low frequency oscillations in power systems. As to achieve impressive performance of a controlled plant, the fuzzy rule matrix (FRM) of a fuzzy logic controller (FLC) is designed by the trial-and-error method, which is a time-consuming process. A systematic procedure is introduced to design FRM for effective damping of these power system oscillations. To design the novel FRM based PSS (FPSS), the existing rule tables in literature are examined on an SMIB power system; consequently, empirical relationships have been drawn. The response validity and rule justification is carried out using linguistic phase-plane trajectory method. The effectiveness of proposed FPSS is examined by nonlinear simulation based analysis on a single-machine and multimachine power system. The response of power systems with proposed FPSS is compared to that of without PSS, with conventional PSS and with FPSS reported in literature. The response comparison is carried out in terms of performance indices (ITAE, IAE and ISE).

5.1. Introduction

Electric power demand is the main cause of large, complex and interconnected power system networks. These are almost operated closer to the transient and dynamic stability limits. The heavy transfer of power on weak transmission lines is one of the causes to develop small signal oscillations. The other sources of low frequency oscillations are sudden changes in operating conditions, continuous changes in load, setting of automatic voltage regulators (AVRs) and some sort of disturbances, including faults within the power system. Some of these low-frequency oscillations (0.2-3.0 Hz) are damped out automatically, not affecting the power transfer capability of a power system, but others may persist for a while, grows in magnitude resulting to system separation and affecting power transmission.

The interconnected synchronous generators are equipped with high gain, fast acting AVRs to hold a generator in synchronism with a power system during transient fault conditions. The elevated gain of an excitation system leads to decrease in damping torque on the generator. To counteract the effect of high-gain AVRs or the sources of negative damping, a supplementary excitation controller referred to as a power system stabilizer (PSS) has been added into the excitation system, which in turn produces a component of electrical torque at the rotor in phase

with speed variations. The most widely used type of PSS is conventional PSS (CPSS) consists of fixed lead-lag structure and is designed under phase compensation for a specific operating condition to work optimally [75]. The designed CPSS gives poor performance under heavy loading conditions within the power system [40, 281].

To improve the performance of CPSS over a wide range of operating conditions, numerous techniques have been proposed for their design, which is based on adaptive control, robust control and intelligent optimization techniques [75]. Adaptive control technique is based on the idea of continuously observing the system contingencies, and updating the PSS parameters accordingly in order to improve damping of the low-frequency oscillations [202]. These adaptive PSSs have poor performance during learning phase, unless they are properly initialized. It requires measurement to satisfy persistent excitation conditions for successful operation, otherwise the adjustment/updating of PSS parameters fails [282, 283]. Robust control is a good example to handle uncertainties introduced by varying operating conditions in a power system. The H_∞ optimization and variable structure control are efficient tools to design PSSs. The H_∞ based design requires exhaustive search and results in a high-order controller up to the order of a plant [284]. In variable structure control, PSS is designed to drive the system to a sliding surface on which the error decays to zero. It gives excellent performance even with uncertainties, but at the cost of high control activities called chattering. Artificial neural network (ANN) based design of PSS is a good performer to stabilize power systems, but it suffers with long training time, selection of layers and the selection of the number of neurons in a layer. Recently, several intelligent optimization techniques have been developed to design CPSS for better performances such as Particle swarm optimization (PSO) [13], small-population-based particle swarm optimization (SPPSO) [13], bacterial foraging algorithm [13], Genetic Algorithm [14, 24], PSO with passive congregation (PSOPC) [14], Modified PSO (MPSO) [15], Combinatorial discrete and continuous action reinforcement learning automata (CDCARLA) [16], Modified artificial immune network (MAINet) [17], multiobjective immune algorithm (MOIA) [17], Bacterial foraging optimization algorithm (BFOA) [18], adaptive mutation breeder genetic algorithm (ABGA) [19], strength-pareto evolutionary algorithm (SPEA) [11], differential evolution (DE) [23], fuzzy gravitational search algorithm (FGSA) [26], Cultural algorithm (CA) [25]. GA and SA have reported revisiting of suboptimal solutions and resulted poor performance.

Fuzzy logic has emerged as the potential technique to design PSS. It is the only technique to design PSS to use knowledge of human expert in linguistic form and represents a nonlinear mapping that can cope with the nonlinear characteristic of a power system. It is reported that FPSS outperforms CPSS over a wide range of operating conditions. As a part of FPSS design, selections of input-output membership function and effect on the performance are reported in [285], while

selection of appropriate defuzzification method is reported in [72]. On selection of scaling factors as normalizing coefficients of input-output signals for FPSS and their tuning using particle swarm optimization (PSO) is well elaborated in [65]. The performance enhancement by proper tuning of scaling factors for input signal using the harmony search algorithm is reported in [286]. General trend to design fuzzy rule matrix (FRM) is by trial and error using knowledge of human expert of the system. Therefore, it becomes a tiresome and difficult process to design FRM. In this chapter, the proper way of design and verification of FRM is presented. The performance of FPSS based on designed FRM is compared to the FPSS used by different researchers in literature, and superiority is validated by comparing performance indices.

The novelty of the proposed design method is to reduce the time burden. In this chapter, a systematic design approach for rule table or fuzzy rule matrix (FRM) is proposed. The rest of this chapter is organized as follows. In section 5.2, the problem formulation is carried out by introducing the systems under consideration and a review on the fuzzy logic controller. In section 5.3, a review of fuzzy rule matrices (FRMs) as reported in literature is presented with response comparison on the SMIB power system. The similar rule tables are named as FRM 1-21. The Fuzzy rule justification by which the proposed FRM and previously published FRM response is validated in section 5.4. The performance of the proposed FPSS is carried out on SMIB system, 4-machine 10-bus system and 10-machine 39-bus power system in section 5.5 - 5.7 with comparison to the FRMs reported in literature. Finally, the observation based conclusion is carried out in section 5.8.

5.2. Problem Formulation

The aim of this chapter is to design, and verification of a new fuzzy rule matrix (FRM) based FPSS to enhance small signal stability of power systems; therefore, the electric power system (EPS) elements such as generators, excitation system and PSS must be modeled. To complete the FRM design process, an overview of the fuzzy logic controller as FPSS is presented. Accordingly, the system model as SMIB and multi machine power system is elaborated.

5.2.1. Test system description

The systems under consideration are single-machine connected to infinite-bus (SMIB), two-area four-machine ten-bus and IEEE New England ten-machine thirty nine-bus power system. The single-line diagram representation of an SMIB power system is shown in Figure 1.6, and the way of connection with AVR and excitation system is shown in Figure 5.1. The small signal models of the SMIB power system can be represented by Figure 5.2 with connection of FPSS. The output

signal of this PSS is added to AVR to modulate the excitation system for enhancing the damping of the minute signal oscillations.

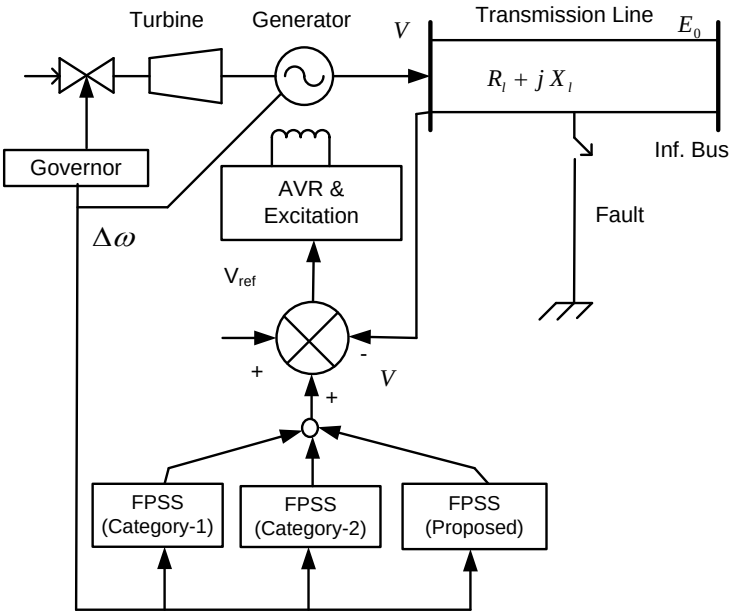

Figure 5.1: Representation of SMIB system in connection with FPSS

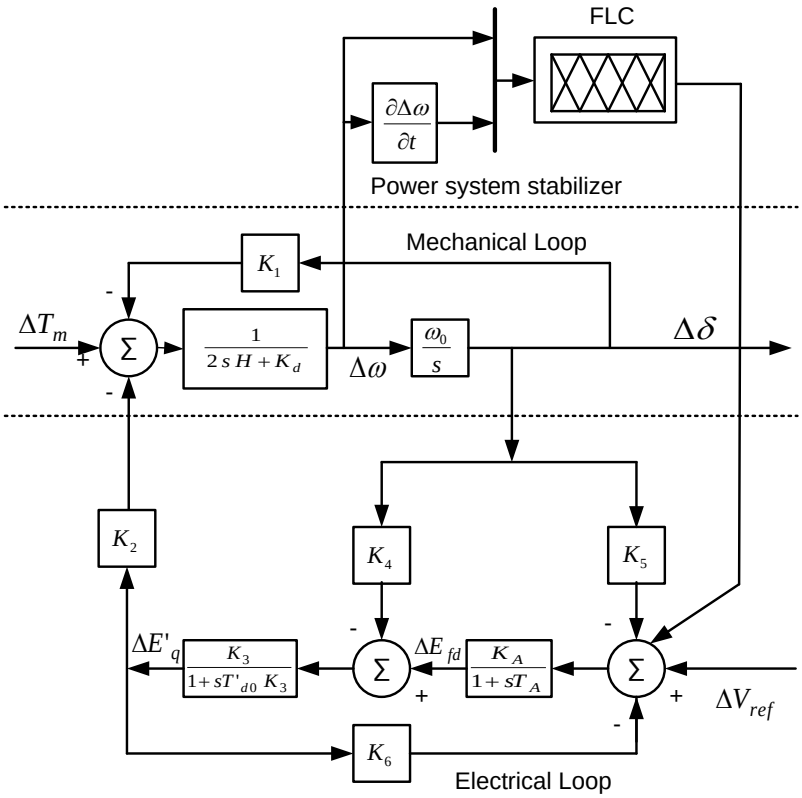

Figure 5.2: Representation of Heffron-Phillip model with FPSS

The single-line diagram representation of four-machine and ten-machine models is shown in Figure 1.14 and Figure 1.15, respectively. Moreover, a general Heffron-Philip representation is shown in Figure 1.13 [24-26]. The considered synchronous machines of SMIB, and multimachine power systems are of a model 1.0 type as discussed in [191]. To cover all operating conditions, the

power system with generators, stabilizers, and excitation systems can be modeled by a set of nonlinear differential equations as described in Eqn. (1.59 – 1.60) [14].

It is necessary to have linearized model of a power system around an operating point to analyze the small signal stability of a power system and consequently, to design power system stabilizer. The power system represented by Eqn. (1.59 – 1.60), is linearized around an equilibrium operating point of the power system and represented by Eqn. (1.64 - 1.65) [14, 23].

5.2.2. On fuzzy logic controller

The pioneer work on fuzzy logic was introduced in 1960s by Prof. Lofti Zadeh [126]. In fuzzy logic, a programmer deals with the natural, "linguistic sets" of states, such as large negative, medium negative, negative, positive, medium positive, large positive, etc. The main parts of the fuzzy logic process are fuzzification (crisp value to fuzzy input), rule evaluation (fuzzy control), and defuzzification (fuzzy output to crisp value) [287, 288]**.**

The FLC has the following main elements as in Figure 5.3.

1. *Rule-Base:* It contains fuzzy logic quantification (a set of If-Then rules) of the expert's linguistic description of the system to get good control.
2. *Inference Mechanism:* It is also called as "inference engine" or "fuzzy inference" module. It emulates the decision making of expert in interpreting and applying to control the plant.
3. *Fuzzification Interface:* It converts controller inputs into fuzzy inputs, which are used by the inference mechanism to activate and apply rules. The crisp value inputs are converted to fuzzy inputs on the basis of membership functions defined for the fuzzy system.
4. *Defuzzification Interface:* It converts the output / conclusions of the inference into crisp inputs to the plant.

The purpose of the fuzzy control system is to replace a human expert by a fuzzy rule-based system. The FLC can convert the linguistic variable based information by use of expert knowledge to an automatic control of the plant. The heart of Fuzzy Systems is a knowledge base, which is formed by the if-then rules of fuzziness.

Fuzzy sets in fuzzy systems are used to map input to output as in Figure 5.3. The Mamdani system [289] type fuzzy system is used in this chapter. The major stages of mapping involve as fuzzification process, inference process and defuzzification process. The triangular membership functions are used in fuzzification stage [289-291]. The major parts of an inference system are application, implication and aggregation [291]. The conjunctive process (MIN) is applied in application part, the truncation process on the implication part while the disjunctive process (MAX) is applied in the aggregation part in this figure. There are many defuzzification methods

like centroid, bisector, LOM, MOM, SOM but most widely used centroid method is considered in the defuzzification stage [291].

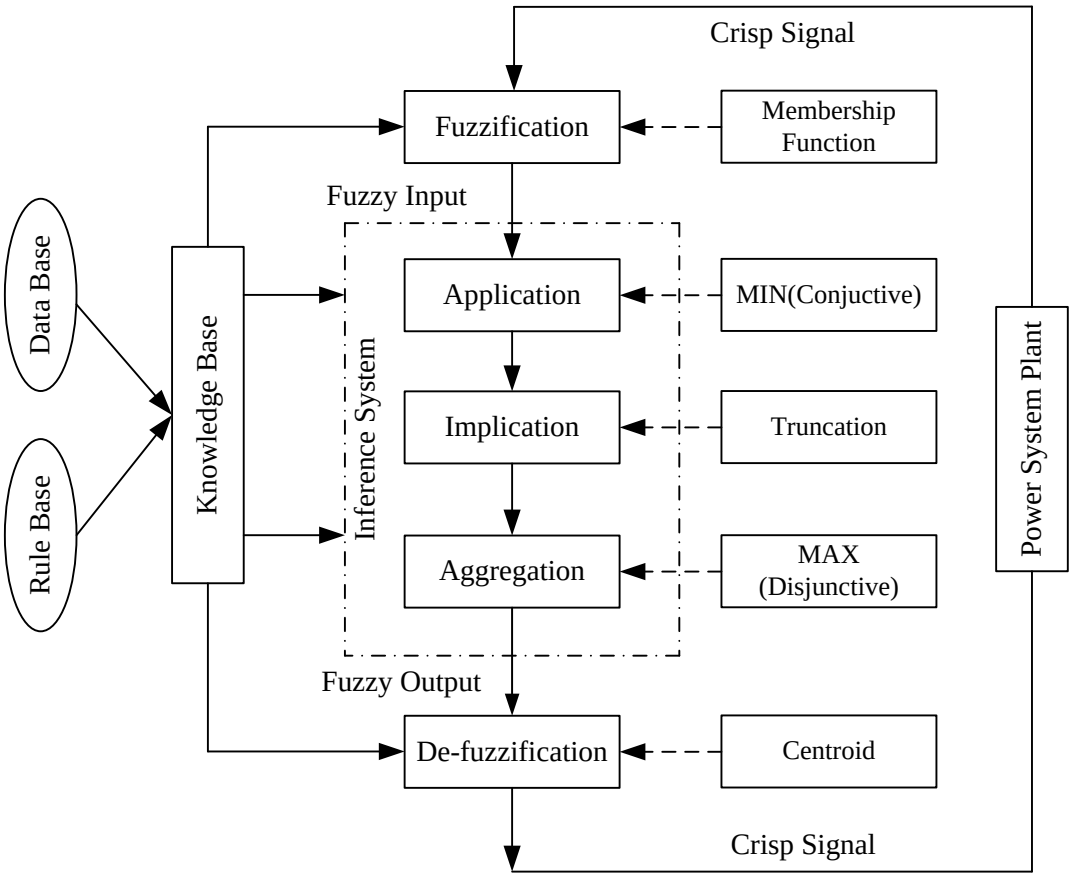

Figure 5.3: Input to Output mapping in a fuzzy system

5.3. Review on Fuzzy Rule Matrices

As per the literature review, 21 different FRMs proposed by different researchers. The similar rule tables (FRM) proposed by different researchers are arranged in a single rule matrix and are represented by FRM-1 to FRM-21. These rule tables are used to design fuzzy PSS for SMIB power system, and the performance is evaluated in terms of the settling time of the speed variation & performance indices as ISE, IAE and ITAE, introduced in section 1.4. The SMIB power system is operated with nominal operating conditions as active power (P_{g0} =1.0) and the reactance as X_l =0.4, mentioned as in Table 5.1.

FRM-1: The similar type of rule table is being proposed by Abdelazim *et al.*, 2003 [43]; Adams *et al.*, 2002 [36]; Shayeghi *et al.*, 2008 [37]; Abdelazim *et al.*, 2005 [38]; Ramirez-Gonzalez *et al.*, 2008 [39], 2010 [40], 2009 [41]; and Vijayaraghavan *et al.*, 2011 [42] at different times for the design of PSS. On application of this rule table; the system shows a stable response as in Figure 5.4 with recorded settling time of 11.11 seconds as in Table 5.1. The

ISE, IAE and ITAE are also observed as 4.192×10^{-5}, 0.009084 and 0.05638 respectively, and mentioned as in Table 5.1. Here, it should be cleared that the eight different researchers have used similar rule table at the distinct time, therefore, represented by single name as FRM-1. The generally used FRM is symmetrical to a diagonal axis (South-West to North-East), with all elements as z and is termed as the z-diagonal.

FRM-2: The rule table proposed by El-Metwally *et al.*, 1996 [44] and Cheng *et al.*, 2003 [45] is also giving the stable response as in Figure 5.4 to the test system with same settling time as in FRM-1 but with different performance indices (PI) as ISE, IAE and ITAE are $4.192\times10^{-5,}$ 0.009084 and 0.05638, respectively. The table is same as in FRM-1, but the element [LN, Z] = LN instead of MN, i.e. slight modification is carried out with respect to FRM-1.

FRM-3: The rule table proposed by Djukanovic et al., 1997 [46] is a table of order 8×7; made the system response unstable as in Figure 5.9. It is neither square nor symmetrical matrix. The ISE, IAE and ITAE observed are 0.6535, 1.7560 and 10.60, respectively. Here, it should be cleared that the system response is forced to be unstable at 2 seconds, while the fault is created at the instant of 5 seconds and cleared at 5.1 seconds. It may be concluded that use of non-square; un-symmetrical rule matrix may render a stable system to behave as an unstable system.

FRM-4: The rule table proposed by Hoang *et al.*, 1996 [47] and Kocaarslan *et al.*, 2005 [48] have been arranged with positive linguistic variables in the left-hand side (LHS) to z-diagonal and negative linguistic variables in the right-hand side (RHS) to the z-diagonal as in Table 5.2, i.e. reverse outputs as in FRM-1 or FRM-2, on simulation, response leads to an unstable system as in Figure 5.9. The ISE, IAE and ITAE observed are 123.70, 57.77 and 1618, respectively as in Table 5.1.

FRM-5: The rule table proposed by Roosta *et al.*, 2010 [49] and Caner *et al.*, 2008 [50] have arranged its axis vertical to the z-diagonal. The LN, MN, N in LHS to z-diagonal and P, MP, LP in RHS to z-diagonal in the vertical axis. It gives the stable response as in Figure 5.5 to the power system. The ISE, IAE and ITAE observed are 4.27×10^{-5}, 0.009604 and 0.06098, respectively, as in Table 5.1.

FRM-6: The rule table proposed by Hasan *et al.*, 1994 [51] is just reversed to FRM-1 and leads not only unstable response, but it leads to make unstable before the fault as in Figure 5.9. The ISE, IAE and ITAE observed are 0.1366, 0.6185 and 4.01, respectively.

FRM-7: Hussein *et al ., 2007* [52], Malik *et al.*, 1995 [53] and Kvasov *et al.*, 2012 [54] have proposed rule table symmetric to the z-diagonal axis. It provides the stable response to

the test system as in Figure 5.4. The ISE, IAE and ITAE observed are 4.192×10^{-5}, 0.009084 and 0.05638 respectively as shown in Table 5.1.

FRM-8: The rule table proposed by Toliyat *et al.*, 1996 [55]; Hsu *et al.*, 1990 [56] and Lakshmi *et al.*, 2000 [57] is a symmetric table to the z-diagonal axis. It leads to the stable response to the test system as in Figure 5.5 with settling time 12.78 seconds. The ISE, IAE and ITAE observed are 4.27×10^{-5}, 0.009604 and 0.06098 respectively as shown in Table 5.1.

FRM-9: The proposed rule table by Sabapathi *et al.*, 2008 [58] and Robandi *et al.*, 2009 [59] is symmetrical to z-diagonal axis and leads to the stable response to the test system as in Figure 5.5. The ISE, IAE and ITAE observed are 4.27×10^{-5}, 0.009604 and 0.06098, respectively as shown in Table 5.1.

FRM-10: The rule table proposed by Hsu *et al.*, 1993 [60] symmetric and gives the stable response to the test system as in Figure 5.5. The ISE, IAE and ITAE observed are 4.27×10^{-5}, 0.009604 and 0.06098, respectively.

FRM-11: The rule table proposed by Chopra *et al.*, 2005 [61] is a matrix of order 9×9 and symmetric to the z-diagonal. It gives stable results but leads to more memory and computational requirements. The ISE, IAE and ITAE observed are 4.188×10^{-5}, 0.009058 and 0.05611, respectively. The corresponding response is shown in Figure 5.4.

FRM-12: Patel *et al.*, 2011 [62], have proposed a rule table of order 8×5, and leads to an unstable response to test system as in Figure 5.9. The ISE, IAE and ITAE observed are 116.50, 55.56 and 1568, respectively.

FRM-13: The rule table proposed by Pasand *et al.*, 1999 [12] is symmetrical to z-diagonal and giving a stable response with settling time 12.78 seconds as in Figure 5.5. The ISE, IAE and ITAE observed are 4.27×10^{-5}, 0.009604 and 0.06098, respectively.

FRM-14: The rule table proposed by Corcau *et al.*, 2007 [63] is symmetrical to the z-diagonal but in reverse pattern of matrix elements, which leads to an unstable response as in Figure 5.9. The ISE, IAE and ITAE observed are 123.70, 57.77 and 1618, respectively.

FRM-15: Gawish *et al.*, 1999 [64], have proposed an unsymmetrical rule table leads to an unstable response as in Figure 5.9. The ISE, IAE and ITAE observed are 29.99, 22.61 and 732.10, respectively.

FRM-16: The rule table proposed by El-Zonkoly *et al.*, 2009 [65] is symmetrical to the z-diagonal except [LP, P] is MP instead of LP and leads to the stable response as in Figure 5.6. The ISE, IAE and ITAE observed are 9.23×10^{-5}, 0.01995 and 0.1508, respectively.

FRM-17: Herron *et al.*, 1994 [66], have proposed a symmetrical rule table with [LN, LN, N, Z, P, LP, LP] in vertical axis leads to a stable response as in Figure 5.6. The ISE, IAE and ITAE observed are 18.49×10^{-5}, 0.03721 and 0.3470, respectively.

FRM-18: The rule table proposed by Rout *et al.*, 2010 [67] and Hosseinzadeh et al., 1999 [68] is symmetrical to z-diagonal leads to a stable response as in Figure 5.7. The ISE, IAE and ITAE observed are 18.49×10^{-5}, 0.03721 and 0.3470, respectively.

FRM-19: The rule table proposed by Elshafei *et al.*, 1997 [69] is symmetrical and gives a stable response to test system as in Figure 5.8. The ISE, IAE and ITAE observed are 18.49×10^{-5}, 0.03721 and 0.3470, respectively.

FRM-20: The rule table proposed by Raouf *et al.*, 2011 [67] is symmetrical and gives stable response to test system as in Figure 5.8. The ISE, IAE and ITAE observed are 18.49×10^{-5}, 0.03721 and 0.3470, respectively.

FRM-21: Renuka *et al.*, 2012 [71], have proposed a symmetrical rule table and gives stable response to the test system as in Figure 5.8. The ISE, IAE and ITAE observed are 18.49×10^{-5}, 0.03721 and 0.3470, respectively.

These FRMs are enlisted in Table 5.1 with the settling time and performance indices as ISE, IAE and ITAE for easy reference. In this table, the FRM-1, 2, 7 and 11 are having similar performance indices and same settling time as 11.11 seconds. The response with proposed FRM is having same settling time but with reduced performance indices value, results, it as the superior to others.

Table 5.1: Performance Indices based comparison of speed response for SMIB System with different Fuzzy Rule Matrices, operated on nominal condition or Plant-6

Category No.	Rule Tables	ISE	IAE	ITAE	Nature of Response	Settling Time (seconds)
1	FRM-1[36-43]	4.192×10^{-05}	0.009084	0.05638	Stable	11.11
	FRM-2[44, 45]	4.192×10^{-05}	0.009084	0.05638		
	FRM-Proposed	**4.188×10^{-05}**	**0.009065**	**0.05622**		
	FRM-7[52-54]	4.192×10^{-05}	0.009084	0.05638		
	FRM-11[61]	4.188×10^{-05}	0.009058	0.05611		
2	FRM-5 [49, 50]	4.27×10^{-05}	0.009604	0.06098	Stable	12.78
	FRM-8 [55-57]	4.27×10^{-05}	0.009604	0.06098		
	FRM-9 [58, 59]	4.27×10^{-05}	0.009604	0.06098		
	FRM-10 [60]	4.27×10^{-05}	0.009604	0.06098		
	FRM-13 [12]	4.27×10^{-05}	0.009604	0.06098		
3	FRM-16 [65]	9.23×10^{-05}	0.01995	0.1508	Stable	17.45
	FRM-17 [66]	0.0001849	0.03721	0.347	Stable	25.42
4	FRM-18 [67, 68]	0.0001849	0.03721	0.347	Stable	23.19
5	FRM-19 [69]	0.0001849	0.03721	0.347	Stable	24.99
	FRM-20 [67]	0.0001849	0.03721	0.347		
	FRM-21 [71]	0.0001849	0.03721	0.347		
6	FRM-3 [46]	0.6535	1.756	10.600	Unstable	∞
	FRM-4 [47, 48]	123.70	57.77	1618.0		
	FRM-6 [51]	0.1366	0.6185	4.0100		
	FRM-12 [62]	116.50	55.56	156800		
	FRM-14 [63]	123.70	57.77	16180		
	FRM-15 [64]	29.99	22.61	732.10		

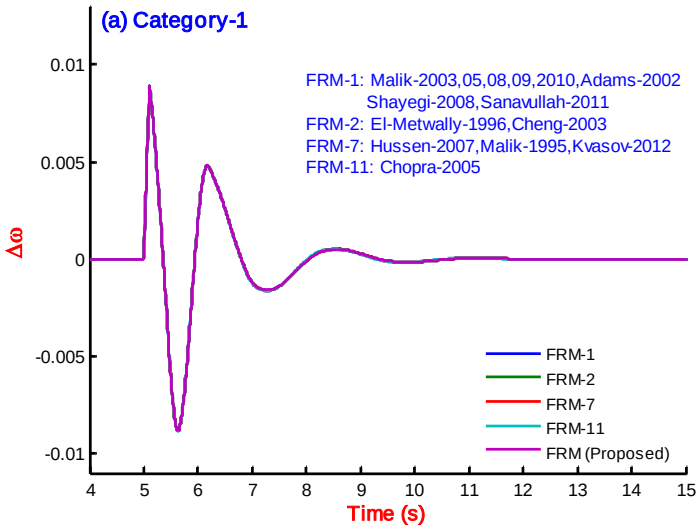

Figure 5.4: Response of system for FRM-1, 2, 7, 11 & Proposed FRM with Settling Time 11.11 seconds

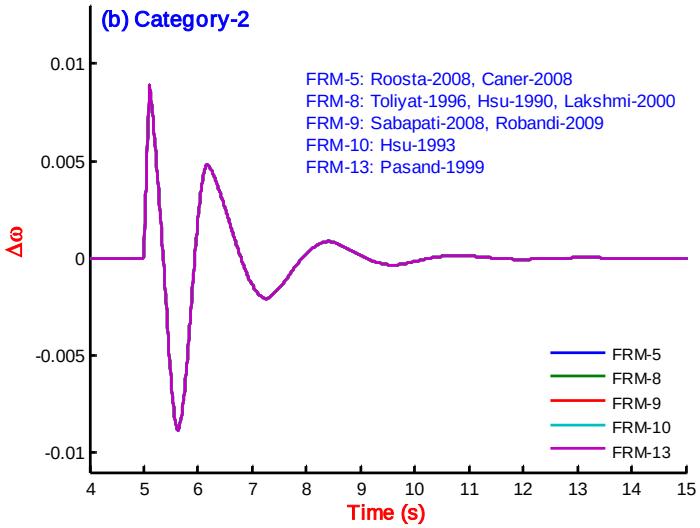

Figure 5.5: Response of system for FRM-5, 8, 9, 10, 13 with Settling Time 12.78 seconds

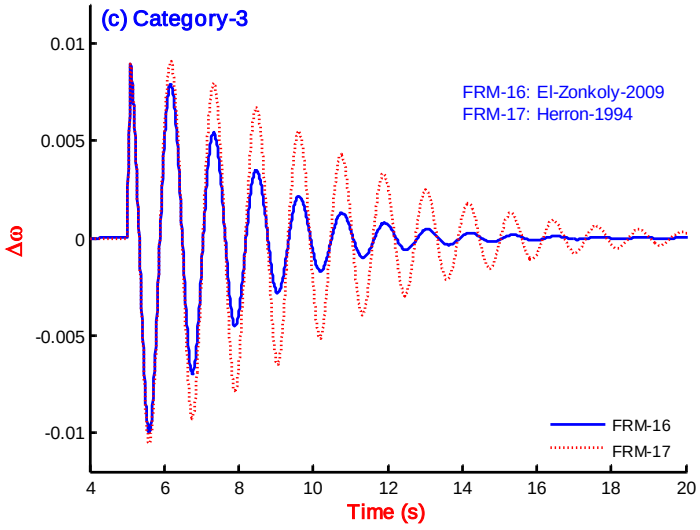

Figure 5.6: Response of system for FRM-16 (red), 17 (blue) with settling time 17.45 and 25.42 seconds, respectively

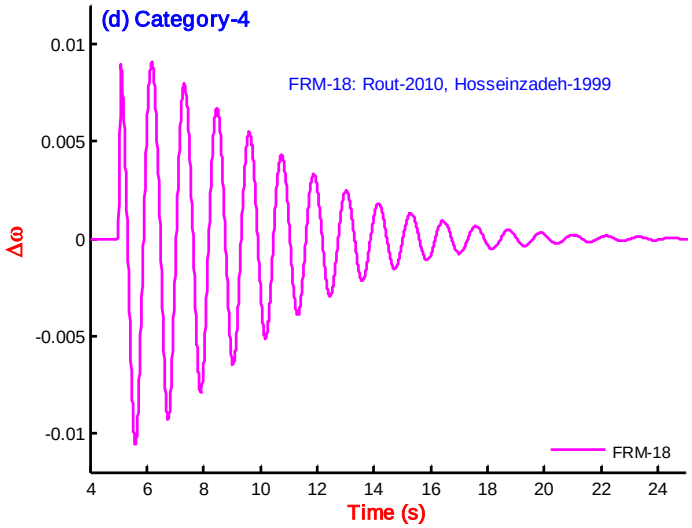

Figure 5.7: Response of system for FRM-18 with settling time 23.19 seconds

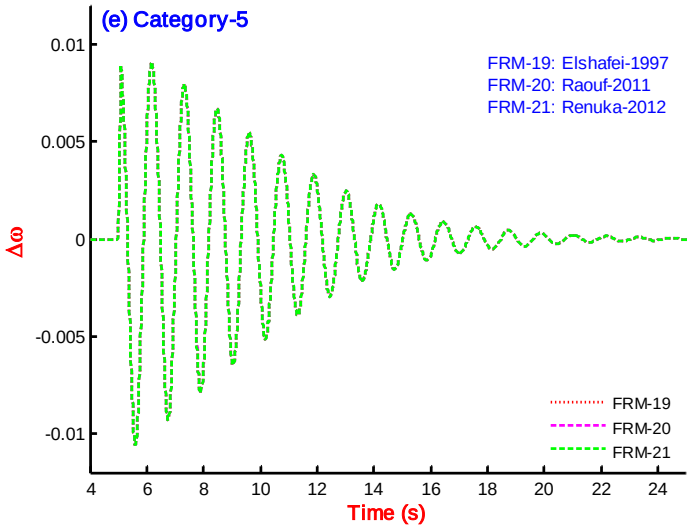

Figure 5.8: Response of system for FRM-19, 20, 21 with settling time 24.99 seconds

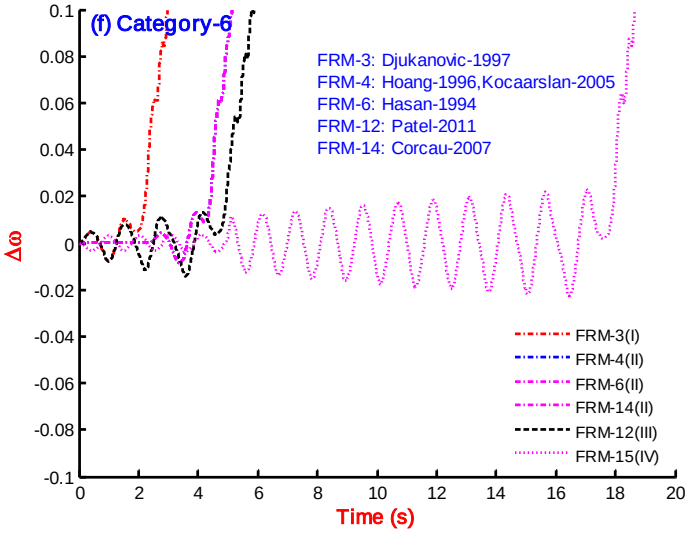

Figure 5.9: Unstable Response of system for FRM-3 (I), FRM-4, 6, 14 (II), FRM-12 (III) & FRM-15 (IV)

The FRM-11 is a rule table of order 9×9, while the proposed FRM and FRM-1, 2, 7 [36-45, 52-54] are of order 7×7. Since, the FRM-1, 2, 7 [36-45, 52-54] are showing best performance as compared with other FRMs reported in literature, therefore, the response with proposed FRM (which outperforms) would be compared to the response with FRM-1, 2, 7 [36-45, 52-54] in forthcoming sections for SMIB, two-area four-machine ten-bus and IEEE New England ten-machine thirty nine-bus power system.

5.4. FRM Design and Justification of Fuzzy Control Rules

The fuzzy control rules can be derived by using heuristic method or deterministic method. In heuristic method, fuzzy control rules are formed by examining the behavioural aspect of a controlled process. These derived fuzzy rules are able to correct the deviation from desired states and able to approach the control requirement of the system. The fuzzy rule derivation relies on the qualitative knowledge of process behaviour and is purely heuristic in nature [292, 293]. In deterministic method, the linguistic structure and/or parameters of the fuzzy control rules are systematically determined to satisfy the control objectives along with the constraints [103, 294, 295]. It is analogous to the conventional controller design by pole placement as described in [293, 296]. In this approach, the low-order linguistic model of a certain open loop system is inverted, but a linguistic inversion mapping is usually incomplete or multi valued. Therefore, an "approximate" strategy, in which heuristic and deterministic process is applied to complete the inverse mapping. It is restricted to low-order systems, but it provides an explicit solution for rule generation of the FLC, where the fuzzy models for an open and closed-loop system are available.

Mamdani and Baaklini [297-299], have introduced a prescriptive algorithm in which the rules are adjusted to getting the system step response within a prescribed band. The method is successful in the considered cases but introduced an added problem of convergence of the adaptive scheme.

Braae and Rutherford [300], have introduced a method for rule justification called as "scale mappings" in which the rules are adjusted for system trajectory termination on a desired state. The rule justification is analogous to the closed-loop system trajectory in a phase plane. The main aspect of the rule justification is to know intuitive feel, overshoot, and rise time by phase plane analysis for a closed-loop system. In this method, a global rule modification in symmetry and monotonicity is also employed. The linguistic trajectory of the system on a "linguistic phase plane”; is tracked to yield approximately the desired trajectory behaviour. The rule modification is carried out by using the linguistic trajectory behaviour to optimize the system response in the linguistic phase plane.

King and Mamdani [292], have introduced useful modifications in rule design. To have global updating of the fuzzy rules is following assumptions are necessary as (a) System symmetry about zero and (b) System monotonicity because, (i) a negative trajectory can be derived from a corresponding positive trajectory and (ii) the control action specified by the fuzzy rules, remain constant or increase with distance from the origin.

5.4.1. Fuzzy rule modification

The method is illustrated by the phase plane and that of the trajectory shown in Figure 5.10 [300] where in the overshoot and settling time are shown for six values of damping factor. It can be noted that the variation in overshoot, and rise time of the system is varied in the given direction of this figure. As in [300], the linguistic phase plane trajectory is similar to phase trajectory as in Figure 5.10. Therefore, to modify the rules of a fuzzy rule table, a similar linguistic phase plane trajectory should be created in the linguistic space. The linguistic trajectory is modified as in Figure 5.10 to modify the fuzzy rules to meet the requirement of overshoot and rise time in the linguistic phase plane [292, 300].

As in Figure 5.10, it is apparently clear that the system rise time should be decreased (i.e. the maximum error derivative should be identified and modified by the trajectory) as in Figure 5.11. It should be noted that the symmetrically positioned rules are altered while that of monotically positioned are ignored as in Figure 5.11(a) and the similar linguistic trajectory as in Figure 5.11(b). On critical observation of Figure 5.11(b) and comparing to Figure 5.10, the system requires rule modification for desired overshoot and rise time. The rule table is slightly modified as in Figure 5.11(c) and linguistic trajectory as in Figure 5.11(d).

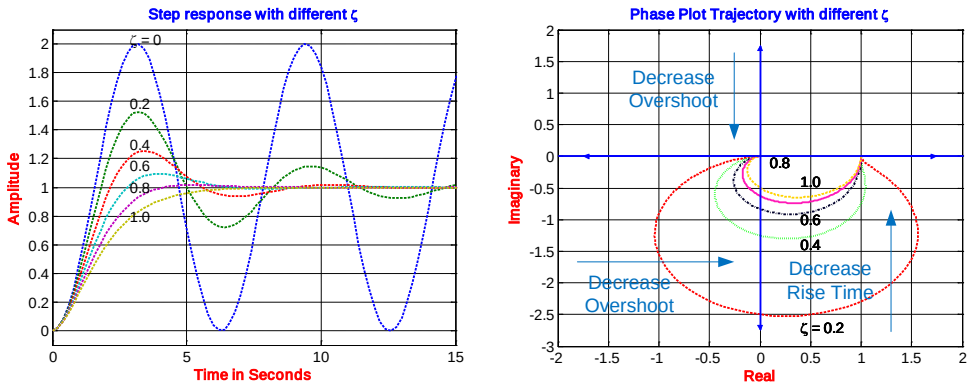

Figure 5.10: Step time response and corresponding phase plane trajectory as proposed in [300]

On a critical comparison of rule table in Figure 5.11(a) and Figure 5.11(c), the rise time is not improved significantly because the derivative error value MP occurs the same number of times in both rule tables. As to improve the system response, further rule modification is required as in

Figure 5.11(e) and corresponding linguistic trajectory in Figure 5.11(f). The final rules as in Figure 5.11(e) are considered to be satisfactory because the overshoot and the rise time both are decreased accordingly.

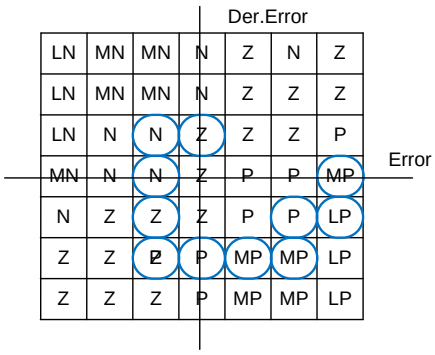

(a) Base Case: FRM

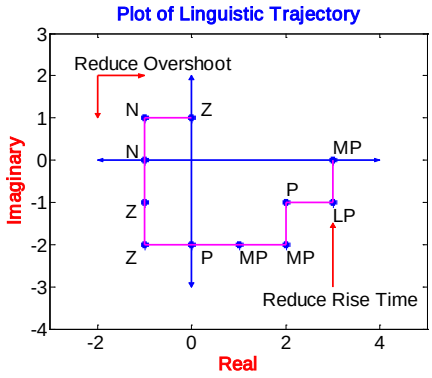

(b) Base Case: Linguistic Phase Plane Trajectory

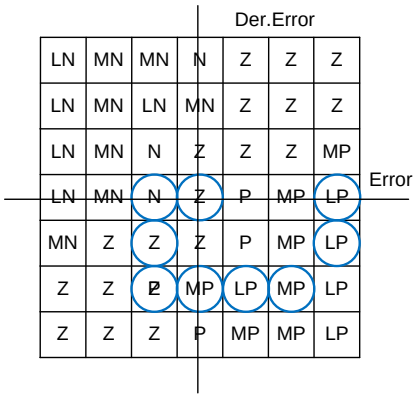

(c) Modified Case-I: FRM

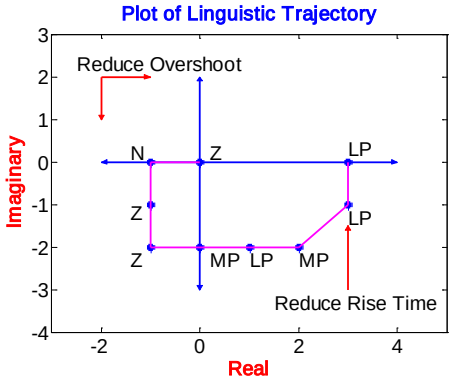

(d) Modified Case-I: Linguistic Phase Plane Trajectory

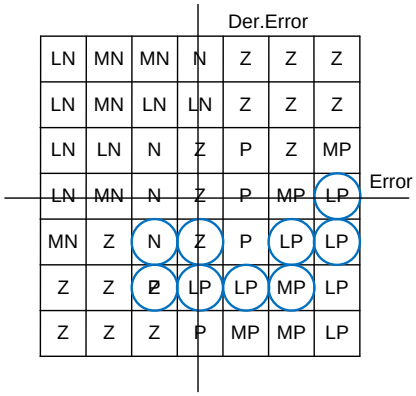

(e) Modified Case-II: FRM

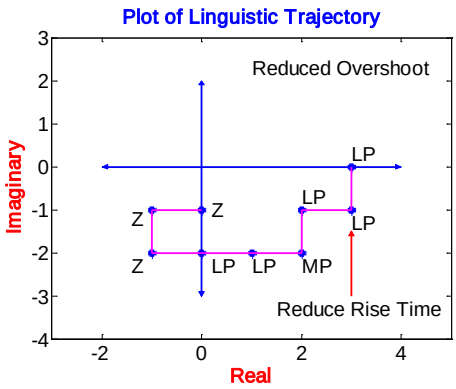

(f) Modified Case-II: Linguistic Phase Plane Trajectory

Figure 5.11: Fuzzy rule table and corresponding Linguistic Phase Plane Trajectory as proposed in [300]

5.4.2. Linguistic trajectory of the category based FRMs

The linguistic phase plane trajectory of the considered fuzzy rule matrix as in Table 5.1, are produced in Figure 5.12. The FRM in category 1, 2, 3, 4, 5 is produced in Figure 5.12 (a) - Figure

5.12 (f). On critical examination & comparison of these trajectories with the phase plane response as in Figure 5.10(b) and corresponding time response of Figure 5.10(a); this system is stable. On the contrary, FRM in category-6, are not having any type of linguistic closed phase plane trajectory.

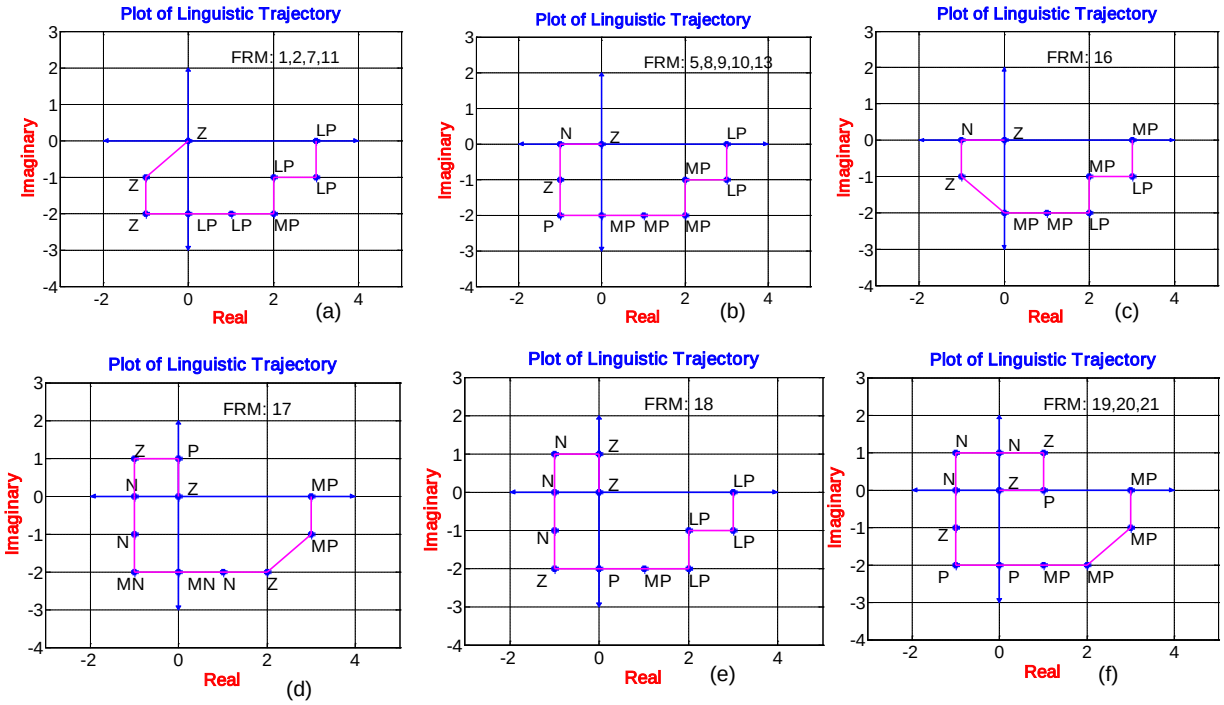

Figure 5.12: Plot of Linguistic Phase Plane Trajectory, (a) for FRM-1,2,7,11, (b) for FRM-5,8,9,10,13, (c) for FRM-16, (d) for FRM-17, (e) for FRM-18 and (f) for FRM-19,20,21.

5.4.3. Proposed fuzzy rule matrix

The analysis with previously published FRM-1 to 21 in section 5.3 and the experiment carried out with different FRMs with the distinct number of linguistic variables, may lead to derive empirical steps in the design of a fuzzy rule matrix as following.

Step-1: The FRM should have z-diagonal [Z, Z, Z, Z, Z, Z, Z] as shown in Table 5.2.

Step-2: If the error and derivative of error linguistic variables (LV) are arranged as [LN, MN, N, Z, P, MP, LP] produced in Table 5.3. To have a stable response, the FRM should have all negative linguistic variables in the left-hand side (LHS) region, and all positive linguistic variables should be in the right-hand side (RHS) region as in a majority of stable rule tables in section 5.3. It can be noted that the FRM - 4, 6, 14 having reverse arrangement of linguistic variables are forcing system response to be unstable. Therefore, an FRM should not have reverse arrangement of linguistic variables to guarantee stability aspects of the power system stabilizer.

Step-3: The stable FRM should have LHS and RHS elements, symmetrical to the z-diagonal but as in point 2 or as in Table 5.2. The diagonal elements arranged in the axis vertical to a z-

diagonal plays a deterministic role as shown in Table 5.2. In FRM-5, 19, 20, 21, the elements are [LN, MN, N, Z, P, MP, LP]. In FRM-1, 2, 7, 16 and 18, the elements are [LN, LN, MN, Z, MP, LP, LP] while in FRM-8, 9, 10, 13, 15 and 17, the elements are [LN, LN, N, Z, P, LP, LP].

Step-4: The number of linguistic variables for error and derivative of error should be same and an odd number to have a symmetrical square matrix for output rule table otherwise; the ability of FPSS would be deteriorated and may lead to worsen performance. The number may be 3, 5, 7 and 9 such as to have an adjustment between accuracy and complexity / memory requirement. It can be observed that the FRM-3 is having order of 7×8 and FRM-12 with an order as 8×5 i.e. non-square / non-symmetric matrix gives an unstable response.

Step-5: The proposed New Fuzzy Rule Matrix is shown in Table 5.3. The elements are arranged in symmetry. The left side of the Z-diagonal elements is as N, MN, LN, while right-side elements are as P, MP, and LP except the elements in vertical axis. It is notable that the arrowed left-side elements to Z-diagonal (i.e. axis vertical to the z-diagonal) are kept as LN while the arrowed diagonal right-side elements to Z-diagonal are kept as LP. The performance of the system is similar to the FRM-1, 2, 7 as the settling time is same but with improved performance indices. The ISE, IAE and ITAE observed are 4.188×10^{-5}, 0.009065 and 0.05622, respectively and found to be lowest for the proposed FRM with respect to available FRMs.

The performance of the proposed FRM is evaluated for SMIB power system, two-area four-machine ten-bus and IEEE New England ten-machine thirty nine-bus power system in section 5.5 - 5.7, respectively.

Table 5.2: Symmetrical Rule Table

Acc / Speed	LN	MN	N	Z	P	MP	LP
LN							Z
MN						Z	
N					Z		
Z				Z			
P			Z				
MP		Z					
LP	Z						

Verticle to z-diagonal

Z-diagonal

LHS should have LN, MN, N

RHS should have P, MP, LP

Table 5.3: Proposed input-output fuzzy rule matrix

Acceleration → Speed deviation ↓	LN	MN	N	Z	P	MP	LP
LN	LN	LN	LN	MN	MN	N	Z
MN	LN	LN	MN	MN	N	Z	P
N	LN	MN	LN	N	Z	P	MP
Z	MN	MN	N	Z	P	MP	MP
P	MN	N	Z	P	LP	MP	LP
MP	N	Z	P	MP	MP	LP	LP
LP	Z	P	MP	MP	LP	LP	LP

5.5. Simulation Results and Discussion: SMIB System

5.5.1. Speed response comparison

To examine performance of the SMIB power system under nonlinear mode by creating fault at 5 seconds and persistent for 0.1 seconds is carried out with a wide range of operating conditions, resulting distinct plant configurations. The system with unlike combinations of different active power and transmission line reactance as in Table 2.2 (eight different plants) and system data as in Table A.1 is considered for nonlinear simulations. Such obtained eight-plants (covering wide range of operating conditions) are examined for the speed response with FPSS (category-1) [36-45, 52-54], FPSS (category-2) [12, 49, 50, 55-60] and FPSS (proposed) in this section. An SIMULINK based block diagram, including all the nonlinear blocks is generated in MATLAB Software.

The comparing Fuzzy logic based PSS (FPSS) is considered as in [21]. The number of linguistic variables is five as LN (large negative), MN (medium negative), Z (zero), MP (medium positive) and LP (large positive). The input signals to FLC are considered as change in speed ($\Delta\omega$) and acceleration (Δa), while that the output signal is considered as correction voltage (ΔV_{pss}). The corresponding 49 rule base is represented in Table 5.3 In the design of FPSS; triangular type membership function is considered for both input and output signals. The crisp value is obtained using centroid type defuzzification method.

The Simulink model of SMIB system is prepared in MATLAB Software with FPSS (category-1) [36-45, 52-54], FPSS (category-2) [12, 49, 50, 55-60] and FPSS (Proposed) and simulations are carried out for all eight plants as created in Table 2.2. The speed response of the SMIB power system equipped with FPSS (category-1) [36-45, 52-54], with FPSS (category-2) [12, 49, 50, 55-60] and with FPSS (Proposed) for plant-6 (Table 2.2) are observed and presented

in Figure 5.13. The SMIB power systems equipped with FPSS (proposed) are simulated for eight plant conditions, and speed response is shown in Figure 5.14.

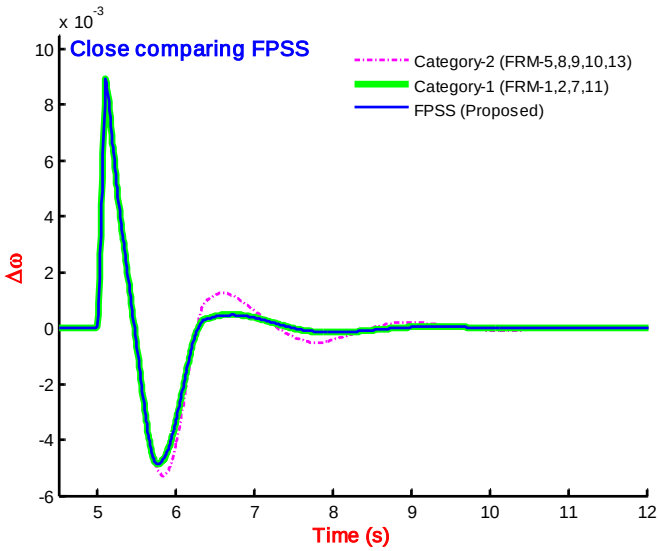

Figure 5.13: Speed response of SMIB power system with close comparing FPSS as in Category-1, Category-2 and FPSS (Proposed)

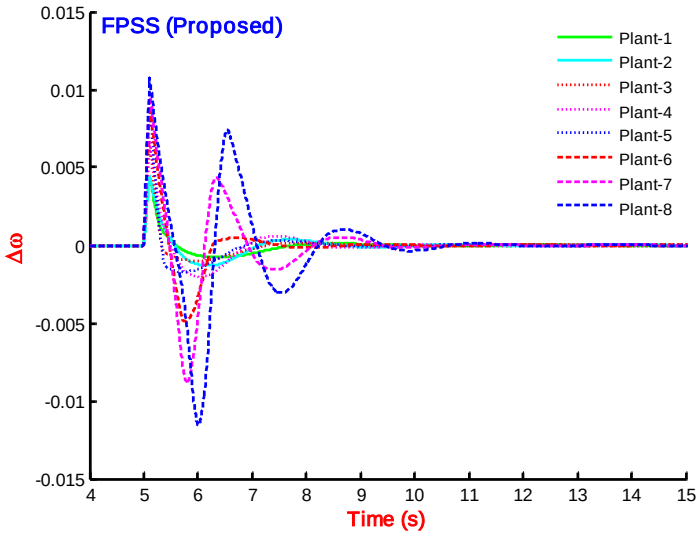

Figure 5.14: Speed response of SMIB power system with close comparing FPSS

5.5.2. PI based performance comparison

The simulation carried out on the SMIB power system with FPSS (Category-2), FPSS (Category-1) [36-45, 52-54] and FPSS (Proposed) for all plant conditions (Table 2.2) and the consecutive performance indices (ITAE, IAE and ISE) are recorded as in Table 5.4. Whenever graphical representation of responses is not differentiable then a quantitative value in terms of performance indices is needed. As the lower value of PI, represents the superior performance of the system with reduced settling time and overshoots. In this table, the value of PIs with FPSS (Proposed) is lesser as compared to others, resulting good performance, i.e. the small signal stability is improved as compared to others.

Table 5.4: Performance indices based comparison of speed response due to close comparing FPSS (Category-1), FPSS (Category-2) and FPSS (Proposed)

Fuzzy PSS	ITAE	IAE	ISE	ITAE	IAE	ISE
	Plant-1			Plant-2		
FRM-5,8,9,10,13	0.0139	0.0023	3.3715×10^{-06}	0.0207	0.0032	5.0300×10^{-06}
FRM-1,2,7	0.0132	0.0022	3.1745×10^{-06}	0.0179	0.0029	4.4550×10^{-06}
FRM Proposed	0.0132	0.0021	3.1652×10^{-06}	0.0178	0.0029	4.4302×10^{-06}
	Plant-3			Plant-4		
FRM-5,8,9,10,13	0.0157	0.0027	6.2253×10^{-06}	0.0287	0.0046	1.0775×10^{-05}
FRM-1,2,7	0.0148	0.0025	5.9284×10^{-06}	0.0245	0.0040	9.4724×10^{-06}
FRM Proposed	0.0148	0.0025	5.9149×10^{-06}	0.0243	0.0040	9.4134×10^{-06}
	Plant-5			Plant-6		
FRM-5,8,9,10,13	0.0218	0.0037	1.1747×10^{-05}	0.0367	0.0061	2.3809×10^{-05}
FRM-1,2,7	0.0203	0.0035	1.1117×10^{-05}	0.0284	0.0049	2.0975×10^{-05}
FRM Proposed	0.0202	0.0035	1.1098×10^{-05}	0.0282	0.0049	2.0911×10^{-05}
	Plant-7			Plant-8		
FRM-5,8,9,10,13	0.0661	0.0103	4.8190×10^{-05}	0.0963	0.0146	8.5088×10^{-05}
FRM-1,2,7	0.0596	0.0096	4.5974×10^{-05}	0.0922	0.0141	8.2756×10^{-05}
FRM Proposed	0.0594	0.0095	4.5908×10^{-05}	0.0921	0.0141	8.2679×10^{-05}

5.6. Simulation Results and Discussion: Four-Machine Power System

5.6.1. Speed response comparison

The two-area four-machine ten-bus power system is described in section 2.3.2 without PSS, and the creations of system models based on operating conditions are elaborated in section 2.3.2.1. The FPSS (category-2) [12, 49, 50, 55-60], FPSS (category-1) [36-45, 52-54, 61] and FPSS (proposed) designed in section 5.4 is connected to the system and simulation carried out for the speed response. In each plant condition as listed in Table 2.4 is considered with fault location as given in Table A.5. The disturbance is considered as self-clearing at different buses at 1.0 second and cleared after 0.05 second. Referring to section 2.3.2.2 and section 2.3.2.3, wherein the simulation and eigenvalue analysis with eight plant conditions without PSS are described and found that none of the generators of plants are showing stable operation; therefore, not needed to compare to the simulation results. As a sample, the speed response of Gen-1 – Gen-4 for plant-2 is compared with FPSS (category-2), FPSS (category-1) and FPSS (proposed) in Figure 5.15 - Figure 5.18. The performance with proposed FPSS clearly outperforms that of with FPSS (category-2), but quite similar to that of with FPSS (category-1). The performance of the system with proposed FPSS and FPSS (category-1) can be differentiated by PI based analysis.

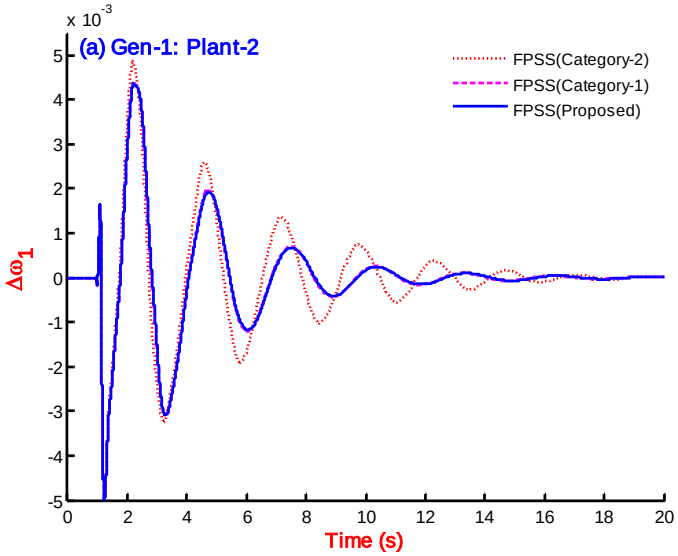

Figure 5.15: Speed response for Gen-1 of Plant-2 with FPSS (Category-1), FPSS (Category-2) and FPSS (Proposed)

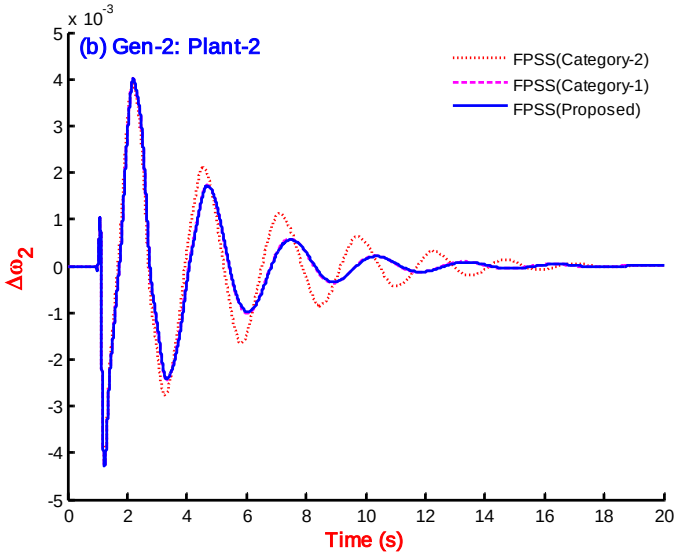

Figure 5.16: Speed response for Gen-2 of Plant-2 with FPSS (Category-1), FPSS (Category-2) and FPSS (Proposed)

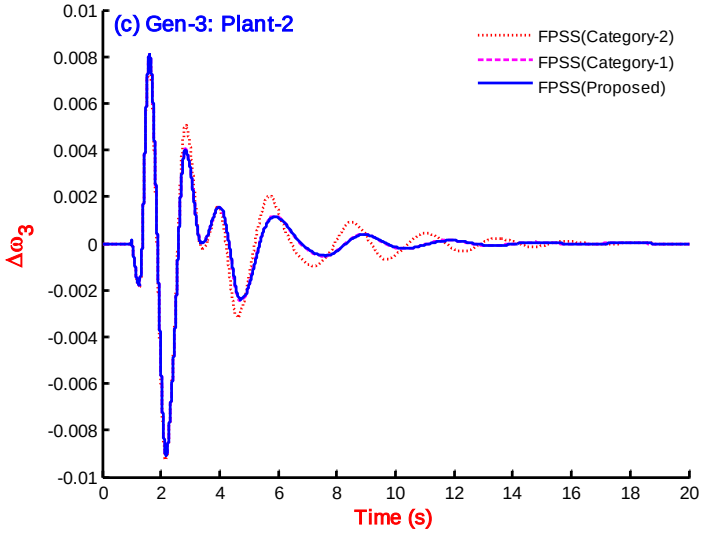

Figure 5.17: Speed response for Gen-3 of Plant-2 with FPSS (Category-1), FPSS (Category-2) and FPSS (Proposed)

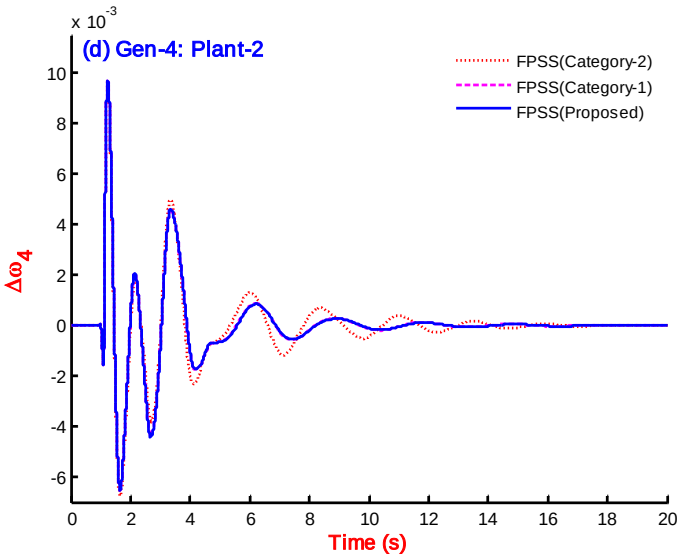

Figure 5.18: Speed response for Gen-4 of Plant-2 with FPSS (Category-1), FPSS (Category-2) and FPSS (Proposed)

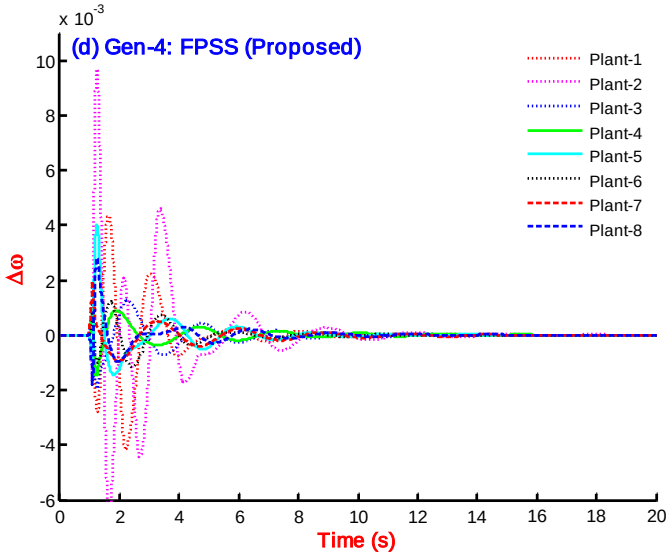

Figure 5.19: Speed response of Gen-4 for eight plant conditions with FPSS (Proposed)

Simulation study on the system with proposed FPSS has been carried out for all eight plant conditions (Table 2.4) to examine robust performance with the system. As a sample, the response of the system with proposed FPSS for Gen-4 with eight plant conditions is shown in Figure 5.19 and response for other generators is not shown because of space constraint.

5.6.2. PI based speed performance comparison

To evaluate the robustness of the proposed FPSS, simulation is carried out for all eight plant configurations which represent the wide range of operating conditions and system configurations. The system is simulated FPSS (category-2) [12, 49, 50, 55-60], FPSS (category-1) [36-45, 52-54] and FPSS (proposed) for comparison purpose with eight plant conditions. Each time the

performance indices (ITAE, IAE and ISE) are recorded and enlisted in Table 5.5. Since the system possesses four generators, therefore, the PI values in this table are the sum of PIs of individual four generators. Comparatively lower value of PI refers to better performance. It is clear from this table, that the performance of the system is enhanced by using proposed FPSS (Proposed) as compared to other controllers.

Table 5.5: Performance indices based comparison of speed response due to close comparing FPSS (Category-1), FPSS (Category-2) and FPSS (Proposed)

Fuzzy PSS	ITAE	IAE	ISE	ITAE	IAE	ISE
	Plant-1			Plant-2		
FRM-5,8,9,10,13	0.1452	0.0316	5.4832×10^{-05}	0.2614	0.0573	1.6153×10^{-04}
FRM-1,2,7	0.0778	0.0233	4.6248×10^{-05}	0.1816	0.0475	1.4384×10^{-04}
FRM (Proposed)	0.0760	0.0231	4.5996×10^{-05}	0.1793	0.0472	1.4331×10^{-04}
	Plant-3			Plant-4		
FRM-5,8,9,10,13	0.1209	0.0248	2.5539×10^{-05}	0.0478	0.0143	1.2477×10^{-05}
FRM-1,2,7	0.0604	0.0171	1.8666×10^{-05}	0.0474	0.0132	1.1329×10^{-05}
FRM (Proposed)	0.0587	0.0168	1.8456×10^{-05}	0.0472	0.0131	1.1294×10^{-05}
	Plant-5			Plant-6		
FRM-5,8,9,10,13	0.0995	0.0223	2.3128×10^{-05}	0.0696	0.0156	1.2589×10^{-05}
FRM-1,2,7	0.0628	0.0168	1.7507×10^{-05}	0.0367	0.0113	1.0234×10^{-05}
FRM (Proposed)	0.0615	0.0166	1.7306×10^{-05}	0.0357	0.0111	1.0156×10^{-05}
	Plant-7			Plant-8		
FRM-5,8,9,10,13	0.0584	0.0154	1.1742×10^{-05}	0.0414	0.0116	8.0938×10^{-06}
FRM-1,2,7	0.0574	0.0148	9.3167×10^{-06}	0.0407	0.0111	6.8588×10^{-06}
FRM (Proposed)	0.0508	0.0148	9.2321×10^{-06}	0.0375	0.0110	6.8405×10^{-06}

5.7. Simulation Results and Discussion: Ten-Machine Power System

The IEEE New England ten-machine thirty nine-bus power system is described in section 2.3.3 without PSS, and the creations of system models based on operating conditions are elaborated in section 2.3.3.1. In each plant condition as listed in Table 2.6 - Table 2.7 are considered with fault location as given in Table A.8. The disturbance is considered as self-clearing at different buses at 1.0 second and cleared after 0.05 second. Referring to section 2.3.3.2 and section 2.3.3.3, wherein the simulation and eigenvalue analysis with eight plant conditions are considered under no-PSS is described and found that none of the generators of plants are showing stable operation; therefore, not needed to compare to the simulation results.

An SIMULINK based block diagram, including all the nonlinear blocks is generated [191]. The speed signals of the machines are considered as output and the initial value of the speed is taken as zero. The output signals of CPSSs are added to V_{ref} via limiters. It is used to damp out the

small signal disturbances via modulating the generator excitation. The output must be limited to preventing the PSS acting to counter action of AVR. Different operating points are taken as the unlike plants for both systems. The limits of PSS outputs are taken as ± 0.05. In decentralized PSS, to activate the proposed controller at same instant, proper synchronization signal is required to be sent to all machines. All PSSs can be applied simultaneously to the respective machines for both power system models.

5.7.1. Speed response comparison

Graphical representation of speed response for New England system with FPSS (category-2), FPSS (category-1) and FPSS (proposed) are carried out by simulation of nonlinear plant-4 configurations (Table 2.6 - Table 2.7). Speed response is recorded and compared and shown only for Gen-4, Gen-6 and Gen-7 in Figure 5.20, Figure 5.21 and Figure 5.22, respectively. In each figure of simulation study, the response with FPSS (proposed) is superior as compared to the response with FPSS (category-2) [12, 49, 50, 55-60]. The settling time and the overshoot of the speed response with proposed FPSS are greatly improved as compared to that of with FPSS (category-2). The response with FPSS (category-1) [36-45, 52-54] is closely related to that of with FPSS (proposed). To distinguish the degree of performance, the performance indices of speed response are to be recorded in next section. The system response with proposed FPSS is carried for all plant conditions but shown only for Gen-2, Gen-4, Gen-8 and Gen-10 in Figure 5.23, Figure 5.24, Figure 5.25 and Figure 5.26, respectively because of space constraints.

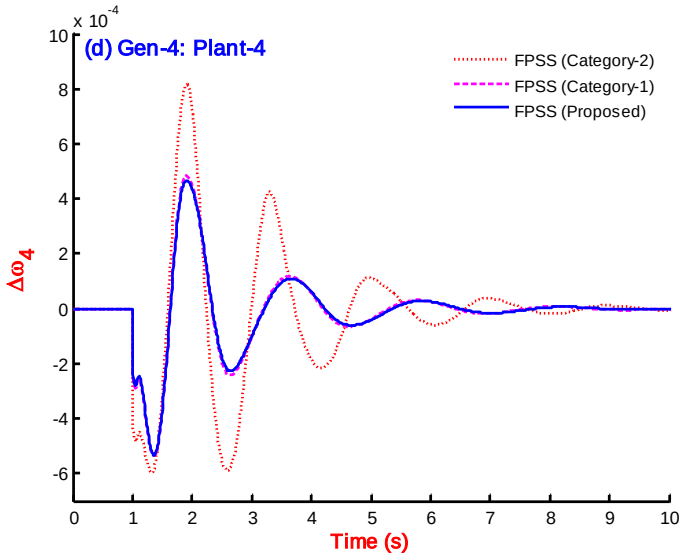

Figure 5.20: Speed response of Gen-4 for Plant-4 with FPSS (Category-2), FPSS (Category-1) and FPSS (Proposed)

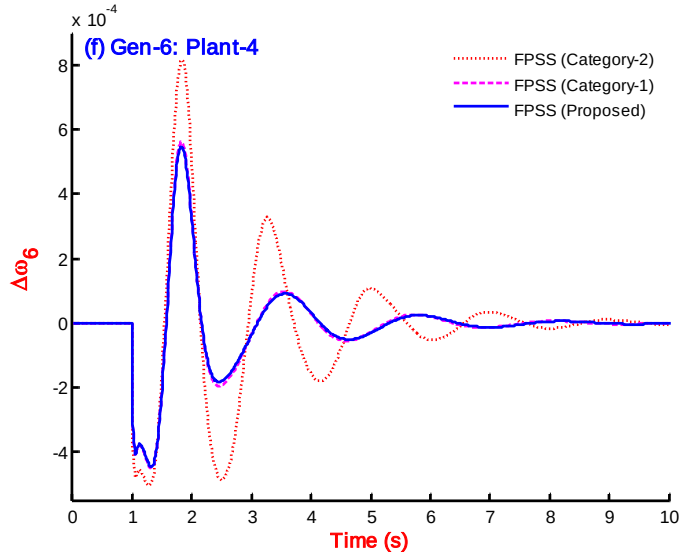

Figure 5.21: Speed response of Gen-6 for Plant-4 with FPSS (Category-2), FPSS (Category-1) and FPSS (Proposed)

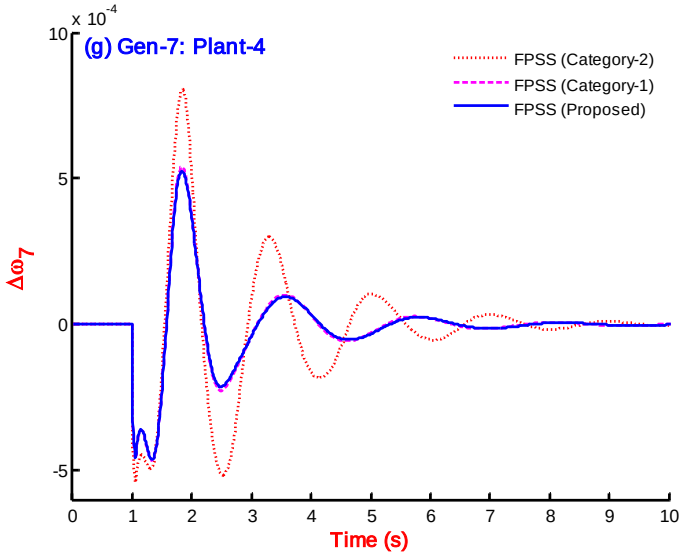

Figure 5.22: Speed response of Gen-7 for Plant-4 with FPSS (Category-2), FPSS (Category-1) and FPSS (Proposed)

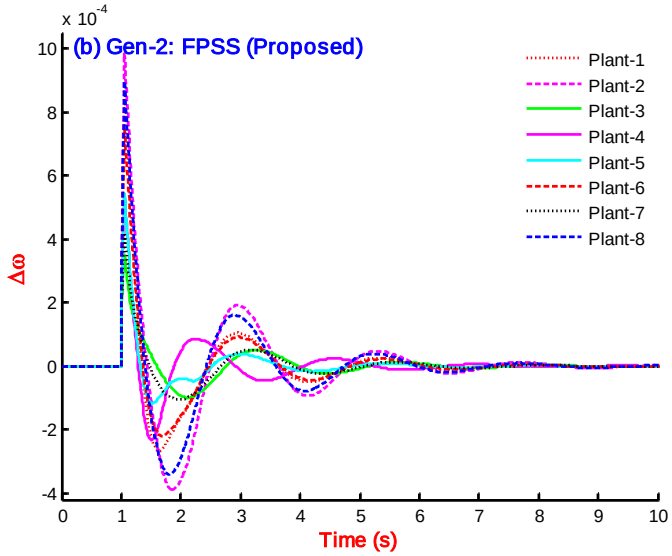

Figure 5.23: Speed response of Gen-2 for eight plants with FPSS (Proposed)

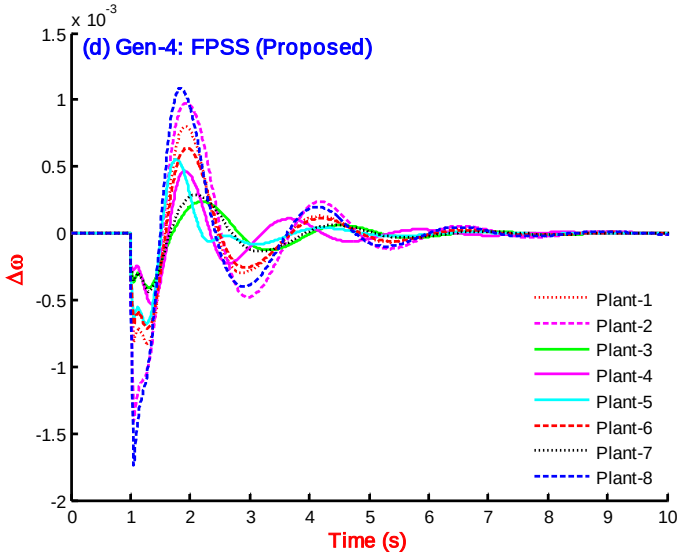

Figure 5.24: Speed response of Gen-4 for eight plants with FPSS (Proposed)

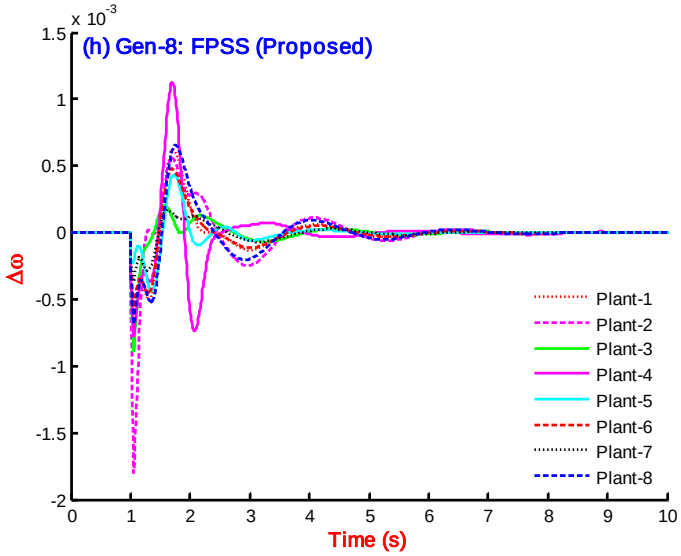

Figure 5.25: Speed response of Gen-8 for eight plants with FPSS (Proposed)

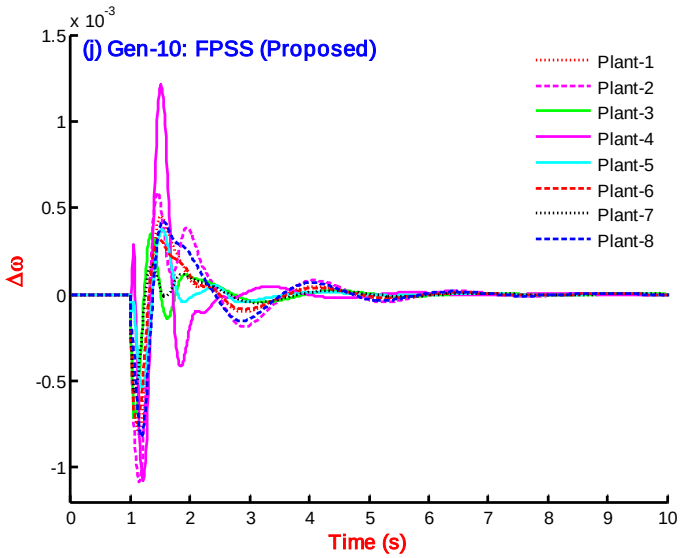

Figure 5.26: Speed response of Gen-10 for eight plants with FPSS (Proposed)

5.7.2. PI based speed response analysis

To evaluate the robustness of the proposed FPSS, simulation is carried out for all eight plant configurations which represent the wide range of operating conditions and system configurations. The system is simulated with FPSS (category-1) [36-45, 52-54] and with FPSS (category-2) [12, 49, 50, 55-60] for comparison purpose with eight plant conditions. Each time the performance indices (ITAE, IAE and ISE) are recorded and enlisted in Table 5.6. Since the system possesses ten generators, therefore, the entries in this table are the sum of respective PIs of ten generators. Comparatively lower value of PI refers to better performance. It is clear from this table, that the performance of the system is enhanced by using proposed FPSS (Proposed) as compared to performance with FPSS (category-1) and with FPSS (category-2). The value of PIs (ITAE, IAE and ISE) with proposed FPSS is improved in the range of 23.19% - 43.85%, 20.37% - 31.39% and 14.32% - 35.91%, respectively as compared to that of with FPSS (category-2). Similarly, the PIs are enhanced in the range of 0.21% - 1.96%, 0.79% - 1.37% and 0.59% - 1.80%, respectively as compared to that of with FPSS (category-1).

It could be easy to say that the performance with proposed FPSS is greatly improved as compared to that of with FPSS (category-2), while it is slightly enhanced as compared to that of with FPSS (category-1). Since, only methodology, to design fuzzy rule table pertains to FPSS (category-2), therefore, the proposed methodology is far better than proposed in [12].

Table 5.6: Performance indices based comparison of speed response with FPSS (category-2), FPSS (Category-1) and FPSS (Proposed) for eight plant conditions.

Fuzzy PSS	ITAE	IAE	ISE	ITAE	IAE	ISE
	Plant-1			Plant-2		
FRM-5,8,9,10,13	0.03532	0.01596	1.0589×10^{-05}	0.04645	0.01877	1.1598×10^{-05}
FRM-1,2,7	0.02392	0.01236	8.4128×10^{-06}	0.03416	0.01507	8.5598×10^{-06}
FRM Proposed	0.02360	0.01222	8.3233×10^{-06}	0.03394	0.01495	8.4324×10^{-06}
	Plant-3			Plant-4		
FRM-5,8,9,10,13	0.01765	0.00858	2.3612×10^{-06}	0.03116	0.01442	1.2250×10^{-05}
FRM-1,2,7	0.01151	0.00640	1.5855×10^{-06}	0.01885	0.01051	1.0396×10^{-05}
FRM Proposed	0.01148	0.00635	1.5598×10^{-06}	0.01848	0.01036	1.0332×10^{-05}
	Plant-5			Plant-6		
FRM-5,8,9,10,13	0.02114	0.01136	8.1754×10^{-06}	0.03222	0.01440	7.9397×10^{-06}
FRM-1,2,7	0.01342	0.00866	7.0461×10^{-06}	0.02067	0.01078	5.9421×10^{-06}
FRM Proposed	0.01318	0.00856	7.0048×10^{-06}	0.02038	0.01065	5.8676×10^{-06}
	Plant-7			Plant-8		
FRM-5,8,9,10,13	0.02131	0.00967	3.0105×10^{-06}	0.04025	0.01709	1.0968×10^{-05}
FRM-1,2,7	0.01211	0.00672	1.9646×10^{-06}	0.02940	0.01366	8.3914×10^{-06}
FRM Proposed	0.01196	0.00664	1.9293×10^{-06}	0.02913	0.01353	8.2817×10^{-06}

5.8. Conclusions

In this chapter, a fuzzy logic based power system stabilizer is designed with a new rule table, and the performance is evaluated for three systems such as single-machine infinite-bus power system (SMIB), two-area four-machine ten-bus power system and IEEE New England ten-machine thirty nine-bus power systems.

The SMIB power system equipped with FPSS (category-1) [36-45, 52-54], FPSS (category-2) [12, 49, 50, 55-60] and FPSS (proposed) are simulated for eight plant conditions and consequently; the speed response of the system for different plants is compared. The performance indices with FPSS (Proposed) are improved as compared to others. Similarly, the two multimachine power systems, equipped with FPSS (category-1) [36-45, 52-54], FPSS (category-2) [12, 49, 50, 55-60] and FPSS (proposed) in the decentralized manner and simulated for eight plant conditions; recorded performance indices (ITAE, IAE and ISE) value reveals superiority of the proposed FPSS performance in both cases.

The performance of speed response is recorded in terms of performance indices (ITAE, IAE and ISE) for a system equipped with proposed FPSS, with FPSS (category-1) and with FPSS (category-2).

In case of the SMIB power system, the value of PIs (ITAE, IAE and ISE) with proposed FPSS is improved in the range of 4.65% - 30.22%, 3.39% - 23.90% and 2.91% - 13.86%, respectively as compared to that of with FPSS (category-2). Similarly, the PIs are enhanced in the range of 0.16% - 0.78%, 0.12% - 0.63% and 0.09% - 0.31%, respectively as compared to that of with FPSS (category-1).

Sanaye-Pasand and Malik, 1999/2010[12] have proposed a standardized rule table for FPSS design, and the performance of speed response has been recorded in terms of ISE. The such designed NFPSS (FPSS with standardized rule table) has reported 1% enhancement of ISE performance index as compared to FPSS (category-2). On the other hand, the proposed FPSS has enhanced ISE in the range of 2.91% - 13.86%; which is much higher than that of with NFPSS [12].

In case of the two-area four-machine ten-bus power system, the value of PIs (ITAE, IAE and ISE) with proposed FPSS is improved in the range of 1.27% - 105.96%, 9.16% - 47.62% and 10.47% - 38.38%, respectively as compared to that of with FPSS (category-2). Similarly, the PIs are enhanced in the range of 0.42% - 12.99%, 0.10% - 1.80% and 0.27% - 1.16%, respectively as compared to that of with FPSS (category-1).

In case of the IEEE New England ten-machine thirty nine-bus power system, the value of PIs (ITAE, IAE and ISE) with proposed FPSS is improved in the range of 23.19% - 43.85%, 20.37% - 31.39% and 14.32% - 35.91%, respectively as compared to that of with FPSS (category-

2) [12, 49, 50, 55-60]. Similarly, the PIs are enhanced in the range of 0.21% - 1.96%, 0.79% - 1.37% and 0.59% - 1.80%, respectively as compared to that of with FPSS (category-1).

It could be easy to say that the performance with proposed FPSS is greatly improved as compared to that of with FPSS (category-2), while it is slightly enhanced as compared to that of with FPSS (category-1). Since, only methodology, to design fuzzy rule table pertains to FPSS (category-2), therefore, the proposed methodology is far better than proposed in [12].

Chapter 6

DESIGN OF INTERVAL TYPE-2 FUZZY LOGIC BASED POWER SYSTEM STABILIZER

In this chapter, the evaluation and performance analysis of an interval type-2 fuzzy logic controller (IT2 FLC) as a power system stabilizer (PSS) is carried out. The single machine infinite bus (SMIB) system is considered for evaluation and implementation of IT2 FLC as PSS. The input signals to the controller are considered as speed deviation & acceleration. The evaluation of the controller is considered with 20 separate types of membership functions (MFs) and treated as IT2 FPSS on SMIB system to evaluate the performance of each. The performance of these Muffs is evaluated graphically as well as in terms of ISE, IAE & ITAE as the performance index. The better suitable MF in design of IT2 FPSS is decided out of considered 20 MFs. The selected MF based IT2 FPSS is tested for small signal performance analysis of an SMIB system with wide operating conditions on a power system. The performance with IT2 FPSS is compared against the performance of the power system without PSS & with conventional PSS. The application of IT2 FPSS is extended to two-area four-machine ten-bus and IEEE New England ten-machine thirty nine-bus power system and speed response comparison is carried out with FPSS. The superiority of performance with IT2 FPSS over type-1 FPSS is validated in terms of ITAE, IAE and ISE.

6.1. Introduction

Electrical power systems (EPSs) are large, interconnected and complex; it generally consists of generating units; transmission lines and load centres are prone to disturbances of temporary or permanent in nature and may result to occur small signal oscillations. These small signal oscillations (SSOs) are of low in magnitude and frequency within the range of 0.2-3.0 Hz. Most of SSOs may be damped out but some of them may persist for a while, grow gradually and result to system separation. The EPS stability is to control excitation of the generator by mean of an automatic voltage regulator (AVR). However, the EPS is dynamically complicated, which often confront with the changes of operating conditions and disturbances.

To enhance dynamic performance, i.e. to provide fast damping to power system, a supplementary control signal in the excitation system to a generating unit can be used. As cheap, simple, easy to install; a power system stabilizer (PSS) has been widely used to suppress the SSOs and to improve dynamic stability of EPS. The most popular structure of PSS is a lead-lag type (phase compensator), whose gain and pole-zeros are determined using linear control theory with a

linearized dynamic model of EPS. The PSS parameter adjustment and damping controller design are reported as root locus and sensitivity analysis method [301], pole placement [302] and robust control [303]. The design of PSS with these techniques depends on linearized model and certain nominal operating conditions. Moreover, such designed PSS shows degraded performance of other operating conditions in case of large disturbances. Intelligent optimization based methods have been adopted to design PSS parameters such as genetic algorithm (GA) [144, 246, 304], Tabu search (TS) [20, 236], simulated annealing (SA) [9, 138], differential evolution (DE) [23], particle swarm optimization (PSO) [92, 149, 224, 245, 304], evolutionary programming (EP) [21], gravitational search algorithm (GSA) [305, 306], artificial bee colony algorithm (ABC) [307, 308], artificial neural network (ANN) based PSS design methods used the gradient algorithm for learning its parameter either with input/output data [193, 309] or on-line at different operating points of the power system..

Fuzzy logic based power system stabilizer (FPSS) has been developed to improve dynamic stability and adapt to changes when the system operation drifts as a result of continuous load changes or unpredictable major disturbances such as three-phase fault. The performance of FPSS outperforms CPSS for improving the stability of the power system. The FPSS uses the human expert knowledge to design its prominent rule base, which usually consists of uncertainties to a certain degree. Zadeh in 1975 [125] have generalized the concept of ordinary fuzzy systems as reported [126], and termed as type-2 (T2) fuzzy systems to handle uncertainties involved in type-1 fuzzy logic systems. Mendel et al. [127, 128], extend this concept and explore many aspects of type-2 fuzzy sets and systems. The reported four possible sources of uncertainty present in type-1 fuzzy logic systems are (1) the antecedents and consequents of rules can be dubious because linguistic terms mean different things to distinct people, (2) consequents may have a set of values associated with them, especially when knowledge is extracted from a group of experts, who do not agree at all, (3) measurements that activate a type -1 fuzzy logic system may be noisy and, therefore, uncertain and (4) the data that are used to tune the parameters of a type -1 fuzzy logic system may also be noisy. Recent research reported the limitations of traditional type-1 fuzzy logic theory in treating large uncertainty factors due to unexpected severe faults on the power system [129]. Application of type-2 fuzzy logic in various fields shows compensation to the limitations with type-1 fuzzy logic [128, 130, 131]. Castillo et al has proposed GA and PSO optimized type-2 fuzzy logic controllers and demonstrated better performance as compared to type-1 controllers [132-135].Type-2 fuzzy logic is computationally intensive because its inference and type reduction are very intensive. Type-2 fuzzy set can be converted to interval type-2 by considering secondary memberships equal to zero or one [136]. The type-2 fuzzy logic controller based on the T2-fuzzy sets includes a third dimension and footprint of uncertainty, which results

to deal with both the linguistic and the numerical uncertainty. The type-2 fuzzy logic controller can obviously outperform its T1 counterpart under the situation of high uncertainty [310]. Because of such a better performance and applicability, interval type-2 fuzzy logic is considered for PSS design.

The later developed fuzzy, i.e. IT2 FS has a few applications in power system-related problems. In [311], fault currents of a power distribution system are calculated based on type-2 fuzzy numbers. The uncertainties associated with the fault current calculations of electrical distribution systems are carried out. A type-2 FLC and a type-2 FSMC (fuzzy sliding-mode controller) is proposed in [312] for control of a buck DC–DC converter. The IT2 FS based TCSC (thyristor controlled series capacitor) has been proposed in [313] to improve stability of the power system. In [314], an Interval Type-2 fuzzy logic controller with Gaussian type-2 MF is proposed for designing an automatic voltage regulator (AVR) system. The choice of Gaussian type-2 MF is not validated[135].

This chapter basically includes two objectives, (1) the evaluation of the IT2-MF in the study of stability enhancement of SMIB system as FPSS & determining the MF with the best performance, (2) the selected IT2-FPSS is applied to an SMIB system as FPSS for a wide range of operating conditions of the power system. The two inputs to the IT2 FPSS are taken as speed deviation ($\Delta\omega$) and acceleration ($\Delta\dot{\omega}$) while the output is taken as stabilizing the voltage (ΔV_{pss}) signal which is applied to the automatic voltage regulator. The application of IT2 FPSS is extended to two-area four-machine ten-bus and IEEE New England ten-machine thirty nine-bus power system and speed response comparison is carried out with FPSS. The superiority of performance with IT2 FPSS over type-1 FPSS is validated in terms of ITAE, IAE and ISE.

The rest of this paper is organized as follows. In Section 6.2, the problem formulation is given by introducing SMIB and multimachine power systems, convention PSS and the objectives are defined simultaneously. The interval type-2 fuzzy logic concept is incorporated in section 6.3. The review on generation of the interval type-2 fuzzy membership function (IT2 FMF) is presented in section 6.4, which includes mathematical and graphical representation of MFs. In section 6.5, the IT2 FMFs (20 in numbers) are evaluated as FPSS with SMIB system, and an FMF is selected with better performance with respect to be other remaining FMFs. The selected IT2 FMF is used to constitute IT2 FPSS and evaluated for the wide range of operating conditions of an SMIB power system. The designed IT2 FPSS is used in analysis with four-machine and ten-machine power systems in section 6.6 and 6.7, respectively. Based on discussion in section 6.5 – 6.7, the conclusion is incorporated in section 6.8.

6.2. Problem Formulation

6.2.1. Test System Model

The systems under consideration are single-machine connected to infinite-bus (SMIB), two-area four-machine ten-bus and IEEE New England ten-machine thirty nine-bus power system. The single-line diagram representation of the SMIB power system is shown in Figure 1.6, and the way of connection with AVR and excitation system is shown in Figure 6.1. The small signal model of the SMIB power system can be represented by Figure 6.2 with connection of FPSS. The output signal of this PSS is added to AVR to modulate the excitation system for enhancing the damping of the small signal oscillations.

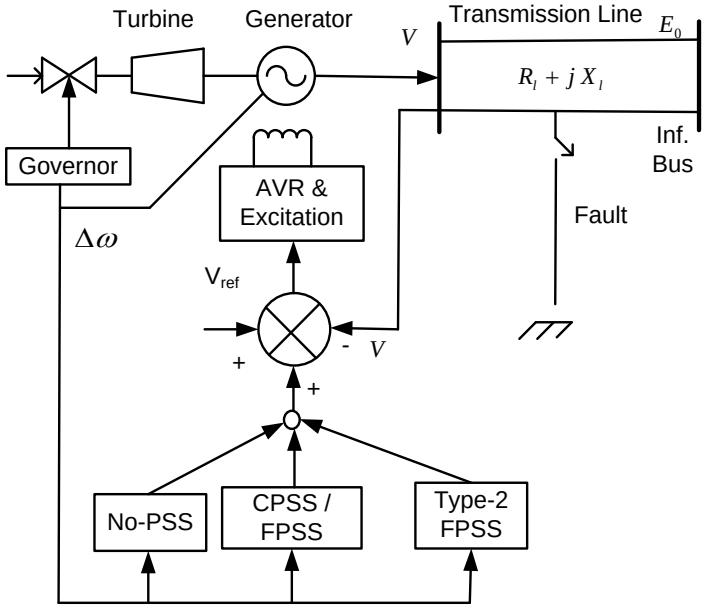

Figure 6.1: Representation of SMIB system with connection to FPSS

The single-line diagram representation of four-machine and ten-machine models is shown in Figure 1.14 and Figure 1.15, respectively. Moreover, a general Heffron-Philip representation is shown in Figure 1.13 [40-42]. The considered synchronous machines of SMIB, and multimachine power systems are of the model 1.0 type as discussed in [191]. To cover all operating conditions, the power system with generators, stabilizers, and excitation systems can be modeled by a set of nonlinear differential equations as in Eqn. (1.59) and (1.60) [191].

It is necessary to have linearized model of the power system around an operating point to analyze the small signal stability of a power system and consequently, to design power system stabilizer. The power system represented by Eqn. (1.59 – 1.60), is linearized around an equilibrium operating point of the power system, and presented in Eqn. (1.64 - 1.65) [14, 23].

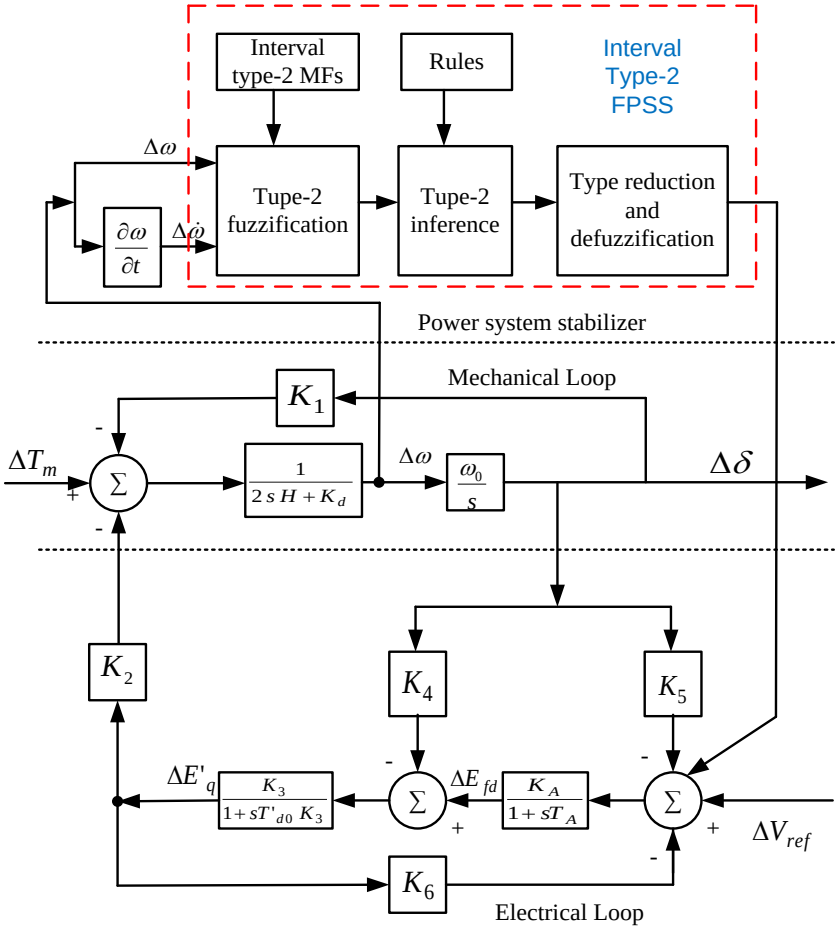

Figure 6.2: Representation of Heffron-Phillip model with IT2 FPSS

6.2.2. Conventional power system stabilizer

In early 1960s, the fast-acting high-gain automatic voltage regulators were used to improve the transient stability but simultaneously reduced damping of the synchronous machines [1]. To improve the damping of the system, a supplementary damping torque proportional to rotor speed deviations is introduced to excitation control loop and was termed as the power system stabilizer. The most widely accepted type of it is known as lead-lag based PSS or conventional PSS. It consists mainly, the gain block, the washout block and the lead-lag block and can be represented by the following equation.

$$\begin{aligned}\Delta V_{pss}(s) &= K_{pss}\frac{sT_{\omega}}{1+sT_{\omega}}\frac{1+sT_1}{1+sT_2}\Delta\omega(s)\\ &= 6.54309\frac{5}{1+sT_{\omega}}\frac{1+0.18987s}{1+0.05s}\end{aligned} \tag{6.1}$$

The $\Delta V_{PSS,}$ is the PSS output and added to the generator excitation as input to modulate the signal. The $\Delta\omega(s)$, is the generator rotor speed deviation being sensed and applied as input to the PSS. The data of CPSS for SMIB power system are considered as in [4].

6.3. Review on IT2-FLS

The type-2 fuzzy sets are an extension of the concept of the type-1 which were introduced by Prof. Zadeh in 1965 [125]. An FLS that uses one type-1 fuzzy set is called a type-1 FLS while using one type-2 fuzzy set is called type-2 FLS.

The MFs of an IT2FLS are in fuzzy and also represents a footprint of uncertainty (FOU) as in Figure 6.3, which is the representation of the area covered in between the upper MFs and lower MFs. FOU represents the capability to handle the uncertainty in the system. Thus, the IT2 FLS can handle both numerical and linguistic uncertainties associated with the inputs and outputs of the FLC. Accordingly, the IT2 FLS can give better performance than its counterpart T1 FLS [131, 315, 316].

6.3.1. Representation of type-2 FS and IT2 fuzzy sets

Let a type-2 fuzzy set in X is represented by $\tilde{A}$. The associated membership grade of $\tilde{A}$ is represented by $\mu_{\tilde{A}}(x,u)$, where $x \in X$ and $u \in J_X \subseteq [0,1]$, which represents a type-1 fuzzy set (T1 FS) in [0,1]. The domain elements of $\mu_{\tilde{A}}(x,u)$ are called primary MFs of x in $\tilde{A}$ [317].

6.3.1.1. Type-2 FS

The T2 FS denoted by $\tilde{A}$, is characterized by a type 2 MF $\mu_{\tilde{A}}(x,u)$, in which $x \in X$ and $u \in J_X \subseteq [0,1]$, i.e.

$$\tilde{A} = \{((x,u), \mu_{\tilde{A}}(x,u)) \,|\, \forall x \in X, \forall u \in J_X \subseteq [0,1]\} \tag{6.2}$$

or,

$$\tilde{A} = \int_{x \in X} \int_{u \in J_X} \mu_{\tilde{A}}(x,u)/(x,u), J_X \subseteq [0,1] \tag{6.3}$$

Here the range of $\tilde{A}$ can represented as $0 \le \mu_{\tilde{A}}(x,u) \le 1$.

At each value of x, say at $x = x'$, the vertical slice of $\mu_{\tilde{A}}(x,u)$ can be represented by axes u and $\mu_{\tilde{A}}(x',u)$ in 2-dimensional plane. Thus, $\mu_{\tilde{A}}(x = x',u)$ for $x \in X$ and $\forall u \in J_{x'} \subseteq [0,1]$, can represented by

$$\mu_{\tilde{A}}(x = x',u) \equiv \mu_{\tilde{A}}(x') = \int_{u \in J_{X'}} f_{x'}(u)/u,\ J_{x'} \subseteq [0,1] \tag{6.4}$$

Where in Eqn. (6.4)[318] the $f_{x'}(u)$ is in between [0, 1]. A T2 FS ($\tilde{A}$), can be represented in terms of embedded fuzzy sets ($\tilde{A}_e^j$). The $\tilde{A}_e^j$ denotes the j^{th} type-2 embedded fuzzy set of $\tilde{A}$.

$$\tilde{A} = \sum_{j=1}^{n} \tilde{A}_e^j \tag{6.5}$$

Where $n \equiv \prod_{i=1}^{N} M_i$ .Further $\tilde{A}_e^j$ can be represented by

$$\tilde{A}_e^j \equiv \left\{\left(u_i^j, f_{x_i}\left(u_i^j\right)\right), i = 1,2,3...,N\right\} \tag{6.6}$$

Where in Eqn. 6.6, $u_i^j \in \{u_{ik}, k = 1,2,...,M_i\}$. If the secondary MF $f_{x'}(u) = 1\ \forall u \in J_x$, then the T2 FS are called as interval type-2 fuzzy sets [317].

6.3.1.2. Interval Type-2 FS

If the T2 FS denoted by $\tilde{A}$, is characterized by an IT2 MF as $\mu_{\tilde{A}}(x,u) = 1$, where $x \in X$ and $u \in J_x \subseteq [0,1]$, i.e. Eqn. (6.1). If the uncertainty of $\tilde{A}$, is denoted by FOU, which is the union of the primary functions, as $FOU(\tilde{A}) = \bigcup_{x \in X} J_x$. If the upper bound of membership function (UMF) is represented by $\overline{\mu}_{\tilde{A}}(x)$ and the lower bound of membership function (LMF) is represented by $\underline{\mu}_{\tilde{A}}(x)$ of $\tilde{A}$ is equal representation as two 'type-1 MF'. Graphical representation of LMF and UMF for triangular MF and trapezoidal MF is represented in Figure 6.3 [317], while the FOU is represented by the shaded area. The embedded fuzzy set $\tilde{A}_e^j$ if represented by a wavy line in Figure 6.4.

6.3.2. Interval type-2 fuzzy logic systems (IT2FLS)

The representation of the IT2 FLS is similar to the type-1 FLS except the defuzzifier block of a type-1 FLS is replaced with the output processing block in a type-2 FLS as shown in Figure 6.5. The output processing block in a T2 FLS consists of a type-reduction block and a defuzzification block.

The type-reduce block maps a T2 FS to a type-1 FS, while the defuzzifier block maps a fuzzy value to a crisp value. The membership function (MF) of an IT2 FS is called FOU, which is represented by two MFs of a type-1 fuzzy set and are called as lower membership function(LMF) and upper membership function (UMF) as in Figure 6.3 [317].

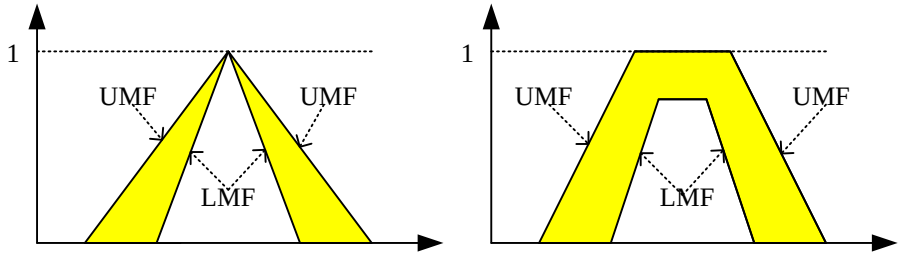

Figure 6.3: The MF, LMF & UMF representation of an IT2 FS

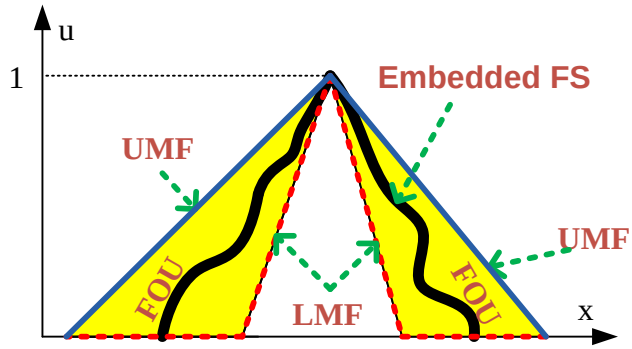

Figure 6.4: Shaded area represents FOU, dashed line denotes LMF, solid boundary line represents UMF and the Wavy line represents embedded Fuzzy System for IT2FS $\tilde{A}$.

In this thesis, Mamdani type fuzzy inference system (FIS) is used, which is normally called as Max - Min method. In Max - Min method, 5-step operation is required to produce an output such as fuzzyfication, membership function (mf) operation (selection of MF), implication function (min - max), aggregation, and defuzzyfication. The defuzzyfication involves a mapping from fuzzy value in fuzzy control area to a crisp value (non-fuzzy) in output control area. The defuzzyfication process on an interval type-2 FLS uses the centroid method which is proposed by Karnik and Mendel [128, 131, 317].

If a lower membership function (LMF) is represented by $\underline{\mu}_{\tilde{A}}(x)$ and an upper membership function (UMF) is denoted by $\overline{\mu}_{\tilde{A}}(x)$ then the centroid (proposed by Karnik and Mendel) is

represented by the interval between C_L and C_R. To determine C_L and C_R, the iterative method proposed by Karnik and Mendel can be used with the following steps.

Step-1: The θ_i can be calculated by the following expression

$$\theta_i = \frac{1}{2}\left[\overline{\mu}(x_i) + \underline{\mu}(x_i)\right] \tag{6.7}$$

Step 2: The value of c' can be evaluated using

$$c' = c(\theta_1, \theta_2, \theta_3, ..., \theta_N) = \frac{\sum_{i=1}^{N} x_i \times \theta_i}{\sum_{i=1}^{N} \theta_i} \tag{6.8}$$

Step 3: The value of k is determined such that $x_k \le c' \le x_{k+1}$

Step 4: If c'' is used for finding C_L, then it can be determined by the following equation,

$$c'' = \frac{\sum_{i=1}^{k} x_i \overline{\mu}(x_i) + \sum_{i=k+1}^{N} x_i \underline{\mu}(x_i)}{\sum_{i=1}^{k} \overline{\mu}(x_i) + \sum_{i=k+1}^{N} \underline{\mu}(x_i)} \tag{6.9}$$

If c'' is used for finding C_R then c'' is determined by the following equation,

$$c'' = \frac{\sum_{i=1}^{k} x_i \underline{\mu}(x_i) + \sum_{i=k+1}^{N} x_i \overline{\mu}(x_i)}{\sum_{i=1}^{k} \underline{\mu}(x_i) + \sum_{i=k+1}^{N} \overline{\mu}(x_i)} \tag{6.10}$$

Step 5: If the value of $c' = c''$ then go to step-6 otherwise go (set) to step-3.

Step 6: Put $C_L = c'$ or put $C_R = c'$ and calculate the mean of centroid, y by using

$$y = \frac{C_R + C_L}{2} \tag{6.11}$$

6.4. Review of Interval Type-2 FMF Generation

The used method to generate FMF is based on heuristics. This method generates the interval type-2 (IT2) FMF based on heuristic type-1 (T1) FMFs and a scaling factor. In this method pre-selected

Type-1 FMF function, such as Gaussian, triangular, trapezoidal, S, or pi functions are used along with specific scaling factor, α. The frequently used heuristic membership functions are as followings.

(1) Triangular Function

$$\mu(x;a,b,c)=\begin{cases}0 & if\ x\le a\\ \dfrac{x-a}{x-b} & if\ a\le x\le b\\ \dfrac{c-x}{c-b} & if\ b\le x\le c\\ 0 & if\ x\le c\end{cases} \tag{6.12}$$

(2) Π-Membership Function

$$\Pi(x;a,b,c)=\begin{cases}S(x;c-b,c-b/2,c & if\ x\le c\\ 1-S(x;c,c+b/2,c+b & if\ x>c\end{cases} \tag{6.13}$$

(3) Gaussian Membership Function

$$\mu(x)=e^{-\frac{(x-c)^2}{2\sigma^2}} \tag{6.14}$$

(4) Trapezoidal Function

$$\mu(x;a,b,c)=\begin{cases}0 & if\ x\le a\\ \dfrac{x-a}{b-a} & if\ a\le x\le b\\ 1 & if\ b\le x\le c\\ \dfrac{c-x}{c-b} & if\ b\le x\le c\\ 0 & if\ x\ge d\end{cases} \tag{6.15}$$

(5) S- Membership Function

$$S(x;a,b,c)=\begin{cases}0 & if\ x\le a\\ 2\left(\dfrac{x-a}{c-a}\right)^2 & if\ a<x\le b\\ 1-2\left(\dfrac{x-a}{c-a}\right)^2 & if\ b<x\le c\\ 1 & if\ x>c\end{cases} \tag{6.16}$$

where, $b=\dfrac{a+c}{2}$.

The appropriate Type-1 FMF which is suitable for PSS design is selected out of MFs as in Eqn. (6.8 – 6.13) or the combinatorial function of these. The heuristic Type-1 FMF represented by

$\mu(x)$ is designed by using the parameters (*a, b, c*) of the function. The selection of parameters is usually provided by experts. As in the previous discussion, the UMF can be represented by $\overline{\mu}_{\tilde{A}}(x)$ of the IT2 FMF. The LMF denoted by $\underline{\mu}_{\tilde{A}}(x)$ is determined using the scaling of the UMF by a factor α in between 0 and 1. The FOU can be expressed as

$$U_{\forall x \in X}[\mu_{\underline{\tilde{A}}}(x), \mu_{\overline{\tilde{A}}}(x)] = U_{\forall x \in X}[\mu_{\tilde{A}}(x), \alpha.\mu_{\tilde{A}}(x)]; \quad 0 < \alpha < 1 \tag{6.17}$$

The FOU can be determined by taking intersections of all lower MFs and upper MFs for all features as in Figure 6.6. If the min operation as intersection is selected then the FOU can be represented by

$$U_{\forall x \in X}[\mu_{\underline{\tilde{A}}}(x), \mu_{\overline{\tilde{A}}}(x)] = U_{\forall x \in X}[\min\{\mu_{\underline{\tilde{A}}}(x)\}, \min\{\mu_{\overline{\tilde{A}}}(x)\}] \tag{6.18}$$

where $\underline{\mu}_{\tilde{A}}(x)$ and $\overline{\mu}_{\tilde{A}}(x)$ are the minimum LMF and UMF among all LMFs and UMFs for all features, respectively. The lower MF is determined by appropriate scaling of the height of upper MF. The area in between the upper MF and scaled LMF represents the FOU for each class in consideration. The heuristic method can be summarized as follows.

(1) The first step involves judicious selection of the heuristic Type-1 Fuzzy MF which is appropriate to represent a system.

(2) Specify the parameters (*a, b, c*) for the selected MF which is generally supplied by an expert.

(3) The UMF and LMF are designed using Eqn. (6.14 - 6.15).

The different 20 interval type-2 FMFs are produced in MATLAB environment & are represented in Figure 6.7 - Figure 6.11.

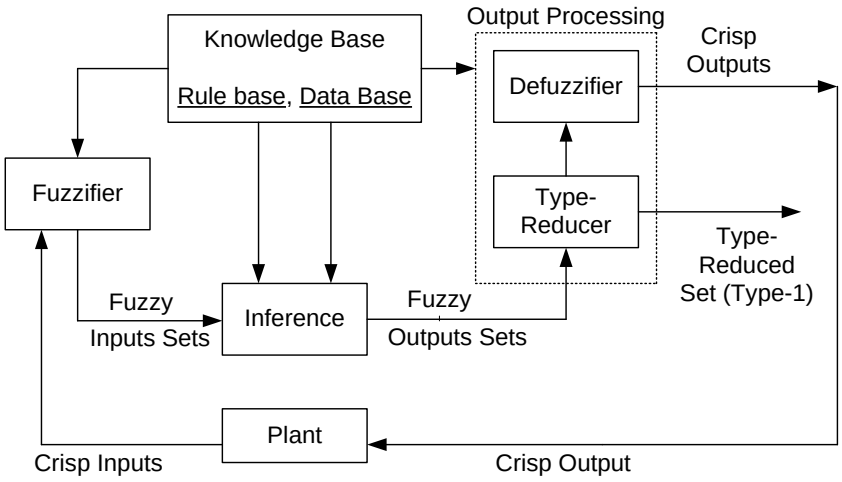

Figure 6.5: Representation of type-2 fuzzy logic system

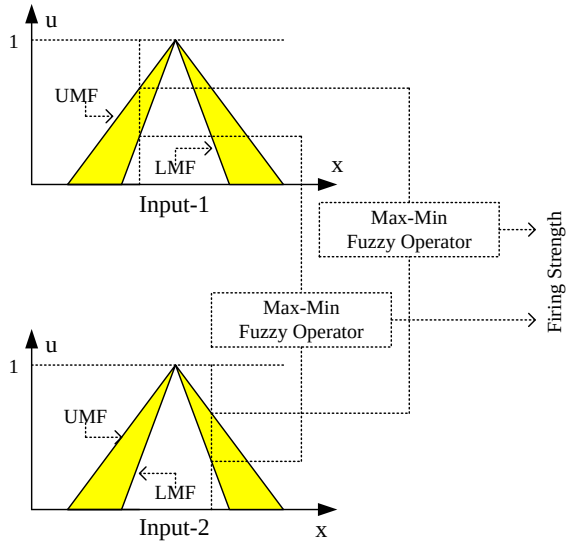

Figure 6.6: The selection of antecedents for a rule of IT2FLS

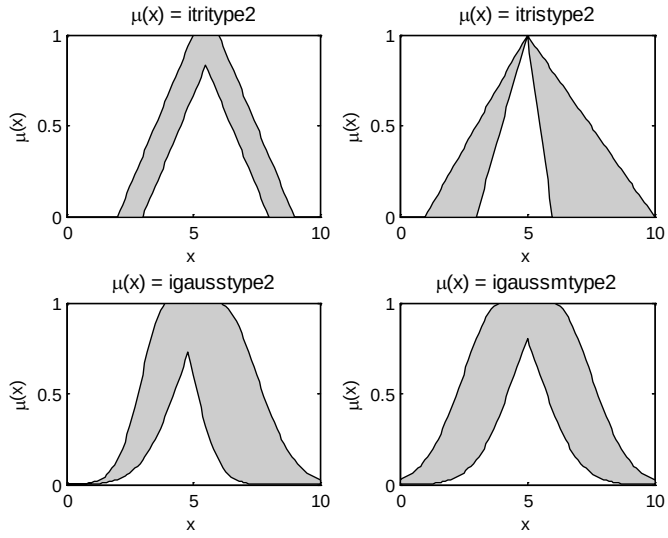

Figure 6.7: The figure represents the itritype2 mf, itristype2 mf, igausstype2 mf and igaussmtype2 membership functions.

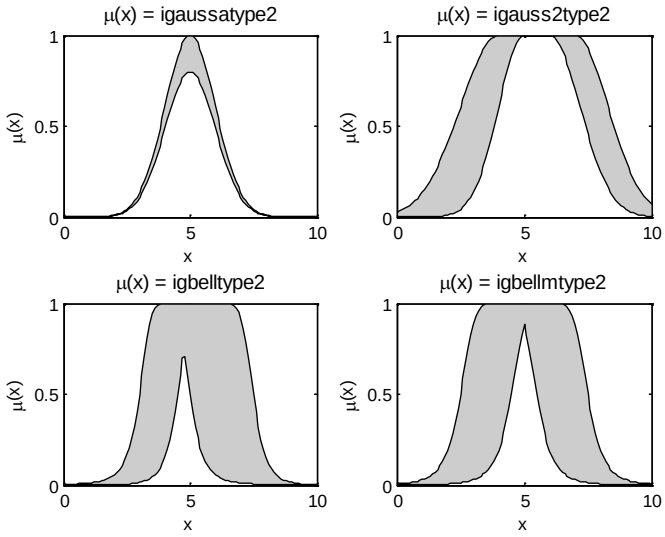

Figure 6.8: The figure represents the igaussatype2 mf, igauss2type2 mf, gbelltype2 mf and igbellmtype2 membership functions.

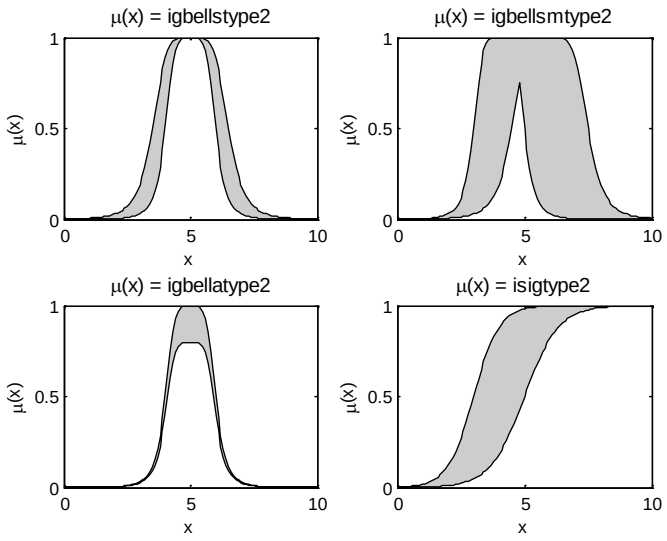

Figure 6.9: The figure represents the igbellstype2 mf, igbellsmtype2 mf, gbellatype2 mf and isigtype2 membership functions.

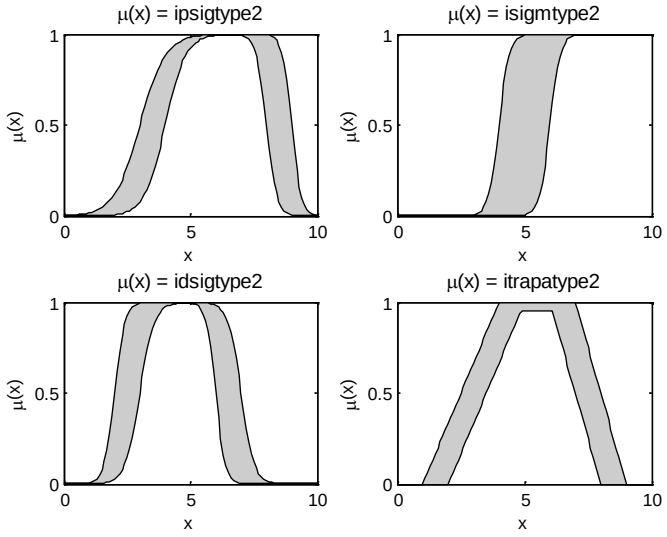

Figure 6.10: The figure represents the ipsigtype2 mf, isigmtype2 mf, idsigtype2 mf and itrapatype2 membership functions.

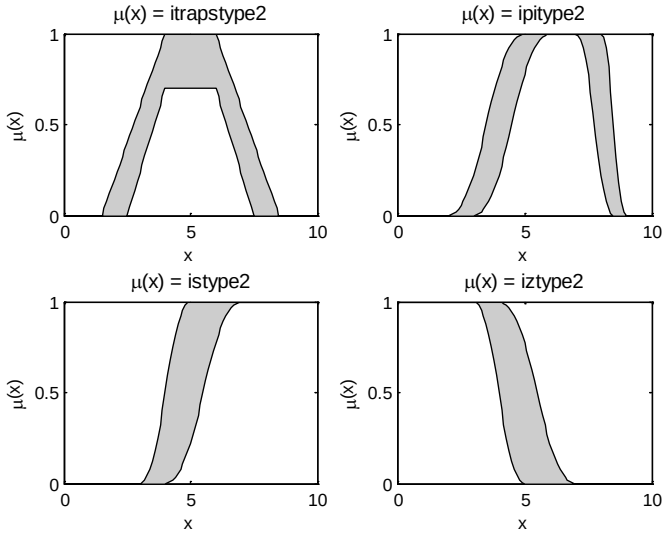

Figure 6.11: The figure represents the itrapstype2 mf, ipitype2 mf, istype2 mf and iztype2 membership functions.

6.5. Simulation Results and Discussions: SMIB Power System

6.5.1. Selection of IT2FMF

The performance study of the different interval type-2 fuzzy MFs (as shown in Figure 6.7 - Figure 6.11) regarding stability enhancement of a single machine-infinite bus system with power system stabilizer is carried out. The linguistic variables (seven in numbers), considered to define inputs (speed deviation & acceleration) and output (voltage) signals are as LN (Large Negative), MN (Medium Negative), N (Negative), Z (Zero), P (Positive), MP (Medium Positive), LP (Large Positive). The input and output linguistic variables are represented in Table 4.4, resulting to 49, "If-Then" rules to define the rule-base of the IT2 fuzzy inference system. A different IT2 fuzzy membership function (FMF) by using this table, constitutes a distinctive IT2 FIS system. Thus, the considered 20 different IT2 FMF results 20 distinctive IT2 FISs. The nonlinear model of the SMIB system is developed in MATLAB Simulink environment, and different FIS systems are used as IT2 fuzzy power system stabilizer (FPSS) to evaluate the performance. The speed response of the SMIB power system using IT2 FPSSs with different MFs is shown in Figure 6.12 - Figure 6.15. The system is stabilized by use of different IT2 FISs with distinct performance indices are recorded in Table 6.1. The observed performance indices (ISE, IAE and ITAE) are having a least value to itritype-2 mf (triangular type-2 membership function) in comparison to other IT2 MFs. The ITAE performance indices are also represented by bar chart in Figure 6.16.

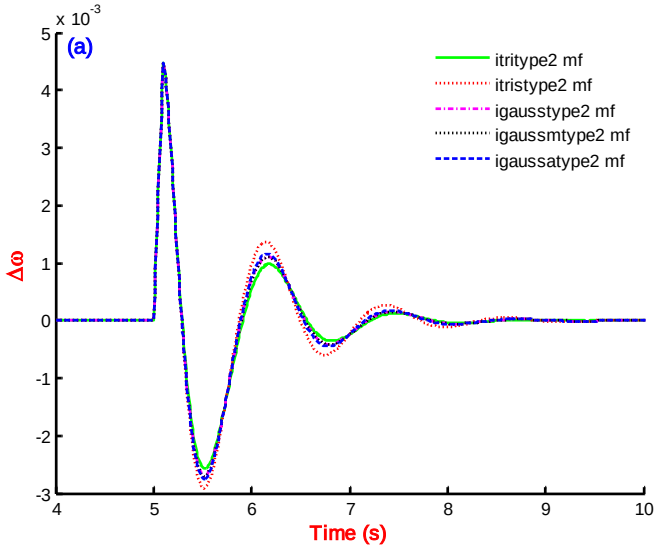

Figure 6.12: Speed response of IT2FPSS with itritype2 mf, itristype2 mf, igausstype2 mf, igaussmtype2 mf, igaussatype2 mf on SMIB power system.

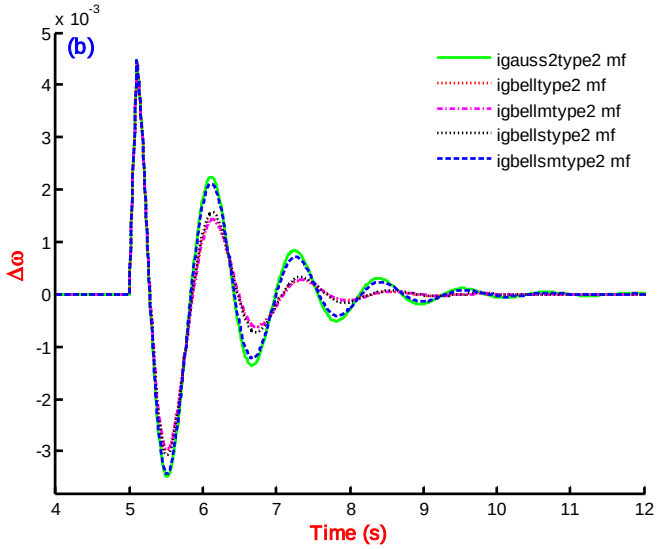

Figure 6.13: Speed response of IT2FPSS with igauss2type2 mf, igbelltype2 mf, igbellmtype2 mf, igbellstype2 mf, igbellsmtype2 mf on SMIB power system

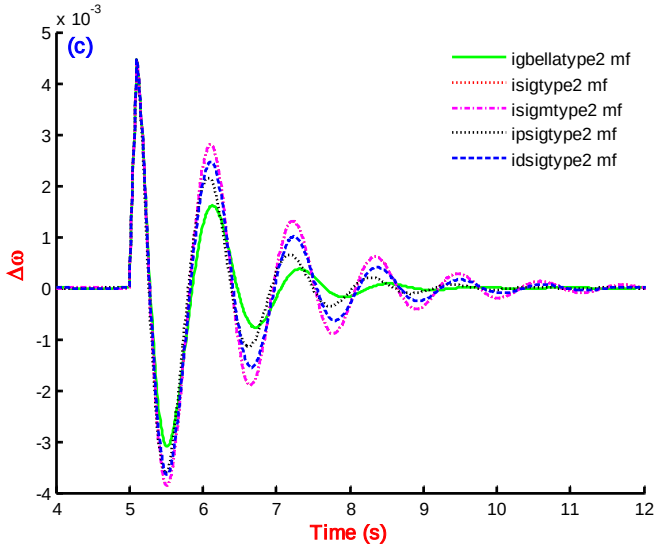

Figure 6.14: Speed response of IT2FPSS with igbellatype2 mf, isigtype2 mf, isigmtype2 mf, ipsigtype2 mf, idsigtype2 mf on SMIB power system

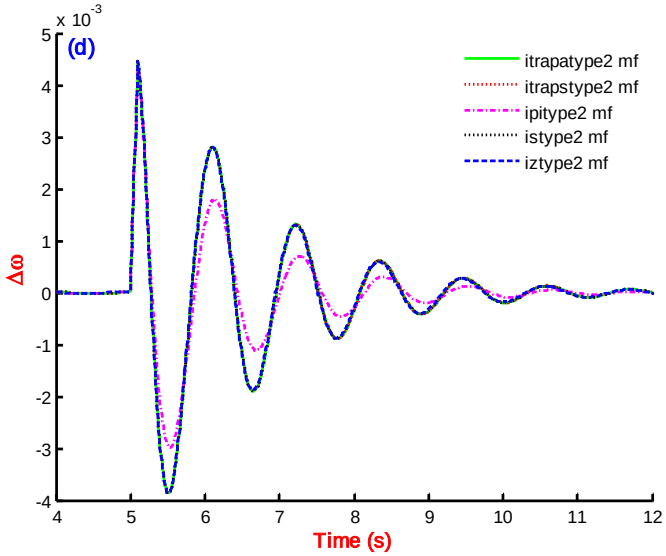

Figure 6.15: Speed response of IT2FPSS with itrapatype2 mf, itrapstype2 mf, ipitype2 mf, istype2 mf, iztype2 mf on SMIB power system

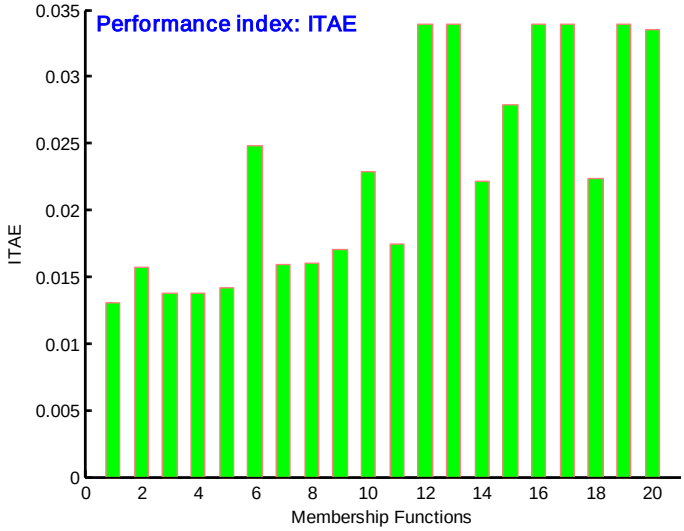

Figure 6.16: Plot of ITAE Performance Index for response with "itritype2 mf, itristype2 mf, igausstype2 mf, igaussmtype2 mf, igaussatype2 mf, igauss2type2 mf, igbelltype2 mf, igbellmtype2 mf, igbellstype2 mf, igbellsmtype2 mf, igbellatype2 mf, isigtype2 mf, isigmtype2 mf, ipsigtype2 mf, idsigtype2 mf.

6.5.2. Speed response performance with IT2FPSS with eight nonlinear plants

As in previous section, due to the superior performance of triangular type-2, fuzzy membership function is used to study the performance of SMIB system over a wide range of operating conditions of it. Eight operating points (plants 01–08 as shown in Table 2.2) of the SMIB power system are considered.

Models of power system and IT2 FPSS are simulated in an SIMULINK working environment of MATLAB. The output of PSS is generally restricted to ±0.25 per unit; hence consequent parameter limit values are set to ±0.25. The plant responses are recorded for system without PSS, with conventional PSS (CPSS) and with IT2 FPSS (itraitype2 mf). The performance summary for plant-1 – plant-8 as follows and as a sample the response comparison to Plant-1, Plant-2 and Plant-7 in Figure 6.17, Figure 6.18 and Figure 6.19, respectively.

Plant-1: In Figure 6.17, the response of plant-1 without considering PSS settles in 11.5 seconds, with CPSS settles in 10.5 seconds and with IT2 FPSS settles in 7.5 seconds.

Plant-2: The plant response settling times recorded without PSS, with CPSS and with IT2 FPSS is around 14.5, 11.0 and 7.75 seconds respectively.

Plant-3: The plant behaviour without PSS is oscillatory while it settles with CPSS and with IT2 FPSS in around 11.25 and 8.0 seconds respectively.

Plant-4: The plant behaviour without PSS is oscillatory and finally making unstable, while it settles with CPSS and with IT2 FPSS in around 11.50 and 9.0 seconds respectively.

Plant-5: The plant response settling times recorded without PSS, with CPSS and with IT2 FPSS is around 15.0, 14.0 and 10.0 seconds respectively.

Plant-6: The plant behaviour without PSS is oscillatory while it settles with CPSS and with IT2 FPSS in around 15.0 and 12.0 seconds respectively.

Plant-7: The plant behaviour without PSS is unstable while it settles with CPSS and with IT2 FPSS in around 13.0 and 9.0 seconds respectively.

Plant-8: The response of the plant-8 without considering PSS settles in approximately 40 seconds, with CPSS settles in 13 seconds and with IT2-FPSS, settles in 9.0 seconds.

Table 6.1: Performance Index of the IT2MFs

S. No.	IT2 FMF	ISE	IAE	IATE
1	itritype2	4.458×10^{-6}	0.002288	0.01306
2	itristype2	5.249×10^{-6}	0.002689	0.01567
3	igausstype2	4.706×10^{-6}	0.002398	0.01375
4	igaussmtype2	4.706×10^{-6}	0.002398	0.01375
5	igaussatype2	4.819×10^{-6}	0.002456	0.01413
6	igauss2type2	7.729×10^{-6}	0.003996	0.02484
7	igbelltype2	5.384×10^{-6}	0.002843	0.01593
8	igbellmtype2	5.382×10^{-6}	0.002743	0.01602
9	igbellstype2	5.688×10^{-6}	0.00289	0.01699
10	igbellsmtype2	7.277×10^{-6}	0.00372	0.02286
11	igbellatype2	5.812×10^{-6}	0.002961	0.01748
12	isigtype2	10.270×10^{-6}	0.005169	0.03394
13	isigmtype2	10.270×10^{-6}	0.005168	0.03393
14	ipsigtype2	7.652×10^{-6}	0.004276	0.02212
15	idsigtype2	8.631×10^{-6}	0.004387	0.02784
16	itrapatype2	10.280×10^{-6}	0.005166	0.03393
17	itrapstype2	10.270×10^{-6}	0.005165	0.03392
18	ipitype2	6.1980×10^{-6}	0.003564	0.0224
19	istype2	10.270×10^{-6}	0.005164	0.03391
20	iztype2	10.210×10^{-6}	0.005239	0.03354

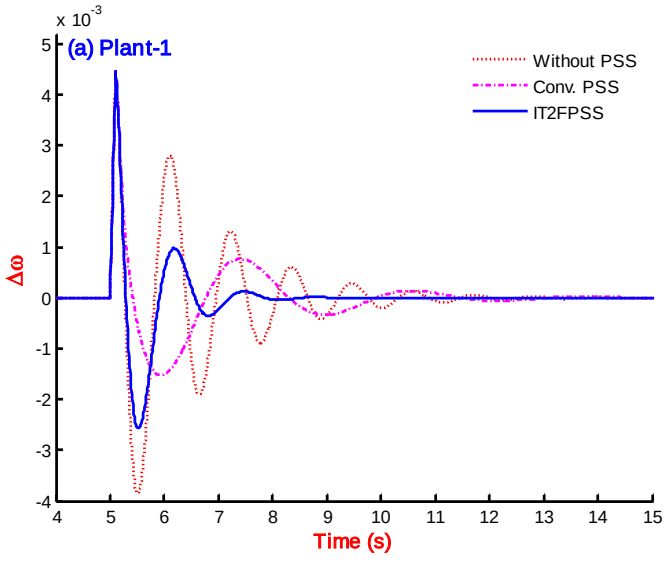

Figure 6.17: Speed response without PSS, with CPSS and with IT2FPSS on Plant-1

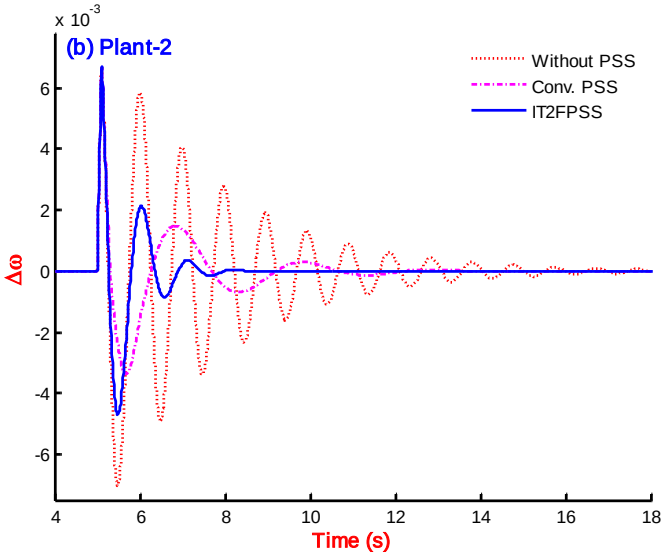

Figure 6.18: Speed response without PSS, with CPSS and with IT2FPSS on Plant-2

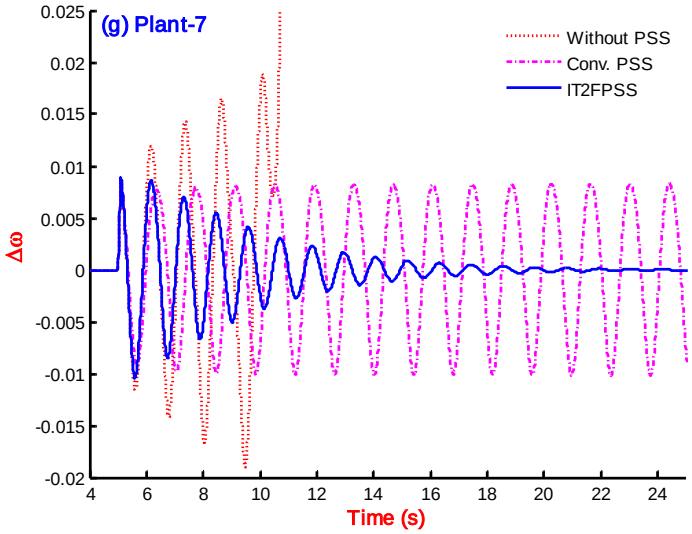

Figure 6.19: Speed response without PSS, with CPSS and with IT2FPSS on Plant-7

6.6. Simulation Results and Discussions: 4-Machine System

6.6.1. Speed response comparison

The two-area four-machine ten-bus power system is described in section 2.3.2 without PSS, and the creations of system models based on operating conditions are elaborated in section 2.3.2.1. The FPSS [40, 41] and IT2 FPSS (Proposed) is connected to the system and simulation carried out for the speed response. In each plant condition as listed in Table 2.4 is considered with fault location as given in Table A.5. The disturbance is considered as self-clearing at different buses at 1.0 second and cleared after 0.05 second. Referring to section 2.3.2.2 and section 2.3.2.3, wherein the simulation and eigenvalue analysis with eight plant conditions without PSS are described and found that none of the generators of plants are showing stable operation; therefore, not needed to

compare to the simulation results.

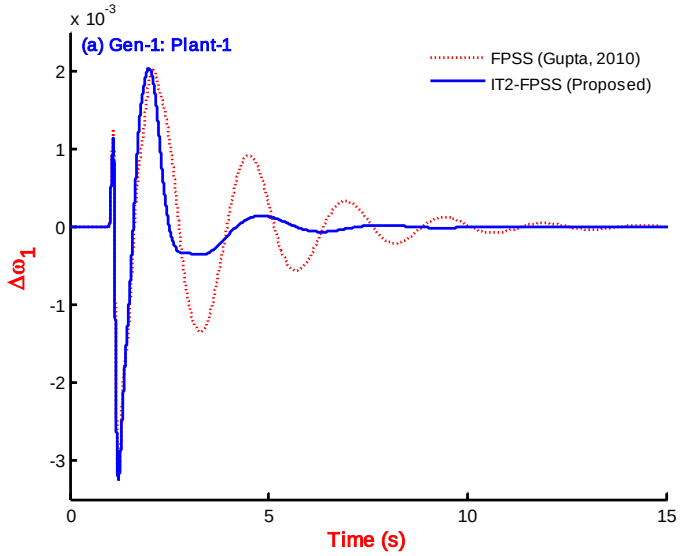

Figure 6.20: Speed response for generator-1 of four-machine system with FPSS and IT2-FPSS

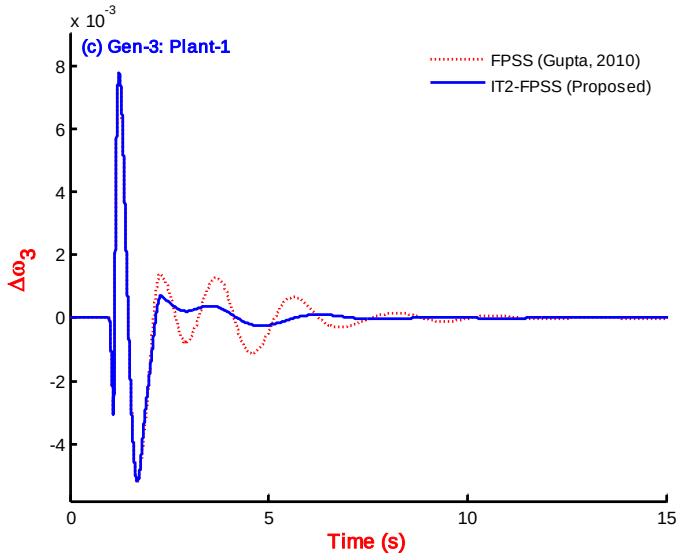

Figure 6.21: Speed response for generator-3 of four-machine system with FPSS and IT2-FPSS

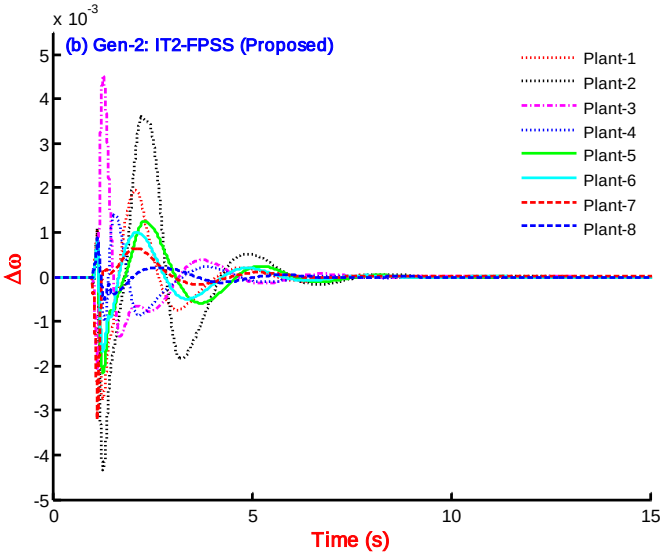

Figure 6.22: Speed response of generator-2 for eight plants of four-machine system with IT2-FPSS

As a sample, the speed response of Gen-1 and Gen-3 for plant-1 is compared with FPSS [40, 41] and IT2 FPSS (proposed) in Figure 6.20 and Figure 6.21. The response with IT2 FPSS is appreciably outperforming the FPSS [40, 41]. The speed response of the four-machine system with FPSS [40, 41] considering all eight plant conditions is shown in Figure 6.22 for Gen-2.

6.6.2. PI based analysis of speed response

As the speed responses of the four-machine system with FPSS [40, 41] and IT2 FPSS (Proposed) are shown graphically in Figure 6.20 and Figure 6.21, but the performance indices are recorded during each simulation carried out for 40 seconds and being recorded in Table 6.2. Clearly, the performance of the system with IT2 FPSS is greatly improved as compared to FPSS.

Table 6.2: PIs based comparison of FPSS and IT2-FPSS response for Plant-1 -Plant-8: 4-Machine system

Controller	ITAE	IAE	ISE	ITAE	IAE	ISE
	Plant-1			Plant-2		
FPSS [40, 41]	0.0760	0.0231	4.5996×10^{-05}	0.1793	0.0472	1.4331×10^{-04}
IT2-FPSS	0.0322	0.0144	3.4774×10^{-05}	0.0739	0.0291	1.0037×10^{-04}
	Plant-3			Plant-4		
FPSS [40, 41]	0.0587	0.0168	1.8456×10^{-05}	0.0477	0.0131	1.1294×10^{-05}
IT2-FPSS	0.0227	0.0092	1.0777×10^{-05}	0.0184	0.0077	8.2026×10^{-06}
	Plant-5			Plant-6		
FPSS [40, 41]	0.0615	0.0166	1.7306×10^{-05}	0.0357	0.0111	1.0156×10^{-05}
IT2-FPSS	0.0285	0.0103	1.0973×10^{-05}	0.0217	0.0086	9.1479×10^{-06}
	Plant-7			Plant-8		
FPSS [40, 41]	0.0584	0.0148	9.2321×10^{-06}	0.0414	0.0111	6.8405×10^{-06}
IT2-FPSS	0.0168	0.0064	3.5080×10^{-06}	0.0111	0.0046	2.5390×10^{-06}

6.7. Simulation Results and Discussions: 10-Machine System

The IEEE New England ten-machine thirty nine-bus power system is described in section 2.3.3 without PSS, and the creations of system models based on operating conditions are elaborated in section 2.3.3.1. In each plant condition as listed in Table 2.6 - Table 2.7 are considered with fault location as given in Table A.8. The disturbance is considered as self-clearing at different buses at 1.0 second and cleared after 0.05 second. Referring to section 2.3.3.2 and section 2.3.3.3, wherein the simulation and eigenvalue analysis with eight plant conditions are considered without-PSS (no-PSS) is described and found that none of the generators of plants are showing stable operation; therefore, not needed to compare to the simulation results.

An SIMULINK based block diagram, including all the nonlinear blocks is generated [191]. The speed signals of the machines are considered as output and the initial value of the speed is

taken as zero. The output signals of CPSSs are added to V_{ref} via limiters. It is used to damp out the small signal disturbances via modulating the generator excitation. The output must be limited to preventing the PSS acting to counter action of AVR. Different operating points are taken as the distinct plants for both systems. The limits of PSS outputs are taken as ± 0.05. In decentralized PSS, to activate the proposed controller at same instant, proper synchronization signal is required to be sent to all machines. All PSSs can be applied simultaneously to the respective machines for both power system models.

6.7.1. Speed response comparison with nonlinear plants

Speed response of New England system with IT2 FPSS (proposed) is carried out by simulation of nonlinear plant-1 configurations (Table 2.6 - Table 2.7). The performance of the proposed controller is to be compared that of with the FPSS [40], cultural algorithms based CPSS [25], adaptive mutation breeder genetic algorithm based CPSS [19], strength pareto evolutionary algorithm based CPSS [11]; therefore, the speed response of plant-1 configuration for Gen-2, Gen-3, Gen-8 and Gen-10 is recorded and compared in Figure 6.23, Figure 6.24, Figure 6.25 and Figure 6.26, respectively. In theses figures, the response with IT2 FPSS (Proposed) is superior as compared to the response with FPSS [40], CA-CPSS [25], ABGA-CPSS [19], SPEA- CPSS [11]. The simulation results with all comparing controllers for all plant conditions is impossible because of space constraint, as a result, speed response of the system with IT2 FPSS for all plant conditions of Gen-1, Gen-4 and Gen-8 is shown in Figure 6.27, Figure 6.28 and Figure 6.29, respectively. Clearly, the proposed IT2 FPSS can stabilize all plant conditions (covering wide range of operating conditions and different system configurations in each case).

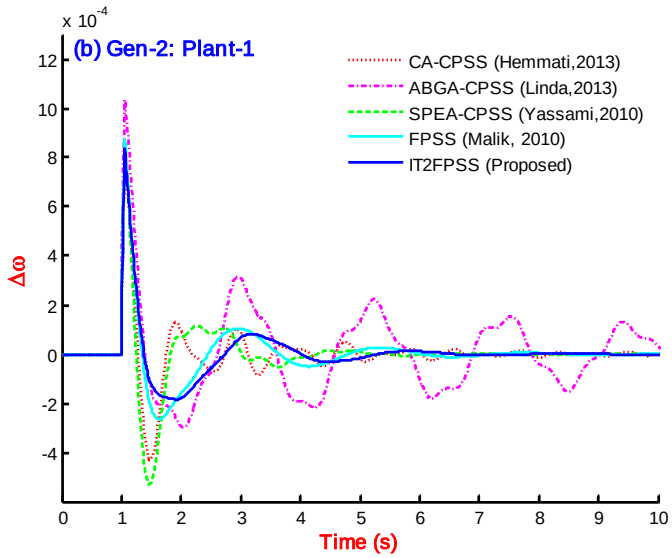

Figure 6.23: Speed response of Gen-2 of Plant-1 with CA-CPSS, ABGA-CPSS, SPEA-CPSS, FPSS and IT2-FPSS

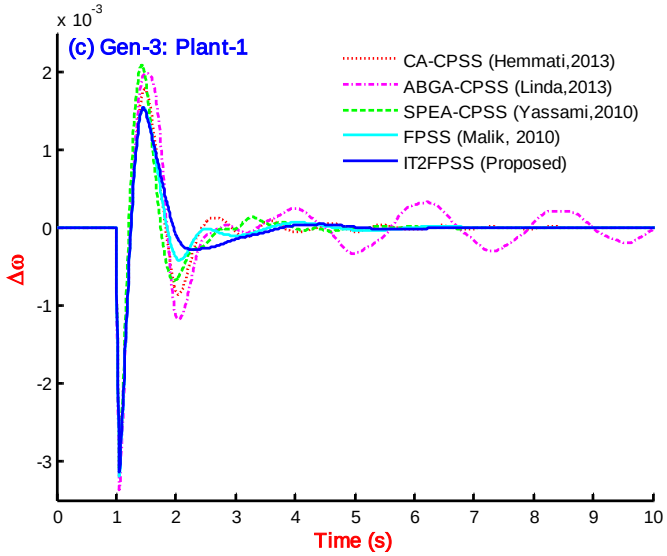

Figure 6.24: Speed response of Gen-3 of Plant-1 with CA-CPSS, ABGA-CPSS, SPEA-CPSS, FPSS and IT2-FPSS

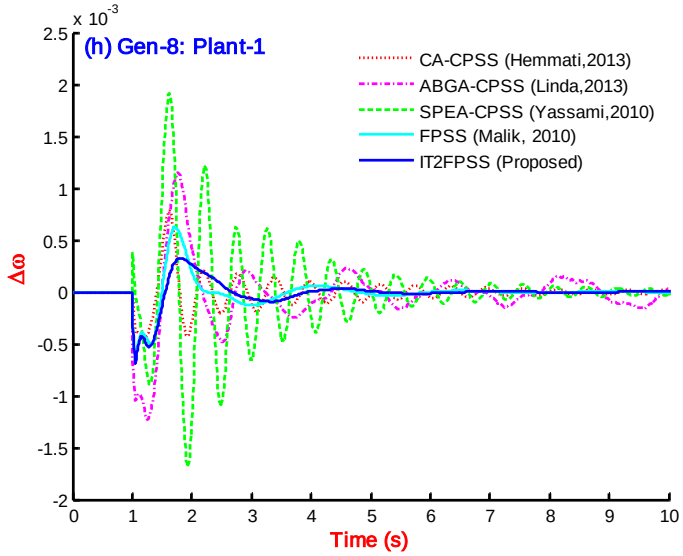

Figure 6.25: Speed response of Gen-8 of Plant-1 with CA-CPSS, ABGA-CPSS, SPEA-CPSS, FPSS and IT2-FPSS

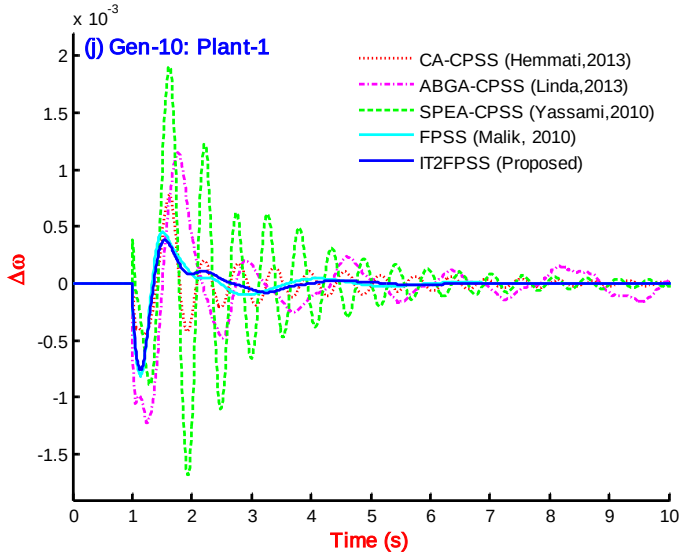

Figure 6.26: Speed response of Gen-10 of Plant-1 with CA-CPSS, ABGA-CPSS, SPEA-CPSS, FPSS and IT2-FPSS

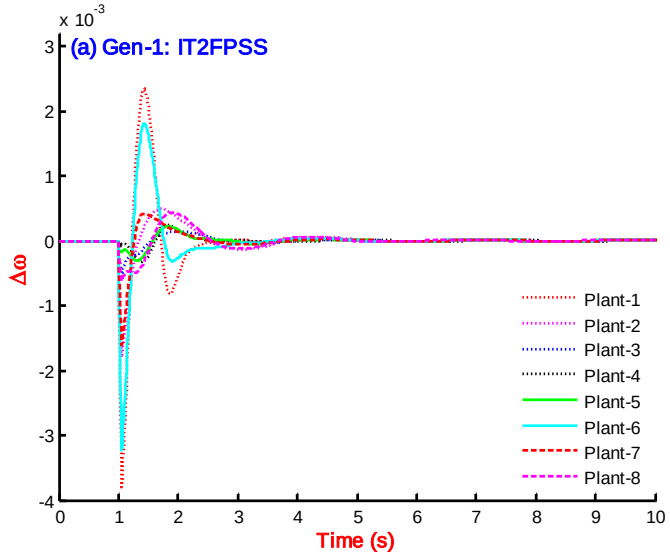

Figure 6.27: Speed response of Gen-1 with all eight plants using IT2-FPSS

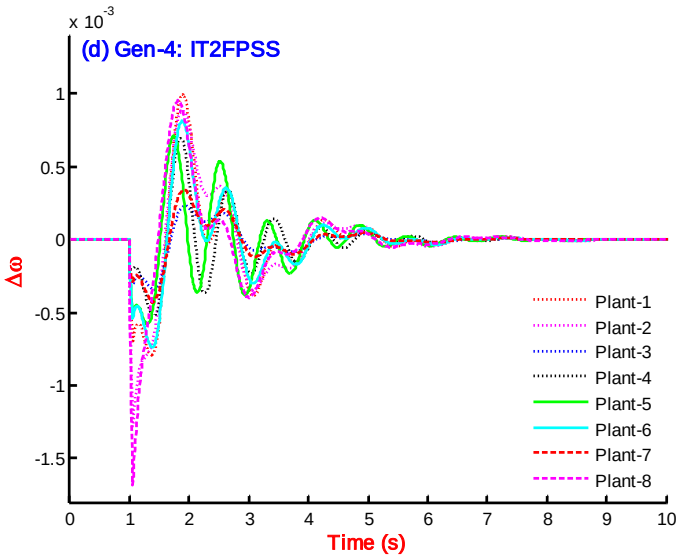

Figure 6.28: Speed response of Gen-4 with all eight plants using IT2-FPSS

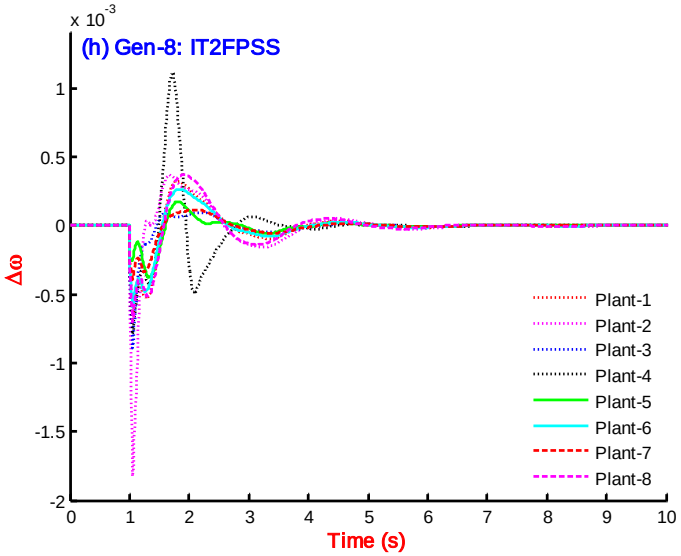

Figure 6.29: Speed response of Gen-8 with all eight plants using IT2-FPSS

6.7.2. PI based performance comparison

To evaluate the robustness of the proposed IT2 FPSS, simulation is carried out for all eight plant configurations which represent the wide range of operating conditions and system configurations. The system is simulated with FPSS [40, 41], CA-CPSS [25], ABGA-CPSS [19], SPEA- CPSS [11] for comparison purpose with eight plant conditions. Each time the performance indices (ITAE, IAE and ISE) are recorded and enlisted in Table 6.3. Since the system possesses ten generators, therefore, the PI values recorded for a particular type in these tables is the sum of PIs of ten generators. Comparatively lower value of PI refers to better performance. It is clear from this table, that the performance of the system is enhanced by using proposed IT2 FPSS (Proposed) as compared to performance with FPSS [40, 41], CA-CPSS [25], ABGA-CPSS [19], SPEA- CPSS [11].

Table 6.3: PIs based comparison of FPSS, IT2-FPSS and CPSSs response for plant-1 - plant-8: 10-machine system

Controller	ITAE	IAE	ISE	ITAE	IAE	ISE
	Plant-1			Plant-2		
CA-CPSS [25]	0.0357	0.0139	1.1636×10^{-05}	0.0339	0.0127	7.5570×10^{-06}
ABGA-CPSS [19]	0.2550	0.0427	2.7732×10^{-05}	0.3413	0.0513	3.0041×10^{-05}
SPEA-CPSS [11]	0.0358	0.0164	1.3156×10^{-05}	0.0371	0.0175	1.4232×10^{-05}
FPSS [40, 41]	0.0236	0.0122	8.3233×10^{-06}	0.0339	0.0149	8.4324×10^{-06}
IT2-FPSS (Proposed)	0.0216	0.0117	8.1003×10^{-06}	0.0256	0.0126	7.1406×10^{-06}
	Plant-3			Plant-4		
CA-CPSS [25]	0.0202	0.0073	2.5068×10^{-06}	0.0200	0.0098	1.0399×10^{-05}
ABGA-CPSS [19]	0.2042	0.0314	1.1968×10^{-05}	0.5749	0.0759	6.8650×10^{-05}
SPEA-CPSS [11]	0.0214	0.0094	4.0660×10^{-06}	0.0614	0.0242	3.8760×10^{-05}
FPSS [40, 41]	0.0115	0.0063	1.5598×10^{-06}	0.0185	0.0104	1.0332×10^{-05}
IT2-FPSS (Proposed)	0.0094	0.0057	1.3692×10^{-06}	0.0147	0.0091	9.4697×10^{-06}
	Plant-5			Plant-6		
CA-CPSS [25]	0.0235	0.0101	7.8741×10^{-06}	0.0317	0.0122	8.5154×10^{-06}
ABGA-CPSS [19]	0.2498	0.0403	2.4133×10^{-05}	0.2227	0.0382	2.1782×10^{-05}
SPEA-CPSS [11]	0.0320	0.0144	1.1481×10^{-05}	0.0328	0.0144	9.5331×10^{-06}
FPSS [40, 41]	0.0132	0.0086	7.0048×10^{-06}	0.0204	0.0107	5.8676×10^{-06}
IT2-FPSS (Proposed)	0.0143	0.0085	6.3510×10^{-06}	0.0181	0.0100	5.6160×10^{-06}
	Plant-7			Plant-8		
CA-CPSS [25]	0.0216	0.0080	3.0716×10^{-06}	0.0282	0.0112	7.4942×10^{-06}
ABGA-CPSS [19]	0.1909	0.0312	1.2801×10^{-05}	0.2537	0.0442	2.9079×10^{-05}
SPEA-CPSS [11]	0.0220	0.0096	4.1197×10^{-06}	0.0384	0.0172	1.3420×10^{-05}
FPSS [40, 41]	0.0120	0.0066	1.9293×10^{-06}	0.0291	0.0135	8.2817×10^{-06}
IT2-FPSS (Proposed)	0.0107	0.0062	1.7528×10^{-06}	0.0224	0.0115	6.9639×10^{-06}

6.8. Conclusions

In this chapter, an interval type-2 fuzzy logic based power system stabilizer (IT2 FPSS) is designed, and the performance is evaluated for three systems such as single-machine infinite-bus power system (SMIB), two-area four-machine ten-bus power system and IEEE New England ten-machine thirty nine-bus power systems.

Initially, IT2 FPSS is designed by considering 20 different type of interval type-2 membership functions and each is subjected to simulation, based on the performance index of speed response; better one is selected. The performance indices (ITAE, IAE and ISE) of speed response on the SMIB power system with as itritype-2 membership function based power system stabilizer recorded as 0.01306, 0.002288 and 4.458×10-6, respectively. Since these values of PIs are least as compared to other interval type-2 fuzzy membership function based PSSs. The best performer IT2 MF is found as itritype-2 mf; therefore, itriatype-2 mf based IT2 FPSS is considered to compare the speed responses over eight plant conditions of SMIB power system and compared to the response of CPSS. The plant behaviour without PSS is oscillatory while it settles with CPSS and with IT2 FPSS in around 15.0 and 12.0 seconds, respectively. It could be easy to state that the IT2 FPSS outperforms the considered CPSS.

An IT2 FPSS is designed by considering rule base in [72] with itritype-2 membership function and connected to the four-machine system in the decentralized manner. The designed IT2 FPSS and FPSS [40, 41] are subjected to simulate over eight plant conditions and found that the IT2 FPSS outperforms over FPSS [40, 41]. The comparative results are validated by considering performance indices of speed response of the system with IT2-FPSS and FPSS [40, 41].

The performance indices (ITAE, IAE and ISE) of speed response on the four-machine system with proposed IT2-FPSS are recorded and found in the range of 0.0168 - 0.0739, 0.0046 - 0.0291 and 2.5390×10^{-6} – 1.0037×10^{-4}, respectively; while that of with FPSS are as 0.0477 – 0.1793, 0.0111 – 0.0472 and 6.8405×10^{-6} – 1.4331×10^{-4}, respectively. The lower value of PIs with proposed IT2 FPSS proves its better performance over the FPSS[72].

Similarly, An IT2 FPSS is designed by considering rule base in [40, 41] and itritype-2 mf; it is connected to the ten-machine system in the decentralized manner. The such designed IT2 FPSS and FPSS [40, 41] are subjected to simulate over eight plant conditions and found that the IT2 FPSS outperforms over FPSS [40, 41], CA - CPSS [25], ABGA - CPSS [19], and SPEA - CPSS [11]. The comparative results are validated by considering performance indices of speed response of the system with IT2 FPSS and FPSS [40, 41], CA - CPSS [25], ABGA - CPSS [19], SPEA - CPSS [11].

The performance indices (ITAE, IAE and ISE) of speed response on the IEEE New England ten-machine power system with proposed IT2-FPSS are recorded and found acceptable and lower in magnitude as compared to other controllers under subject FPSS [40, 41], CA - CPSS [25], ABGA - CPSS [19], and SPEA - CPSS [11].

The comparatively lower value of performance indices represents early settlement of transient response with reduced overshoot. Here, the speed response with proposed IT2 FPSS on SMIB power system, four-machine power system and ten-machine power system observed to be lower as compared to the FPSSs and CPSSs under consideration.

Chapter 7

CONCLUSIONS AND FUTURE WORK

Electric power demand is the main cause of large, complex and interconnected power system networks. These are almost operated closer to the transient and dynamic stability limits. The heavy transfer of power on weak transmission lines is one of the causes to develop small signal oscillations. The other sources of low frequency oscillations are sudden changes in operating conditions, continuous changes in load, setting of automatic voltage regulators (AVRs) and some sort of disturbances, including faults within the power system. Some of these low-frequency oscillations (0.2-3.0 Hz) are damped out automatically, not affecting the power transfer capability of a power system, but others may persist for a while, grows in magnitude resulting to system separation and affecting power transmission.

The interconnected synchronous generators are equipped with high gain, fast acting AVRs to hold a generator in synchronism with a power system during transient fault conditions. The elevated gain of an excitation system leads to decrease in damping torque on the generator. To counteract the effect of high-gain AVRs or the sources of negative damping, a supplementary excitation controller referred to as a power system stabilizer (PSS) has been added into the excitation system, which in turn produces a component of electrical torque at the rotor in phase with speed variations. The optimal PSS design is always the requirement of the electric power system networks to enhance small signal stability.

This thesis examines the design of conventional PSS; PID based PSS, Type-1 FPSS (optimized input scaling factors), Type-1 FPSS (optimized input-output scaling factors), Type-1 FPSS (with new rule table) and Interval Type-2 FPSS in order to design globally optimal PSSs that will ensure a stable and robust operation of a single-machine connected to infinite-bus, two-area four-machine ten-bus and IEEE New England ten-machine thirty nine-bus power system, for each operating point within a wide range.

This thesis presents the CPSS design using the bat algorithm for SMIB power systems and outperforms to the performances with much of works reported in literature using different optimization techniques [2-11]. The problem of CPSS design is formulated as an optimization with eigenvalue based objective function to shift eigenvalue in D-shape sector of s-plane. The robustness and effectiveness of the BA-CPSS for SMIB power system are examined with 231 plant conditions using eigenvalue analysis to prove superiority of performance as compared to 12 distinct controllers designed by distinct algorithms as reported in literature [2-11]. The application

of the bat algorithm is extended to the four-machine power system for optimal design of CPSSs parameters. The problem of tuning CPSS parameters is formulated as an optimization problem using an eigenvalue based objective function to place the eigenvalue in the wedge-shaped sector in the LHS of s-plane. The performance of designed BA-CPSS outperforms the 12 different controllers designed by distinct algorithms as reported in literature [11, 13-19]. The bat algorithm based design of CPSSs for IEEE ten-machine power system is carried out with an objective function as to increase damping ratio with thresh hold value as 0.1. The performance comparison of BA-CPSSs is carried out with nine different algorithm based CPSSs reported in literature [11, 19-26] and proved to be superior in performance.

The bat algorithm is also employed to tune parameters of PID based PSS in above three power system scenario. The design of PID based PSS is formulated as an optimization problem using a simple time-domain based minimization of ISE of error signal. The designed PSSs outperform the comparing nine different PSSs designed by other optimization techniques as reported in literature [27-33]. It is also examined for 231 operating conditions of SMIB power system and found excellent to others using eigenvalue plots on s-plane. The BA-CPSS designed is examined for performance and found to be superior in performance as compared to [34].

An analogy between parameters of PD controller and input scaling factors of type-1 FPSS by considering the small-signal model of FPSS is developed and presented. The two input signals to FPSS are considered as speed and acceleration and output as voltage. These scaling factors have been optimized using harmony search algorithm and bat algorithm; the performance with BA-FPSS outperforms to HSA-FPSS and FPSS [72] in above three power system scenario.

It presents an optimization of input-output scaling factors of type-1 FPSS; where in two input signals are speed and power while output is considered as voltage. The scaling factors have been optimized using harmony search algorithm and bat algorithm and performance comparison is carried out also with PSO-FPSS [65]. The BA tuned FPSS again outperforms to the controllers in subject.

It includes design steps of a rule table with verification on linguistic phase plane. The designed FPSS using new rule table outperforms to other FPSSs in literature [12, 36-60, 62-69, 71] for above three power systems.

An application of interval type-2 fuzzy logic control is included to design IT2-FPSSfor single-machine and multimachine scenario. The IT2-FPSS with same rule base as that of comparing FPSS outperforms to it. In case of the SMIB power system the performance with IT2-FPSS proved to be outperforming CPSS [4]. An IT2-FPSS is designed by considering rule base in [72] with itritype-2 membership function and connected to the four-machine system in the decentralized manner. The such designed IT2-FPSS and FPSS [72] are subjected to simulate over

eight plant conditions and found that the IT2-FPSS outperforms over FPSS [72]. Similarly, An IT2 FPSS is designed by considering rule base in [40] and itritype-2 mf; it is connected to the ten-machine system in the decentralized manner. The such designed IT2 FPSS and FPSS[40] are subjected to simulate over eight plant conditions and found that the IT2 FPSS outperforms over FPSS [40], CPSSs reported in [11, 19, 25].

The performance indices for SMIB system with different controllers have been included in Table 2.10, Table 3.2, Table 4.6, Table 4.12, Table 5.4 and Table 6.1. It is found that system performance with IT2 FPSS outperformes to others and BA-PID-PSS turned up as worst performer. Howere, BA-CPSS is 2nd good performer w.r.t. others except IT2 FPSS.

7.1. Salient Features of the Present Work

- The thesis provides a broad-ranging overview of the research work carried out in the area of PSS tuning over the past three decades and brings out the main research issues that have been addressed.
- The thesis provides a detailed description of the development of the system mathematical models, both for single-machine infinite-bus power system as well as multimachine power system under small perturbations. These models are generic enough and can be applied to large sized power systems.
- The thesis provides an exhaustive analysis of bat algorithm based simultaneous tuning of CPSSs parameters for single-machine as well as multimachine power system. Actually, the design of lead-lag type PSS using classical control is carried out using sequential tuning method. The simultaneous tuning procedure also used in the design of PID type PSS, Type-1 FPSS (optimized input scaling factors) and Type-1 FPSS (optimized input-output scaling factors) using heuristic algorithms.
- The thesis demonstrates the effective and efficient approach of bat algorithm in the field of PSS design because these controllers outperform as compared to the PSS design by other technique.
- It includes an exhaustive review for each type of controller and would lead to design an efficient controller for power system.

7.2. Scope of Future Work in This Area

- Tuning of PSS for large interconnected power systems has been a challenging task for power engineers and though a lot of work has been reported in this area, several issues

remain unresolved. based on the work reported in this thesis, brief review on some issues that need to be addressed within the same framework are discussed here, in order to gain understanding of the problem of PSS tuning and its characteristics.

- The system investigated has been limited to a ten-machine thirty nine bus power system. It would be desirable to examine all proposed methods of PSS design for somewhat higher order and realistic (i.e. of more than 4^{th} order machine models) power systems. Based on the experience accumulated during simulations and due to development of both the system model and the tuning methods in a generic manner, the extension of the work could be done without difficulties.
- The systems considered in the thesis assume that the loads are of constant impedance type load. It would be of interest to the designer to understand how the dynamics of the system will be affected by the load dependence on voltage and consequently, how the optimal PSS parameters will be affected.
- The designed FPSS (optimized input scaling factors) and FPSS (optimized input-output scaling factors) are lacking the optimization of rule base and membership function. Therefore, the optimal number of rules and optimal shape of membership functions can be included as an extension to this work.
- As per Table 2.2, the case of leading power factor is left, therefore the analysis may also be considered under leading power conditions. The leading power factor operation of generator is more problematic than lagging power factor operation.
- In Figure 2.30, A slack bus, Bus -10, is like an infinite bus. How does the speed of an infinite bus can changes? It is necessary to examine the system modelling and other relevant aspects.
- In the design of IT2 FPSS, only type of fuzzy logic (i.e. the membership functions) is changed from type-1 to type-2, but much of work can be included by optimizing scaling factors, number of linguistic variables (i.e. rules) and the shape of membership function using heuristic optimization technique.

Appendix

POWER SYSTEM DATA

A.1. SMIB power system

Table A.1: SMIB Power System

Single machine connected to an infinite bus power system data are considered on a base of 1000 MVA are given as following [191]:	
Generator data	Ra = 0.0, $x_d = 1.97$, $x_q = 1.90$, $x'_d = 0.30$, $T'_{d0} = 6.0$, $H = 5.0$, $\omega_0 = 2\pi \times 50$
Transmission line (per circuit)	The parameters are representative of 400 kV and 400 Km long lossless lines with reactance as: $X_l = 0.02$
Excitation Data	Static exciter with single time constant AVR is used with gain and time constants as: $K_A = 100$, $T_A = 0.02$, $E_{fd}^{\min} = -5.0$, $E_{fd}^{\max} = 5.0$
Operating data	$E_b = 1.0$, $P_{g0} = 1.0$, $V_t = 1.0$
Fault	A three phase fault at the sending end of one of the circuits of the transmission line followed by clearing the fault.

A.2. Two-Area 4-Machine 10-Bus Power System

It is a 4 generator, 10 bus system where in, the two areas are connected by three AC tie lines. The transmission line data are considered on 100 MVA base [191, 196, 232].

Table A.2: Line Data: Four-machine ten-bus power system

From Bus Number	To Bus Number	Series resistance (R_s) pu	Series Reactance (X_s) pu	Shunt Reactance (B_s) pu
1	6	0.010	0.012	0.000
2	5	0.010	0.012	0.000
9	10	0.022	0.220	0.330
9	10	0.022	0.220	0.330
9	10	0.022	0.220	0.330
9	5	0.022	0.020	0.030
9	5	0.022	0.020	0.030
3	8	0.001	0.012	0.000
4	7	0.001	0.012	0.000
10	7	0.002	0.020	0.030
10	7	0.002	0.020	0.030
6	5	0.005	0.050	0.075
6	5	0.005	0.050	0.075
8	7	0.005	0.050	0.075
8	7	0.005	0.050	0.075

Table A.3: Load flow data: four-machine ten-bus power system[196]

Bus No.	V (pu)	θ (pu)	P_G (pu)	Q_G (pu)	P_L (pu)	Q_L (pu)	B_l (pu)
1	1.03	8.2154	7.0	1.3386	0.0	0.0	0.0
2	1.01	-1.5040	7.0	1.5920	0.0	0.0	0.0
3	1.03	0.0	7.2122	1.4466	0.0	0.0	0.0
4	1.01	-10.2051	7.0	1.8083	0.0	0.0	0.0
5	1.0108	3.6615	0.0	0.0	0.0	0.0	0.0
6	0.9875	-6.2433	0.0	0.0	0.0	0.0	0.0
7	1.0095	-4.6997	0.0	0.0	0.0	0.0	0.0
8	0.9850	-14.9443	0.0	0.0	0.0	0.0	0.0
9	0.9761	-14.4194	0.0	0.0	11.59	2.12	3.0
10	0.9716	-23.2977	0.0	0.0	15.75	2.88	4.0

Table A.4: Machine data: Four-machine ten-bus power system

Generator	R_a	x_d	x'_d	x_q	x'_q	H	T'_{d0}	T'_{q0}	x_l	K_d	K_A	T_A
1	0.00028	0.20	0.033	0.19	0.061	54.0	8.0	0.4	0.022	0.00	200	0.05
2	0.00028	0.20	0.033	0.19	0.061	54.0	8.0	0.4	0.022	0.00	200	0.05
3	0.00028	0.20	0.033	0.19	0.061	54.0	8.0	0.4	0.022	0.00	200	0.05
4	0.00028	0.20	0.033	0.19	0.061	54.0	8.0	0.4	0.022	0.00	200	0.05

Table A.5: Location of fault at a particular bus in the plant configurations: Four-machine ten-bus power system

S. No.	Power system model	Fault location at bus
1	Plant – 1	Bus – 3
2	Plant – 2	Bus – 4
3	Plant – 3	Bus – 5
4	Plant – 4	Bus – 6
5	Plant – 5	Bus – 7
6	Plant – 6	Bus – 8
7	Plant – 7	Bus – 9
8	Plant – 8	Bus – 10

A.3. IEEE New England 10-Machine 39-Bus Power System

Table A.6: Machine data: Ten-machine thirty nine - bus power system[191, 196, 319]

Gen.	R_a	x_d	x'_d	x_q	x'_q	H	T'_{d0}	T'_{q0}	T_c	K_d	K_A	T_A
1	0.00	0.2950	0.0647	0.282	0.0647	30.30	6.560	1.50	0.01	0.0	25	0.025
2	0.00	0.2000	0.0060	0.019	0.0060	500.0	6.000	0.70	0.01	0.0	25	0.025
3	0.00	0.2495	0.0531	0.237	0.0531	35.8	5.700	1.50	0.01	0.0	25	0.025
4	0.00	0.3300	0.0660	0.310	0.0660	26.0	5.400	0.44	0.01	0.0	25	0.025
5	0.00	0.2620	0.0436	0.258	0.0436	28.6	5.690	1.50	0.01	0.0	25	0.025
6	0.00	0.2540	0.0500	0.241	0.0500	34.8	7.300	0.40	0.01	0.0	25	0.025
7	0.00	0.2950	0.0490	0.292	0.0490	26.4	5.660	1.50	0.01	0.0	25	0.025
8	0.00	0.2900	0.0570	0.280	0.0570	24.3	6.700	0.41	0.01	0.0	25	0.025
9	0.00	0.2106	0.0570	0.205	0.0570	34.5	4.790	1.96	0.01	0.0	25	0.025
10	0.00	0.2000	0.0040	0.196	0.0040	42.0	5.700	0.50	0.01	0.0	25	0.025

Table A.7: Load flow data: Ten-machine thirty nine - bus power system [191, 319]

Bus No.	V (pu)	θ (degree)	P_G (pu)	Q_G (pu)	P_L (pu)	Q_L (pu)
1	0.98200	0.00000	5.519816	1.6180980	0.0920	0.04600
2	1.03000	-10.96807	10.00000	2.2622770	11.0400	2.50000
3	0.98310	2.340665	6.500000	1.6603620	0.00000	0.00000
4	1.01230	3.166466	5.080000	1.5509820	0.00000	0.00000
5	0.99720	4.189765	6.320000	0.8379978	0.00000	0.00000
6	1.04930	5.198208	6.500000	2.8103410	0.00000	0.00000
7	1.06350	7.991468	5.600000	2.2966220	0.00000	0.00000
8	1.02780	1.842515	5.400000	0.27572774	0.00000	0.00000
9	1.02650	7.544687	8.300000	0.5969476	0.00000	0.00000
10	1.04750	-4.006471	2.500000	1.83865	0.00000	0.00000
11	1.03501	-9.319072	0.000000	0.000000	0.00000	0.00000
12	1.01664	-6.441693	0.000000	0.000000	0.00000	0.00000
13	0.98552	-9.439605	0.000000	0.000000	3.22000	0.02400
14	0.94983	-10.37121	0.000000	0.000000	5.00000	1.84000
15	0.95056	-9.118281	0.000000	0.000000	0.00000	0.00000
16	0.95205	-8.345428	0.000000	0.000000	0.00000	0.00000
17	0.94408	-10.80150	0.000000	0.000000	2.33800	0.84000
18	0.944796	-11.36434	0.000000	0.000000	5.22000	1.76000
19	1.00709	-11.18251	0.000000	0.000000	0.00000	0.00000
20	0.95848	-5.588706	0.000000	0.000000	0.00000	0.00000
21	0.98490	-4.339794	0.000000	0.000000	2.74000	1.15000
22	1.01487	0.1908752	0.000000	0.000000	0.00000	0.00000
23	1.01216	-0.081575	0.000000	0.000000	2.74500	0.84660
24	0.97347	-6.801041	0.000000	0.000000	3.08600	0.92200
25	1.02567	-4.973582	0.000000	0.000000	2.24000	0.47200
26	1.01236	-6.207839	0.000000	0.000000	1.39000	0.17000
27	0.99181	-8.328811	0.000000	0.000000	2.81000	0.75500
28	1.01636	-2.467062	0.000000	0.000000	2.06000	0.27600
29	1.01874	0.4586534	0.000000	0.000000	2.83500	0.26900
30	0.98423	-2.018678	0.000000	0.000000	8.28000	1.03000
31	0.95493	-6.528843	0.000000	0.000000	0.00000	0.00000
32	0.93491	-6.512507	0.000000	0.000000	0.07500	0.88000
33	0.95597	-6.377243	0.000000	0.000000	0.00000	0.00000
34	0.95464	-8.215876	0.000000	0.000000	0.00000	0.00000
35	0.95675	-8.534196	0.000000	0.000000	3.20000	1.53000
36	0.97367	-6.891177	0.000000	0.000000	3.29400	0.32300
37	0.98141	-8.100629	0.000000	0.000000	0.00000	0.00000
38	0.98149	-9.085413	0.000000	0.000000	1.58000	0.30000
39	0.98489	-1.018596	0.000000	0.000000	0.00000	0.00000

Table A.8: Location of fault at a particular bus: Ten-machine power system[196]

S. No.	Power system model	Fault location at bus
1	Plant – 1	Bus – 16
2	Plant – 2	Bus – 13
3	Plant – 3	Bus – 11
4	Plant – 4	Bus – 9
5	Plant – 5	Bus – 7
6	Plant – 6	Bus – 17
7	Plant – 7	Bus –19
8	Plant – 8	Bus – 21

Table A.9: Transformer data: Ten-machine thirty nine - bus power system [191, 319]

From bus number	To bus number	R_T	X_T	Tap
39	30	0.0007	0.0138	1.00
39	5	0.0007	0.0142	1.00
32	33	0.0016	0.0435	1.00
32	31	0.0016	0.0435	1.00
30	4	0.0009	0.0180	1.00
29	9	0.0008	0.0156	1.00
25	8	0.0006	0.0232	1.00
23	7	0.0005	0.0272	1.00
22	6	0.0000	0.0143	1.00
20	3	0.0000	0.0200	1.00
16	1	0.0000	0.0250	1.00
12	10	0.0000	0.0181	1.00

Table A.10: Line data: Ten-machine thirty nine - bus power system [191, 319]

From bus number	To bus number	R_L	X_L	B_c
37	27	0.0013	0.0173	0.3216
37	38	0.0007	0.0082	0.1319
36	24	0.0003	0.0059	0.0680
36	21	0.0008	0.0135	0.2548
36	39	0.0016	0.0195	0.3040
36	37	0.0007	0.0089	0.1342
35	36	0.0009	0.0094	0.1710
34	35	0.0018	0.0217	0.3660
33	34	0.0009	0.0101	0.1723
28	29	0.0014	0.0151	0.2490
26	29	0.0057	0.0625	1.0290
26	28	0.0043	0.0474	0.7802
26	27	0.0014	0.0147	0.2396
25	26	0.0032	0.0323	0.5130
23	24	0.0022	0.0350	0.3610
22	23	0.0006	0.0096	0.1846
21	22	0.0008	0.0135	0.2548
20	33	0.0004	0.0043	0.0729
20	31	0.0004	0.0043	0.0729
19	2	0.0010	0.0250	1.2000
18	19	0.0023	0.0363	0.3804
17	18	0.0004	0.0046	0.0780
16	31	0.0007	0.0082	0.1389
16	17	0.0006	0.0092	0.1130
15	18	0.0008	0.0112	0.1476
15	16	0.0002	0.0026	0.0434
14	34	0.0008	0.0129	0.1382
14	15	0.0008	0.0128	0.1342
13	38	0.0011	0.0133	0.2138
13	14	0.0013	0.0213	0.2214
12	25	0.0070	0.0086	0.1460
12	13	0.0013	0.0151	0.2572
11	12	0.0035	0.0411	0.6987
11	2	0.0010	0.0250	0.7500

PUBLICATIONS FROM THE RESEARCH WORK

SCI Indexed Journals

[1]. D. K. Sambariya and R. Prasad, “Robust tuning of power system stabilizer for small signal stability enhancement using metaheuristic bat algorithm”, *International Journal of Electrical Power & Energy Systems*, 2014, Vol. 61, No. 0, pp. 229-238. DOI: 10.1016/j.ijepes.2014.03.050

[2]. D. K. Sambariya and R. Prasad, “Power System Stabilizer Design for Multimachine Power System Using Interval Type-2 Fuzzy Logic Controller”, *International Review of Electrical Engineering (IREE)*, 2013, Vol. 8, No. 5, pp. 1556-1565. DOI: 10.15866/iree.v8i5.2113

[3]. D. K. Sambariya and R. Prasad, “Design of Harmony Search Algorithm Based Tuned Fuzzy Logic Power System Stabilizer”, *International Review of Electrical Engineering (IREE)*, 2013, Vol. 8, No. 5, pp. 1594-1607. DOI: 10.15866/iree.v8i5.2117

[4]. D. K. Sambariya and R. Prasad, "Evaluation of Interval Type-2 Fuzzy Membership Function & Robust Design of Power System Stabilizer for SMIB Power System", Sylwan Journal, 2014, Vol. 158, No. 5, pp. 289-307.

[5]. D. K. Sambariya and R. Prasad, "Optimal Tuning of Fuzzy Logic Power System Stabilizer Using Harmony Search Algorithm," *International Journal of Fuzzy Systems*, 2015, Vol. xx, No. xx, pp. 1-14. DOI: 10.1007/s40815-015-0041-4

[6]. D. K. Sambariya and R. Prasad, "Design of Robust PID Power System Stabilizer for Multimachine Power System Using HS Algorithm," *American Journal of Electrical and Electronic Engineering*, 2015, Vol. 3, No. 3, pp. 75-82. DOI: 10.12691/ajeee-3-3-3

[7]. D. K. Sambariya, “Power system stabilizer design using compressed rule base of fuzzy logic controller,” *Journal of Electrical and Electronic Engineering*, 2015, Vol. 3, No. 3, pp. 52-64. DOI: 10.11648/j.jeee.20150303.16.

[8]. D. K. Sambariya and R. Prasad, "Design and small signal stability enhancement of power system using interval type-2 fuzzy PSS", Journal of Intelligent and Fuzzy Systems, 2015 (Accepted).

International Conferences

[9]. D. K. Sambariya and R. Prasad, "Robust Power system stabilizer design for single machine infinite bus system with different membership functions for fuzzy logic controller," in 7th International Conference on Intelligent Systems and Control (ISCO-2013) 2013, pp. 13-19. [doi: 10.1109/isco.2013.6481115].

[10]. Sambariya, D.K. and Prasad, R., 'Fuzzy PSS for Single Machine Infinite Bus Power System', International Conference on Power Electronics and Energy Systems (PEES-2012), ISBN : 978-81-920249-8-1; Department of Electrical Engineering, Chitkara University, 2012, pp. 23-27.

[11]. D. K. Sambariya and R. Prasad, "Small signal stability enhancement by optimally tuned conventional power system stabilizer using bat algorithm," in *International Conference on Advances in Power Generation from Renewable Energy Sources*, ed. Rajasthan Technical University, Kota, 2015, pp. 366-380.

[12]. D. K. Sambariya and R. Prasad, "Evaluation of Membership Functions in the design of Fuzzy Logic Power System Stabilizer," in *International Conference on Advances in Power Generation from Renewable Energy Sources, 'APGRES-2015'*, Rajasthan Technical University, Kota, 2015, pp. 352-365.

Papers Under Review in SCI Indexed Journals

[13]. Sambariya, D.K. and Prasad, R.,' A novel fuzzy rule matrix design for Fuzzy logic based Power System Stabilizer', Electric power components and systems: 2nd Review Sent

[14]. Sambariya, D.K. and Prasad, ' Optimal design of power system stabilizer for multimachine power system using harmony search algorithm', Control Engineering and Applied Informatics: Under Review.

[15]. Sambariya, D.K. and Prasad, 'Bat algorithm based PID controller tuning for desired system performance for small signal stability improvement of a power system', Journal of Electrical Engineering & Technology: Under review.

[16]. Sambariya, D.K. and Prasad, 'Application of bat algorithm to optimize scaling factors of fuzzy logic based power system stabilizer for multimachine power system', International journal of nonlinear sciences and numerical simulation: Under review.

BIBLIOGRAPHY

[1] F. P. Demello and C. Concordia, "Concepts of Synchronous Machine Stability as Affected by Excitation Control," *IEEE Transactions on Power Apparatus and Systems,* vol. PAS-88, pp. 316-329, 1969.

[2] M. A. Abido, "A novel approach to conventional power system stabilizer design using tabu search," *International Journal of Electrical Power & Energy Systems,* vol. 21, pp. 443-454, 1999.

[3] M. A. Abido, "Analysis of Power System Stability Enhancement via Excitation and Facts-Based Stabilizers," *Electric Power Components and Systems,* vol. 32, pp. 75-91, 2004/01/01 2004.

[4] M. A. Abido and Y. L. Abdel-Magid, "A GENETIC-BASED POWER SYSTEM STABILIZER," *Electric Machines & Power Systems,* vol. 26, pp. 559-571, 1998/07/01 1998.

[5] S.-J. Kim, S. Kwon, and Y.-H. Moon, "Low-order robust power system stabilizer for single-machine systems: An LMI approach," *International Journal of Control, Automation and Systems,* vol. 8, pp. 556-563, 2010/06/01 2010.

[6] H. M. Soliman, E. H. E. Bayoumi, and M. F. Hassan, "Power System Stabilizer Design for Minimal Overshoot and Control Constraint Using Swarm Optimization," *Electric Power Components and Systems,* vol. 37, pp. 111-126, 2008/12/30 2008.

[7] S. Sheetekela and K. A. Folly, "Breeder Genetic Algorithm for Power System Stabilizer design," in *IEEE Congress on Evolutionary Computation (CEC, '10')*, 2010, pp. 1-7.

[8] S. Abd-Elazim and E. Ali, "Power System Stability Enhancement via Bacteria Foraging Optimization Algorithm," *Arabian Journal for Science and Engineering,* vol. 38, pp. 599-611, 2013/03/01 2013.

[9] M. A. Abido, "An efficient heuristic optimization technique for robust power system stabilizer design," *Electric Power Systems Research,* vol. 58, pp. 53-62, 2001.

[10] S. Tripathi and S. Panda, "Tuning of Power System Stabilizer Employing Differential Evolution Optimization Algorithm," in *Swarm, Evolutionary, and Memetic Computing*. vol. 7076, B. Panigrahi, P. Suganthan, S. Das, and S. Satapathy, Eds., ed: Springer Berlin Heidelberg, 2011, pp. 59-67.

[11] H. Yassami, A. Darabi, and S. M. R. Rafiei, "Power system stabilizer design using Strength Pareto multi-objective optimization approach," *Electric Power Systems Research*, vol. 80, pp. 838-846, 2010.

[12] M. Sanaye-Pasand and O. P. Malik, "A Fuzzy Logic Based PSS Using a Standardized Rule Table," *Electric Machines & Power Systems*, vol. 27, pp. 295-310, 1999/02/01 1999.

[13] T. K. Das, G. K. Venayagamoorthy, and U. O. Aliyu, "Bio-Inspired Algorithms for the Design of Multiple Optimal Power System Stabilizers: SPPSO and BFA," *IEEE Transactions on Industry Applications* vol. 44, pp. 1445-1457, 2008.

[14] M. Eslami, H. Shareef, A. Mohamed, and S. P. Ghoshal, "Tuning of power system stabilizers using particle swarm optimization with passive congregation," *International Journal of the Physical Sciences*, vol. 5, pp. 2574-2589, 18 December, 2010 2010.

[15] M. Eslami, H. Shareef, A. Mohamed, and M. Khajehzadeh, "An efficient particle swarm optimization technique with chaotic sequence for optimal tuning and placement of PSS in power systems," *International Journal of Electrical Power & Energy Systems*, vol. 43, pp. 1467-1478, 2012.

[16] M. Kashki, Y. L. Abdel-Magid, and M. A. Abido, "Parameter optimization of multimachine power system conventional stabilizers using CDCARLA method," *International Journal of Electrical Power & Energy Systems*, vol. 32, pp. 498-506, 2010.

[17] M. Khaleghi, M. M. Farsangi, H. Nezamabadi-pour, and K. Y. Lee, "Pareto-Optimal Design of Damping Controllers Using Modified Artificial Immune Algorithm," *IEEE Transactions on Systems, Man, and Cybernetics, Part C: Applications and Reviews* vol. 41, pp. 240-250, 2011.

[18] M. Kiani, H. Soloklo, M. A. Mohammadi, and M. Farsangi, "Design of a Supplementary Controller for Power System Stabilizer Using Bacterial Foraging Optimization Algorithm," in *Computational Intelligence and Information Technology*. vol. 250, V. Das and N. Thankachan, Eds., ed: Springer Berlin Heidelberg, 2011, pp. 405-410.

[19] M. M. Linda and N. K. Nair, "A new-fangled adaptive mutation breeder genetic optimization of global multi-machine power system stabilizer," *International Journal of Electrical Power & Energy Systems*, vol. 44, pp. 249-258, 2013.

[20] M. A. Abido and Y. L. Abdel-Magid, "Eigenvalue assignments in multimachine power systems using tabu search algorithm," *Computers & Electrical Engineering*, vol. 28, pp. 527-545, 2002.

[21] M. A. Abido and Y. L. Abdel-Magid, "Optimal Design of Power System Stabilizers Using Evolutionary Programming," *IEEE Transactions on Energy Conversion*, vol. 17, pp. 429-436, 2002.

[22] M. A. Abido, "Optimal design of power-system stabilizers using particle swarm optimization," *IEEE Transactions on Energy Conversion,* vol. 17, pp. 406-413, 2002.

[23] M. A. Abido, "Robust Design of Power System Stabilizers for Multimachine Power Systems Using Differential Evolution," in *Computational Intelligence in Power Engineering*. vol. 302, B. Panigrahi, A. Abraham, and S. Das, Eds., ed: Springer Berlin Heidelberg, 2010, pp. 1-18.

[24] Y. L. Abdel-Magid and M. A. Abido, "Optimal multiobjective design of robust power system stabilizers using genetic algorithms," *IEEE Transactions on Power Systems,* vol. 18, pp. 1125-1132, 2003.

[25] A. Khodabakhshian and R. Hemmati, "Multi-machine power system stabilizer design by using cultural algorithms," *International Journal of Electrical Power & Energy Systems,* vol. 44, pp. 571-580, 2013.

[26] A. Ghasemi, H. Shayeghi, and H. Alkhatib, "Robust design of multimachine power system stabilizers using fuzzy gravitational search algorithm," *International Journal of Electrical Power & Energy Systems,* vol. 51, pp. 190-200, 2013.

[27] K. A. Hameed and S. Palani, "Robust Design of Power System Stabilizer using Harmony Search Algorithm," *Automatika – Journal for Control, Measurement, Electronics, Computing and Communications,* vol. 55, pp. 1-8, 2014.

[28] K. A. Hameed and S. Palani, "Robust design of power system stabilizer using bacterial foraging algorithm," *ARCHIVES OF ELECTRICAL ENGINEERING,* vol. 62, pp. 141-152, 2013.

[29] H. I. Abdul-Ghaffar, E. A. Ebrahim, and M. Azzam, "Design of PID Controller for Power System Stabilization Using Hybrid Particle Swarm-Bacteria Foraging Optimization," *WSEAS Transactions on power systems,* vol. 8, pp. 12-23, January 2013 2013.

[30] S. Duman and A. Öztürk, "Robust Design of PID Controller for Power System Stabilization by Using Real Coded Genetic Algorithm," *International Review of Electrical Engineering (I.R.E.E.),* vol. 5, pp. 2159-2170, September-October 2010 2010.

[31] G. Kasilingam, "Particle swarm optimization based PID power system stabilizer for a synchronous machine," *International Journal of Electrical, Electronic Science and Engineering,* vol. 8, pp. 118-123, 2014.

[32] B. S. Theja, A. Rajasekhar, D. P. Kothari, and S. Das, "Design of PID controller based power system stabilizer using Modified Philip-Heffron's model: An artificial bee colony approach," in *IEEE Symposium on Swarm Intelligence (SIS)*, 2013, pp. 228-234.

[33] K. Karthikeyan and P. Lakshmi, "Optimal Design of PID Controller for Improving Rotor Angle Stability using BBO," *Procedia Engineering,* vol. 38, pp. 889-902, 2012.

[34] M. Soliman, A. L. Elshafei, F. Bendary, and W. Mansour, "Robust decentralized PID-based power system stabilizer design using an ILMI approach," *Electric Power Systems Research,* vol. 80, pp. 1488-1497, 2010.

[35] M. M. Linda and N. K. Nair, "Optimal design of multi-machine power system stabilizer using robust ant colony optimization technique," *Transactions of the Institute of Measurement and Control,* vol. 34, pp. 829-840, October 2012 2012.

[36] J. M. Adams and K. S. Rattan, "Backpropagation learning for a fuzzy controller with partitioned membership functions," in *Proceedings, 'NAFIPS- '02', Annual Meeting of the North American Fuzzy Information Processing Society* 2002, pp. 172-177.

[37] H. Shayeghi, A. Jalili, and H. A. Shayanfar, "Multi-stage fuzzy load frequency control using PSO," *Energy Conversion and Management,* vol. 49, pp. 2570-2580, 2008.

[38] T. Abdelazim and O. P. Malik, "Power System Stabilizer Based on Model Reference Adaptive Fuzzy Control," *Electric Power Components and Systems,* vol. 33, pp. 985-998, 2005/09/01 2005.

[39] M. Ramirez-Gonzalez and O. P. Malik, "Power System Stabilizer Design Using an Online Adaptive Neurofuzzy Controller With Adaptive Input Link Weights," *IEEE Transactions on Energy Conversion,* vol. 23, pp. 914-922, 2008.

[40] M. Ramirez-Gonzalez and O. P. Malik, "Self-tuned Power System Stabilizer Based on a Simple Fuzzy Logic Controller," *Electric Power Components and Systems,* vol. 38, pp. 407-423, 2010/02/26 2010.

[41] M. Ramirez-Gonzalez and O. P. Malik, "Simplified Fuzzy Logic Controller and Its Application as a Power System Stabilizer," in *15th International Conference on Intelligent System Applications to Power Systems(ISAP '09)* 2009, pp. 1-6.

[42] M. Vijayaraghavan and M. Y. Sanavullah, "A Supervisory Hierarchical Fuzzy logic controller for power system stabilizer," in *Electronics Computer Technology (ICECT), 2011 3rd International Conference on*, 2011, pp. 275-279.

[43] T. Abdelazim and O. P. Malik, "An adaptive power system stabilizer using on-line self-learning fuzzy systems," in *IEEE Power Engineering Society General Meeting*, 2003, pp. 1715-1720 Vol. 3.

[44] K. A. El-Metwally and O. P. Malik, "Application of fuzzy logic stabilisers in a multimachine power system environment," *IEE Proceedings-Generation, Transmission and Distribution*, vol. 143, pp. 263-268, 1996.

[45] Y. J. Cheng and S. Elangovan, "Enhanced power system stabilizer via integrated tabu–fuzzy knowledge based controller," *International Journal of Electrical Power & Energy Systems*, vol. 25, pp. 543-550, 2003.

[46] M. B. Djukanovic, D. M. Dobrijevic, M. S. Calovic, M. Novicevic, and D. J. Sobajic, "Coordinated stabilizing control for the exciter and governor loops using fuzzy set theory and neural nets," *International Journal of Electrical Power & Energy Systems,* vol. 19, pp. 489-499, 1997.

[47] P. Hoang and K. Tomsovic, "Design and analysis of an adaptive fuzzy power system stabilizer," *IEEE Transactions on Energy Conversion,* vol. 11, pp. 455-461, 1996.

[48] I. Kocaarslan and E. Cam, "Fuzzy logic controller in interconnected electrical power systems for load-frequency control," *International Journal of Electrical Power & Energy Systems,* vol. 27, pp. 542-549, 2005.

[49] A. R. Roosta, H. Khorsand, and M. Nayeripour, "Design and analysis of fuzzy power system stabilizer," in *Innovative Smart Grid Technologies Conference Europe (ISGT Europe), 2010 IEEE PES,* 2010, pp. 1-7.

[50] M. Caner, N. Umurkan, S. Tokat, and S. V. Üstün, "Determination of optimal hierarchical fuzzy controller parameters according to loading condition with ANN," *Expert Systems with Applications,* vol. 34, pp. 2650-2655, 2008.

[51] A. R. Hasan, T. S. Martis, and A. H. M. S. Ula, "Design and implementation of a fuzzy controller based automatic voltage regulator for a synchronous generator," *IEEE Transactions on Energy Conversion,* vol. 9, pp. 550-557, 1994.

[52] T. Hussein, A. L. Elshafei, and A. Bahgat, "Design of a hierarchical fuzzy logic PSS for a multi-machine power system," in *Mediterranean Conference on Control & Automation (MED '07')* 2007, pp. 1-6.

[53] K. A. El-Metwally and O. P. Malik, "Fuzzy logic power system stabiliser," *IEE Proceedings-Generation, Transmission and Distribution,* vol. 142, pp. 277-281, 1995.

[54] D. E. Kvasov, D. Menniti, A. Pinnarelli, Y. D. Sergeyev, and N. Sorrentino, "Tuning fuzzy power-system stabilizers in multi-machine systems by global optimization algorithms based on efficient domain partitions," *Electric Power Systems Research,* vol. 78, pp. 1217-1229, 2008.

[55] H. A. Toliyat, J. Sadeh, and R. Ghazi, "Design of augmented fuzzy logic power system stabilizers to enhance power systems stability," *IEEE Transactions on Energy Conversion,* vol. 11, pp. 97-103, 1996.

[56] Y. Y. Hsu and C. H. Cheng, "Design of fuzzy power system stabilisers for multimachine power systems," *IEE Proceedings C-Generation, Transmission and Distribution,* vol. 137, pp. 233-238, 1990.

[57] P. Lakshmi and M. Abdullah Khan, "Stability enhancement of a multimachine power system using fuzzy logic based power system stabilizer tuned through genetic algorithm," *International Journal of Electrical Power & Energy Systems,* vol. 22, pp. 137-145, 2000.

[58] D. Sabapathi, R. Dhanasekaran, and R. Lakshmipathy, "Design of Fuzzy Based Power System Stabilizer for a Multimachine System," *International Journal of Electric and Power Engineering,* vol. 2, pp. 248-253, 2008.

[59] I. Robandi and B. Kharisma, "Design of Interval Type-2 Fuzzy Logic Based Power System Stabilizer," *International Journal of Electrical and Electronics Engineering* vol. 3, pp. 593-600, 2009.

[60] Y. Y. Hsu and C. H. Cheng, "A Fuzzy Controller for Generator Excitation Control," *IEEE Transactions on Systems, Man, and , Cybernetics,* vol. 23, pp. 532-539, 1993.

[61] S. Chopra, R. Mitra, and V. Kumar, "Fuzzy Controller: Choosing an Appropriate and Smallest Rule Set," *International Journal of Computational Cognition,* vol. 3, pp. 73-79, 2005.

[62] H. D. Patel and C. Majmudar, "Fuzzy logic application to single machine power system stabilizer," in *Nirma University International Conference on Engineering (NUiCONE, '11')* 2011, pp. 1-6.

[63] J. I. Corcau and E. Stoenescu, "Fuzzy logic controller as a power system stabilizer," *International Journal of Circuits, Systems and Signal Processing,* vol. 1, pp. 266-273, 2007.

[64] S. A. Gawish, F. A. Khalifa, W. Sabry, and M. A. L. Badr, "Large Power Systems Stability Enhancement Using a Delayed Operation Fuzzy Logic Power System Stabilizer," *Electric Machines & Power Systems,* vol. 27, pp. 157-168, 1999/01/15 1999.

[65] A. M. El-Zonkoly, A. A. Khalil, and N. M. Ahmied, "Optimal tunning of lead-lag and fuzzy logic power system stabilizers using particle swarm optimization," *Expert Systems with Applications,* vol. 36, pp. 2097-2106, 2009.

[66] J. Shi, L. H. Herron, and A. Kalam, "Optimization of fuzzy controllers as real-time power system stabilizers," *Engineering Applications of Artificial Intelligence,* vol. 7, pp. 545-558, 1994.

[67] K. Rout and P. C. Panda, "Power System Dynamic Stability Enhancement of SMIB Using Fuzzy Logic Based Power System Stabilizer," in *Power Electronics and Instrumentation Engineering*. vol. 102, V. Das, J. Stephen, and N. Thankachan, Eds., ed: Springer Berlin Heidelberg, 2010, pp. 10-14.

[68] N. Hosseinzadeh and A. Kalam, "A rule-based fuzzy power system stabilizer tuned by a neural network," *IEEE Transactions on Energy Conversion,* vol. 14, pp. 773-779, 1999.

[69] A.-L. Elshafei and K. El-Metwally, "Power System Stabilization Via Adaptive Fuzzy-Logic Control," *Proceedings of the 12th IEEE International Symposium on Intelligent Control 16-18 July 1997, Istanbul, Turkq*, pp. 89-94, 1997.

[70] M. H. Raouf, H. Lesani, E. R. Anarmarzi, and J. Olamaei, "Study of fuzzy multi-input power system stabilizer by using communication lines active power deviations input," in *10th International Conference on Environment and Electrical Engineering (EEEIC, '11')*, 2011, pp. 1-4.

[71] T. K. Renuka and S. Manakkal, "A tuned fuzzy based power system stabilizer for damping of Low Frequency Oscillations," in *International Conference on Power, Signals, Controls and Computation (EPSCICON,'12')*, 2012, pp. 1-6.

[72] D. K. Sambariya and R. Gupta, "Fuzzy Applications in a Multi-Machine Power System Stabilizer," *Journal of Electrical Engineering & Technology*, vol. 5, pp. 503-510, 2010.

[73] D. K. Sambariya, R. Gupta, and A. K. Sharma, "Fuzzy Applications to Single Machine Power System Stabilizers," *Journal of Theoretical and Applied Information Technology*, vol. 5, pp. 317-324, 2009.

[74] M. E. El-Hawary, *Electric Power Applications of Fuzzy Systems*: Wiley-IEEE Press, 1998.

[75] P. Kundur, *Power system stability and control*. New Delhi, India: Tata McGraw-Hill Education Pvt. ltd., 2011.

[76] E. V. Larsen and D. A. Swann, "Applying Power System Stabilizers Part I: General Concepts," *IEEE Transactions on Power Apparatus and Systems*, vol. PAS-100, pp. 3017-3024, 1981.

[77] K. Bollinger, A. Laha, R. Hamilton, and T. Harras, "Power stabilizer design using root locus methods," *IEEE Transactions on Power Apparatus and Systems*, vol. 94, pp. 1484-1488, 1975.

[78] P. Kundur, D. C. Lee, and H. M. Zein El-Din, "Power System Stabilizers for Thermal Units: Analytical Techniques and On-Site Validation," *IEEE Transactions on Power Apparatus and Systems*, vol. PAS-100, pp. 81-95, 1981.

[79] R. A. Jabr, B. C. Pal, N. Martins, and J. C. R. Ferraz, "Robust and coordinated tuning of power system stabiliser gains using sequential linear programming," *IET - Generation, Transmission and Distribution*, vol. 4, pp. 893-904, 2010.

[80] J. Heydeman and G. Honderd, "Adaptive and supplementary intelligent control of power system stabilizers," *Annual Review in Automatic Programming*, vol. 17, pp. 177-182, 1992.

[81] G. P. Chen, O. P. Malik, G. S. Hope, Y. H. Qin, and G. Y. Xu, "An adaptive power system stabilizer based on the self-optimizing pole shifting control strategy," *IEEE Transactions on Energy Conversion,* vol. 8, pp. 639-645, 1993.

[82] A. Ghosh, G. Ledwich, O. P. Malik, and G. S. Hope, "Power System Stabilizer Based on Adaptive Control Techniques," *IEEE Transactions on Power Apparatus and Systems,* vol. PAS-103, pp. 1983-1989, 1984.

[83] R. A. F. Saleh and H. R. Bolton, "Comparison of an adaptive stabilizer and a fuzzy logic stabilizer for superconducting generator governor control," *Electric Power Systems Research,* vol. 57, pp. 65-71, 2001.

[84] M. L. Kothari, K. Bhattacharya, and J. Nanda, "Adaptive power system stabiliser based on pole-shifting technique," *IEE Proceedings - Generation, Transmission and Distribution,* vol. 143, pp. 96-98, 1996.

[85] T. C. Yang, "Applying H∞ optimisation method to power system stabiliser design Part 1: Single-machine infinite-bus systems," *International Journal of Electrical Power & Energy Systems,* vol. 19, pp. 29-35, 1997.

[86] M. Bouhamida, A. Mokhtari, and M. A. Denai, "Power system stabilizer design based on robust control techniques," *ACSE Journal,* vol. 5, Nov., 2005 2005.

[87] Y. Meng and R. A. Schlueter, "μ-synthesis power system stabilizer design using a bifurcation subsystem based methodology," *IEEE Transactions on Power Systems,* vol. 18, pp. 1497-1506, 2003.

[88] A. Khodabakhshian and R. Hemmati, "Robust decentralized multi-machine power system stabilizer design using quantitative feedback theory," *International Journal of Electrical Power & Energy Systems,* vol. 41, pp. 112-119, 2012.

[89] V. Bandal and B. Bandyopadhyay, "Robust decentralised output feedback sliding mode control technique-based power system stabiliser (PSS) for multimachine power system," *IET Control Theory & Applications,* vol. 1, pp. 1512-1522, 2007.

[90] A. Al-khazraji, N. Essounbouli, A. Hamzaoui, F. Nollet, and J. Zaytoon, "Type-2 fuzzy sliding mode control without reaching phase for nonlinear system," *Engineering Applications of Artificial Intelligence,* vol. 24, pp. 23-38, 2011.

[91] V. A. Maslennikov and S. M. Ustinov, "Method and software for coordinated tuning of power system regulators," *IEEE Transactions on Power Systems,* vol. 12, pp. 1419-1424, 1997.

[92] H. Shayeghi, H. A. Shayanfar, A. Safari, and R. Aghmasheh, "A robust PSSs design using PSO in a multi-machine environment," *Energy Conversion and Management,* vol. 51, pp. 696-702, 2010.

[93] E. De Tuglie, M. La Scala, R. Sbrizzai, and M. Trovato, "Sequential design of a decentralized control structure for power system stabilizers," *Electric Power Systems Research,* vol. 50, pp. 91-98, 1999.

[94] R. A. Jabr, B. C. Pal, and N. Martins, "A Sequential Conic Programming Approach for the Coordinated and Robust Design of Power System Stabilizers," *IEEE Transactions on Power Systems,* vol. 25, pp. 1627-1637, 2010.

[95] C. M. Lim and S. Elangovan, "Design of stabilisers in multimachine power systems," *IEE Proceedings C-Generation, Transmission and Distribution,* vol. 132, pp. 146-153, 1985.

[96] C.-L. Chen and Y.-Y. Hsu, "Coordinated Synthesis of Multimachine Power System Stabilizer Using an Efficient Decentralized Modal Control (DMC) Algorithm," *IEEE Transactions on Power Systems,* vol. 2, pp. 543-550, 1987.

[97] Y. N. Yu and Q. H. Li, "Pole-placement power system stabilizers design of an unstable nine-machine system," *IEEE Transactions on Power Systems,* vol. 5, pp. 353-358, 1990.

[98] E. Zhou, O. P. Malik, and G. S. Hope, "Design of stabilizer for a multimachine power system based on the sensitivity of PSS effect," *IEEE Transactions on Energy Conversion,* vol. 7, pp. 606-613, 1992.

[99] Y.-Y. Hsu and C.-L. Chen, "Identification of optimum location for stabiliser applications using participation factors," *IEE Proceedings-Generation, Transmission and Distribution,* vol. 134, pp. 238-244, 1987.

[100] X.-S. Yang, "A New Metaheuristic Bat-Inspired Algorithm," in *Nature Inspired Cooperative Strategies for Optimization (NICSO 2010)*. vol. 284, J. González, D. Pelta, C. Cruz, G. Terrazas, and N. Krasnogor, Eds., ed: Springer Berlin Heidelberg, 2010, pp. 65-74.

[101] Y. Zhang, G. P. Chen, O. P. Malik, and G. S. Hope, "An artificial neural network based adaptive power system stabilizer," *IEEE Transactions on Energy Conversion,* vol. 8, pp. 71-77, 1993.

[102] H. Yuan-Yin and C. Chao-Rong, "Tuning of power system stabilizers using an artificial neural network," *IEEE Transactions on Energy Conversion,* vol. 6, pp. 612-619, 1991.

[103] C. C. Lee, "Fuzzy logic in control systems: fuzzy logic controller. I," *IEEE Transactions on Systems, Man and Cybernetics,* vol. 20, pp. 404-418, 1990.

[104] C. C. Lee, "Fuzzy logic in control systems: fuzzy logic controller. II," *IEEE Transactions on Systems, Man and Cybernetics,* vol. 20, pp. 419-435, 1990.

[105] E. Handschin, W. Hoffmann, F. Reyer, T. Stephanblome, U. Schlucking, D. Westermann, *et al.*, "A new method of excitation control based on fuzzy set theory," *IEEE Transactions on Power Systems,* vol. 9, pp. 533-539, 1994.

[106] K. A. El-Metwally, G. C. Hancock, and O. P. Malik, "Implementation of a fuzzy logic PSS using a micro-controller and experimental test results," *IEEE Transactions on Energy Conversion,* vol. 11, pp. 91-96, 1996.

[107] Y. Kitauchi and H. Taniguchi, "Experimental verification of fuzzy excitation control system for multi-machine power system," *IEEE Transactions on Energy Conversion,* vol. 12, pp. 94-99, 1997.

[108] S. Pillutla and A. Keyhani, "Power system stabilization based on modular neural network architecture," *International Journal of Electrical Power and Energy Systems,* vol. 19, pp. 411-418, 1997.

[109] L. Wenxin, G. K. Venayagamoorthy, and D. C. Wunsch, II, "A heuristic dynamic programming based power system stabilizer for a turbogenerator in a single machine power system," in *38th IAS Annual Meeting, Conference Record of the Industry Applications Conference* 2003, pp. 270-276 vol.1.

[110] R. Segal, A. Sharma, and M. L. Kothari, "A self-tuning power system stabilizer based on artificial neural network," *International Journal of Electrical Power & Energy Systems,* vol. 26, pp. 423-430, 2004.

[111] B. Chaudhuri, R. Majumder, and B. C. Pal, "Application of multiple-model adaptive control strategy for robust damping of interarea oscillations in power system," *IEEE Transactions on Control Systems Technology,* vol. 12, pp. 727-736, 2004.

[112] O. Wolkenhauer, *Data Engineering: Fuzzy Mathematics in Systems Theory and Data Analysis*. New York: John Wiley & Sons, Inc., 2001.

[113] S. P. Ghoshal, A. Chatterjee, and V. Mukherjee, "Bio-inspired fuzzy logic based tuning of power system stabilizer," *Expert Systems with Applications,* vol. 36, pp. 9281-9292, 2009.

[114] T. Hiyama, "Real time control of micro-machine system using micro-computer based fuzzy logic power system stabilizer," *IEEE Transactions on Energy Conversion,* vol. 9, pp. 724-731, 1994.

[115] Z. Yi-Sheng and L. Lin-Ying, "Optimal design for fuzzy controllers by genetic algorithms," in *International IEEE/IAS Conference on Industrial Automation and Control: Emerging Technologies,* 1995, pp. 429-435.

[116] N. A. Singh, K. A. Muraleedharan, and K. Gomathy, "Particle swarm intelligence tuned fuzzy controller for damping modal oscillations of power system," in *IEEE Region 10 Conference,'TENCON-08',* 2008, pp. 1-6.

[117] H. Shayeghi, H. A. Shayanfar, S. Jalilzadeh, and A. Safari, "Multi-machine power system stabilizers design using chaotic optimization algorithm," *Energy Conversion and Management,* vol. 51, pp. 1572-1580, 2010.

[118] M. M. Beno, N. A. Singh, M. C. Therase, and M. M. S. Ibrahim, "Design of PSS for damping low frequency oscillations using bacteria foraging tuned non-linear neuro-fuzzy controller," in *IEEE GCC Conference and Exhibition (GCC '11')*, 2011, pp. 653-656.

[119] A. Chatterjee, S. P. Ghoshal, and V. Mukherjee, "Chaotic ant swarm optimization for fuzzy-based tuning of power system stabilizer," *International Journal of Electrical Power & Energy Systems*, vol. 33, pp. 657-672, 2011.

[120] B. Shaw, A. Banerjee, S. P. Ghoshal, and V. Mukherjee, "Comparative seeker and bio-inspired fuzzy logic controllers for power system stabilizers," *International Journal of Electrical Power & Energy Systems*, vol. 33, pp. 1728-1738, 2011.

[121] H. E. Mostafa, M. A. El-Sharkawy, A. A. Emary, and K. Yassin, "Design and allocation of power system stabilizers using the particle swarm optimization technique for an interconnected power system," *International Journal of Electrical Power & Energy Systems*, vol. 34, pp. 57-65, 2012.

[122] K. Belarbi and F. Titel, "Genetic algorithm for the design of a class of fuzzy controllers: an alternative approach," *IEEE Transactions on Fuzzy Systems*, vol. 8, pp. 398-405, 2000.

[123] C. C. Chen and C. C. Wong, "Self-generating rule-mapping fuzzy controller design using a genetic algorithm," *IEE Proceedings -Control Theory and Applications*, vol. 149, pp. 143-148, 2002.

[124] M. Dubey and N. E. Mastorakis, "Tunning of Fuzzy Logic Power System Stabilizers using Genetic Algorithm in Multimachine Power System," *WSEAS Transactions on Power Systems*, vol. 3, pp. 105-114, March 2009 2009.

[125] L. A. Zadeh, "The concept of a linguistic variable and its application to approximate reasoning—I," *Information Sciences*, vol. 8, pp. 199-249, 1975.

[126] L. A. Zadeh, "Fuzzy Sets," *Information Control*, vol. 8, pp. 338-353, 1965.

[127] J. M. Mendel, "Uncertainty, fuzzy logic, and signal processing," *Signal Processing*, vol. 80, pp. 913-933, 2000.

[128] L. Qilian and J. M. Mendel, "Interval type-2 fuzzy logic systems: theory and design," *IEEE Transactions on Fuzzy Systems*, vol. 8, pp. 535-550, 2000.

[129] Z. Sun, N. Wang, D. Srinivasan, and Y. Bi, "Optimal tunning of type-2 fuzzy logic power system stabilizer based on differential evolution algorithm," *International Journal of Electrical Power & Energy Systems*, vol. 62, pp. 19-28, 2014.

[130] Y. Li and Y. Du, "Indirect adaptive fuzzy observer and controller design based on interval type-2 T–S fuzzy model," *Applied Mathematical Modelling*, vol. 36, pp. 1558-1569, 2012.

[131] J. M. Mendel, R. I. John, and L. Feilong, "Interval Type-2 Fuzzy Logic Systems Made Simple," *IEEE Transactions on Fuzzy Systems*, vol. 14, pp. 808-821, 2006.

[132] D. Wu and W. Wan Tan, "Genetic learning and performance evaluation of interval type-2 fuzzy logic controllers," *Engineering Applications of Artificial Intelligence,* vol. 19, pp. 829-841, 2006.

[133] O. Castillo, P. Melin, A. Alanis, O. Montiel, and R. Sepulveda, "Optimization of interval type-2 fuzzy logic controllers using evolutionary algorithms," *Soft Computing,* vol. 15, pp. 1145-1160, 2011/06/01 2011.

[134] O. Castillo, R. Martínez-Marroquín, P. Melin, F. Valdez, and J. Soria, "Comparative study of bio-inspired algorithms applied to the optimization of type-1 and type-2 fuzzy controllers for an autonomous mobile robot," *Information Sciences,* vol. 192, pp. 19-38, 2012.

[135] O. Castillo and P. Melin, "A review on the design and optimization of interval type-2 fuzzy controllers," *Applied Soft Computing,* vol. 12, pp. 1267-1278, 2012.

[136] S. S. Sidhu, J. S. Saini, and A. Khosla, "Interval type-2 fuzzy system for autonomous navigational control of non-holonomic vehicles," *International Journal of Information Technology and Knowledge Management,* vol. January-June 2012, Volume 5, No. 1, pp. 195-200, pp. 195-200, 2012.

[137] M. A. Abido, "Thyristor controlled phase shifter based stabilizer design using simulated annealing algorithm," in *International Conference on Electric Power Engineering. PowerTech Budapest 99.* , 1999, p. 307.

[138] M. A. Abido, "Robust design of multimachine power system stabilizers using simulated annealing," *IEEE Transactions on Energy Conversion,* vol. 15, pp. 297-304, 2000.

[139] M. A. Abido, "Pole placement technique for PSS and TCSC-based stabilizer design using simulated annealing," *International Journal of Electrical Power and Energy Systems,* vol. 22, pp. 543-554, 2000.

[140] V. A. Maslennikov and S. M. Ustinov, "The optimization method for coordinated tuning of power system regulators," *Proc. 12th Power Syst. Comput. Conf. , Dresden, Germany,* pp. 70-75, 1996.

[141] Y. L. Abdel-Magid, M. Bettayeb, and M. M. Dawoud, "Simultaneous stabilisation of power systems using genetic algorithms," *IEE Proceedings-Generation, Transmission and Distribution,* vol. 144, pp. 39-44, 1997.

[142] Y. L. Abdel-Magid, M. A. Abido, S. Al-Baiyat, and A. H. Mantawy, "Simultaneous stabilization of multimachine power systems via genetic algorithms," *IEEE Transactions on Power Systems,* vol. 14, pp. 1428-1439, 1999.

[143] Y. L. Abdel-Magid and M. M. Dawoud, "Tuning of power system stabilizers using genetic algorithms," *Electric Power Systems Research,* vol. 39, pp. 137-143, 1996.

[144] M. Eslami, H. Shareef, and M. Khajehzadeh, "Genetic algorithm for damping of power system oscillations," *Przegląd Elektrotechniczny (Electrical Review),* vol. 89, pp. 219-222, 2013.

[145] A. Phiri and K. A. Folly, "Application of Breeder GA to power system controller design," in *IEEE Swarm Intelligence Symposium (SIS '08')* 2008, pp. 1-5.

[146] S. Sheetekela, K. Folly, and O. P. Malik, "Design and implementation of power system stabilizers based on evolutionary algorithms," in *IEEE AFRICON, (AFRICON '09')*, 2009, pp. 1-6.

[147] K. A. Folly, "Performance evaluation of power system stabilizers based on Population-Based Incremental Learning (PBIL) algorithm," *International Journal of Electrical Power & Energy Systems,* vol. 33, pp. 1279-1287, 2011.

[148] A. D. Falehi, "Design and Scrutiny of Maiden PSS for Alleviation of Power System Oscillations Using RCGA and PSO Techniques," *Journal of Electrical Engineering & Technology*, vol. 8, pp. 402-410, 2013.

[149] M. A. Abido, "Particle swarm optimization for multimachine power system stabilizer design," in *IEEE Power Engineering Society Summer Meeting*, 2001, pp. 1346-1351 vol.3.

[150] H. Shayeghi, A. Safari, and H. A. Shayanfar, "PSS and TCSC damping controller coordinated design using PSO in multi-machine power system," *Energy Conversion and Management,* vol. 51, pp. 2930-2937, 2010.

[151] H. M. Soliman and M. S. Mahmoud, "Resilient static output feedback power system stabiliser using PSO-LMI optimisation," *Int. J. Syst., Control Commun.,* vol. 5, pp. 74-91, 2013.

[152] A. Ali and A. Mehdi, "A multi-objective gravitational search algorithm based approach of power system stability enhancement with UPFC," *Journal of Central South University,* vol. 20, pp. 1536-1544, 2013/06/01 2013.

[153] T. Mulumba and K. A. Folly, "Design and comparison of Multi-machine Power System Stabilizer base on Evolution Algorithms," *46th International Universities Power Engineering Conference (UPEC '11'),* pp. 1-6, 2011.

[154] H. Shayeghi and A. Ghasemi, "A multi objective vector evaluated improved honey bee mating optimization for optimal and robust design of power system stabilizers," *International Journal of Electrical Power & Energy Systems,* vol. 62, pp. 630-645, 2014.

[155] H. Na, L. Ruiye, and X. Dianguo, "The Study of UPFC Fuzzy Control with Self-adjustable Factor," in *IEEE/PES Transmission and Distribution Conference and Exhibition (Asia and Pacific '05')*, 2005, pp. 1-5.

[156] G. K. Venayagamoorthy, "Optimal control parameters for a UPFC in a multimachine using PSO," in *Proceedings of the 13th International Conference on Intelligent Systems Application to Power Systems*, 2005, p. 6 pp.

[157] A. T. Al-Awami, Y. L. Abdel-Magid, and M. A. Abido, "A particle-swarm-based approach of power system stability enhancement with unified power flow controller," *International Journal of Electrical Power & Energy Systems,* vol. 29, pp. 251-259, 2007.

[158] L. Wenxin, G. K. Venayagamoorthy, and D. C. Wunsch, II, "Adaptive neural network based power system stabilizer design," in *Proceedings of the International Joint Conference on Neural Networks* 2003, pp. 2970-2975 vol.4.

[159] P. Shamsollahi and O. P. Malik, "Design of a neural adaptive power system stabilizer using dynamic back-propagation method," *International Journal of Electrical Power & Energy Systems,* vol. 22, pp. 29-34, 2000.

[160] P. Young-Moon, C. Myeon-Song, and K. Y. Lee, "A wide range operation power system stabilizer design with neural networks using power flow characteristics," in *Proceedings, ISAP '96', International Conference on Intelligent Systems Applications to Power Systems*, 1996, pp. 294-298.

[161] P. Pugliese, R. Sbrizzai, M. Trovato, and M. La Scala, "Intelligent control of inter-area oscillations in power systems," in *8th Mediterranean Electrotechnical Conference (MELECON '96')*, 1996, pp. 737-741 vol.2.

[162] A. S. Yilmaz, E. Esiyok, and E. Yanikoglu, "An analysis of relative performance of state variables in the design of power system stabilizer through neural networks," in *9th Mediterranean Electrotechnical Conference (MELECON '98')*, 1998, pp. 1052-1056 vol.2.

[163] J. He and O. P. Malik, "An adaptive power system stabilizer based on recurrent neural networks," *IEEE Transactions on Energy Conversion,* vol. 12, pp. 413-418, 1997.

[164] M. K. El-Sherbiny, A. M. Sharaf, G. El-Saady, and E. A. Ibrahim, "A novel fuzzy state feedback controller for power system stabilization," *Electric Power Systems Research,* vol. 39, pp. 61-65, 1996.

[165] J. Lu, M. H. Nahrir, and D. A. Pierre, "A fuzzy logic-based adaptive power system stabilizer for multi-machine systems," *Electric Power Systems Research,* vol. 60, pp. 115-121, 2001.

[166] N. Hossein-Zadeh and A. Kalam, "An indirect adaptive fuzzy-logic power system stabiliser," *International Journal of Electrical Power & Energy Systems,* vol. 24, pp. 837-842, 2002.

[167] A. L. Elshafei, K. A. El-Metwally, and A. A. Shaltout, "A variable-structure adaptive fuzzy-logic stabilizer for single and multi-machine power systems," *Control Engineering Practice,* vol. 13, pp. 413-423, 2005.

[168] P. Mitra, S. Chowdhury, S. P. Chowdhury, S. K. Pal, R. N. Lahiri, and Y. H. Song, "Performance of A Fuzzy Power System Stabilizer With Tie Line Active Power Deviation Feedback," in *IEEE PES Power Systems Conference and Exposition (PSCE '06')*, 2006, pp. 884-889.

[169] M. Soliman, A. L. Elshafei, F. Bendary, and W. Mansour, "LMI static output-feedback design of fuzzy power system stabilizers," *Expert Systems with Applications,* vol. 36, pp. 6817-6825, 2009.

[170] X. Lei, H. Huang, S. L. Zheng, D. Z. Jiang, and Z. W. Sun, "Global tuning of power-system stabilizers in multi-machine systems," *Electric Power Systems Research,* vol. 58, pp. 103-110, 2001.

[171] T. Hussein, M. S. Saad, A. L. Elshafei, and A. Bahgat, "Robust adaptive fuzzy logic power system stabilizer," *Expert Systems with Applications,* vol. 36, pp. 12104-12112, 2009.

[172] K. Saoudi and M. N. Harmas, "Enhanced design of an indirect adaptive fuzzy sliding mode power system stabilizer for multi-machine power systems," *International Journal of Electrical Power & Energy Systems,* vol. 54, pp. 425-431, 2014.

[173] P. Kundur, *Power System Stability and Control*. New York: McGraw-Hill, 1994.

[174] T. Hussein, M. S. Saad, A. L. Elshafei, and A. Bahgat, "Damping inter-area modes of oscillation using an adaptive fuzzy power system stabilizer," *Electric Power Systems Research,* vol. 80, pp. 1428-1436, 2010.

[175] I. E. E. E. Digital Excitation System Subcommittee Report, "Computer models for representation of digital-based excitation systems," *IEEE Transactions on Energy Conversion,* vol. 11, pp. 607-615, 1996.

[176] P. Yadav, R. Kumar, S. K. Panda, and C. S. Chang, "An Intelligent Tuned Harmony Search algorithm for optimisation," *Information Sciences,* vol. 196, pp. 47-72, 2012.

[177] D. Manjarres, I. Landa-Torres, S. Gil-Lopez, J. Del Ser, M. N. Bilbao, S. Salcedo-Sanz, *et al.*, "A survey on applications of the harmony search algorithm," *Engineering Applications of Artificial Intelligence,* vol. 26, pp. 1818-1831, 2013.

[178] J. Fourie, S. Mills, and R. Green, "Harmony filter: A robust visual tracking system using the improved harmony search algorithm," *Image and Vision Computing,* vol. 28, pp. 1702-1716, 2010.

[179] J. Fourie, R. Green, and Z. W. Geem, "Generalised Adaptive Harmony Search: A Comparative Analysis of Modern Harmony Search," *Journal of Applied Mathematics,* vol. 2013, pp. 1-13, 2013.

[180] L. Wang, R. Yang, Y. Xu, Q. Niu, P. M. Pardalos, and M. Fei, "An improved adaptive binary Harmony Search algorithm," *Information Sciences,* vol. 232, pp. 58-87, 2013.

[181] Y. Zhang and A. Bose, "Design of Wide-Area Damping Controllers for Interarea Oscillations," *IEEE Transactions on Power Systems,* vol. 23, pp. 1136-1143, 2008.

[182] X.-S. Yang and A. H. Gandomi, "Bat Algorithm: A Novel Approach for Global Engineering Optimization," *Engineering Computations,* vol. 29, pp. 464-483, 2012.

[183] J. Usmana, M. W. Mustafaa, G. Aliyua, and B. U. Musab, "Coordinated AVR-PSS for Transient Stability Using Modified Particle Swarm Optimization," *Jurnal Teknologi (Sciences & Engineering),* vol. 67, pp. 9–16, January, 2014 2014.

[184] F. S. Al-Ismail, M. A. Hassan, and M. A. Abido, "RTDS Implementation of STATCOM-Based Power System Stabilizers," *Electrical and Computer Engineering, Canadian Journal of,* vol. 37, pp. 48-56, 2014.

[185] P. Bera, D. Das, and T. K. Basu, "Tuning of Excitation and TCSC -based stabilizers for multimachine power system," *International Journal of Engineering,* vol. 23, pp. 37-52, 2010.

[186] W. Peres, E. J. de Oliveira, J. A. Passos Filho, and I. C. da Silva Junior, "Coordinated tuning of power system stabilizers using bio-inspired algorithms," *International Journal of Electrical Power & Energy Systems,* vol. 64, pp. 419-428, 2015.

[187] P. Mitra, Y. Chuan, L. Grant, G. K. Venayagamoorthy, and K. Folly, "Comparative Study of Population Based Techniques for Power System Stabilizer Design," in *15th International Conference on Intelligent System Applications to Power Systems (ISAP '09')* 2009, pp. 1-6.

[188] A. Stativa, M. Gavrilas, and O. Ivanov, "Optimal Power System Stabilizer design using multiple wide-area input signals," in *Environment and Electrical Engineering (EEEIC), 2014 14th International Conference on*, 2014, pp. 34-39.

[189] V. Keumarsi, M. Simab, and G. Shahgholian, "An integrated approach for optimal placement and tuning of power system stabilizer in multi-machine systems," *International Journal of Electrical Power & Energy Systems,* vol. 63, pp. 132-139, 2014.

[190] S. Panda, B. K. Sahu, and P. K. Mohanty, "Design and performance analysis of PID controller for an automatic voltage regulator system using simplified particle swarm optimization," *Journal of the Franklin Institute,* vol. 349, pp. 2609-2625, 2012.

[191] K. R. Padiyar, *Power System Dynamics Stability and Control*. Hyderabad, India: BS Publications, 2008.

[192] G. Gurrala and I. Sen, "Synchronizing and Damping Torques Analysis of Nonlinear Voltage Regulators," *IEEE Transactions on Power Systems,* vol. 26, pp. 1175-1185, 2011.

[193] E. Abu-Al-Feilat, M. Bettayeb, H. Al-Duwaish, M. Abido, and A. Mantawy, "A neural network-based approach for on-line dynamic stability assessment using synchronizing and damping torque coefficients," *Electric Power Systems Research,* vol. 39, pp. 103-110, 1996.

[194] Hardiansyah, S. Furuya, and J. Irisawa, "A robust H∞ power system stabilizer design using reduced-order models," *International Journal of Electrical Power & Energy Systems,* vol. 28, pp. 21-28, 2006.

[195] S. M. Radaideh, I. M. Nejdawi, and M. H. Mushtaha, "Design of power system stabilizers using two level fuzzy and adaptive neuro-fuzzy inference systems," *International Journal of Electrical Power & Energy Systems,* vol. 35, pp. 47-56, 2012.

[196] R. Gupta, "Robust Nondynamic Multirate Output Feedback Technique based Power System Stabilizers," Ph. D., Systems and Control Engineering Indian Institute of Technology Bombay, Mumbai, 2003.

[197] A. R. Fereidouni, B. Vahidi, T. Hoseini Mehr, and M. Tahmasbi, "Improvement of low frequency oscillation damping by allocation and design of power system stabilizers in the multi-machine power system," *International Journal of Electrical Power & Energy Systems,* vol. 52, pp. 207-220, 2013.

[198] J. Talaq, "Optimal power system stabilizers for multi machine systems," *International Journal of Electrical Power & Energy Systems,* vol. 43, pp. 793-803, 2012.

[199] H. Bevrani, T. Hiyama, and H. Bevrani, "Robust PID based power system stabiliser: Design and real-time implementation," *International Journal of Electrical Power & Energy Systems,* vol. 33, pp. 179-188, 2011.

[200] K. Sebaa and M. Boudour, "Optimal locations and tuning of robust power system stabilizer using genetic algorithms," *Electric Power Systems Research,* vol. 79, pp. 406-416, 2009.

[201] Z. Peng and O. P. Malik, "Design of an Adaptive PSS Based on Recurrent Adaptive Control Theory," *IEEE Transactions on Energy Conversion,* vol. 24, pp. 884-892, 2009.

[202] G. Ramakrishna and O. P. Malik, "Adaptive PSS using a simple on-line identifier and linear pole-shift controller," *Electric Power Systems Research,* vol. 80, pp. 406-416, 2010.

[203] H. N. Al-Duwaish and Z. M. Al-Hamouz, "A neural network based adaptive sliding mode controller: Application to a power system stabilizer," *Energy Conversion and Management,* vol. 52, pp. 1533-1538, 2011.

[204] B. Changaroon, S. C. Srivastava, and D. Thukaram, "A neural network based power system stabilizer suitable for on-line training-a practical case study for EGAT system," *IEEE Transactions on Energy Conversion,* vol. 15, pp. 103-109, 2000.

[205] B. Changaroon, S. C. Srivastava, and D. Thukaram, "Closure to discussion of "Nneural network based power system stabilizer suitable for on-line training"a practical case study for egat system"," *IEEE Transactions on Energy Conversion,* vol. 15, pp. 494-494, 2000.

[206] V. Mukherjee and S. P. Ghoshal, "Intelligent particle swarm optimized fuzzy PID controller for AVR system," *Electric Power Systems Research,* vol. 77, pp. 1689-1698, 2007.

[207] P. S. Bhati and R. Gupta, "Robust fuzzy logic power system stabilizer based on evolution and learning," *International Journal of Electrical Power & Energy Systems,* vol. 53, pp. 357-366, 2013.

[208] J. M. Ramirez, R. E. Correa, and D. C. Hernández, "A strategy to simultaneously tune power system stabilizers," *International Journal of Electrical Power & Energy Systems,* vol. 43, pp. 818-829, 2012.

[209] E. Nechadi, M. N. Harmas, A. Hamzaoui, and N. Essounbouli, "A new robust adaptive fuzzy sliding mode power system stabilizer," *International Journal of Electrical Power & Energy Systems,* vol. 42, pp. 1-7, 2012.

[210] D. K. Chaturvedi and O. P. Malik, "Neurofuzzy Power System Stabilizer," *IEEE Transactions on Energy Conversion,* vol. 23, pp. 887-894, 2008.

[211] M. A. Awadallah and H. M. Soliman, "A Neuro-fuzzy Adaptive Power System Stabilizer Using Genetic Algorithms," *Electric Power Components and Systems,* vol. 37, pp. 158-173, 2009/01/28 2009.

[212] S. C. Srivastava and B. Changaroon, "A Hybrid Power System Stabilizer Using Neuro-identifier and Predictive Controller," *Electric Machines & Power Systems,* vol. 27, pp. 637-651, 1999/05/01 1999.

[213] H. Alkhatib and J. Duveau, "Dynamic genetic algorithms for robust design of multimachine power system stabilizers," *International Journal of Electrical Power & Energy Systems,* vol. 45, pp. 242-251, 2013.

[214] A. Al-Hinai, "Dynamic stability enhancement using Genetic Algorithm Power System Stabilizer," in *International Conference on Power System Technology (POWERCON), 2010,* 2010, pp. 1-7.

[215] R. Gupta, B. Bandyopadhyay, and A. M. Kulkarni, "Robust decentralized fast-output sampling technique based power system stabilizer for a multi-machine power system," *International Journal of Systems Science,* vol. 36, pp. 297-314, 2005/04/15 2005.

[216] S. M. Abd-Elazim and E. S. Ali, "A hybrid Particle Swarm Optimization and Bacterial Foraging for optimal Power System Stabilizers design," *International Journal of Electrical Power & Energy Systems,* vol. 46, pp. 334-341, 2013.

[217] H. M. Soliman, E. H. E. Bayoumi, and M. F. Hassan, "PSO–based Power System Stabilizer for Minimal Overshoot and Control Constraints," *Journal of Electrical Engineering,* vol. 59, pp. 153–159, 2008.

[218] S. Panda, "Multi–Objective Non–Dominated shorting Genetic Algorithm–II for Excitation and TCSC–based Controller Design," *Journal of Electrical Enginnering,* vol. 60, pp. 86-93, 2009.

[219] L. H. Hassan, M. Moghavvemi, H. A. F. Almurib, K. M. Muttaqi, and V. G. Ganapathy, "Optimization of power system stabilizers using participation factor and genetic algorithm," *International Journal of Electrical Power & Energy Systems,* vol. 55, pp. 668-679, 2014.

[220] S. Panda, "Robust coordinated design of multiple and multi-type damping controller using differential evolution algorithm," *International Journal of Electrical Power & Energy Systems,* vol. 33, pp. 1018-1030, 2011.

[221] M. A. Abido, "Simulated annealing based approach to PSS and FACTS based stabilizer tuning," *International Journal of Electrical Power & Energy Systems,* vol. 22, pp. 247-258, 2000.

[222] C. Li-Jun and I. Erlich, "Simultaneous coordinated tuning of PSS and FACTS damping controllers in large power systems," *IEEE Transactions on Power Systems,* vol. 20, pp. 294-300, 2005.

[223] R. Poli, J. Kennedy, and T. Blackwell, "Particle swarm optimization: An overview," *Swarm Intell,* vol. 1, pp. 33-57, 2007.

[224] M. Eslami, H. Shareef, A. Mohamed, and M. Khajehzadeh, "A hybrid PSO technique for damping electro-mechanical oscillations in large power system," in *IEEE Student Conference on Research and Development (SCOReD '10')*, 2010, pp. 442-447.

[225] X.-S. Yang, "Firefly Algorithms for Multimodal Optimization," in *Stochastic Algorithms: Foundations and Applications*. vol. 5792, O. Watanabe and T. Zeugmann, Eds., ed: Springer Berlin Heidelberg, 2009, pp. 169-178.

[226] A. Gandomi, X.-S. Yang, and A. Alavi, "Cuckoo search algorithm: a metaheuristic approach to solve structural optimization problems," *Engineering with Computers,* vol. 29, pp. 17-35, 2013/01/01 2013.

[227] Y. Xin-She and S. Deb, "Cuckoo Search via Levy flights," in *World Congress on Nature & Biologically Inspired Computing, 2009. NaBIC 2009.*, 2009, pp. 210-214.

[228] S. Mirjalili, S. Mirjalili, and X.-S. Yang, "Binary bat algorithm," *Neural Computing and Applications*, pp. 1-19, 2013/12/27 2013.

[229] A. Pal and J. Maiti, "Development of a hybrid methodology for dimensionality reduction in Mahalanobis–Taguchi system using Mahalanobis distance and binary particle swarm optimization," *Expert Systems with Applications*, vol. 37, pp. 1286-1293, 2010.

[230] İ. Babaoglu, O. Findik, and E. Ülker, "A comparison of feature selection models utilizing binary particle swarm optimization and genetic algorithm in determining coronary artery disease using support vector machine," *Expert Systems with Applications*, vol. 37, pp. 3177-3183, 2010.

[231] B. Seung-Mook, P. Jung-Wook, and I. A. Hiskens, "Optimal Tuning for Linear and Nonlinear Parameters of Power System Stabilizers in Hybrid System Modeling," *IEEE Transactions on Industry Applications*, vol. 45, pp. 87-97, 2009.

[232] P. W. Sauer and M. A. Pai, *Power System Dynamics and Stability*. New Delhi, India: Prentice-Hall of India Pvt. Limited, 1998.

[233] Y. L. Abdel-Magid, M. A. Abido, and A. H. Mantawy, "Robust tuning of power system stabilizers in multimachine power systems," in *IEEE Power Engineering Society Winter Meeting*, 2000, p. 1425 vol.2.

[234] A. Hariri and O. P. Malik, "Self-learning adaptive-network-based fuzzy logic power system stabilizer," in *International Conference on Intelligent Systems Applications to Power Systems (ISAP '96')*, 1996, pp. 299-303.

[235] M. Kashki, M. A. Abido, and Y. L. Abdel-Magid, "Pole placement approach for robust optimum design of PSS and TCSC-based stabilizers using reinforcement learning automata," *Electrical Engineering*, vol. 91, pp. 383-394, 2010/03/01 2010.

[236] M. A. Abido and Y. L. Abdel-Magid, "A tabu search based approach to power system stability enhancement via excitation and static phase shifter control," *Electric Power Systems Research*, vol. 52, pp. 133-143, 1999.

[237] M. A. Abido, "Coordinated Design of Power System Stabilizers and Static Phase Shifters Using Genetic Algorithm," *Electric Machines and Power Systems*, vol. 27, pp. 1069-1084, 1999/09/01 1999.

[238] A. T. Al-Awami, Y. L. Abdel-Magid, and M. A. Abido, "Simultaneous Stabilization of Power System Using UPFC-Based Controllers," *Electric Power Components and Systems*, vol. 34, pp. 941-959, 2006/09/01 2006.

[239] M. Kashki, M. A. Abido, and Y. L. Abdel-Magid, "Power System Dynamic Stability Enhancement Using Optimum Design of PSS and Static Phase Shifter Based Stabilizer," *Arabian Journal for Science and Engineering*, vol. 38, pp. 637-650, 2013/03/01 2013.

[240] M. A. M. Hassan, O. P. Malik, and G. S. Hope, "A fuzzy logic based stabilizer for a synchronous machine," *IEEE Transactions on Energy Conversion*, vol. 6, pp. 407-413, 1991.

[241] M. A. M. Hassan, O. P. Malik, and G. S. Hope, "A fuzzy logic based self-tuned power system stabilizer," in *Third International Conference on Power System Monitoring and Control* 1991, pp. 146-151.

[242] R. Gupta, B. Bandyopadhyay, and A. M. Kulkarni, "Design of power system stabiliser for single-machine system using robust periodic output feedback controller," *IEE Proceedings-Generation, Transmission and Distribution*, vol. 150, pp. 211-216, 2003.

[243] R. Gupta, B. Bandyopadhyay, and A. M. Kulkarni, "Design of power system stabilizer for single machine system using robust fast output sampling feedback technique," *Electric Power Systems Research*, vol. 65, pp. 247-257, 2003.

[244] G. Rogers, *Power system oscillations*. New York: Springer: Kluwer Academic Publishers, 2000.

[245] T. K. Das and G. K. Venayagamoorthy, "Optimal design of power system stabilizers using a small population based PSO," in *IEEE Power Engineering Society General Meeting*, 2006, pp. 1-7.

[246] M. A. Abido, "Parameter optimization of multimachine power system stabilizers using genetic local search," *International Journal of Electrical Power & Energy Systems*, vol. 23, pp. 785-794, 2001.

[247] M. A. Abido and Y. L. Abdel-Magid, "A genetic-based fuzzy logic power system stabilizer for multimachine power systems," in *IEEE International Conference on Systems, Man, and Cybernetics, 1997. Computational Cybernetics and Simulation*, 1997, pp. 329-334 vol.1.

[248] T. Hiyama and T. Sameshima, "Fuzzy logic control scheme for on-line stabilization of multi-machine power system," *Fuzzy Sets and Systems*, vol. 39, pp. 181-194, 1991.

[249] X.-S. Yang, "Bat algorithm for multi-objective optimisation," *International Journal of Bio-Inspired Computation*, vol. 3, pp. 267-274, 2011.

[250] P. Kundur, *Power System Stability and Control*. New York: McGraw-Hill, 1974.

[251] R. Grondin, I. Kamwa, G. Trudel, L. Gerin-Lajoie, and J. Taborda, "Modeling and closed-loop validation of a new PSS concept, the multi-band PSS," in *IEEE Power Engineering Society General Meeting*, 2003, p. 1809 Vol. 3.

[252] P. M. Anderson and A. A. Foud, *Power System Control and Stability*. Lowa, USA: Lowa State University Press, 1997.

[253] F. Milano, "Power system analysis toolbox," Version 2.1.6 ed. University college Dublin, 2010.

[254] M. Ramirez-Gonzalez, R. Castellanos B, and O. P. Malik, "Application of simple fuzzy PSSs for power system stability enhancement of the Mexican Interconnected System," in *IEEE Power and Energy Society General Meeting-2010*, 2010, pp. 1-8.

[255] R. Gupta, D. K. Sambariya, and R. Gunjan, "Fuzzy Logic based Robust Power System Stabilizer for Multi-Machine Power System," in *IEEE International Conference on Industrial Technology, ICIT 2006.*, 2006, pp. 1037-1042.

[256] A. Bagis, "Tabu search algorithm based PID controller tuning for desired system specifications," *Journal of the Franklin Institute,* vol. 348, pp. 2795-2812, 2011.

[257] S. Panda, "Multi-objective evolutionary algorithm for SSSC-based controller design," *Electric Power Systems Research,* vol. 79, pp. 937-944, 2009.

[258] S. Panda, "Differential evolution algorithm for SSSC-based damping controller design considering time delay," *Journal of the Franklin Institute,* vol. 348, pp. 1903-1926, 2011.

[259] J. Zhang, J. Zhuang, H. Du, and S. Wang, "Self-organizing genetic algorithm based tuning of PID controllers," *Information Sciences,* vol. 179, pp. 1007-1018, 2009.

[260] W.-D. Chang and S.-P. Shih, "PID controller design of nonlinear systems using an improved particle swarm optimization approach," *Communications in Nonlinear Science and Numerical Simulation,* vol. 15, pp. 3632-3639, 2010.

[261] M. Soliman, H. Emara, A. Elshafei, A. Bahgat, and O. P. Malik, "Robust output feedback power system stabilizer design: an LMI approach," in *IEEE Power and Energy Society General Meeting - Conversion and Delivery of Electrical Energy in the 21st Century*, 2008, pp. 1-8.

[262] B. C. Pal, A. H. Coonick, I. M. Jaimoukha, and H. El-Zobaidi, "A linear matrix inequality approach to robust damping control design in power systems with superconducting magnetic energy storage device," *IEEE Transactions on Power Systems,* vol. 15, pp. 356-362, 2000.

[263] P. Bera, D. Das, and T. K. Basu, "Design of P-I-D power system stabilizer for multimachine system," in *IEEE First India Annual Conference (INDICON-2004)*, 2004, pp. 446-450.

[264] P. Bera, T. K. Basu, and D. Das, "Design of P-I Power System Stabilizers for Damping Inter-area Oscillation," in *Frontiers in Computer Education*. vol. 133, S. Sambath and E. Zhu, Eds., ed: Springer Berlin Heidelberg, 2012, pp. 551-558.

[265] L. Wang, R. Yang, P. M. Pardalos, L. Qian, and M. Fei, "An adaptive fuzzy controller based on harmony search and its application to power plant control," *International Journal of Electrical Power & Energy Systems*, vol. 53, pp. 272-278, 2013.

[266] J. Pahasa and I. Ngamroo, "Adaptive Power System Stabilizer Design Using Optimal Support Vector Machines Based on Harmony Search Algorithm," *Electric Power Components and Systems*, vol. 42, pp. 439-452, 2014/04/04 2014.

[267] J. Reddy and M. J. Kishore, "Real time implementation of H∞ loop shaping robust PSS for multimachine power system using dSPACE," *International Journal of Electrical Power & Energy Systems*, vol. 33, pp. 1750-1759, 2011.

[268] M. A. Abido and Y. L. Abdel-Magid, "Hybridizing rule-based power system stabilizers with genetic algorithms," *IEEE Transactions on Power Systems*, vol. 14, pp. 600-607, 1999.

[269] P. Zhang and A. Coonick, "Coordinated synthesis of PSS parameters in multi-machine power systems using the method of inequalities applied to genetic algorithms," in *IEEE Power Engineering Society Winter Meeting*, 2000, p. 1424 vol.2.

[270] S. Mishra, M. Tripathy, and J. Nanda, "Multi-machine power system stabilizer design by rule based bacteria foraging," *Electric Power Systems Research*, vol. 77, pp. 1595-1607, 2007.

[271] V. Bandal, B. Bandyopadhyay, and A. M. Kulkarni, "Output feedback fuzzy sliding mode control technique based power system stabilizer (PSS) for single machine infinite bus (SMIB) system," in *IEEE International Conference on Industrial Technology (ICIT-2005)*, 2005, pp. 341-346.

[272] Zong Woo Geem, Joong Hoon Kim, and G. V. Loganathan, "A New Heuristic Optimization Algorithm: Harmony Search," *Simulation*, vol. 76, pp. 60-68, February 1, 2001 2001.

[273] Z. W. Geem, "Harmony Search Applications in Industry," in *Studies in Fuzziness and Soft Computing, Volume 226, Soft Computing Applications in Industry*. vol. 226, B. Prasad, Ed., ed: Springer-Verlag Berlin Heidelberg, 2008, pp. 117-134.

[274] J. Yu and P. Guo, "Improved PSO Algorithm with Harmony Search for Complicated Function Optimization Problems," in *Advances in Neural Networks – ISNN 2012*. vol. 7367, J. Wang, G. Yen, and M. Polycarpou, Eds., ed Shenyang, China: Springer-Verlag Berlin Heidelberg, 2012, pp. 624-632.

[275] N. Sinsuphan, U. Leeton, and T. Kulworawanichpong, "Optimal power flow solution using improved harmony search method," *Applied Soft Computing*, vol. 13, pp. 2364-2374, 2013.

[276] A. Verma, B. K. Panigrahi, and P. R. Bijwe, "Harmony search algorithm for transmission network expansion planning," *IET Proceedings-Generation, Transmission & Distribution*, vol. 4, pp. 663-673, 2010.

[277] R. Sirjani, A. Mohamed, and H. Shareef, "Optimal allocation of shunt Var compensators in power systems using a novel global harmony search algorithm," *International Journal of Electrical Power & Energy Systems*, vol. 43, pp. 562-572, 2012.

[278] D. Drainkov, H. Hellendoorn, and M. Reinfrank, *An introduction to fuzzy control*. Berlin: Springer, 1996.

[279] R. Gupta, B. Bandyopadhyay, and A. M. Kulkarni, "Design of decentralized power system stabilizers for multimachine power system using model reduction and fast output sampling techniques," in *5th Asian Control Conference-2004*, 2004, pp. 1384-1392 Vol.2.

[280] R. Gupta, B. Bandyopadhyay, and A. M. Kulkarni, "Power system stabiliser for multimachine power system using robust decentralised periodic output feedback," *IEE Proceedings -Control Theory and Applications*, vol. 152, pp. 3-8, 2005.

[281] B. C. Pal, "Robust pole placement versus root-locus approach in the context of damping interarea oscillations in power systems," *IEE Proceedings-Generation, Transmission and Distribution*, vol. 149, pp. 739-745, 2002.

[282] A. J. Saavedra-Montes, J. M. Ramirez-Scarpetta, C. A. Ramos-Paja, and O. P. Malik, "Identification of excitation systems with the generator online," *Electric Power Systems Research*, vol. 87, pp. 1-9, 2012.

[283] J. Ritonja, "Adaptive stabilization for generator excitation system," *COMPEL: The International Journal for Computation and Mathematics in Electrical and Electronic Engineering*, vol. 30, pp. 1092-1108, 2011.

[284] C. Y. Chung, C. T. Tse, A. K. David, and A. B. Rad, "A new H∞ based PSS design using numerator–denominator perturbation representation," *Electric Power Systems Research*, vol. 52, pp. 37-42, 1999.

[285] D. K. Sambariya and R. Prasad, "Power System Stabilizer Design for Single Machine Infinite Bus System with different Membership Functions for Fuzzy Logic Controller," *International Conference on Advances in Technology and Engineering, ICATE-2012 [IEEE-Conference] at Mukesh Patel School of Technology Management & Engineering, Behind Homeopathy College, Bhakti Vedant Swami Marg, JVPD Scheme, Vile Parle West, Mumbai, Maharashtra.*, pp. 151-162, January 23-25, 2013 2013.

[286] D. K. Sambariya and R. Prasad, "Design of Harmony Search Algorithm based tuned Fuzzy logic Power System Stabilizer," *International Review of Electrical Engineering (IREE)*, vol. 8, pp. 1594-1607, October 2013 2013.

[287] D. Flynn, B. W. Hogg, E. Swidenbank, and K. J. Zachariah, "Expert control of a self-tuning automatic voltage regulator," *Control Engineering Practice,* vol. 3, pp. 1571-1579, 1995.

[288] K. J. Åström and B. Wittenmark, "On self tuning regulators," *Automatica,* vol. 9, pp. 185-199, 1973.

[289] E. H. Mamdani and S. Assilian, "An experiment in linguistic synthesis with a fuzzy logic controller," *International Journal of Man-Machine Studies,* vol. 7, pp. 1-13, 1975.

[290] J. Dombi, "Membership function as an evaluation," *Fuzzy Sets and Systems,* vol. 35, pp. 1-21, 1990.

[291] A. Gegov and N. Gobalakrishnan, "Advanced Inference in Fuzzy Systems by Rule Base Compression," *Mathware & Soft Computing,* vol. 14, pp. 201-216, 2007.

[292] P. J. King and E. H. Mamdani, "The application of fuzzy control systems to industrial processes," *Automatica,* vol. 13, pp. 235-242, 1977.

[293] M. Braae and D. A. Rutherford, "Theoretical and linguistic aspects of the fuzzy logic controller," *Automatica,* vol. 15, pp. 553-577, 1979.

[294] M. Sugeno and G. T. Kang, "Structure identification of fuzzy model," *Fuzzy Sets and Systems,* vol. 28, pp. 15-33, 1988.

[295] T. Takagi and M. Sugeno, "Fuzzy identification of systems and its applications to modeling and control," *Systems, Man and Cybernetics, IEEE Transactions on,* vol. SMC-15, pp. 116-132, 1985.

[296] M. Braae and D. A. Rutherford, "Fuzzy Relations in a control setting," *Kybernetes,* vol. 7, pp. 185 - 188, 1978.

[297] E. H. Mamdani, "Advances in the linguistic synthesis of fuzzy controllers," *International Journal of Man-Machine Studies,* vol. 8, pp. 669-678, 1976.

[298] E. H. Mamdani, "Application of fuzzy algorithms for control of simple dynamic plant," *Electrical Engineers, Proceedings of the Institution of,* vol. 121, pp. 1585-1588, 1974.

[299] N. Baaklini and E. H. Mamdani, "Prescriptive methods for deriving control policy in a fuzzy-logic controller," *Electron. Lett.,* vol. 11, pp. 625-626, 1975.

[300] M. Braae and D. A. Rutherford, "Selection of parameters for a fuzzy logic controller," *Fuzzy Sets and Systems,* vol. 2, pp. 185-199, 1979.

[301] C. Y. Chung, K. W. Wang, C. T. Tse, X. Y. Bian, and A. K. David, "Probabilistic eigenvalue sensitivity analysis and PSS design in multimachine systems," *IEEE Transactions on Power Systems,* vol. 18, pp. 1439-1445, 2003.

[302] A. Venkateswara Reddy, M. Vijay Kumar, G. Gurrala, and I. Sen, "New approach for the design of pole placement power system stabilizers," in *International Conference on Clean Electrical Power (ICCEP-2011)*, 2011, pp. 324-327.

[303] M. Chilali and P. Gahinet, "H∞ design with pole placement constraints: an LMI approach," *IEEE Transactions on Automatic Control*, vol. 41, pp. 358-367, 1996.

[304] M. Eslami, H. Shareef, A. Mohamed, and M. Khajehzadeh, "Damping of Power System Oscillations Using Genetic Algorithm and Particle Swarm Optimization," *International Review of Electrical Engineering (I.R.E.E.)*, vol. 5, pp. 2745-2753, 2010.

[305] M. Eslami, H. Shareef, A. Mohamed, and M. Khajehzadeh, "Gravitational search algorithm for coordinated design of PSS and TCSC as damping controller," *Journal of Central South University*, vol. 19, pp. 923-932, 2012/04/01 2012.

[306] M. Eslami, H. Shareef, A. Mohamed, and M. Khajehzadeh, "PSS and TCSC Damping Controller Coordinated Design Using GSA," *Energy Procedia*, vol. 14, pp. 763-769, 2012.

[307] M. Eslami, H. Shareef, and M. Khajehzadeh, "Optimal design of damping controllers using a new hybrid artificial bee colony algorithm," *International Journal of Electrical Power & Energy Systems*, vol. 52, pp. 42-54, 2013.

[308] M. Eslami and H. Shareef, "Artificial bee colony algorithm for optimal design of power system stabilizer," in *IPEC '12', Conference on Power and Energy*, 2012, pp. 1-6.

[309] J. Shin, S. Nam, J. Lee, S. Baek, Y. Choy, and T. Kim, "A Practical Power System Stabilizer Tuning Method and its Verification in Field Test," *Journal of Electrical Engineering & Technology*, vol. 5, pp. 400-406, 2010.

[310] A. Abbadi, L. Nezli, and D. Boukhetala, "A nonlinear voltage controller based on interval type 2 fuzzy logic control system for multimachine power systems," *International Journal of Electrical Power & Energy Systems*, vol. 45, pp. 456-467, 2013.

[311] J. R. Aguero and A. Vargas, "Calculating Functions of Interval Type-2 Fuzzy Numbers for Fault Current Analysis," *IEEE Transactions on Fuzzy Systems*, vol. 15, pp. 31-40, 2007.

[312] P. Z. Lin, C. M. Lin, C. F. Hsu, and T. T. Lee, "Type-2 fuzzy controller design using a sliding-mode approach for application to DC-DC converters," *IEE Proceedings-Electric Power Applications*, vol. 152, pp. 1482-1488, 2005.

[313] M. Tripathy and S. Mishra, "Interval type-2-based thyristor controlled series capacitor to improve power system stability," *IET Proceedings-Generation, Transmission & Distribution*, vol. 5, pp. 209-222, 2011.

[314] M. K. Panda, G. N. Pillai, and V. Kumar, "Power system stabilizer design: Interval type-2 fuzzy logic controller approach," in *2nd International Conference on Power, Control and Embedded Systems (ICPCES), 2012* 2012, pp. 1-10.

[315] H. A. Hagras, "A hierarchical type-2 fuzzy logic control architecture for autonomous mobile robots," *IEEE Transactions on Fuzzy Systems*, vol. 12, pp. 524-539, 2004.

[316] D. Wu and W. W. Tan, "Type-2 FLS Modeling Capability Analysis," in *The 14th IEEE International Conference on Fuzzy Systems, 2005. FUZZ '05.* , 2005, pp. 242-247.

[317] L. T. Ngo, D. D. Nguyen, L. T. Pham, and C. M. Luong, "Speedup of Interval Type 2 Fuzzy Logic Systems Based on GPU for Robot Navigation," *Advances in Fuzzy Systems*, vol. 2012, p. 11, 2012.

[318] B.-I. Choi and F. Chung-Hoon Rhee, "Interval type-2 fuzzy membership function generation methods for pattern recognition," *Information Sciences,* vol. 179, pp. 2102-2122, 2009.

[319] M. A. Pai, *Energy Function Analysis for Power System Stability*. Norwell, Massachusetts 02061 USA: K1uwer Academic Publishers, 1989.